The efficiency of bacterial self-healing concrete inculcated in ground condition

A submission in partial fulfilment of the requirements of the University of Derby for the Doctor of Philosophy degree in Civil Engineering

Mohamed Esaker

College of Science and Engineering

The University of Derby

October 2021

Declaration

I declare that this thesis is my own work, and the content of this thesis has not been previously submitted to any other university for a degree. Any published work used in this thesis was fully referenced at the point of use in accordance with a standard referencing style and fully described in the reference section of this thesis.

Mohamed Esaker

Derby, October 2021

Acknowledgement

My honest thanks to my supervisors: Dr. Omar Hamza, and Dr. David Elliott who gave me the chance to work on this research project, and for providing supervision and unlimited support during this research project. I would like to thank the University of Derby for funding this research.

I would like also to thank the technical staff in the laboratory: Richard Duff, Matt Whomsley, and Graham Souch for their support and providing all required materials for this research and giving me an opportunity to access and use the equipment in the laboratory and other facilities.

Finally, a special thanks goes to my wife, for her support and continuous encouragement through my study.

Abstract

The innovative bacterial self-healing concrete is a promising solution to improve the sustainability of concrete structures by sealing the cracks in an autonomous way. Regardless of the types of bacterial-based approach, the provision of a suitable incubation environment is essential for the activation of bacteria and thus for a successful self-healing application. However, the research to date has mainly focused on the self-healing process within humid air or water environment. This research aims to investigate the performance of bacterial self-healing concrete within ground conditions which can potentially benefit the development of more sustainable underground concrete structures such as deep foundations, retaining walls and tunnels.

The research method is comprised of a laboratory experimental program with several stages/ phases. In the first stage, control tests were conducted to examine the influence of different delivery techniques of healing agents such as the material of capsules on the healing performance in water. The outputs from this stage were used as a control test to inform the next stages where the fine-grained concrete/mortar specimens were incubated inside the soil. In this stage, three different delivery techniques of the healing agent were examined namely Direct add, Calcium alginate beads and Perlite. The results showed that the crack-healing capacity was significantly improved with using of bacterial agent for all delivery techniques and the maximum healed crack width was about 0.57 mm after 60 days of incubation for specimens incorporated with perlite (set ID: M4). The volume stability of the perlite capsules has made them more compatible with the cement mortar matrix in comparison with the calcium alginate capsule. The results from Scanning Electron Microscope (SEM) and Energy Dispersive X-ray (EDX) indicated that the mineral precipitations on crack surfaces were calcium carbonate.

The second stage investigates the effect of different ground conditions on the efficiency of bio self-healing concrete. This stage presents a major part of the experimental programme and contains three experimental parts based on the types of soils and their conditions where bio self-healing of cement mortar

specimens was examined. The first part investigates the effect of the presence of microbial and organic materials within the soil on the performance of self-healing by incubating cracked mortar specimens into sterilized and non-sterilized soil. This part aims to investigate if the existing bacteria in the soil can produce any self-healing.

In the second part, the investigation focused on the bio self-healing in specimens incubated in coarse-grained soil (sand). The soil was subjected to fully and partially saturated cycles and conditioned with different pH and sulphate levels representing industrially recognised classes of exposure (namely, X0, XA1, and XA3). These classes were selected according to BS EN 206:2013+A1:2016 - based on the risk of corrosion and chemical attack from an aggressive ground environment. In the third part, cement mortar specimens were incubated into fully and partially saturated fine-grained soil (clay) with similar aggressive environments as in part 2. The results showed that the indigenous bacteria naturally present within the soil can enhance the mortar self-healing process. For specimens incubated within coarse-grained soil (sand), the reduction in pH of the incubation environment affected the bio self-healing performance. However, for fine-grained soil (clay) the healing ratios of specimens incubated in the same identical exposure conditions were almost similar, with better results observed in the pH neutral condition. The results showed also that the self-healing efficiencies in both the control and bio-mortar specimens were significantly affected by the soil's moisture content. This indicates that the mineral precipitation of calcium carbonate caused by the metabolic conversion of nutrients by bacteria is heavily reliant on the moisture content of the soil. The hydration of un-hydrated cement particles representing the primary source of autogenous healing is also influenced by soil moisture content.

The third stage investigated the use of a non-destructive technique utilising the concrete electrical resistivity to monitor the crack healing performance of specimens incubated within the soil. The results showed that the improvement in electrical resistivity of bio-mortar specimens was remarkably higher in comparison

with control specimens. This improvement can be used as an indication of the healing performance of bio-mortar specimens in comparison with autogenous healing in control specimens.

In general, the study suggests that the bio self-healing process can protect underground concrete structures such as foundations, bridge piers, and tunnels in a range of standard exposure conditions and that this is facilitated by the commonly applied bacterial agent Bacillus subtilis or similar strains. However, as the experimental findings indicated the exposure conditions could affect the healing efficiency. Therefore, future work should consider how formulations, application methods, and ground preparation can be optimised to achieve the best possible incubation environment and thus improved protection for underground concrete structures.

List of Publications from this work

The author is named as the first author and co-author on the following journal papers:

1- Souid, A., Esaker, M., Elliott, D. and Hamza, O., 2019. Experimental data of bio self-healing concrete incubated in saturated natural soil. Data in brief, 26, p.104394.

2- Hamza, O., Esaker, M., Elliott, D. and Souid, A., 2020. The effect of soil incubation on bio self-healing of cementitious mortar. Materials Today Communications, 24, p.100988.

3- Esaker, M., Hamza, O., Souid, A. and Elliott, D., 2021. Self-healing of bio-cementitious mortar incubated within neutral and acidic soil. Materials and Structures, 54(2), pp.1-16.

4- Esaker, M., Hamza, O., Souid, A. and Elliott, D. The performance of bio self-healing of cementitious mortar incubated within clay soil. (Manuscript).

The author is named as the first author and co-author on the following conference papers and proceedings:

1- Esaker, M. and Hamza, O. (2019). The effect of delivery technique of bacterial healing agent on efficiency of self-healing concrete. ICSHM 2019: The 7th International Conference on Self-Healing Materials, 3rd5th June 2019, Yokohama, Japan.

2- Souid, A., Esaker, M., Elliott, D. and Hamza, O. (2019). Microbiological self-healing of structural concrete underground incubation for geotechnical applications. ICSHM 2019: The 7th International Conference on Self-Healing Materials, 3rd5th June 2019, Yokohama, Japan.

3- Esaker, M., Hamza, O., Elliott, D. and Souid, A. (2020). Evaluation of the self-healing of cracked mortars incubated within sterilized and non-

sterilized natural soil. RM4L: Resilient Materials 4 Life International Conference, 20-22 September 2020, Cambridge, UK.

4- Souid, A., Hamza, O., Elliott, D. and Esaker, M. (2020). Microbial induced calcite precipitations of bio self-healing concrete underground exposure conditions. RM4L: Resilient Materials 4 Life International Conference, 20-22 September 2020, Cambridge, UK.

Table of content

List of Figures

List of Tables

List of symbols and abbreviation

BMS	Bio Mortar Specimens
CF	Carbon Fibre
CFU	Colony Forming Unit
CMS	Control Mortar Specimens
CP	Coated Perlite
CSH	Calcium Silicate Hydrate
CSI	Cement Sustainability Initiative
DIC	Dissolved Inorganic Carbon
EDX	Energy Dispersive X-ray
FSC	Fully Saturated Clay
I	Coefficient of absorption
LVDT	Linear Variable Differential Transducers
MICCP	Microbiologically Induced Calcium Carbonate Precipitation
NSS	Non-Sterilized Soil
PBS	Phosphate Buffered Saline
PVA	poly vinyl alcohol
PSC	Partially Saturated Clay
PSD	Particle Size Distribution
SEM	Scanning Electron Microscopy
SST	Spore Stain Test
UCP	Uncoated Perlite
UMS	Miniature-Tensiometer
S	Coefficient of sorptivity
SS	Sterilized Soil
u	Pore-water pressure in soil

Chapter 1

Introduction

1.1 Background

Concrete is the most common construction material utilised worldwide for buildings and infrastructures. The high performance and quality of concrete structures have become extremely important for the economies of all countries. Since the days of the Roman and Greek civilisation, concrete has been the primary material used to provide a reliable and stable infrastructure [1]. Although it is efficient in resisting compression, it has low tensile strength and starts to crack when subjected to tension. To resist these internal tensile stresses, concrete constructions are often combined with various types of reinforcement such as steel.

Reinforced concrete is considered an economical construction material and has been utilised for decades. According to the Cement Sustainability Initiative [CSI, 2009], approximately 25 billion tons of concrete are utilised per annum. It is easy to cast in different shapes and is strong and durable throughout its service life [2]. Although steel reinforcement is used to control concrete cracking, complete crack prevention is almost impossible due to factors such as thermal shrinkage and expansion [3]. In addition, poor design and the inappropriate selection of materials can lead to inadequate performance [2] as concrete structures often suffer from cracks caused by service loads, resulting in early deterioration and shorter service life [4]. The rate of deterioration of concrete structures is influenced by two primary factors: concrete permeability and the development of micro-cracks [5]. Although micro-cracks do not affect the strength of the concrete, they can accelerate permeability and allow aggressive chemicals such as chlorides, sulphates, and acids to ingress structural elements and corrode the reinforcing steel, thus damaging the entire structure [6].

The high alkaline environment can prevent reinforcing steel in concrete from corroding by creating a passive film on the surface of the steel. However, the passive film will not last long, and the steel immediately corrodes under the chloride attack. Rust products are approximately four to six times larger in volume than steel. This creates internal tensile stresses in the concrete cover that result in delamination and cracking when the tensile strength of the concrete is exceeded [7].

1.2 Research motivation

The financial cost for the rehabilitation and monitoring of concrete structures is extremely high and the process is time-consuming. Koch et al. [8] warned that the deterioration of structures is having a serious impact on the economy of multiple countries. For instance, in the USA, approximately $140 billion is spent on maintenance and repair work on 10% of its bridges [9].

In Europe, approximately half of the annual construction budgets are allocated to repairing existing infrastructures [10]. For instance, around one-third of the annual budget for large civil engineering projects in the Netherlands is set aside for monitoring, inspection, maintenance, and repair. In the UK, approximately £8 billion per annum is spent on maintenance works, representing approximately 45% of the total activity of the construction and building industry [11]. In the Middle East, a survey report indicates that 70% of concrete bridges on the Gulf Coast in Saudi Arabia are suffering from deterioration damage. Sea salts and polluted aggregates or water are the main reasons for severe deterioration within 10 years of the construction of jetty pile caps, service duct covers, oil tank foundations, and bridge piers [12]. In Japan, the East Japan Railway Company states that more than $10 billion is spent on the maintenance and repair of railway bridges and tunnels [13].

In 2009, the American Society of Civil Engineers reported that the USA infrastructure had been awarded a grade of “D” due to delays in maintenance and funding. To increase this to a “B”, they estimated that approximately $2.2 trillion would be needed over the next five years [14].

In addition to the direct costs, there are indirect costs of up to $63 billion per year in the USA due to a severe economic loss in productivity and the occurrence of traffic jams, [15]. Therefore, “enhancing the longevity of our built infrastructure will undoubtedly reduce the impact of mankind’s activities on the stability of the biosphere” [16].

It can be inferred that sustaining infrastructure assets, which are made of reinforced concrete such as bridges and utilities, is essential for economic growth. Therefore, inspection, maintenance and repair works are needed to seal the concrete cracks and hence reduce permeability, prevent the corrosion of steel reinforcement, and restore the durability of the structure. Extending the service life of existing infrastructure can reduce the demand for new infrastructure, cost, and levels of pollution. However, manual repair works can sometimes be difficult, time-consuming, and extremely expensive because cracks are either invisible or their location is inaccessible.

1.3 Proposed solutions

A large body of research has been conducted by engineers and material scientists to explore techniques developed to repair micro-cracks and design structures and ensure high durability, good performance, and a long maintenance-free service life [17]. An alternative approach to damage prevention is that of damage management. This is predicated on the rule that structural damage can be tolerated if it is healed or corrected in sufficient time [18]. This approach was translated into the development of self-healing concrete by C. Dry in 1994 [19]. In the ensuing years, several researchers began to investigate this topic. The current state of the art concerning cementitious self-healing is given in [20, 21].

The different approaches available today can be grouped into two broad categories: (i) Intrinsic, and (ii) Autonomous. The former strives to enhance the natural healing mechanism taking place within autogenous cracks. Self-healing is an ancient and well-known phenomenon in concrete that possesses several natural autogenous healing properties.

Due to the ongoing hydration of clinker minerals or carbonation of calcium hydroxide ($Ca(OH)_2$), cracks may heal after a time [22-24]. However, as well as being dependent on the age of the concrete, autogenous healing is limited to small cracks, is only effective when water is available, and is difficult to control.

There are two approaches in which the concrete cracks are self-healed in an autonomous manner: vascular or capsules-based self-healing. The vascular approach is not self-healing per se because the external intervention is required to supply the healing agent and ensure it is effective. Moreover, although feasible at a laboratory scale, it is difficult to cast concrete with a network of pipes on actual construction sites [20, 21].

Capsules-based self-healing involves one of two techniques: (i) Healing by Chemical Agents and (ii) Healing by Bacteria [20, 21] (Eco-Bio solution). By encapsulating chemical agents, a variety of materials such as glass tubes, ceramic tubes [25, 26] and polymers [27-29] have been utilised to develop the self-healing process. However, several problems with the encapsulated chemical agents have been reported in the literature. For instance, nanosized capsule debris has been found to accumulate in the host matrix of the concrete and these can initiate cracking. In addition, although glass capsules with chemical healing agents are located at the predicted locations of cracks, in most civil reinforced concrete structures it is not always possible to predict these locations. It may therefore be better to randomly (but uniformly) distribute the capsules in pairs in all areas susceptible to cracking [21]. A problem has also been reported with synthetic polymer products such as organic polymers, which have a high level of toxicity, and epoxy treatment. Regrettably, these materials are costly, need frequent maintenance, and are harmful to the environment [30]. The (EU) 305/2011 regulation, which relates to the Construction Products Regulation, aims to decrease the use of hazardous materials [31]. Therefore, alternative healing strategies, particularly the use of a biological repair technique in concrete, have attracted increasing attention [30]. Over the last few years, bio-based healing agents have yielded promising results concerning the performance of crack

healing [32] and can address the problems discussed above. The carbonate precipitate induced by bacteria is regarded as an environmental-friendly and economic material that offers promising potential for a wide range of engineering applications aimed at reducing the cost of repair and maintenance work [33].

Self-healing concrete can repair and protect itself by forming calcium carbonate to seal concrete micro-cracks, thereby preventing the ingression of any gasses and liquids into the concrete [32]. This technique is in great demand, especially in underground structures where maintenance in hidden locations is difficult or impossible. Recently, several studies have been conducted to prevent concrete deterioration using a bacterial self-healing concrete technique. However, only a small amount of information on this area was found to assist in the protection of concrete using this system. Research to date has focused on self-healing in air or water environments. However, almost all structures, including bridges and buildings, have foundations that are exposed to soil environments (Figure 1.1); therefore, the efficiency of this technique in ground conditions requires further investigation.

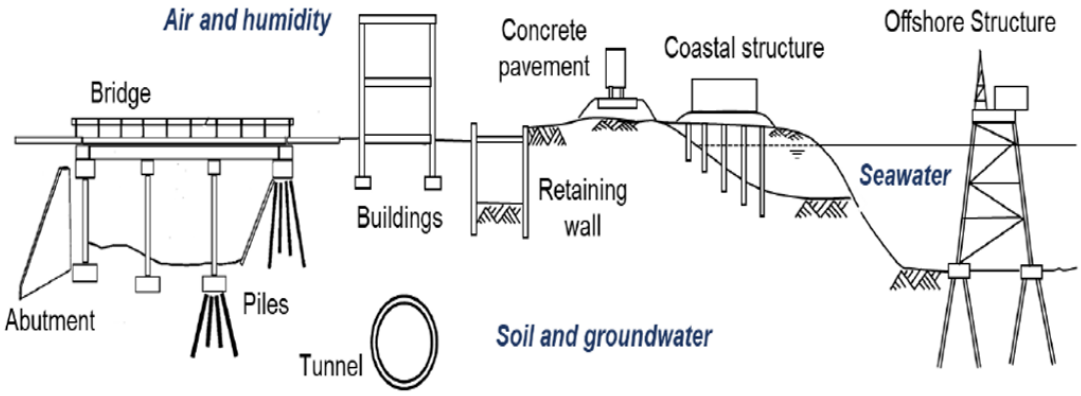

Figure 1.1: Structures and their environmental exposures [34]

1.4 Problem statement

It is well established that cracks appearing at the surface of structural elements are a significant problem for concrete structures and can reduce their durability, thereby damaging the entire structure. If such cracks are not mitigated, serviceability problems will arise, and the cost of maintenance will increase. Several strategies have been proposed by different researchers to overcome concrete cracks. One of these is to utilise specific types of bacteria to seal concrete cracks by forming calcium carbonate. This carbonate precipitate is an environment-friendly and economical material that can potentially be employed across a large number of engineering applications [35]. However, the precipitation of calcium carbonate can be influenced by a range of factors such as crack age, depth and width, incubation period, and incubation conditions.

The aim of the current research, therefore, is to generate novel information to enhance our understanding of bacterial self-healing concrete in ground conditions. This has the potential to eliminate or reduce the environmental and economic cost of maintenance activities, especially for underground structures.

1.5 Research aim and objectives

The research hypothesises that the bacterial self-healing process (which has been previously examined in humid air and water) will be influenced in different ways by different ground conditions.

The specific aim of this research is to investigate the efficiency of a bacterial self-healing concrete solution in different ground conditions. This will help to facilitate the application of this technique in underground concrete structures such as pile foundations, retaining walls, and tunnels.

To achieve this aim, the following objectives have been set.

1- To select an appropriate delivery technique for healing agents by investigating different delivery systems and encapsulation materials.

2- To test the efficiency of the bacterial self-healing technique in different types of soil (course and fine-grained soil).
3- To test the efficiency of self-healing in different types of aggressive environmental exposures classified according to BS EN 206-1 2000, namely X0, XA1, and XA3.
4- To test the efficiency of self-healing in different ground regimes, including partially, fully saturated, and different cycles.
5- To investigate the suitability of the non-destructive method, namely concrete electrical resistivity, for assessing the efficiency of the self-healing system for concrete elements embedded with soils.

These objectives are divided into three chapters, as illustrated in the following chart:

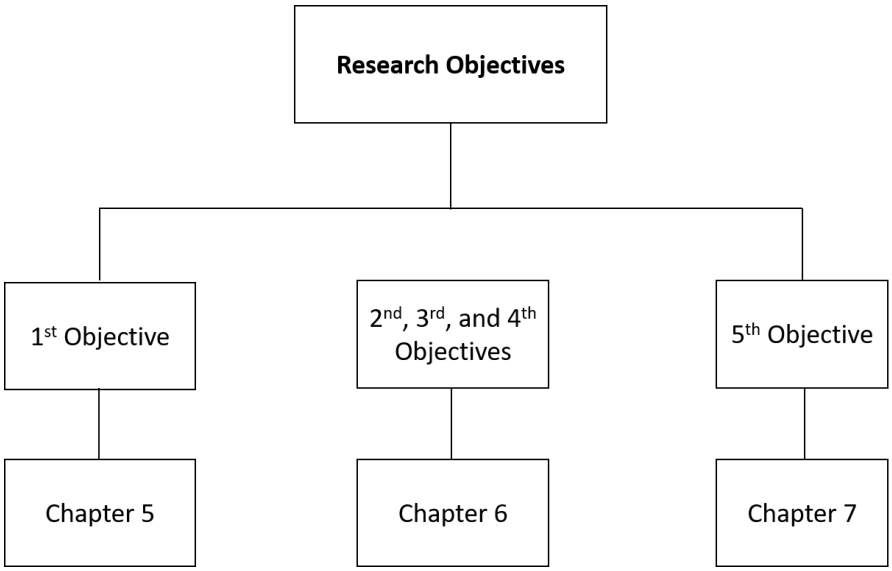

1.6 Thesis outline:

The contents of the thesis are organised in the following chapters:

Chapter 1: Presents a background and introduction to the study, as well as the research motivation, problem definition, research aim, and the objectives that will address the research problem.

Chapter 2: Presents a critical review of the literature to discuss the state of the art on types and causes of cracks in concrete structures and topics relevant to the classification and development of self-healing concrete techniques. Different techniques employed to assess the performance of the self-healing system are also discussed.

Chapter 3: Reviews the literature on the application of bacterial based self-healing concrete and factors affecting the healing performance.

Chapter 4: Presents the properties of used materials, preparation of healing agents, mix procedures, preparations, and production of samples to produce self-healing. The chapter also describes and explains the equipment and experimental work conducted to assess the efficiency of self-healing.

Chapter 5: Presents an approach to study the influence of delivery techniques for the bacterial agent on the efficiency of the self-healing system. This involves using different capsule materials to study their compatibility with cement mortar matrix and their effect on healing performance.

Chapter 6: Presents an extensive and critical evaluation of the experimental results to evaluate the efficiency of bacterial self-healing concrete incubated in different types of soil such as sand and clay, and in different ground regimes, including partially, fully saturated, and different cycles. Self-healing performance is also assessed in different types of aggressive environmental exposures classified according to BS EN 206-1 2000, namely X0, XA1, and XA3.

Chapter 7: Discusses the potential application of non-destructive testing methods such as concrete electrical resistivity and steel corrosion to assess the healing performance of concrete specimens incubated inside the soil.

Chapter 8: Concludes the thesis by discussing the main findings of the research and making recommendations for further work on the performance of the bacterial based self-healing concrete within ground conditions.

Chapter 2

A review of the development of self-healing techniques in construction materials

2.1 Overview

This chapter presents a review of the existing literature on self-healing concrete techniques, as well as the methodologies adopted in this research area. Its purpose is to contextualise the literature within the domain of material science and civil engineering. Although there is some degree of overlap, the following three topics are considered:

- Types and causes of cracks – before and after hardening of concrete as well as the effect of cracks on corrosion of reinforced steel bars.
- Development of self-healing – relevant approaches are discussed, including the concept of self-healing, along with a consideration of the different forms it takes (i.e., autogenous, autogenomic, and autonomic self-healing).
- Methods for assessing self-healing performance – Different approaches (i.e., based on the recovery of mechanical properties and durability) and techniques used to assess healing performance are introduced.

2.2 Introduction

Today's concrete is a more sophisticated blend than concrete at the beginning of the last century. Several chemical and mineral admixtures are added to enhance the concrete properties. Consequently, the ingress of harmful materials through today's concrete pores is a prolonged process. Unfortunately, all concrete structures suffer from cracks, and access harmful materials through cracks is faster than through pores. The presence of cracks in concrete structures has a significant

impact on initiating corrosion of steel bars and deteriorating concrete structures [36]. One of the greatest challenges facing the global construction industry is the deterioration of concrete structures [37].

To produce concrete structures with high durability performance, researchers are investigating the self-healing concrete phenomenon. This phenomenon could occur naturally, where induced calcium carbonate can seal concrete cracks by concrete exposure to water and further hydration of unreacted cement by the expansion of hydrated cementitious materials [38]. Furthermore, self-healing in concrete can be produced by using chemical admixtures such as polymers and geo-materials [39]. In addition, calcium carbonate can be formed by microorganisms to seal concrete's cracks [17, 32, 35, 40].

2.3 Types and causes of cracks in concrete structures

The tensile strength of concrete is generally weak and rarely constitutes more than 10% of compressive strength.; therefore, as a result of the weaknesses within the tension zone, cracks may occur due to inescapable imposed tensile stresses. Cracks are common in concrete and cannot be avoided. A combination of applied stresses and exposure to a severe environment is likely to be the primary cause of cracking in concrete structures [41].

Several factors cause the ready occurrence of cracks on the surface of structural features. These include tensile stresses, excessive heat and water, creep drying shrinkage, freeze-thawing, and incorrect curing of concrete. Furthermore, when hydration is at an early stage, chlorides and carbon dioxide can enter concrete structures via cracks, causing additional harm and speeding up the degradation process. [42, 43]. Cracks in concrete may only influence concrete surface appearance, or they may cause serious structural ordeal or decrease structures' service life. The significance of cracks relies on the nature of cracking type and on the importance of structure. For instance, cracks that are acceptable for residential building may not be acceptable in water-retaining structures or nuclear structures [41].

In most cases, concrete cracks do not cause a failure to structure, but they can decrease the performance of structures and adding extra cost for repairing and maintenance work [44]. Concrete cracks can be classified into two categories according to their physical state; cracks that occur before hardening and those which occur after hardening of concrete.

Cracks that appear before concrete hardening can be classified as follows: construction movement, which can occur as a result of the sub-grade settlement of formwork due to swelling of timber or lack of formwork strength and plastic shrinkage cracks as a result of the rapid hydration of mix water from the surface of the concrete.

Cracks that occur after hardening are divided into six types: chemical, physical thermal, structural design, stress concentration and accidental overload [44]. Figure 2.2 illustrates the most common types of concrete cracks that appear on the concrete surface as well as an indication of their potential time of occurrence.

Cracks may also be classified as structural and non-structural cracks. In such cases, structural cracks may include accidental overload, creep, and subgrade movement cracks, whereas non-structural cracks may include physical, chemical, and thermal cracks [41]. The following chart shown in Figure 2.1 summarizes the typical forms for different types of concrete cracks.

Content removed due to copyright reasons

Figure 2. 1: Chart showing the main categories of concrete cracks [44]

Content removed due to copyright reasons

Figure 2. 2: Examples of different types of cracks in a hypothetical concrete structure [45]

When concrete starts to harden, cracks could be induced due to drying shrinkage or environmentally as a result of different reasons such as the use of unsound cement, sulfate attack, alkali-aggregate reaction, freezing-thawing, corrosion of steel bars, and thermal cycling. Table 2.1 presents the classification of intrinsic cracks that may occur in a typical situation for a hypothetical concrete structure.

Table 2.1: Classification of intrinsic cracks according to Figure 2.2 [44]

Content removed due to copyright reasons

2.4 Effect of cracks on corrosion of steel bars

In recent years, several studies [46, 47] have been undertaken to examine the impact of cracks on steel corrosion. Previous research has established that cracks allow chlorides ready access to concrete, which means that the corrosion of steel in cracked concrete takes place earlier than normal. The rate of corrosion, however, is impacted by several factors, including water-to-binder ratio, binder type, quality of concrete, and cover depth [48, 49]. Using ordinary Portland cement and silica fume concrete with water to binder ratio of 0.3, Pettersson and Jorgensen [49] examined the effect of crack width on corrosion. Their results indicated that corrosion rates were higher for crack widths of 0.4 mm or above. This was attributable to the area of steel exposed and/or availability of oxygen. Similar results were obtained by Arya and Ofori-Darko [50] who reported that the rate of corrosion increased in line with the frequency of cracks, although this may not be the case for all forms of binders. Using different binder types, a cover of 20 and 40 mm, and crack widths of 0.2 and 0.7 mm, Scott and Alexander [48] found that a change in cover only affected ordinary Portland cement concretes where oxygen availability tends to govern the rate of corrosion, rather than blended cements where the dominant factor is high concrete resistivity. Their results suggested that a reduction in cover significantly increases the rate of corrosion at a certain crack width for ordinary Portland cement concrete but not for concrete composed of blended cements. Conversely, other researchers assert that no direct relationship exists between the rate of corrosion and crack width [51]. They argue that the initiation of corrosion is accelerated by cracks, whereas its propagation is not. Among the essential factors are exposure conditions (i.e. service environment) and crack properties (e.g. active or dormant). Beeby [52] performed a decade of tests on specimens exposed to an outdoor environment with surface crack widths ranges between 0.13 to 1.27 mm. They reported that an increase in crack width did not result in any significant increases in corrosion rate.

These seemingly contradictory results are attributable to the way in which the type, depth, frequency, width, length, and orientation of concrete structures with respect to reinforcement affect their durability [47].

Furthermore, whether cracks fully or partially heal is vital in determining the extent to which chlorides penetrate the concrete and thus the corrosion rate of the steel within [46].

2.5 The significance of controlling cracks

In practice, it is very difficult to stop the creation of cracks, if not impossible. Inadequate selection of materials, reinforcement steel or exposure conditions can harmfully lead to serious cracks. Not only cracks can lead to serviceability problems such as water leakage but also can lead to durability problems such as decrease in strength and steel corrosion [53].

The high alkaline environment can prevent steel reinforcing in concrete from corrosion by creating a passive film on the steel surface. However, the passive film will not last long, and the steel immediately corrodes under the chloride and carbon dioxide attack, which have been seeped to reinforced steel through cracks. The volume of the rust products is around four to six times greater than the original steel volume. This increase causes internal tensile stresses in concrete cover and when these stresses skip the concrete tensile strength, the concrete cover deteriorated by delamination and cracking [7]. According to some research work, it has been proven that there is a slight relationship between the corrosion rate of steel and width of crack, though at the early stage of the exposure period only. However, the existence of a crack itself is significant with regard to corrosion of reinforced steel in concrete when the service life of a structure is considered. Therefore, to meet the service life, aesthetics requirements, and to avoid any dangerous situations caused by deterioration, an appropriate maintenance system should be applied to control the development of cracks [54].

2.6 Development of self-healing concrete techniques

In recent years, the development of intelligent materials in different research fields has been extensively focused. The design approach of these materials is based on installing smart tools such as sensors (Science and Technology Agency 1989) [4]. Shahinpoor [55] defined intelligent materials as " materials capable of automatically and inherently sensing or detecting changes in their environmental conditions and responding to those changes with some kind of actuating or reaction". From this definition, once the sensors detect any changes, a required assessment should be undertaken to evaluate the performance of the structure [4]. To recruit such a tool, advanced apparatus such as shape memory, optical fibre sensors and piezoelectric devices are commonly used to develop intelligent materials.

For conventional concrete and under certain conditions self-healing of concrete can be obtained by the natural phenomenon where concrete demonstrate an inherent self-healing capacity, which comes from the un-hydrated particles of cement in concrete mixtures. The continuity in hydration has a positive aspect on self-healing as no strange materials were mixed with concrete which could cause further problems for concrete. Based on this concept, the use of capsules containing a self-healing agent based on cement is preferable [16].

The self-healing of concrete can be achieved artificially (physical [56, 57], chemical [58, 59] and biological processes [60, 61] by using different techniques such as adding additive materials to the concrete mix or fibre reinforced cementitious composites (FRCC). Polymers and microorganisms or adding some admixtures have been proposed in the application of mineral-producing bacteria and geo-materials [4]. Figure 2.3 summarize the approaches to the development of self-healing [38].

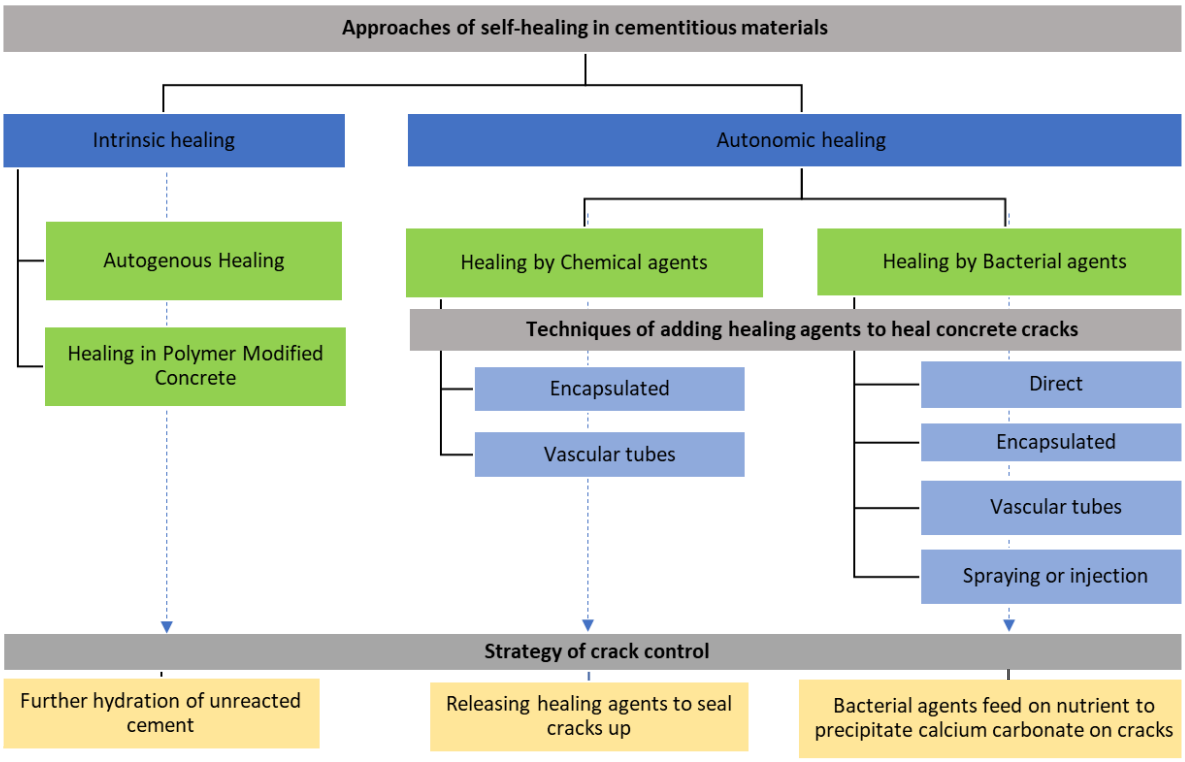

Figure 2.3: General overview of the approaches of self-healing in cementitious materials

2.7 Concept of self-healing approach

The phenomenon of self-healing or autogenous of concrete has been studied by many researchers [4, 35, 62]. The researchers have defined the term of self-healing with differences. According to Ghosh [63], self-healing can be defined as "the ability of a material to heal (recover/repair) damages automatically and autonomously, that is, without any external intervention", whereas Davies and Jefferson [64] described the self-healing as " Any process by the material itself involving the recovery and hence an improvement of performance after an earlier action that had reduced the performance of the material". De Rooij et al. [65] has classified the self-healing materials as autogenic or autonomic as presented in the following definitions.

“Autogenic: The self-healing process is autogenic when the recovery process uses materials components that could otherwise also be present when not specifically designed for self-healing (own generic materials).”

“Autonomic: The self-healing process is autonomic when the recovery process uses materials components that would otherwise not be found in the material (engineered additions).” [64]

The Japan Concrete Institute (JCI) committee proposed several definitions for self-healing concrete as follow:

- Natural healing
- Autonomic healing
- Activated healing
- Autogenous healing covers natural and autonomic healing
- Engineered healing covers activated healing and autonomic healing
- Self-healing covers all healing categories

Figure 2.4 illustrates the terminology which has been used for classifying self-healing materials.

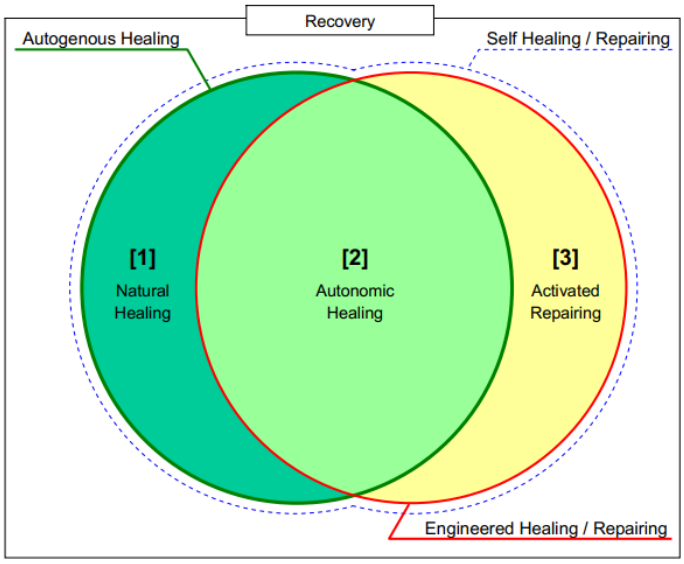

Figure 2.4: Diagram illustrating the terminology of self-healing according to JCI TC-075B [4]

2.7.1 Autogenous self-healing

The interest in using the ability of concrete micro-cracks to heal in the presence of moisture was first detected by the French Academy of Science in the 19th century [66]. Since then, there have been several cases where healing of cracks in concrete structures either has been unexpectedly detected or deliberately applied to regain strength or water-tightness.

During the last century, the recovery of the mechanical properties of cracked concrete, such as tensile, compressive, shear and flexural strength, have been focused. Similar interests have been detected related to recovery in frost resistance, elastic modulus, stiffness and deformation of cracked concrete. However, the term "autogenous healing" has been used to generally describe the recovery of mechanical properties or water-tightness, assuming that it is solely caused by continued hydration or calcium carbonate formation in the cracked area. The RILEM report [65], defines a mechanism as autogenous if it is entirely reliant on elements of the material that exist because they are created to self-heal. The autogenous phenomenon can be defined as the ability of cementitious material to heal itself and prevent water ingress by filling up the cracks [67]. Over the past years, the autogenous phenomenon has been investigated by many authors. Wang et al. [35] have considered the effect of hydrogel on promoting of autogenous healing; Edvardsen [62] studied the influence of autogenous healing of cracks on water permeability; Zhang, et al. [68] investigated the relationship between the cement composition and cracks' healing performance, and the result revealed that mixes with higher binder particles tend to have better crack healing performance. This state is caused as a result of the delay of hydration in un-hydrated cement particles when contacted with water that ingresses through cracks [69].

The recent researches concluded that the compressive strength of concrete could be recovered only up to 4–5% as a result of autogenous [63]. However, Edvardsen [62] noticed that the possibility of autogenous healing has a great chance to present in early age concrete. More recent studies on autogenous healing have

focused on the evaluation of not only the reduction in permeability of cracked concrete but also the recovery of concrete mechanical properties [70, 71].

Water is essential in ensuring successful autogenous self-healing, with crack widths less than 100 µm and ideally smaller than 50 µm [72, 73]. A recent study on autogenous healing has been conducted by Japanese researchers: Kishi et al. ; Hosoda et al. [74], and; Yamada et al. The results of the microscopic observations and water permeability tests revealed that cracks of up to 0.3 - 0.4 mm could be healed by implication of expansive agents in the concrete. In addition to that, the results have also shown that adding a small portion of soda bicarbonate can enhance the ability of self-healing by precipitation of calcium carbonate on cracks [75]. Self-healing of a crack having a width of up to 200 µm within six weeks was achieved for concrete mixed with alternative binders (blast furnace slag and fly ash). Similarly, Sisomphon and Koenders, [76] found that when pre-cracked cement-based materials were treated with calcium sulfo-aluminate (CSA), complete sealing was only evident in cracks up to 150µm. However, these results cannot be purely considered as autogenous healing as expensive agents were added to the concrete matrix.

Characteristics associated with the environment can significantly influence the self-healing process [77, 78]. From cyclic wet-dry exposures to underwater immersion, various environmental conditions can support autogenous healing. For instance, Yang et al. [79] verified total crack sealing under 0.05 mm, after 4 to 5 cycles of immersion in water for 24 hours and drying for 24 hours. The analysis proposed by Wang et al. [35], in wet and dry cycles at 12 hours in each situation, cracks under 0.15 mm were completely sealed after seven cycles. For submersed curing specimens, this same phenomenon in the same period did not occur. Some studies report the phenomenon of self-healing at young ages, with satisfactory results after three consecutive cycles [79] or four to five cycles [80]. It is important to note that these are specific conditions of cracks under 0.15 mm, cement composites mortar, and the use of the cycles without renewal water the environmental exposure [81]. For most types of infrastructure, especially transportation, these are practical conditions, and therefore it is easy to fulfil this

criterion for effective self-healing. Furthermore, the existence of a large volume of un-hydrated or partially hydrated cement grains in concrete mixes with high cement content means it is also easier to fulfil the second criterion, which is to ensure sufficient concentrations of vital chemical species. Other elements that support self-healing are NaCl in seawater and de-icing salt and CO_2 in air.

To date, there have been no definitive results regarding the impact of crack widths on autogenous self-healing. Yang et al [79] contend that the most difficult challenge in designing and applying self-healing concrete materials is to maintain a crack width of less than 150µm and ideally below 50 µm [62, 73, 82]. Although feedback control load-frames have been successfully employed in the laboratory to maintain a crack width in concrete structures of less than 150µm, it has not yet been possible to consistently achieve this in the field. Consequently, in actual reinforced concrete structures, reliable autogenous healing is generally lacking. Table 2.2 summarising some of the maximum healed crack width in different results reported in the literature.

Table 2.2: The maximum healed crack widths in autogenous healing

Maximum healed crack width (mm)	Reference No.
0.15	[71]
0.3	[83]
0.2	[62]
0.1	[73]

Autogenous healing can be caused by three different mechanisms namely physical, chemical and mechanical as shown in Figure 2.5.

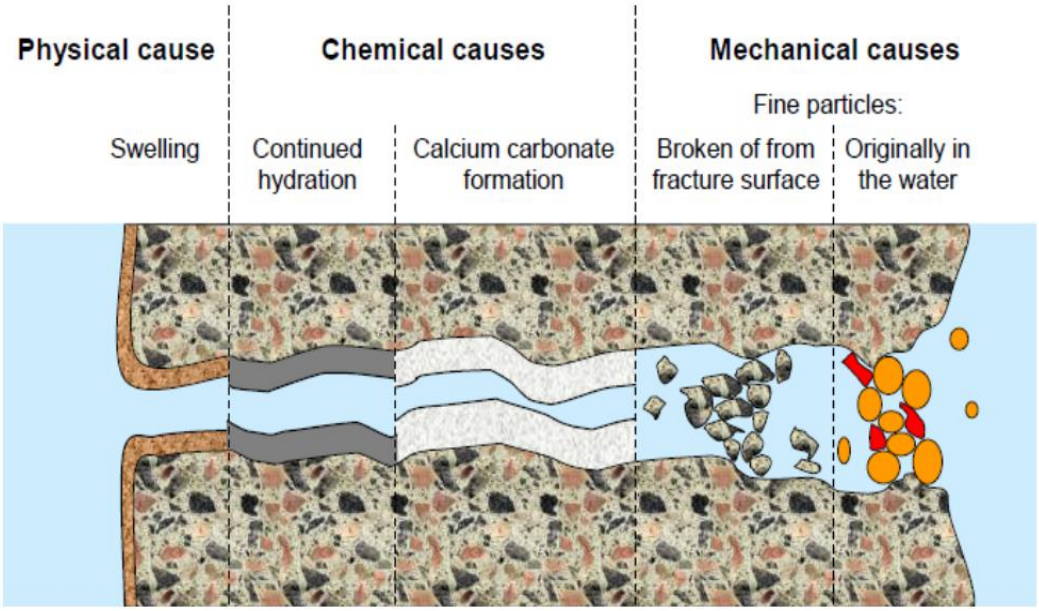

Figure 2.5: Different mechanisms of autogenic self-healing [64]

According to Hearn [67], the physical mechanism occurs when water seeps through cracks to contact the un-hydrated cement particles and then these particles starts to hydrate and swell to close cracks. This swelling can be promoted by adding some dilatable agents such as swelling clay minerals, where these agents can swell and tighten up the cracks [13]. The effect of continuing hydration on the reduction of permeability was investigated by Hearn [84]. As it is shown in Figure 2.6, the continuing hydration can drop the permeability of hydrated concrete up to four times in comparison to the initial permeability of young concrete.

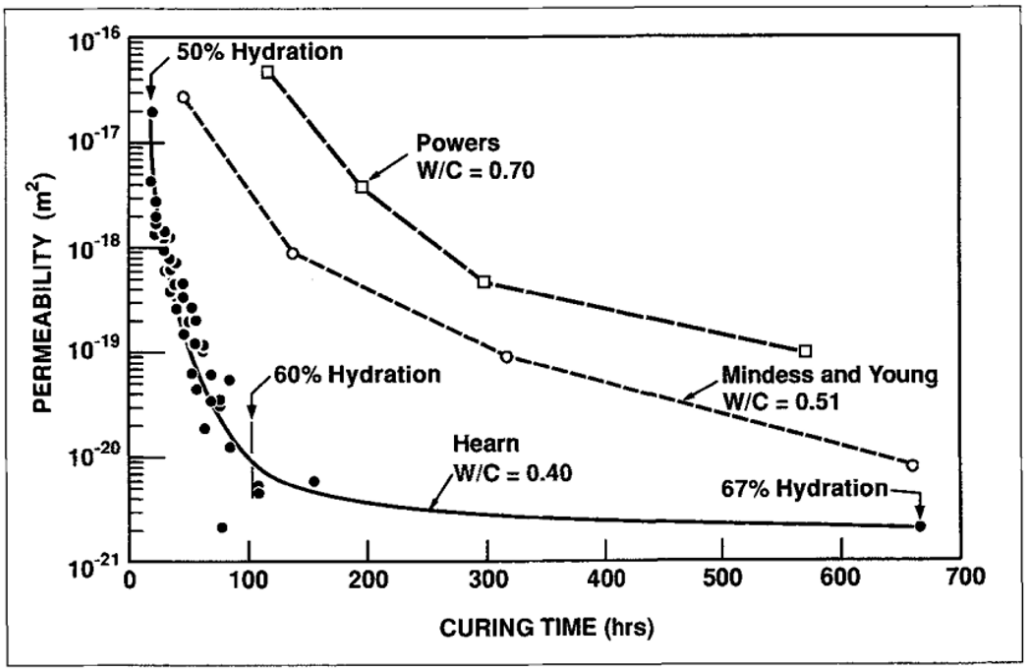

Figure 2.6: The effect of continuing hydration on concrete permeability [84]

The mechanical mechanism can be caused as a result of the un-bonded fine particles within the hardened cement composition. During the process of crack forming, these particles can move with water through cracks. After a while, these particles will be precipitated in the crack and partially block it up. The second mechanical approach is when small concrete fractures, which have been produced during the generation of cracks, remain on the top of the crack surface and partially blocking the flow paths through the crack.

The chemical mechanism is mainly caused as a result of the reaction between water that ingresses through cracks and un-reacted cement particles to form new components into the crack space which eventually bridge it. Also, some chemical reaction such as the reactions between carbonate ions and calcium ions from the pore water of concrete encourages the growth of crystals to form calcium carbonate ($CaCO_3$) on the crack surface [67].

From a practical view, autogenous healing concrete is more attractive and economical compared to other engineering materials such as chemical encapsulation or other techniques that have been proposed. Concrete has a

unique feature, where un-hydrated cement particles can be gathered in micro-reservoirs and stay a long time after concrete hardening to be available for self-healing. However, the presence and the amount of un-hydrated cement particles depends on many factors such as the w/c ratio. For example, the amount of un-hydrated cement in concrete with a low w/c ratio is expected to be higher by 25%. According to what has been mention above, the autogenous phenomenon can effectively benefit the transport properties and recover the mechanical properties of concrete. Unfortunately, due to the lack of information about the mechanism of autogenous healing, so the phenomenon is still unreliable. The main concern in any healing process is dependence on tight crack width [85]. The autogenous healing depends on significant factors such as the existence of humidity or water in the surrounding environment, the amount of un-hydrated cement particles, and the composition of concrete mix. In order to improve autogenous healing, the water to cement (w/c) ratio should be reduced, but on the other hand, increasing cement portion to reduce w/c ratio has a negative impact on workability and shrinkage and requires more cement production [86].

This is because it is only possible to heal small cracks. Steel reinforcement, therefore, has a vital role to play in controlling crack width. The reliability of this approach has, however, recently been questioned. In the latest version of the ACI code, the allowable crack width is no longer specified. This means that, before adapting autogenous healing, those tasked with engineering materials have several key challenges to overcome [85].

Compared with autonomous methods, autogenous self-healing techniques based on traditional concrete technology are generally cheaper, safer, and easier than autonomous methods. However, based on the various results from the literature, we can conclude that the mechanism behind the autogenous self-healing concrete is not fully understood.

2.7.2 Autogenomic or improved autogenous healing

Different researchers have proposed various mechanisms by using artificial solutions that can seal cracks in concrete with widths greater than 0.1mm, which

cannot be sealed by autogenous healing [69]. So to restrict the crack width, different studies have proposed different techniques such as fibre reinforced strain hardening engineered cementitious composite (ECC) [87] and poly vinyl alcohol (PVA) fibres [22]. As concrete cracks form in a unique pattern with mutable cracks and different widths, it is more complicated to achieve narrow cracks by using fibres.

The presence of water in autogenous is another factor that can improve the healing process [20]. In order to provide more water into the concrete matrix, many researchers have studied the possibility of adding super absorbent polymers (SAP, hydrogels) to concrete mix [88]. SAP has the ability to absorb a large amount of water and swell virtually to create an insoluble and soft gel to block the cracks. The alkalinity and ionic concentration play an essential role that can influence the swelling capacity of SAP. Once cement starts to hydrate, SAP release the absorbed water and shrink, leaving behind small macro-pores. However, SAP has some drawbacks, where they reduce concrete compressive strength as a result of forming of pores during concrete mixing. In order to promote the autonomic healing, other techniques have been studied by many researchers such as using nano-clay as an internal water reservoir in ECC [89], and by encapsulated pure water with paraffin [90] or by adding expansive additives such as calcium sulfo-aluminate based agents and crystalline admixtures to form crystals when water ingress into cracks and therefor sealing the cracks [91].

2.7.3 Autonomic or Engineered self-healing

Experimental results of autogenous self-healing have been previously discussed and the results showed that the ability of crack healing mechanism in the autogenous phenomenon is limited to small crack [73]. However, in some cases manual intervention is required to guarantee a successful crack-healing process [92]. Many engineers have attempted to investigate different approaches to autonomic solutions in order to improve crack healing efficiency. The autonomic self-healing can be defined "as a self-healing process where the recovery process uses materials components that would otherwise not be found in the material"

[64]. Recently, the autonomic self-healing of cementitious composites has received significantly high attention as a result in developing of engineering materials. According to Schlangen, and Sangadji [17] the autonomic materials can be classified into two different modes called active and passive modes. In the active mode, in order to complete the healing process, smart material needs human intervention such as multi-channel vascular system. Whereas in the passive mode, smart material has the ability to react and heal cracks without any external intervention such as capsule-based delivery system and one channel vascular system. Both systems have been investigated, with regard to concrete by Dry [19], and they are shown in Figures 2.7 and 2.8.

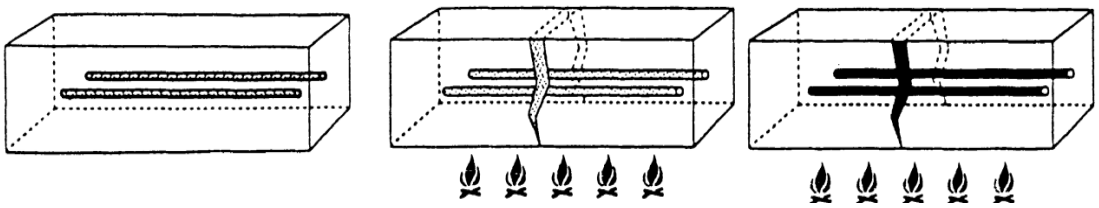

(a) (b) (c)

Figure 2.7. Illustration of timed active release mode using methylmethacrylate as a healing agent impregnated within porous fibres coated with melted wax. (a) Fibres impregnated with methylmethacrylate and coated with wax. (b) Wax coating melted with initial heating. Methylmethacrylate released from fibres into cracks. (c) Polymerized Methylmethacrylate during the second heating, closing previous cracks [19]

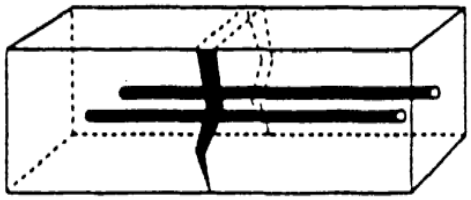

Figure 2.8. Illustration of passive release mode via the physical cracking of the brittle fibre under loading [19]

Although there has been notable progress in autonomic self-healing over the last years, the ability to repair or heal concrete cracks is still a significant challenge to engineers. There are three different healing approaches, which can be summarised as follows:

2.7.3.1 Capsule-based delivery of healing agents

Different healing agents included chemicals and bacterial agents have been investigated in various studies related to the self-healing of concrete. The properties of the healing agents are playing a significant role in the final result of crack healing. According to Joseph [93], the efficiency of chemical healing agents is impacted by two factors: the viscosity of the healing agent, where the repaired area increases as the viscosity of the agent decreases, and the capillary force, which decreases as crack width increases. In addition to that, in order to prevent the crack from reopening, the filling created by the healing agent must have adequate strength. For practical and economic considerations, the healing agent should be cheap and available to use like concrete.

The healing agents are added to concrete either directly such as bacterial agents or impregnated in capsules. The idea for encapsulating materials was drawn from natural phenomena such as birds' eggs or seeds and its principal aim is to protect healing agents [94]. The healing agents could be bacterial [6, 32, 68, 95, 96] or chemical agents [27, 56, 97, 98] such as epoxy resins, cyanoacrylates, alkali-silica solutions. To achieve this in the harsh conditions associated with fresh concrete,

such as high temperature and pH, and ensure optimally efficient self-healing, bacteria have been encapsulated in several studies as part of a bacteria-based system [35, 68, 96, 99]. Such materials need to be sufficiently sensitive to the pressure created by cracks in order to release the healing agents that seal them. They must also inhibit the undesirable release of the agent during the mix [94]. Another advantage derived from using capsules to safeguard the healing agent is that it enhances the efficacy and utility of the bacterial agent for a substantial amount of time [86]. Tittelboom et al. [26] contend that the use of capsules is an extremely efficient way to ensure total healing of the crack using chemical agents and therefore to prevent seepage of harmful materials such as chloride and sulphate, and on occasion, to partially recover mechanical properties of the concrete. The latter is important in enhancing long-lasting structural performance.

To transport chemicals and bacterial self-healing agents, chemical materials such as gelatine, glass, ceramics [26] and urea-formaldehyde [28] have been included in different types of capsules. Numerous researchers have introduced these agents as autonomic self-healing materials, the most frequent tools of which are encapsulation by chemical agents and bacterial spore encapsulation.

The encapsulation of polymeric material entails sealing concrete cracks by converting the healing agent to foam in the presence of moisture. Numerous researchers have employed capsules to safeguard the bacterial healing agent from the strongly alkaline environment of concrete. For example, Jonkers [6] utilised porous expanded clay particles to immobilise B. sphaericus bacteria. Adding the lightweight aggregate to replace 50% of the total aggregate, samples were pre-cracked and then cured in water for two months. The results indicated that all bacterial specimens were healed, compared with just two out of six control specimens. Moreover, the bacterial spores were viable for more than six months, rather than two months only. Among the first researchers to study the self-healing of concrete were Wang et al. [100], who proposed using diatomaceous earth as a caring agent. Their results suggested that bacteria immobilised in diatomaceous earth exhibited high ureolytic activity (12–17 g/l urea decomposed within 3 days)

in the cement slurry, whereas un-immobilised bacteria exhibited low ureolytic activity (less than 1 g/l urea decomposed within 3 days). Furthermore, cracks of widths 0.15 to 0.17 mm were entirely filled by calcium carbonate, and the optimal diatomaceous earth concentration for immobilisation was 60% (w/v, weight of diatomaceous earth/volume of bacterial suspension).

A bacteria-based healing agent was incorporated into silica gel by Tittelboom et al. [101]. They cured their specimens in an air-conditioned room with a humidity greater than 90% and a temperature of 20 °C for 28 days. Using thin copper plates in fresh concrete during the casting, they created standard cracks with depths between 10 mm to 20 mm and a width of 0.3 mm. Authentic cracks with widths ranging from 0.05 mm to 0.87 mm were initiated in concrete cylinder specimens 75 mm in height and 80 mm in diameter using a splitting test. The specimens were then subjected to a water permeability test. The results indicated that healing occurred in cracks treated with silica gel immobilised bacteria. In contrast to specimens treated with epoxy, these samples also exhibited low water permeability.

Experiments performed by Wang et al. [102] reported higher activity in silica gel immobilised bacteria than polyurethane immobilised bacteria. A thermogravimetric analysis also identified greater precipitation of calcium carbonate in silica gel (25% by mass) than in polyurethane (11% by mass). Notably, the cracked mortar samples healed by polyurethane immobilised bacteria exhibited greater strength regain (60%) than the samples healed by silica gel.

Wang et al. [103] also examined the use of melamine-based microcapsules and found that 48% to 80% of crack areas in specimens with healing agents exhibited healing, compared with 18% to 50% in specimens without bacteria. However, the largest crack width in specimens healed with bacteria was 970 µm, four times as large as that for control specimens.

In another study, Wang et al. [35] investigated the addition of a hydrogel capsule constituting 2% of the weight of the cement. The hydrogel can absorb and retain water, which assists in activating bacteria and ensuring the spores are viable. Four

cylinders 78 mm in diameter and 22 mm in height were constructed along with a 30 x 30 x 360 mm prism reinforced with a 6 mm diameter bar. For a period of four weeks, the specimens were cured in an air-conditioned room with a relative humidity greater than 95% and a temperature of 20 °C. Cracks were then created by applying a specific tensile force to the specimens. The results indicated an average fall in water permeability of 68% and a maximum healed crack width of 0.5 mm. By contrast, the average fall in water permeability for specimens without a bacterial agent ranged from 15% to 55% while the maximum healed crack width was 0.3 mm. Zhang et al. [68] examined and compared the effects of expanded perlite and expanded clay capsules. Following 28 days of healing, for specimens incorporated with expanded perlite, complete sealing was observed for crack widths of up to 0.79 mm. This compares to a crack width of 0.45 mm in specimens incorporated with expanded clay. However, the mechanical properties of concrete can be harmed by the use of these capsules. For example, a 50% reduction in compressive strength was identified following 28 days of curing in comparison with samples with identical aggregate percentages and no substitution of expanded clay particles with sand and gravel fractions [6].

To prevent rupture of the microcapsule during concrete mixing, Mostavi et al. [104] added dual shell layers comprising polyurethane and poly (ureaformaldehyde) with sodium silicate as the healing material.

The additional amount of shell material required means that a significant relationship exists between the size of the micro-capsule and the thickness of the shell. Dong et al. [105] created micro-capsules with an average size of 415.3 µm and three different shell thicknesses, and then assessed the resistance of each shell in a simulated concrete solution. The results indicated that with lower shell thickness, a reduction was noted in the high pH level along with an increase in the release of the healing material. The authors concluded that ensuring a precise agitation rate, pH level, and temperature during fabrication will achieve the preferred shell thickness.

Another factor that can affect the effectiveness of capsules is the shape. Spherical capsules can be more controlled, and the healing agents can be released easily and also the stress will be equally distributed around the capsule. Whereas the tubular capsules cover a large area for the same volume of healing agents. Therefore the release of healing agents will be nonhomogeneous and mutable cracks might not be covered by the healing agents [93]. Table 2.3 shows different types of capsules materials used as protection for the bacterial agent and their effect on healing performance.

Table 2.3: Overview of different types of capsules that have been used to deliver self-healing agents

Delivery technique	Ref. No	Best results
Expanded clay aggregate	[6, 32, 68, 95, 97]	Cracks up to 0.46 mm were healed
Silica gel	[101, 102]	Cracks of 0.3mm were filled completely
Expanded perlite	[68, 96]	Cracks up to 0.79 mm were healed
polyurethane	[102]	Strength regains up to 60% and lower water permeability
Urea and formaldehyde	[1, 28]	Cracks up to 0.46 mm were healed
Hydrogel	[35]	Decrease water permeability by 68%
calcium alginate beads	[99, 106]	Decrease water permeability of cracks 0.4 mm by 95%
modified alginate hydrogel	[107]	Able to keep more than 90% of the encapsulated spores from releasing during mixing
Direct	[61, 68, 108-118]	Improve compressive strength up to 30%

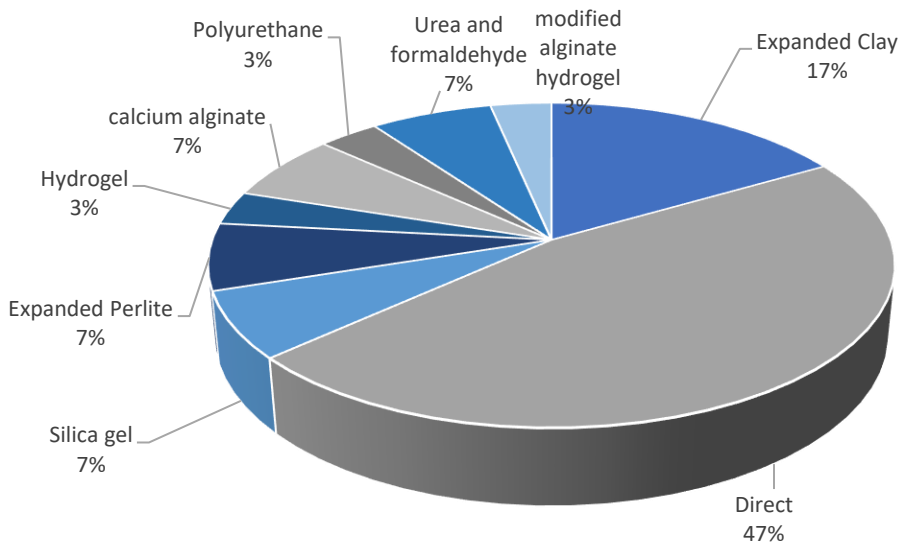

Figure 2.9: Pie chart illustrating the percentages of using capsules and direct delivery for references listed in Table 2.3

Even though in most studies releasing chemical agents from capsules can block the cracks, but in some cases, they do not behave the same as other concrete matrices and they can worsen the situation of the current cracks. Furthermore, capsules are needed for this technique to carry and protect the healing agents for a long period.

Thus, from the above literature it can be inferred that all the encapsulation materials have shown promising results related to the sealing of cracks. Still, on the other hand they have negative impacts on the mechanical properties of fresh and hardened concrete, so in order to obtain an efficient bacterial self-healing mechanism to seal concrete cracks, investigation of those protective factors which can preserve bacteria for longer periods and enhance concrete mechanical properties are in demand.

2.7.3.2 Vascular autonomic self-healing approach

The main idea of the vascular technique has been inspired by the human's bone. The human bone consists of two parts. The outer part is cortical and compacted and the inner part is tending to be such a spongy layer. The vascular system can be a multi-channel system [119], where the healing agents can be supplied from outside of structural element through an emended tubular network, which has been prepared before concrete casting, or it can be one channel vascular system [120], where the system is consisted from one tube to carry the healing agent in order to be released when cracks occur (See Figure 2.9). As cracks start to occur, the healing agents will be released through the broken vessels to move towards the crack to seal it up.

The vascular self-healing technique was first investigated by Dry in 1994 [19]. The author has examined single and multiple hallow vascular fibres on different types of structural elements such as beams and bridge decks. The results revealed that the released methylmethacrylate from inside wax-coated, hollow, porous-walled polypropylene fibres into concrete had filled the voids, and improved concrete permeability [121].

In many research works, different healing agents have been investigated by other authors [102, 122, 123]. Huang and Shui [124] has investigated the use of saturated calcium hydroxide as a healing agent.

Sangadji and Schlangen [125] used a different tool based on vascular networks system, where they simulated vascular networks with cylindrical concrete consisted of core and outer porous parts to represent the "spongious bone". After forming cracks, the healing agent has been distributed manually through the porous core concrete matrix and then activated in order to seal the cracks. The outcome results revealed that the micro-cracks had been completely sealed and concrete strength was notably recovered.

The viscosity of the healing agent is an extremely crucial parameter that can have an impact on the healing system. To enable it to flow out of the capsules and fill the crack, the viscosity should not be overly high. However, if it becomes too low,

the agent may leak from the crack or vanish as a result of absorption by the matrix that surrounds it [20]. In Table 2.4, an overview is given of healing agents used for application inside self-healing concrete.

Table 2.4: Types of vascular materials and healing agents which have been reported in the literature

Vascular materials	Healing agent	Reference
glass pipettes	Silicon	306
Glass fiber	Alkali silica	307
glass tubes	Cyanoacrylate adhesive	330
glass tubes	Alkali-silica solution	331
holes inside the concrete	Epoxy	332
capillary glass tubes	Spore suspension	22

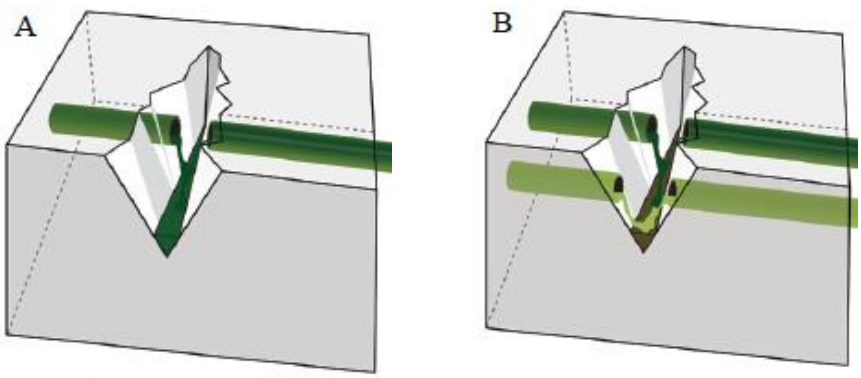

Figure 2.10: Embedded tubular network carrying healing agents in vascular self-healing technique. (A) Vascular single-channel system, (B) Vascular milt-channel system [20]

Vascular systems possess a key advantage in that cracks can be supplied with large volumes of the healing agent, and potentially different healing agents can be used to top up external reservoirs. This means that the system will continue to be

effective following numerous damage events, which could facilitate a substantial increase in the extent of healing [126].

However, using the vascular technique in the field appears to be impractical due to several restrictions summarized as follow:

- Pathways for undesirable and harmful substances to enter the material may be created as a result of vascular channels
- In order to guarantee flowing the healing agents through the embedded tubular network, the healing agents should have constant viscosity during the structure's service life, which is quite impossible for some materials.
- Aesthetic problems might be caused for structures, due to the inadequate release for the healing agents.
- The difficulty to distribute the tubular network homogeneously due to several obstacles such as steel bears, electrical and ventilation links.
- Because the embedded tubular network forms part of the cross-sectional area of the concrete, the bond between materials may be weakened and there may be an associated decrease in concrete strength.

2.7.3.3 Porous network

Sangadji and Schlangen [127] devised the notion of a porous network healing concrete system based on the fracture healing taking place in an animal's bones. They investigated the utility of a hollow network comprising porous concrete. Porous concrete cylinders were cast and surrounded by a PVA film contained within concrete beams. The PVA film then dissolves as the dense concrete matrix is cast around the porous section, facilitating exchange between the inner and outer layers. Schematic diagrams of the conceptual working principle underpinning transport of the healing agent in the porous concrete are presented in Figure 2.11. A concrete vascular structure was installed by the system without the need for an additional method of delivery. The porous network system comprises two parts: the main concrete body and the prefabricated porous core.

When cracks emerge in the concrete system, they move towards these porous structures, transporting the healing agent that heals the cracks. Within this structure, both bacteria-based and polymer healing agents can be used. When the bacteria-based healing agent was applied, a liquid tightness was achieved in the cracked porous network self-healing system, despite limited mechanical regain. Conversely, when the epoxy was utilised as a healing agent, the crack faces were glued and the crack zone sealed, which helped recover the stiffness and strength of crack specimens. Further research is required to assess the up-scaling ability and reusability of this system [128].

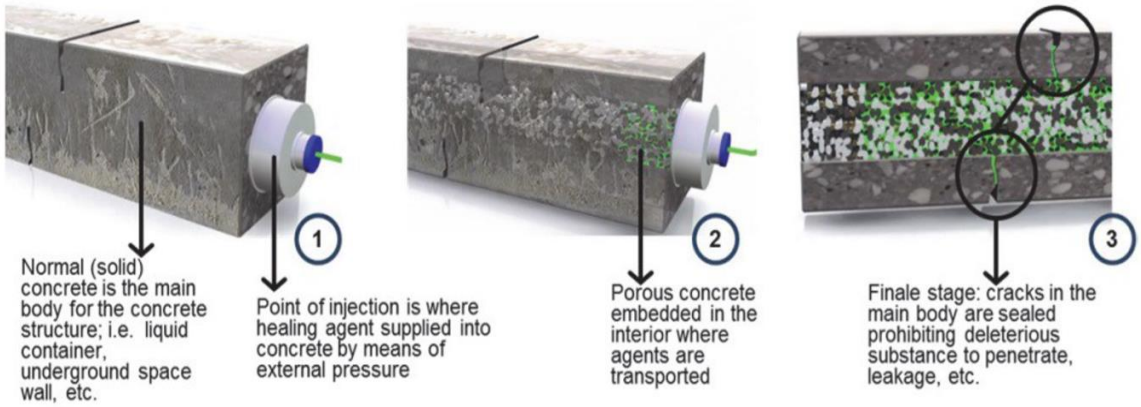

Figure 2.11: The conceptual working system of healing agent transported in the porous concrete [128]

2.8 Methods for assessing self-healing performance

A vital requirement in research on self-healing technology is to perform a robust evaluation of healing efficiency. High levels of healing efficiency indicate full or almost full recovery of mechanical strength and durability. In terms of design and with potential applications in mind, the effectiveness of self-healing technology needs to be characterised and evaluated with respect to at least one material property. A distinction has been made in the scientific community [4, 65, 129] between self-healing and self-sealing. The former alludes to the material properties being recovered as a result of crack sealing. Such recovery is considered strong for mechanical and durability properties if there has been effective blocking of cracks and pores.

In the last ten years, flourishing research and development activity has led to the concept and the validation of significant numbers of techniques [20, 21, 130, 131] to promote and enhance the self-healing capacity of cementitious materials. Figure 2.12 illustrates the methodology and techniques commonly used to develop and assess self-healing performance. These methods are developed for the laboratory-scale specimen; however, only few studies have been conducted on full-scale models.

As shown in Figure 2.12, the methodology is based on four phases; following the preparation of specimens, a controlled preliminary level of pre-cracking (damage) is initiated in a diffused (multiple) cracking patterns or in a localised crack. After a period of incubation in appropriate conditions, quantitative and qualitative techniques are employed to assess the efficiency of the self-healing process.

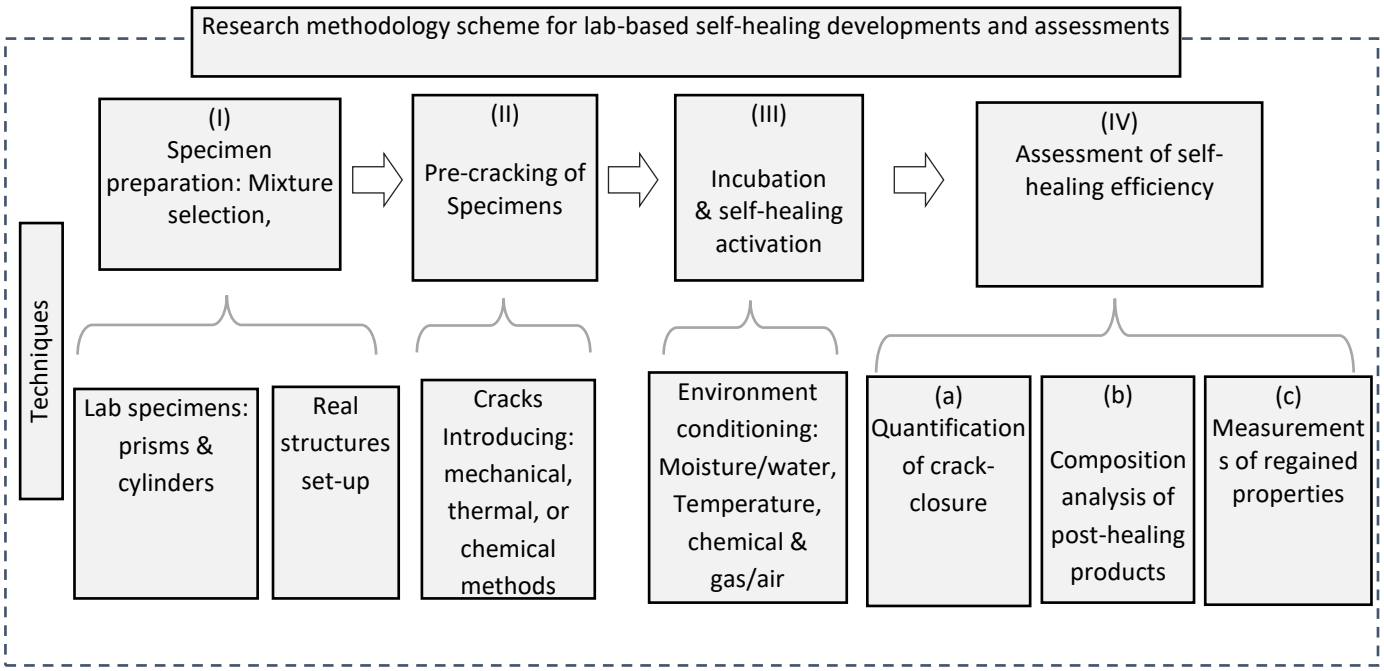

Figure 2.12: Scheme of research methodology for the developments and assessments of self-healing in cementitious materials

2.8.1 Pre-cracking of specimens

For the pre-cracking phase, cracks are commonly introduced using one the following mechanical experiments Figure 2.13:

- Tensile tests: Direct or splitting tests which are used for durability measurements.
- Bending tests: three or four-point bending tests.
- Splitting tensile test.

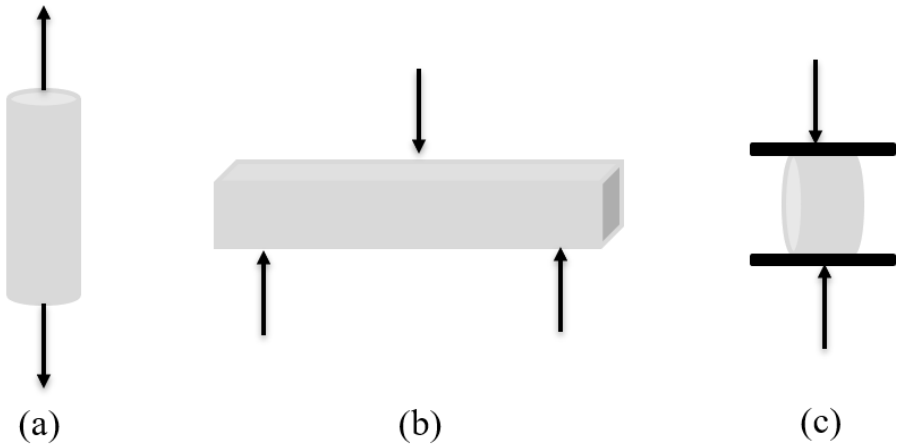

Figure 2.13: A schematic diagram shows different types of laboratory-based concrete tests: (a) Direct tensile test (b) Three-point bending test (c) Splitting tensile test

The selection of a pre-cracking test [131] is based on two considerations:

- The shape of the specimen: this can be associated with the type of test employed to assess recovery with respect to durability parameters.
- The specimen shape: which can be related to the type of the test to be used to assess the recovery in the durability parameters.
- The desired crack shape: which can refer to the real structural crack's mode due to solicitations of bending, shear, mixed bending with shear, uniform tension or compression. The width of a crack generated by bending tests varies with depth. It is widest at the mouth and narrowest towards the tip.

Beams and plate elements offer this bending or mixed shear-bending cracking mode. On the other hand, cracks of specimens under direct tensile or splitting tests are more uniform width lengthwise. These types of cracks can be typically found in structural elements under uniform tension like tension piles or under restrained deformation elements as well as cracks in two dimensional elements suffering membrane stress states.

- The type of material which has to be tested: it can be very difficult to do a controlled testing to pre-crack plain concrete specimens without reinforcements under direct tensile test or bending tests. However, the other configurations of mechanical pre-cracking tests with concrete and reinforced concrete are possible.

2.8.2 Assessment of the efficiency of self-healing

This type of assessment measures whether mechanical properties have been regained in comparison with the initial undamaged state, and also whether cracks have been closed or sealed. The former must be measured straight after pre-cracking and then once again after the healing period.

The methods employed to assess the efficiency of self-healing/sealing are summarised in Figure 2.14:

a) Quantification of cracks closure: to quantify surface and internal cracks by imaging approaches (Table 2.5).

b) Composition analyses of post-self-healing products (Table 2.5).

c) Measurements of regained properties: experimental approaches commonly used in durability testing (Table 2.6) and solid mechanics (Table 2.7 to measure the tightness and mechanical properties regaining.

Correlation between results obtained from the implementation of different experimental assessment testing (Figure 2.14) can be done to improve robustness criteria (e.g., quality of results, reliability, operational considerations and in-situ

applicability), which are required for standardisation, normalisation and commercialisation purposes [130, 131].

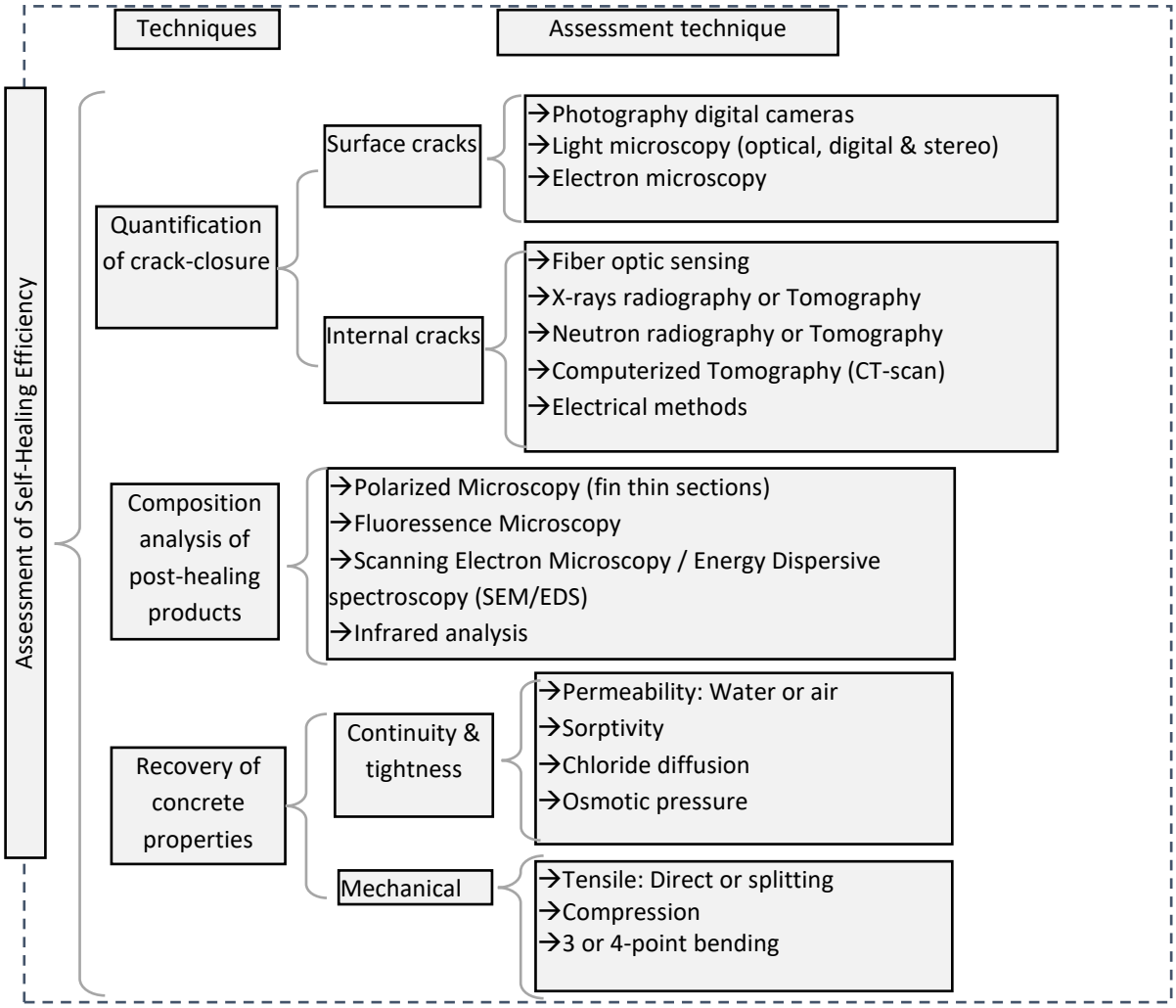

Figure 214: Techniques and tests used commonly to assess the self-healing concrete technologies and can be employed for bacterial self-healing concrete efficiency assessments

2.8.2.1 Quantification of crack closure

These assessment methods primarily employ qualitative analysis to depict the composition and structure of the healed concrete, release of the encapsulated healing agent, crystal deposition, and crack closure. The latter is the most obvious indicator of self-healing and is therefore the initial step required to evaluate and assess self-healing [131]. Table 2.5 presents a review of the experimental testing

methods based on imaging, microscopy and spectroscopy techniques with their advantages and limitations to visualize and to determine the cracks closure (surface and internal cracks).

To assess self-healing as a result of crack closure, the initial crack width must be compared with that after the healing process. To avoid subjectivity, areas where the growth in crack width is measured must be determined prior to healing. Self-healing can also be random; therefore, the greater the length of crack assessed, the more representative the analysis. To perform such an analysis, a size reference and standard photography software or specific measuring software from microscopes is required. The parameters that can be assessed are as follows:

Crack width:

This is measured as the average width along a pre-determined length [132, 133] or at specific points [134]. It can be assessed as the area under the plot of initial vs final crack width, or the average of values measured at different points on the same specimen [76].

Crack area:

To calculate the crack area in a specific section before and after healing, a picture of the crack path needs to be digitalised and appropriately filtered so that the crack area can be evaluated by calculating the crack area in a specific section before and after the healing process [131].

The healing performance based on crack width, area or volume is commonly used in the following expression:

$$Crack\ closure\ (\%)\ \frac{(\mathrm{Wf}-\mathrm{Wi})}{Wi}\ x\ 100 \qquad (2.1)$$

Where:

W_i = is the initial crack width, area or volume

W_f = is the final crack width, area or volume

2.8.2.2 Composition analysis of post-healing products

To assess the self-healing technology of cementitious materials, contemporary instrumented analytic methods can be employed to characterise and determine the healing process, chemical composition, crystalline materials, and precipitated products. Table 2.5 gives a review of the advantages and limitations of the experimental testing used for this purpose.

Table 2.5: Review of experimental testing methods commonly used to analyze the cracks closures of self-healing concrete and can be employed for bacterial self-healing efficiency assessments [20, 21, 130, 131].

Technique	Type	Testing	Targets/purposes/advantages	Limitations/Disadvantages	References
CRACK CLOSING MEASUREMENTS, VISUALISATION, ANALYSES AND DETERMINATIONS	Surface cracks closure	Photography cameras: *(high resolution or digital single-lens)*	• Largest area of visualization • Allow acquisition of data during testing. • Easy continuous monitoring for fast self-healing methods	• Generally, needs certain distance to cover the whole specimen • Less detail for a specific crack	[102, 135, 136]
		Light microscopy (optical, digital and stereo) Electron microscopy: *- (SEM) Scanning Electron Microscopy* *- (TEM) Transmission Electron Microscopy*	• Visualization of the surface crack as seen by the eye but at improved resolution while showing natural colours. • Visualization of crystal deposition and healing rate • Cheap and easy to implement. • Easy preparation of samples. • Larger area visualization • Good results for 0.05–0.30 mm cracks	• Not able to evaluate internal crack width, unless through thin sections taken in ‘‘tailored” mode • Not able to evaluate the composition of precipitates	[13, 91, 97, 102, 134, 137-143]
			• Generally, focus on small size cracks. • Good for verifying autogenous healing (like bacterial concrete)	• Expensive compared with light microscopy techniques. • Only in grey scale depending on the atomic number of the element	[13, 43, 61, 105, 130, 137, 142, 144-147]
	Internal cracks closure	Tomography and CT-scans (*X-rays and neutron)*	• Internal crack evaluation, in the damage and healing stage. • Allows the differentiation by densities of the materials • In the case of neutron tomography, high sensitivity for hydrogen detection, good for analysis of water uptake	• Extremely expensive and low availability of equipment • Health and safety hazard due to radiation risks • Time-consuming • High resolution only for small samples	[26, 148-155]
		Fibre optic sensing	• Predetermination of crack locations is not required. • Reveals time-variation of crack widths. • Non-destructive and absence of radiation risks	• Delicate specimen preparation works with embedded sensors. • Risk of damaging the sensors	[156-158]
		Electrical methods	• Reveals time-variation of crack width • Can be applied to specimens and structural elements under load • Non-destructive	• May require dedicated and expensive equipment and suitable post-processing model to correlate electrical measure with crack width	[159-170]
	Post self-healing composition analyses	Polarized and fluorescence functions for light microscopy	• High contrast in the borders between matrix and voids or cracks • Allows identification of crystalline solids from optical properties	• Needs time-consuming preparation of samples with polarized epoxy or fluorescence filter sets	[76, 152, 171, 172]
		Scanning Electron Microscopy + Energy Dispersive Spectroscopy *(SEM-EDS or EDX*)	• Allows complementary tests of the composition of precipitates, • Generally, focus on small size cracks. • Good for verifying autogenous healing (like bacterial concrete)	• Expensive compared with light microscopy techniques. • Only in grey scale depending on the atomic number of the element	[13, 61, 87, 137, 142, 145-147, 151, 173]

		+Back scattered Electrons *(SEM-BSE)* +Powder X-ray Diffraction (p-XRD)	• Qualitative and quantitative analysis of crystalline phases		[43, 71, 97, 103, 109, 174-183]
		Infrared analysis	• Determination of precipitated products	• Presence of moisture in concrete may affect accuracy • Infrared is suitable only to see prominent components and thus minor depositions may not be discernible • Limited detection for some substances	[95, 184, 185] [97, 176, 177, 186]

2.8.2.3 Measurements of regained properties

The mechanical properties (stiffness and strength) of concrete may be substantially weakened by the presence of cracks in the concrete matrix. These may disrupt the fundamental integrity of the matrix, rendering it more vulnerable to penetration by fluids and/or gases. Thus, the essential criteria for determining the efficiency of crack healing methods in concrete are whether the mechanical and tightness properties of the cement have been regained once healing is complete.

Methods based on the recovery of durability and tightness

Following consumption of nutrients, activation of the bacteria, and the filling of cracks with deposited carbonate precipitation crystals, which enhance the continuity of the concrete medium [187], [144], [20], cracks in bacterial self-healing concrete become both gas and watertight. However, some scholars contend that the precipitation of calcium carbonate may be associated with a decrease [97, 102, 130, 188-194]or increase [21] in porosity, or both, at different areas within the same matrix [195].

Transport properties and the integrity of the healed concrete medium are the primary indicators of regained resistance and tightness within the concrete following self-healing. Tests employed to assess these indicators measure water and air permeability, chloride diffusivity, sorptivity, and osmotic pressure in the healed specimen. Of these, the water permeability test has been utilised frequently by researchers to assess the efficiency of bio-self-healing concrete. A

summary of the experimental tests to evaluate concrete and Bio-concrete self-healing through the recovery of tightness and durability features is reported in Table 2.6.

Table 2.6: Review of experimental testing methods to assess healing and recovery of durability properties [20, 21, 130, 131]

Technique	Type	Testing	Targets/purposes/advantages	Limitations/Disadvantages	References
REGAINED RESISTANCE AND TIGHTNESS (Durability features)	Transport properties	Water permeability (low & high pressure)	Water permeability coefficient can be determined by flow of water through healed cracks	Effectiveness is dependent on how the cracks were introduced Very sensitive to composition of the specimen. Require water/air-tight seal	[26, 35, 43, 62, 73, 91, 100-103, 130, 137, 143, 176-178, 189, 196-207]
		Air/Gas permeability	Flow rate of air after healing has occurred measures the resistance against moisture/ foreign substance penetration through healed cracks		[144, 205, 208, 209]
		Sorptivity	To measure the rate of ingress of water in concrete specimen		[97, 102, 130, 188-194]
		Chloride diffusivity	Measurement of resistance against chloride penetration. Relevant and applicable for coastal structures		[78, 145, 210-220]
		Osmotic pressure	Resistance against ion ingress	Moisture content and temperature of the surrounding environment as well as the specimen may affect the accuracy of results	[219, 221]

Methods based on the recovery of mechanical properties

To identify any differences between healing and the natural time-gain of the properties concerned, a comparison is needed between the strain capacity [22, 71, 208], mechanical properties (stiffness, strength [22, 79, 137, 222], and energy absorption capacity [223, 224] of the healed specimens and those of undamaged natural specimens subject to an identical curing/incubation history. Such an approach provides important data on the efficiency of the healing mechanism. The methods most commonly employed to assess whether mechanical properties have been regained in self-healing concrete are mechanical tests such as the 3-

point and 4-point bending tests [22, 134, 147, 225, 226], compression test [43, 227], tensile test [22, 137, 222]. These experimental methods are the same tests employed for pre-damaging of the tested specimens. A review of the employed experimental tests is reviewed in Table 2.7.

It may also be useful to assess whether the recovery of different mechanical properties (strength, stiffness, strain and deformation capacity) correlates with each other and with crack closure. For instance, concerning autogenous healing, a minimum 60% crack closure must be obtained before any substantive recovery of stiffness and strength can be said to have occurred [134, 147]. Likewise, when water permeability is compared with crack closure, higher crack closure ratios than sealing ratios were more likely to be exhibited by specimens [203]. Thus, crack closure is the initial step that needs to be taken prior to facilitating the recovery of durability and/or mechanical properties. However, using crack closure alone as a healing indicator could mean the healing capability of the material is overestimated [205, 206].

Table 2.7: Review of test methods used to assess the efficiency of self-healing concrete technology: Healing and recovery of Mechanical and Durability properties after healing.

Technique	Type	Testing	Targets/purposes/advantages	Limitations/Disadvantages	References
RECOVERY OF MECHANICAL PROPERTIES	Mechanical	Direct tensile tests & Compression test	• Techniques used commonly to introduce pre-cracking onto the tested specimens • Measure recovery in strength, stiffness and/or energy due to self-healing when reloaded healed specimens	• Strongly influenced by moisture content, size and curing of specimens and the rate of application of load	[35, 43, 71, 79, 103, 137, 139, 155, 190, 223, 227, 228]
		Bending test (3-point bending test & 4-point bending test)			[19, 24, 26, 97, 107, 112, 146, 229-242]
	Non-mechanical	Acoustic emission analysis	• Signals from sensors that are attached to surface are captured and analysed to detect capsule breakage and regain in energy	• Sensitive to the quality of environmental noise and signal • High signal quality is required	[71, 141, 208, 218, 243-245]
		Resonance frequency analysis	• Measurement of recovery of stiffness	• Resonance frequency results are affected by size and geometrical effect of specimen • Crumbling of the surface on impact may affect the accuracy of results	[39, 71, 79, 218, 221, 246, 247]

2.9 Concluding remarks

In this chapter, the types and causes of cracks along with the development of techniques to assess self-healing performance were reviewed, the main points of which are as follows:

- As reviewed in section 2.2, concrete structures can be exposed to different types of cracks either before or after hardening. These cracks may occur at early stages ranging from ten minutes to three weeks due to plastic shrinkage, plastic settlement, early thermal contraction, and early shrinkage as a result of self-desiccation. Alternatively, cracks can occur in later stages (several weeks to several years) as a result of long-term

shrinkage caused by crazing, external moisture loss, alkali-silica reactions, and the corrosion of reinforcement. Such cracks arise at different depths and widths.

- In this review, three different categories of self-healing techniques were presented: natural, chemical, and biological. Natural healing, which is known as autogenous healing, is more economical and friendly to the environment. However, to achieve noticeable self-healing, the crack widths of concrete specimens should be less than 150µm and ideally below 50 µm [71].

- Chemical and biological agents can be added to concrete either directly or by impregnation in capsules. However, the effect of the delivery of the healing agent on self-healing performance has yet to be investigated.

- Various types of capsules have been reviewed, such as light weight aggregate, expanded perlite, silica gel, hydrogel, and calcium alginate beads. These capsules have yielded promising results in terms of protecting healing agents and then releasing them when cracks form. However, most of these capsules have drawbacks as the volume of both healing agents and capsules can form a part of concrete specimens due to partial replacement with aggregate when mixing with a concrete matrix, which decreases the strength of the concrete.

- Numerous methods have been employed to assess self-healing, including uniaxial tensile strength, water permeability, chloride ion permeability, ultrasonic measurements, SEM, oxygen consumption, and XRD. However, observing the healing process of samples inside the soil is difficult and complicated as it is important not to disturb the specimens; an electrical resistivity test with electrodes made of carbon fibre sheets could therefore be used to assess the healing process during the incubation period.

Chapter 3

A review of the mechanisms and factors affecting bacterial-based self-healing

3.1 Introduction

Internal stresses in concrete are one of the main factors that can induce micro-cracks on the concrete surface. These cracks lead to the ingression of harmful chemical materials such as sodium chloride and sulphates and, ultimately, the corrosion of steel bars and a reduction in the durability of concrete.

Over the last few decades, several materials have been used as self-healing agents to heal concrete cracks [248-250]. Although these have yielded promising results, they also have serious drawbacks in terms of their environmental impact. Furthermore, their thermal expansion coefficients are different compared to concrete. Increasing levels of environmental awareness throughout the world have motivated researchers to develop and investigate a new technique called “Bacteria-based self-healing concrete” or “Bio-concrete” [251]. Restoration of the durability of concrete can be achieved by utilising an innovative approach that consists of the precipitation of calcium carbonate induced by bacteria.

This technique is based on adding specific types of bacteria to the concrete mix, either directly or encapsulated, to precipitate calcium carbonate and therefore heal the cracks. When applying this technique, small cracks in the concrete can be repaired via the precipitation of calcium carbonate whereby bacterial activity provides heterogenous sites of crystal nucleation in a highly saturated solution of $CaCO_3$. The successful use of this rehabilitation technique could extend the lifespan of concrete structures and lead to a considerable reduction in cement production and structural replacement [86].

Recently, extensive research has been conducted on the use of bacteria to produce self-healing concrete. This shows how the use of bacteria as a healing agent has increasingly attracted the attention of researchers over the years. However, there are numerous problems with this process that engineers must resolve, particularly in relation to

bacterial self-healing. This chapter, therefore, reviews different aspects and factors that might affect the efficiency of the healing process.

3.2 General Classification of Bacteria

The classification of bacteria the most basic level is based on morphology. In general, it is possible to separate them into Rod-shaped bacteria (*Bacilli*), Sphere-shaped bacteria (*Cocci*) and Spiral-shaped bacteria (*Spirilla*) [252]. Bacteria can also be classified according to the Gram staining method as Gram-positive (e.g., *bacillus subtilis*) or Gram-negative (e.g., *Escherichia coli*). The staining of Gram-positive is a crystal violet-blue colour, whereas Gram-negative produces a safranin/simple fuchsine pink coloured stain. Gram staining is dependent on the existence of teichoic acid within the bacteria's cell wall, and only gram-positive bacteria contain teichoic acid [253].

The requirement for oxygen can also be used as a basis for classifying bacteria into four groups: obligate aerobic or strict (using molecular oxygen as terminal electron acceptors), whose growth occurs when oxygen is present. The growth of facultative anaerobic bacteria can happen regardless of the presence or absence of oxygen. Certain kinds of bacteria are defined as microaerophilic, meaning that their growth is optimal when the molecular concentration of oxygen is reduced [254].

3.3 Type of Bacteria used as Self-healing agent

The precipitation of calcium carbonate $CaCO_3$ is the most important element in the self-healing process. Various categories of bacteria are capable of precipitating calcium carbonate, which generally exists in environments such as soil, sand, or natural minerals [255]. However, to obtain a high level of precipitation, accelerated healing is needed to select the most efficient type of bacteria.

Researchers have investigated different types of bacteria, including *Sporosarcina pasteurii* [256], *Bacillus Lentus* [257], and *Bacillus pseudofirmus* [96].

For instance, in the majority of the research work conducted by Wang et al, Bacillus *sphaericus* LMG 22557 was utilised as the self-healing agent, whereas Bacillus *pseudofirmus* DSM 8715 and B. *cohnii* DSM 6307 were employed by Jonkers et al. [35,

61, 102, 155]. *Bacillus Megaterium* is a different Bacillus species that has been demonstrated to have potential as a healing agent for concrete [258]. According to prior research, bacteria that belongs to the *Bacillus genus* has been broadly utilised and has demonstrated the capacity to resist the increased alkalinity of the concrete medium. These researchers have also shown that Bacillus-type bacteria are capable of precipitating $CaCO_3$ after activation via water.

Ramachandranet et al. [259] reported that the contribution of *pseudomonas aeruginosa* to the precipitation of calcium carbonate was inconsiderable. Alazhari [106] studied three different types of bacteria: *B.cohnii, B.halodurans*, and *B.pseudofirmus*. The results showed that all three are capable of sealing concrete cracks and producing calcium carbonate as part of the process of self-healing. However, *B.pseudofirmus* was the most efficient and economical. In another study, calcium carbonate precipitation was assessed for 13 different strains of bacteria obtained from mangrove sediment and soda lake sediment. The results showed that strain H4 (a type of bacteria strain identified as Bacillus species) exhibited the highest level of calcium carbonate precipitation. This precipitation can be affected by compounds such as sodium lactate and sodium nitrate, which serve as a source of carbon and nitrogen [260]. Table 3.1 summarises the several types of bacteria that have been used in different studies and the achieved results.

Table 3.1: Types of bacteria used in different studies

Type of bacteria	Ref.	Results
B. sphaericus	[102]	Decrease water permeability and crack visually sealed
B. subtilis	[108]	Decrease water permeability
B. sphaericus	[35]	Decrease water permeability by 68%
Pseudomonas aeruginosa	[259]	Improve compressive strength
B. cohnii,	[68]	crack widths up to 0.79 mm were healed
S. pasteurii	[261]	Improve compressive strength by 22% and decrease in water absorption
Bacillussp.	[262]	Improve compressive strength by 36% and decrease in water absorption
Bacillus halmapalus	[99]	Decrease water permeability of cracks 0.4 mm by 95%
Sporosarcina pasteurii	[263]	cracks up to 0.417 mm were healed

Nonetheless, the majority of studies have utilised isolated bacterial strains produced in laboratory conditions. The dependence on such strains can elevate the production costs for self-healing concrete. Different research employed non-axenic bacteria whose growth was achieved utilising a sub-stream of the vegetable plant as the source of nutrients [264]. The findings revealed that the costs of using non-axenic bacteria as self-healing agents are reduced in comparison to bacteria produced in laboratories. They demonstrated that the bacteria could heal a 0.45mm fracture within 28 days, compared with bacteria from the Bacillus genus that could seal a 0.33mm fracture within 20 days [109].

3.4 The effect of bacteria on concrete

Fresh and hardening properties should not be affected if the bacterial spores are encapsulated prior to mixing them with concrete, whereas adding bacteria directly to

concrete as a suspension has a significant effect on both fresh and hardening concrete properties [265]. However, previous research [61, 266] suggests that bacteria cells and spores have a limited impact on concrete as they can survive for a short time in the early-age properties of concrete.

Alazhari [106] investigated the influence of self-healing agents on the properties of fresh concrete such as hydration kinetics and early and final setting times. The results indicated that hydration kinetics were significantly affected when the concentration of healing agents was greater than 0.05% of the cement mass, and that the setting time was slightly retarded when the concentration of healing agent by cement mass was 0.5%.

The effect of adding vegetative bacterial (*S. pasteuri*) cells to a cement paste on early-age cement mortar properties was investigated by Bundur et al. [267]. The results indicated that this addition significantly affected hydration kinetics and early and 28-day strength. The results also revealed that adding live and dead cells to cement paste delayed hydration kinetics. However, the negative effect on hydration kinetics during the hydration process might be reduced by the metabolic activity of live cells.

With regard to the influence of bio-based healing agents on concrete compressive strength, numerous studies have been conducted with different types of bacteria. These have yielded contradictory results. As suggested by Jonkers et al. [61], the addition of different healing agents to cement paste mixtures has a negative impact on compressive strength. The findings of their experiments indicated that a reduced compressive strength of lower than 10% was observed for samples subjected to curing for 3,7 and 28 days via the addition of a large volume of bacterial spores (6×10^8 cm ^{3}) (See Figure 3.1). On the other hand, the addition of Bacillus spore cells to cement mortar caused the compressive strength to rise to 36% [268]. This is an indication that the enhancement in the compressive strength is likely caused by calcium carbonate precipitation that occurs inside the cement mortar pores Andalib et al. [269] explored the impact that Bacillus megaterium bacteria with a concentration of 30×10^5 CFU/ml had on the compressive strength of concrete. Their findings indicated that greater amounts of

calcite precipitation occurred in high-grade concrete compared to low-grade concrete, which exhibited respective strength development rates of 24% and 12.8%.

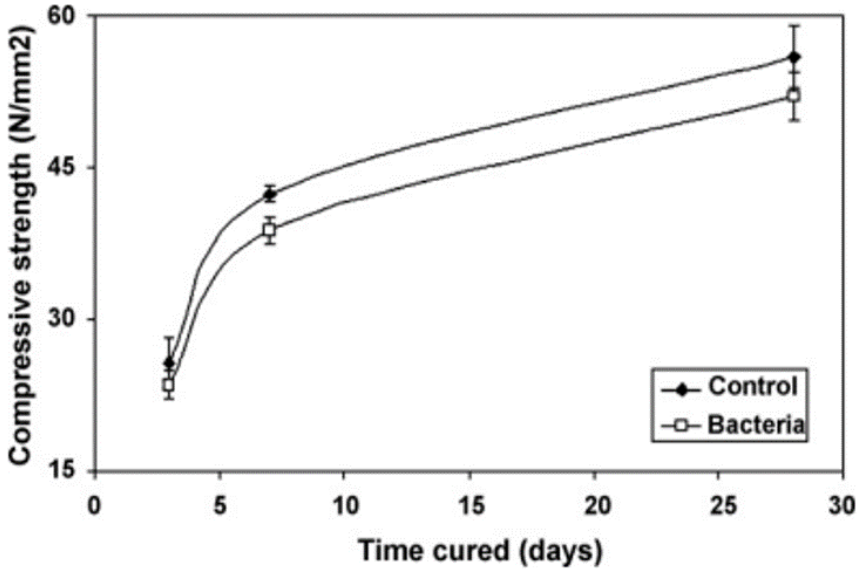

Figure 3.1: The effect of bacterial agent on concrete compressive strength [61].

The effect of three different bacterial concentrations (10^3, 10^5, 10^7 cells-ml^{-1}) on concrete strength was investigated by Chahal et al. [261]. The results showed that maximum compressive strength was achieved with a bacterial concentration of 10^5 cells-ml^{-1} (Figure 3.2).

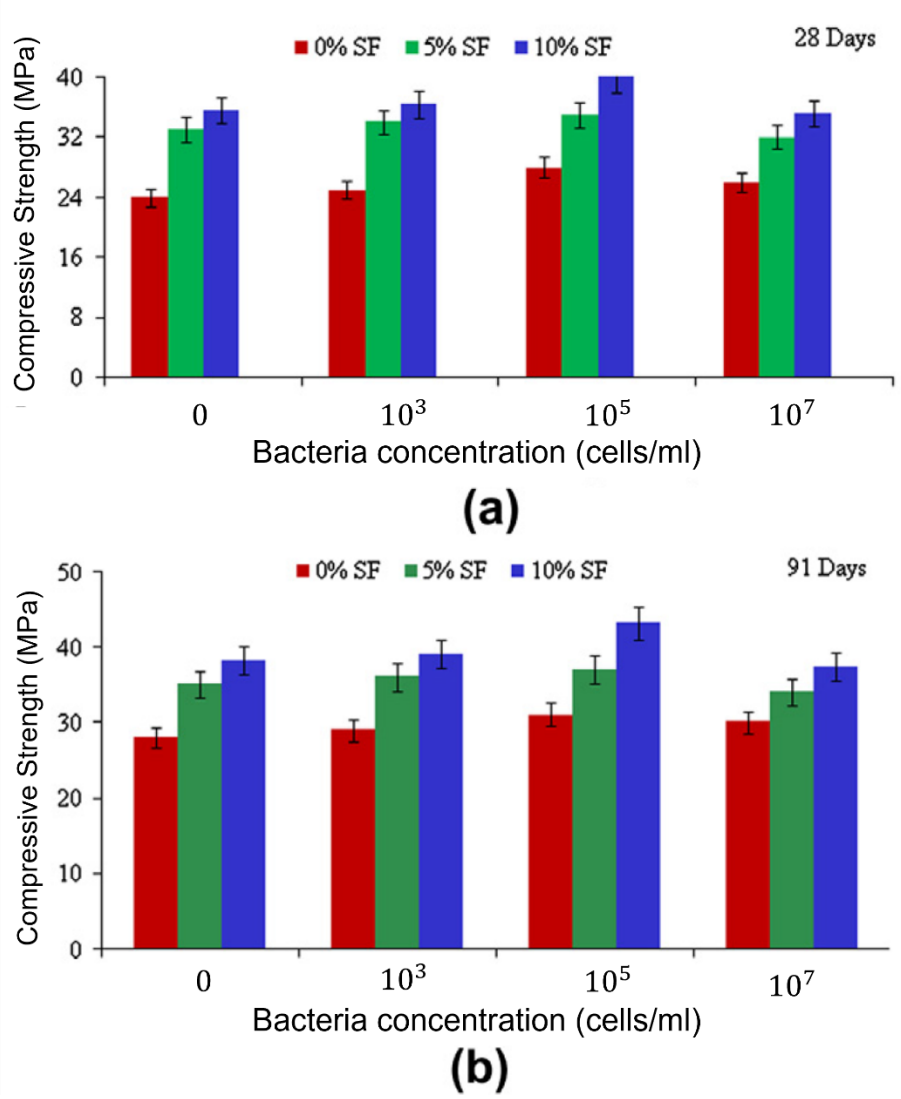

Figure 3.2: The effect of bacterial concentration on concrete compressive strength (a) after 28 days of curing (b) after 91 days of curing [261]

These differences in outcomes may be caused by the brittle nature of the precipitated calcium carbonate. Furthermore, the use of varied culture mediums, bacteria concentrations and nutrients in addition to the variety of environmental states such as incubation, temperature and the volume of carbon dioxide and oxygen could have been contributory factors that generated the variation.

3.5 Viability of bacteria in concrete

Bacterial surfaces are significant factors in the precipitation of calcium [270]; as a result of the existence of groups with a negative charge at elevated pH, it is possible to find

ions with a positive charge on such surfaces. Carbonate precipitates are frequently formed on the outer surfaces of bacterial cells via successive stratification, while the embedding of bacteria in developing carbonate crystals can occur [271]. Hammes et al. [272] explained the primary contributions of pH and calcium metabolism in the process of microbial carbonate precipitation. It is possible to apply the bacterial agent externally to repair external fractures in the concrete; alternatively, it can be used as an additive in the concrete mix either to serve as a spore that functions as a self-sufficient self-healing agent or in a capsular form within tubers or chemical substances [35, 99, 101, 102] or within lightweight aggregate [6, 32, 68, 96].

The activation of bacteria embedded within concrete should occur when a crack forms, followed by the optimal precipitation of calcium carbonate. To achieve this, they should be capable of surviving despite the harsh environment of concrete. The structure of a concrete matrix exhibits high density where the porosity is lower than 10% and the sizes of the pores are less than 1µm. Contrastingly, the size of the bacteria varies between 1 and 4µm. Hence, there is a strong likelihood that the bacteria will be compressed when the cement is hydrated [273]. The pH level of cement is generally around 12 and only minimal levels of oxygen and moisture are present, which are not very hospitable conditions for bacteria. It was ascertained that Microbially-induced calcium carbonate (MICP) necessitates a certain amount of aeration and the bacteria's viability is lowered as the pH rises in what is otherwise an advantageous environment for MICP [274]. Additionally, the presence of high shear forces in the concrete mix process could also negatively impact the bacteria's survivability. Hence, it is essential to evaluate the survivability and long-run viability of bacteria embedded within concrete [273]. As the resistance of spores to harsh environments is greater than vegetative cells, a recommendation to optimise the survivability of the bacteria is to insert either spores or spores in capsule form, as mentioned previously. Measurement of the survivability of concrete-embedded bacterial spores has been assessed utilising various techniques and species. The application of the dilution-to-extinction approach (in other words, the most probable-number method), involved the crushing of cement stone, followed by grinding of the stone with a strong mechanical force, and then suspension through ultrasonic treatment to acquire an individual cell suspension of the bacteria that was

not bound to the concrete [61]. It was observed that the amount of cells that showed viability declined proportionally to the age of the specimen, suggesting that spores embedded in cement experience a decrease in viability over time. Most of the spores that had been directly incorporated into the cement paste mixture only survived for under 4 months, which is line with the results of similar studies in the literature. In terms of Bacillus megaterium embedded in samples of mortar, the amount of cells was observed to significantly decrease within 3 days 10^7 to 10^5 CFU-ml^{-1}) and 28 days (10^4 CFU-ml^{-1}); only 0.1% of the cells survived for up to 28 days [113]. Spores of *Bacillus sphaericus* were only capable of surviving for 2 days within concrete without suitable protection, and if this was provided, they started to germinate and grow within 48 h of being extracted from the concrete dust [275]. The survival time of the *Shewanella* strain is approximately 6-7 days inside the mortar [118], with analogous findings being reported for *S. pasteurii*. The amount of cells considered viable declined by 80% after 24 h within the cement paste. Furthermore, the survival rates for 7 and 28 days were limited to 1 and 0.4% respectively, where around half of the cells showing viability were spores [276]. The abovementioned findings emphasise the sub-standard performance of naked cells after being inserted into concrete. While the survivability of bacterial spores was enhanced, compression caused by the progressive reduction in the size of concrete ultimately also causes the spores to be destroyed. Hence, it is essential that the bacterial cells are incorporated into carriers for the production of concrete that is capable of self-healing for extended periods. The effectiveness of carriers has been demonstrated; for example, research that assessed the ability of extracted vegetative cells to reduce NO_3 after being embedded within concrete for 28 days determined that protective carriers were critical for the survivability of the cells within the harsh conditions of the concrete [176]. The time required to resuscitate the cells ranged from 3 to 7 days. In the absence of a protecting or encapsulating carrier, it is typically not possible for spores and bacterial cells to continue to live in the inhospitable environment found within cementitious matrices [277].

3.6 The mechanism of bacterial based self-healing concrete

The use of bacterial-based self-healing concrete was first suggested by Gollapudi in the mid-1990s. Gollapudi's aim was to incorporate ureolytic bacteria, which assists in the precipitation of calcium carbonate, to seal micro-cracks in an environmentally friendly way [94]. The concept of bacterial self-healing concrete was inspired by autonomous healing in organisms such as animals and plants [38].

Bacillus Sphaericus is the most common bacteria used in research studies and is recognised as harmless to humans and the environment. The possibility of reinforcement corrosion is also reduced due to the consumption of oxygen during the healing process [278]. It is difficult to repair cracks wider than 0.8mm; however, these can be healed by the use of bacteria in calcite precipitation [109]. The healing of micro cracks or damaged structures through a bacterial self-healing technique, in which the selective cementation of porous media by microbiologically induced calcium carbonate occurs, represents a new generation of concrete. Numerous studies have reported that bacteria from different habitats can precipitate calcium carbonate in natural and laboratory conditions [30].

Calcium carbonate can be produced by the natural or artificial activities of microbes [279]. However, the self-healing mechanism starts when water ingresses through cracks that have formed on the concrete surface. When the water contacts the spores, the bacteria start to germinate and get activated by the water and nutrients such as calcium lactate. The bacteria then consume the oxygen, and the soluble calcium lactate is transformed into calcium carbonate. The calcium carbonate then consolidates and seals the cracks (Figure 3.3). At this point, bacteria return to the hibernation stage. If any future cracks occur, the bacteria will be re-activated to heal the cracks. This phenomenon is called Microbiologically Induced Calcium Carbonate Precipitation (MICP) [69].

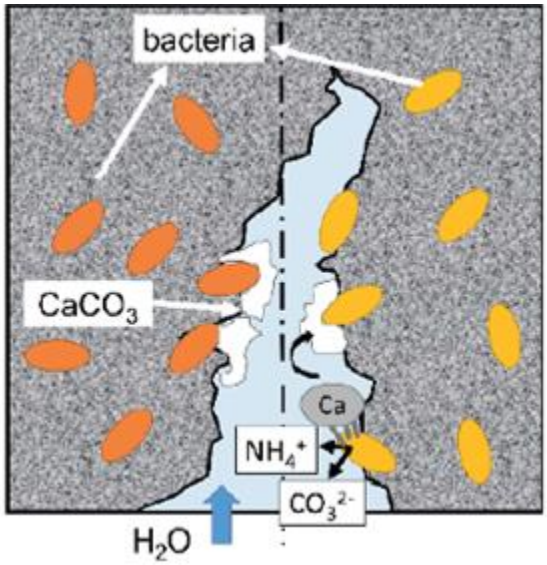

Figure 3.3: Bacterial-based self-healing approach [280]

Oxygen is an essential element in the process of steel corrosion. The consumption of oxygen during the bacterial transformation of calcium lactate to calcium carbonate, therefore, has the additional advantage of increasing the durability of reinforced concrete structures. In most studies, both agent parts of bacteria spores and nutrition are added within capsules to protect the agents from activation during the concrete mix process. When cracks occur, water seeps into the concrete to activate the bacteria with nutrition. Laboratory experiments have shown that bacteria can convert nutrition to calcium carbonate within seven days, whereas in the outdoor environment, where the temperature is low, the process takes several weeks [30].

Another common way to precipitate calcium carbonate is through the decay of urea by ureoltic bacteria. To produce dissolved ammonium, carbon dioxide, and dissolved inorganic carbon, the urea is hydrolysed by the microbial urease enzyme. Furthermore, an increase in pH due to the ammonia released in the surroundings leads to an accumulation of insoluble calcium carbonate in a calcium-rich environment.

Figure 3.5 depicts a simplified representation of events occurring during ureolytic-induced carbonate precipitation [31]. Calcium ions in the solution are attracted to the negative charge of the bacterial cell wall. Following the addition of urea to the bacteria, dissolved inorganic carbon (DIC) and ammonium are released in the microenvironment of the bacteria (Figure 3.4A). In the presence of calcium ions, this can result in local

supersaturation and hence heterogeneous precipitation of calcium carbonate on the bacterial cell wall (Figure 3.4B). Over time, the entire cell becomes encapsulated (Figure 3.4C), limiting nutrient transfer and resulting in cell death.

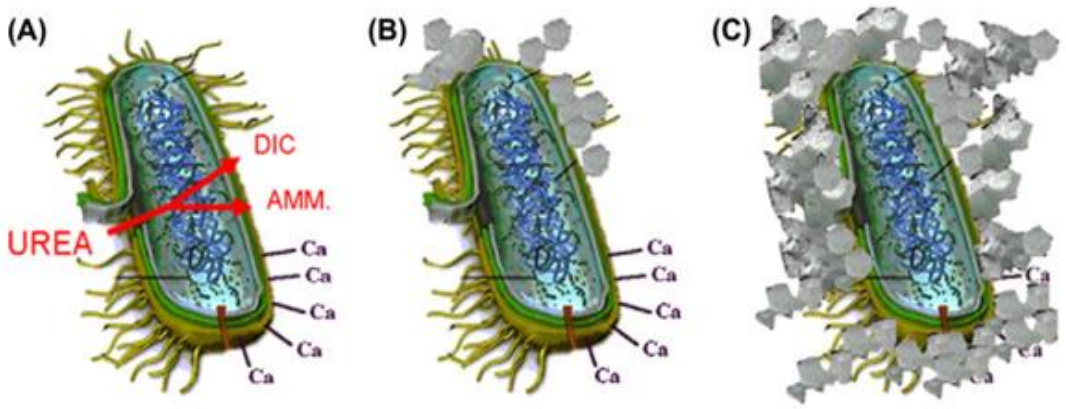

Figure 3.4: Simplified performance of the stages occurring during the ureolytic induced carbonate precipitation [31].

According to Palin, et al. [99], the highest concentration of carbon dioxide on the crack surface results in rapid precipitation of calcium carbonate, which then closes the crack. The precipitation of calcium carbonate in a natural environment depends on conditions connected with the concrete matrix such as calcium ion concentration, the pH of the solution, and the concentration of dissolved inorganic carbon. At the same time, the availability of nucleation sites is related to the bacterial cell [281] (Figure 3.5).

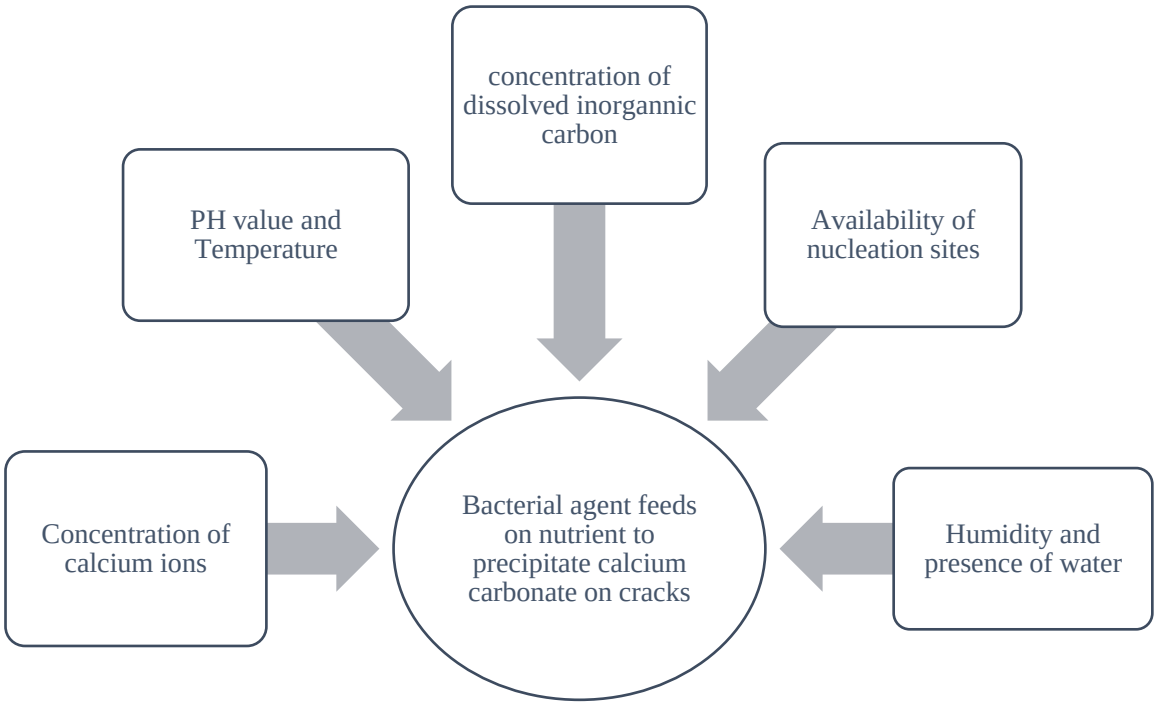

Figure 3.5. The factors affecting the precipitation of calcium carbonate natural environment

The concentration of dissolved inorganic carbon relies on environmental factors such as the partial pressure of carbon dioxide and temperature. The following equations show the equilibrium reactions and constants that control the dissolving of CO_2 in a watery environment at a temperature of 25 ℃ and 1 atm of atmospheric pressure [282].

$$CO_{2\,(g)} \leftrightarrow CO_{2\,(aq.)} \; (pk_H = 1.468) \tag{3.1}$$

$$CO_{2\,(aq.)} + H_2O \leftrightarrow H_2CO_3^{*} \; (pK = 2.84) \tag{3.2}$$

$$H_2CO_3^{*} \leftrightarrow H^+ + HCO_3^- \; (pK_1 = 6.352) \tag{3.3}$$

$$HCO_3^- \leftrightarrow CO_3^{2-} + H^+ \; (pK_2 = 10.329) \tag{3.4}$$

$$\text{With } H_2CO_3^{*} = CO_{2\,(aq.)} + H_2CO_3 \tag{3.5}$$

3.7 Pathways of calcium carbonate precipitation

Researchers have previously investigated various kinds of carbon-producing pathways. Nevertheless, the most frequent type is aerobic respiration, which is dependent on the respiration features of bacteria for the direct conversion of organic calcium compounds into calcium carbonate [86, 183]. This procedure involves the production of microorganisms in an extracellular manner via two metabolic pathways: heterotrophic and autotrophic.

3.7.1. Autotrophic pathway

The autotrophic pathway occurs when carbon dioxide is present, whereby the carbon dioxide is converted into carbonate by the microbes in three different processes: (i) non-methylotrophic methanogenesis (via Methanogenic archaea); (ii) oxygenic photosynthesis (via Cyanobacteria), and (iii) anoxygenic photosynthesis (via Purple bacteria [283].

In the non-methylotrophic pathway, hydrogen and carbon dioxide are converted into methane (Eq 3.6). Resultantly, the anaerobic oxidation of methane via electron acceptors such as sulphate causes bicarbonate to be produced, as demonstrated in Eq 3.7 [284]. The carbonate generated will subsequently lead to the precipitation of calcium carbonate when calcium ions are present, as revealed in Eq 3.8. This pathway has a greater prevalence among marine sediments.

$$CO_2 + 4H_2 \rightarrow CH_4 + 2H_2O \quad (3.6)$$

$$CH_4 + SO_4^{2-} \rightarrow HCO_3^- + HS^- + H_2O \quad (3.7)$$

$$Ca^{2+} + 2HCO_3^- \leftrightarrow CaCO_3 + CO_2 + H_2O \quad (3.8)$$

Additionally, the process of photosynthesis is an autotrophic pathway that produces calcium carbonate when calcium ions are present. Photosynthetic bacteria are divided into two groups: oxygenic and anoxygenic photosynthetic bacteria. Distinct kinds of electron donors are used by oxygenic and anoxygenic photosynthesising organisms in the production of methanol. As demonstrated by Eq. 3.9, the electron donor that facilitates oxygenic photosynthesis is water. On the other hand, for anoxygenic photosynthesis, the electron donor within the redox reaction (Eq. 3.10) is hydrogen

sulphide (H_2S), meaning there is no generation of oxygen [285]. The extraction of carbon dioxide as part of microbial photosynthesis from bicarbonate solutions causes carbonate to be produced [286]. This activity results in a constrained rise in pH and ultimately, the precipitation of calcium carbonate when calcium ions are present [281]. The equations shown below summarise the photosynthesis chemical reactions involved in the production of calcium carbonate.

$$CO_2 + H_2O \rightarrow^{(Oxygenic\ Photosynthesis)} (CH_2O) + O_2 \quad (3.9)$$

$$CO_2 + 2H_2S + H_2O \rightarrow^{(Anoxygenic\ Photosynthesis)} (CH_2O) + 2S + 2H_2O \quad (3.10)$$

$$2HCO_3^- \leftrightarrow CO_2 + CO_3^{2-} + H_2O \quad (3.11)$$

$$CO_3^{2-} + H_2O \leftrightarrow HCO_3^- + OH^- \quad (3.12)$$

Although it is possible to precipitate calcium via photosynthesis, it can only be realised in the presence of sufficient carbon dioxide. This suggests that it is only possible to utilise the photosynthesis pathway for parts of the concrete construction that have increased exposure to sunlight and carbon dioxide.

3.7.2 Heterotrophic pathway

Precipitation of crystals could be caused by microbial communities due to their expansion within natural environments. The production of crystals is ascribed to the composition of the medium utilised for growing heterotrophic bacteria and can be frequently observed in natural habitats. The heterotrophic expansion of distinct genera of bacteria like species on organic acid salts (acetate, lactate, citrate, succinate, oxalate, malate, and glyoxylate) cause carbonate minerals to be produced. Organic compounds provide the energy needed by such bacteria. According to the different types of salts and carbon that constitute the medium, the aforementioned bacteria are capable of producing a variety of different crystals including magnesium carbonate and calcium carbonate. Eqs. 3.13-3.15 show the chemical reactions that occur in the formation of calcium carbonate when calcium carbonate as the source of low molecular weight acid and calcium ions are present [287].

$$CH_3COO^- + 2O_2 \rightarrow^{(Heterotrophic\ bacteria)} 2CO_2 + H_2O + OH^- \quad (3.13)$$

$$2CO_2 + OH^- \rightarrow CO_2 + HCO_3^- \quad (3.14)$$

$$2HCO_3^- + Ca^{2+} \rightarrow CaCO_3 + CO_2 + H_2O \quad (3.15)$$

The precipitation of calcium carbonate via the usage of organic acids has been broadly recorded in varied substrate conditions, such as caves (caves walls and ceilings, cave formations), marines, lakes and soils. Researchers found that isolates of heterotrophic bacterial communities (*Arthrobacter and Rhodococcus species*) extracted from cave stalactites could be used for the production of calcium carbonate when calcium acetate was present [288]. Furthermore, extensive research has been conducted on the roles of *Arthrobacter* and *Rhodococcus species* isolated from extreme cold conditions in the process of precipitating calcium carbonate crystals where the carbon was sourced from calcium acetate and calcium citrate [289]. Cacchio et al. [290] performed a different conceptual study and determined that Bacillus and Arthrobacter species are able to precipitate calcium carbonate in an alkaline carbonate medium.

The primary benefit of this pathway is the existence of organic acid as the solitary provider of carbon and energy. It is also important to note that characteristics of the cell surfaces of bacteria (as nucleation locations), proteins, and extracellular polymeric substances have important impacts on the morphological and mineralogical properties of the calcium carbonate generated. Hence, it is possible to precipitate various morphologies of calcium carbonate including (rhombohedra crystal), vaterite (hexagon-shaped crystal) or aragonite (needle-shaped crystal) according to the chemical characteristics of the cell wall of the bacteria.

Sulphur and nitrogen cycles are additional mechanisms that enable calcium carbonate to be produced. The former involves the dissimilatory reduction of sulphate. Resultantly, the production of calcium carbonate occurs if the medium contains a source of calcium, organic substance and sulphate. Due to the rise in the pH level caused by degasifying the hydrogen sulphide, the reaction is shifted towards calcium carbonate precipitation [283]. Eqs. 3.16-3.19 demonstrate how calcium carbonate is produced via the reduction of calcium sulphate ($CaSO_4$) to calcium sulphide (CaS) using sulphate-reducing bacteria [291].

$$CaSO_4 + 2(CH_2O) \rightarrow CaS + 2CO_2 + 2H_2O \quad (3.16)$$

$$CaS + 2H_2O \rightarrow Ca(OH)_2 + H_2S \quad (3.17)$$

$$CO_2 + H_2O \rightarrow H_2CO_3 \quad (3.18)$$

$$Ca(OH)_2 + H_2CO_3 \rightarrow CaCO_3 + 2H_2O \quad (3.19)$$

Carbonate or bicarbonate can be produced via the nitrogen cycle by following three primary pathways: (i) the degradation of urea or uric acid (ureolysis), (ii) by ammonifying amino acids, and (iii) dissimilatory nitrate reduction [284, 292]. Due to the nitrogen cycle, precipitation of calcium carbonate can be achieved if enough calcium ions are present within the medium [283].

3.8 Factors affecting self-healing performance

In the comparison of different studies that have addressed the self-healing properties of cementitious substances, it is not only important to consider the testing approaches used, but also the starting and boundary conditions adopted, which can have a significant impact on the final outcomes. First, according to the pre-cracking time, the presence of un-hydrated cement particles and/or additional cementitious substances could still be detected. This can influence the extent of autogenous healing with regard to the overall healing. Second, the healing process efficiency can be significantly affected by various factors related to the performance of the healing agent such as the concentration of bacteria, the effect of pH and temperature on the growth of bacteria, type of nutrient, long-term survival of bacteria within the concrete matrix, incubation conditions, and surrounding environments [33].

Third, the healing properties could be affected by a stress condition standard to the surfaces of cracks, whereby compressive strength causes a mechanical crack to close, whereas tensile stress causes it to open. Finally, damage can occur to the healing materials produced, and disruption can occur in the healing procedure due to instability of the crack. Additionally, crack width can play a significant role, since, as will be explained in greater detail, healing efficiency is evidently dependent on, also as a function of the self-healing process, on the starting width of the crack that requires

closure; for example, the process of closing cracks with greater width can be lengthier or may necessitate a better simulating/engineering mechanism to ensure effective healing [131].

3.8.1. Age of pre-cracking

The pre-cracking age should also be taken into consideration in the study of healing phenomena. It is possible to attribute autogenous healing to the precipitation of calcium carbonate and calcium hydroxide, mechanical obstruction and blockage of narrow crack volumes via tiny particles, swelling, as well as the re-hydration of the cement paste in the proximity of the crack [196]. Rehydrating the cement paste leads to a delay in the hydration of cement particles that have yet to react as a result of the absence of water. These types of un-hydrated particles are highly prevalent in cases where the mix is designed with a low ratio of water to cement. This is the overriding mechanism that occurs in newly formed concrete because a large volume of un-hydrated cement grains is present [293].

Calcium hydroxide and calcium carbonate precipitation occur due to the carbonation reaction between carbon dioxide, which exists in both air and water, and calcium ions contained within the concrete [62]. For older cement, the primary mechanism of autogenous healing is carbonation [293]. It is important to note that it is associated with the interactions between the crack and its immediate environment in addition to its level of moisture, which could differ across the same crack. In terms of concrete that contains latent hydraulic or pozzolanic binder substances (e.g., blast furnace slag or fly ash), which hydrate at a slower rate compared to cement, hydration could occur at a later time, thus ensuring that the time that unreacted binder material is accessible is extended [294]. Another significant factor is that the pre-cracking age does not necessarily have an association with a particular kind of healing process, but can be associated with specific kinds of damage, which are expected to materialise through the planned lifecycle of the construction. Cracks can emerge in young concrete as a result of constrained shrinkage and /or thermal deformation[295]. For instance, Formia et al. [204] utilised the ring test to create restrained shrinkage cracks and assess the associated healing capability. Cracks that emerge as the concrete ages are caused by

load or deformation as a result of general service conditions. In typical scenarios, design specifications indicate that the reference age should be assumed to be 28 days, at which point a vast proportion of the hydration process can be considered to be completed for standard concretes. Pre-cracking at subsequent periods (more than 28 days) has additionally been documented and can be used to evaluate how viable healing agents are after being dormant, including the effectiveness of bacteria crystalline admixtures, encapsulated polymers, among others. A similar situation can arise with the usage of additional cementitious substances, such as fly ash or slag, where their activity and therefore role in the autogenous healing process can result in a lengthier period of consumption.

3.8.2 Concentration of bacteria

Sealing effectiveness is not only dependent on the kind of bacteria, but also the quantity of bacteria and nutrients that are included in the concrete. The amount of bacteria spores added to the concrete could enhance the capacity to seal cracks, although nutrients are required for the production of $CaCO_3$ subsequent to activation of the spores with water. As illustrated by the following equation, the volume of nutrients will be constrained by the volume of $CaCO_3$ [61].

$$CaC_6H_{10}O_6 + 6O_2 \rightarrow CaCO_3 + 5CO_2 + 5H_2O \quad (3.20)$$

Wang et al. (2014) [35] conducted a study in which the number of spores contained within $1m^3$ concrete was within 2% of hydrogels, where 10^9 spores/ml was contained within every hydrogel. The resulting mixture facilitated 80-90% healing of a 0.3mm crack, while a 0.3-0.7mm crack was healed up to 30-50% within 28 days. The hydrogel that acted as the healing agent additionally contained nutrients and urea, which facilitated the precipitation of $CaCO_3$. In another research, Bacillus Megaterium was utilised as the bacterial healing agent, where 10^5 cells/ml solution was included in the concrete mixture [269]. Out of this mixture, approximately 186 x 10^5 cell/m^3 was utilised within the concrete composition. A different study employed a virtually identical concentration of 10^8 spores/L, which generated a healing rate that showed strong similarities to that found by Wang et al. [35]. The findings indicated that the impregnation of a bacterial solution of 10^8 spores/L into Light Weight Aggregate (LWA)

enabled 69% of the water tightness to be recovered in 28 days. Although no measurement was taken to determine the width of the crack that had been healed, it was similar to the crack with a width of 0.3-0.7mm documented by Wang et al. [35]. The number of spores embedded equalled 5% of the cement in the overall concrete mixture. Research conducted by Da Silva et al. [264] determined that by adding a bacterial self-healing agent, it was possible to reduce the concrete's compressive strength. When 0.5-1% of Cyclic EnRiched Ureolytic Powder (CERUP) was added as the self-healing agent, this resulted in the smallest decline in compressive strength. However, 3-5% CERUP included in the mixture caused a 35-52% reduction in compressive strength of concrete after 28 days. In summary, in order for the detrimental effects on the mechanical strength of concrete to be minimised, it is recommended that the volume of self-healing agent incorporated into the concrete mix should not exceed 1-2%. A proportion of spores included in a concrete mixture of up to 10^8 spores/L is also capable of producing an identical healing result due to the increased spore concentration contained within the mixing solution. This could be attributed to the fact that the bacteria are capable of reproducing subsequent to activation via the spores.

3.8.3 Effect of the pH on the growth of the bacteria

One of the primary factors that can have an impact on bacterial growth is the pH level (Figure 3.6) The pH range in which microbial species grow can vary [296]. Bang et al. [297] investigated the impact of pH on bacterial growth for different species. The preparation of nutrients with pH levels ranging between 4 and 12 was performed in test tubes. The bacterial culture was subsequently introduced in order to observe how it grew. The test was performed based on the measurement of the sample's turbidity utilising a Photo calorimeter, which indicated a pH range of 7.5-9.0 facilitated growth. *Bacillus pasteurii* grew in pH between 7 and 9, whereas the range of 8-9 was conducive to *Bacillus spaericus* growth.

Reddy [298] found that the most favourable pH for bacterial activity was 7.4. In another study, Lee and Park [277] reported that microbiologically induced calcium carbonate and the survival of bacteria increase as pH decreases.

Wang et al. [100] investigated the ureolytic activity of bacteria with and without immobilisation onto diatomaceous earth in different kinds of pH environments. Their results showed that the amount of urea decomposed by free bacterial cells in a high pH (12.5) cement slurry decreased dramatically from 95% to less than 5%.

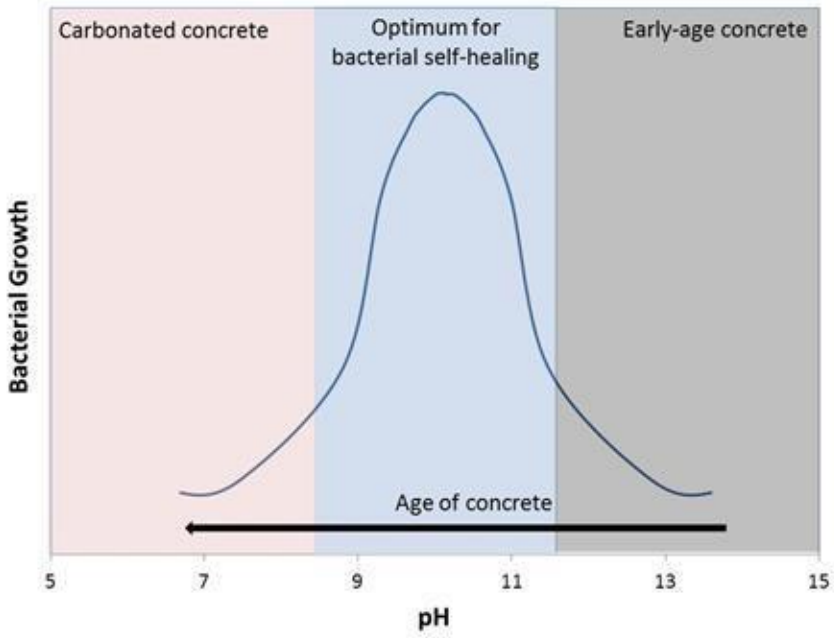

Figure 3.6: The influence of pH on the growth of bacteria [299]

3.8.4 Temperature

Bacteria require different temperatures in which to grow. The temperature at which a bacterium grows is defined as the optimum temperature. Those bacteria whose optimum temperature is in the range between 25 and 40°C are named mesophilic, while those who achieve maximum growth under 20°C are called psychrophilic bacteria. A different collection of non-pathogenic bacteria known as thermophiles have an optimum temperature of between 55 and 80°C. Conversely, the minimum temperature that causes a bacterium to be killed in a normal environment is defined as the thermal death point [300].

With regard to their applicability for concrete that has exposure to different conditions, the selection of bacteria to be utilised is additionally dependent on their capacity to withstand increased temperatures (thermophilic), decreased temperatures

(psychrophilic) as well as fresh and salt-water habitats. The majority of these characteristics have received minimal focus with respect to self-healing concrete and experiments conducted under laboratory conditions have predominantly concentrated on germinating spores and precipitating calcite in conditions approaching optimum for the given species of bacteria, which is generally in the range of 25-4°C for the majority of alkaliphilic bacteria [301].

Nevertheless, psychrophilic behaviour is exhibited by certain alkaliphiles. For instance, strain 207, which is an aerobic coccus, can achieve growth in the temperature range of between -5 and 39°C [301]; if a calcite precipitating alkaliphile was discovered that had analogous growth properties, it would have a considerable impact on the advancement of self-healing concrete based on bacteria.

It has been demonstrated that certain strains of *B. sphaericus*, *B. megaterium* and *B. firmus* even have the ability to precipitate calcite within B4 medium in temperatures as low as 4°C [290]. Although the rate of precipitation was reduced compared to more elevated temperatures, this is an indication that it is possible for self-healing to occur at reduced temperatures utilising bacillus. Palin et al. [99] investigated to determine how efficient the self-healing of cementitious materials was in marine conditions with reduced temperatures (8°C). The findings indicated that the crack-healing ability lowered the permeability of a 0.44m wide crack by approximately 95%, while cracks with a width of 0.6 mm were reduced by 93% after a 56-day period of incubation within artificial seawater. Additionally, Cacchio et al. [290] documented that calcium carbonate was formed when bacteria that belonged to the Arthrobacter species were used. They are oligotrophic bacteria that can achieve growth in the absence of moisture, at reduced temperatures and without the requirement of abundant nutrients. Nonetheless, the majority of bacteria that belong to this genus do not produce spores, which reduces their overall suitability for self-healing concrete.

Ghosh et al. [117] conducted a study that was aimed at enhancing the compressive strength of cement mortars utilising bacteria from the Shewanella genus, with thermophilic anaerobic properties. Nevertheless, their study did not involve an investigation to determine whether the bacteria could be grown in a range of

temperatures but did determine that bacterial growth was achieved and minerals were precipitated until the pH level reached 11 [302].

3.8.5 Nutrient type

As a result of the process of biomineralising calcium carbonate being relatively time-consuming, there is increased demand for specific nutrients that can enhance the speed of this process. Furthermore, researchers prefer to select bacteria that offer reduced risk with an increased capacity to induce calcium carbonate precipitation, enzyme activity and growth rate. Nevertheless, excessive growth of bacteria could cause uncontrolled superficial biofilms and irregular surfaces to be produced [303]. Hence, it is necessary to optimise the volume of nutrients and inoculum magnitude to avert bacterial overgrowth and to maximise precipitation.

Several types of calcium salts can be utilised in bacterial self-healing systems, including calcium chloride, and calcium nitrate [265], calcium acetate [106], and calcium lactate [6]. The type of salt used affects the performance of the self-healing process. Calcium chloride ($CaCl_2$) was not optimal due to the production of chloride [265]. Calcium nitrate ($Ca(NO_3)_2$) was more appropriate as it is often employed as a setting accelerator or anti-freeze agent. It reacts with calcium hydroxide ($Ca(OH)_2$) to form calcium hydroxynitrate – a mineral with needle-shaped crystals that functions as a micro reinforcement for the cement matrix. However, it is unclear whether it can provide a sufficient amount of $Ca2^+$ ions [265]. Calcium lactate ($C_4H_6CaO_4$) was shown to improve concrete strength [6].

The viability of using calcium lactate as a deposition agent in comparison to urea was demonstrated by research in which calcium lactate of 0.5% of cement weight was added to the concrete mix [61]. Hydrolysing urea has the potential to generate large volumes of nitrogen and could elevate the likelihood that the steel reinforcement will be corroded [304]. Additionally, the urea could enable ammonium ions to be formed, which will result in environmental nitrogen loading [265]. Thus, it is necessary to optimise both the concentration and type of the source of calcium to make the process more cost-effective, prevent salt from being formed and maximise the amount of calcium carbonate produced.

A study that used bio-reagents incorporating calcium nitrate and urea additionally demonstrated the viability of the mineralisation process for self-healing concrete [35]. A total of 0.9 g of urea was utilised in the research along with 1.2 g of calcium nitrate. In comparison to [61], the volumes of both urea and calcium nitrate applied to the mixture were increased, which is approximately 1.2% of cement content. The findings indicated that the crack-filling process was more efficient in comparison to the sample without nutrients because the largest crack sealed was 0.5mm wide. Alghamri et al. [97] utilised a broth medium culture containing amounts of calcium lactate and urea of 80 g/l and 20 g/l, respectively. This was a lower volume in comparison to Tziviloglou et al [60] , who added 200 g/l of calcium lactate to their bacterial mixing solution. The purpose of nutrients like calcium nitrate, calcium lactate and urea is to facilitate the formation of calcium carbonate as a result of bacterial metabolic conversion [61]. The majority of studies indicate that white particles precipitate on the surfaces of cracks, which confirms the capabilities of carbonate precipitating bacteria. Further evidence of this was provided by research that involved the immersion of cracked mortar in a solution consisting of calcium gluconate and calcium lactate [305]. The findings suggested that the self-healing kinetic of the mortar was enhanced by both calcium gluconate and calcium lactate as a result of the increased accessibility of carbonate and calcium ions within the cracks.

The nutrients, which enable spores to germinate and offer a source that allows the bacterial cells to grow, also had an impact on the self-healing efficiency in addition to the characteristics of the concrete, particularly when directly incorporated into the concrete mixture [306]. For example, when calcium chloride is used as the source of calcium, this could lead to a chloride ion attack that will ultimately cause the reinforcement bars to be degraded. Hence, it is suggested that either calcium nitrate or calcium lactate are applied.

3.8.6 The efficiency of capsules

Encapsulation of the healing agent into spherical or cylindrical capsules increases the viability of bacteria within concrete specimens for an extended period of time [86].

Depending on their properties, the capsules are likely to ‘attract’ propagating cracks (Figure 3.7). When a crack propagates in a matrix containing particles, three possible fracture mechanisms are possible: (i) particle fracture; (ii) crack deflection; and (iii) interface debonding (shown in Figure 3.8).

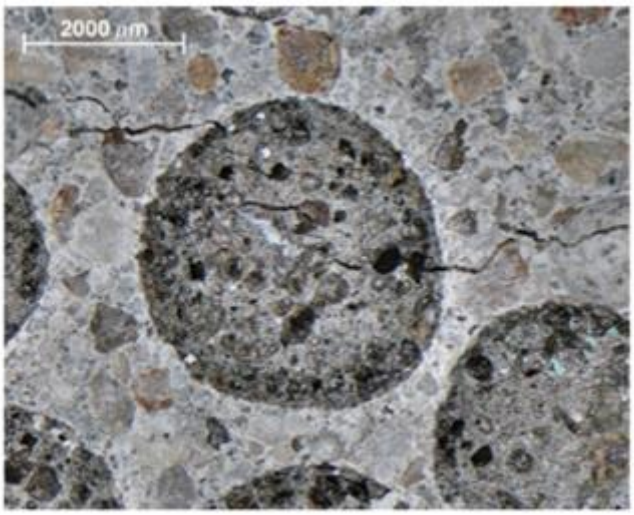

Figure 3.7: Change in crack direction as it moves through the capsule embedded within the mortar matrix [307].

Although a stiffer particle will generally ‘deflect’ a crack, it has been demonstrated, through experimental observations, that a particle fracture is another possibility [308]. In the prediction of crack-particle interaction, particle flaws, interfacial attributes and fracture properties serve an important function. Shells for mechanically triggered capsule-based self-healing systems are modified by using this information.

In order to establish the possibility of a crack intersecting a spherical particle or a capsule, probabilistic paradigms have been used in numerous studies [309, 310]. It has been revealed, through theoretical examination, that the volume of liquid that spherical capsules deliver scales with dosage, and also linearly with diameter [124]. Furthermore, it has been calculated that if elongated capsules are orientated properly, their use increases the healing potential for an identical volume fraction of spherical capsules (Figure 3.9).

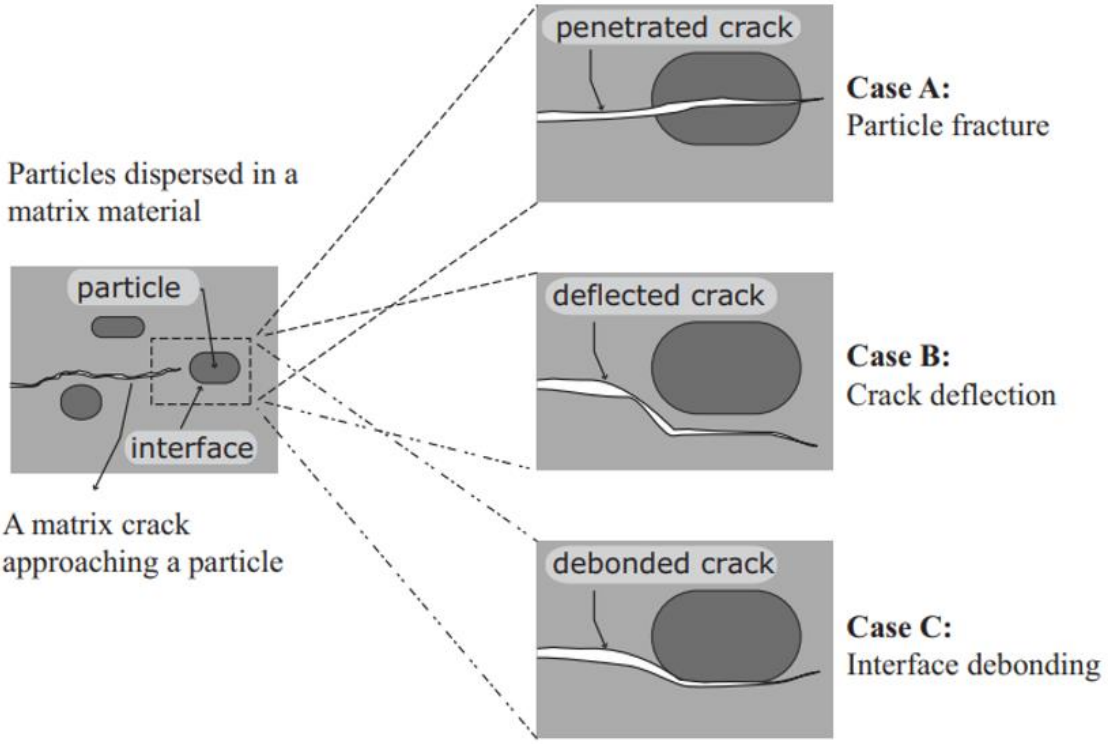

Figure 3.8: Possible fracture mechanisms of crack in a particulate system; (i) particle fracture; (ii) crack deflection; and (iii) interface debonding [308]

Nevertheless, there is also more probabilistic variation in the volume of the healing agent that is released. It is generally considered that, upon breakage, spherical capsules give a better and more controlled release of healing agent than elongated capsules do. Moreover, they reduce concentrations of stress around the void that remains from empty capsules [63]. Theoretical probability values do not consider the physical properties of concrete, although they are given a lower estimate of the number of intersected capsules [307].

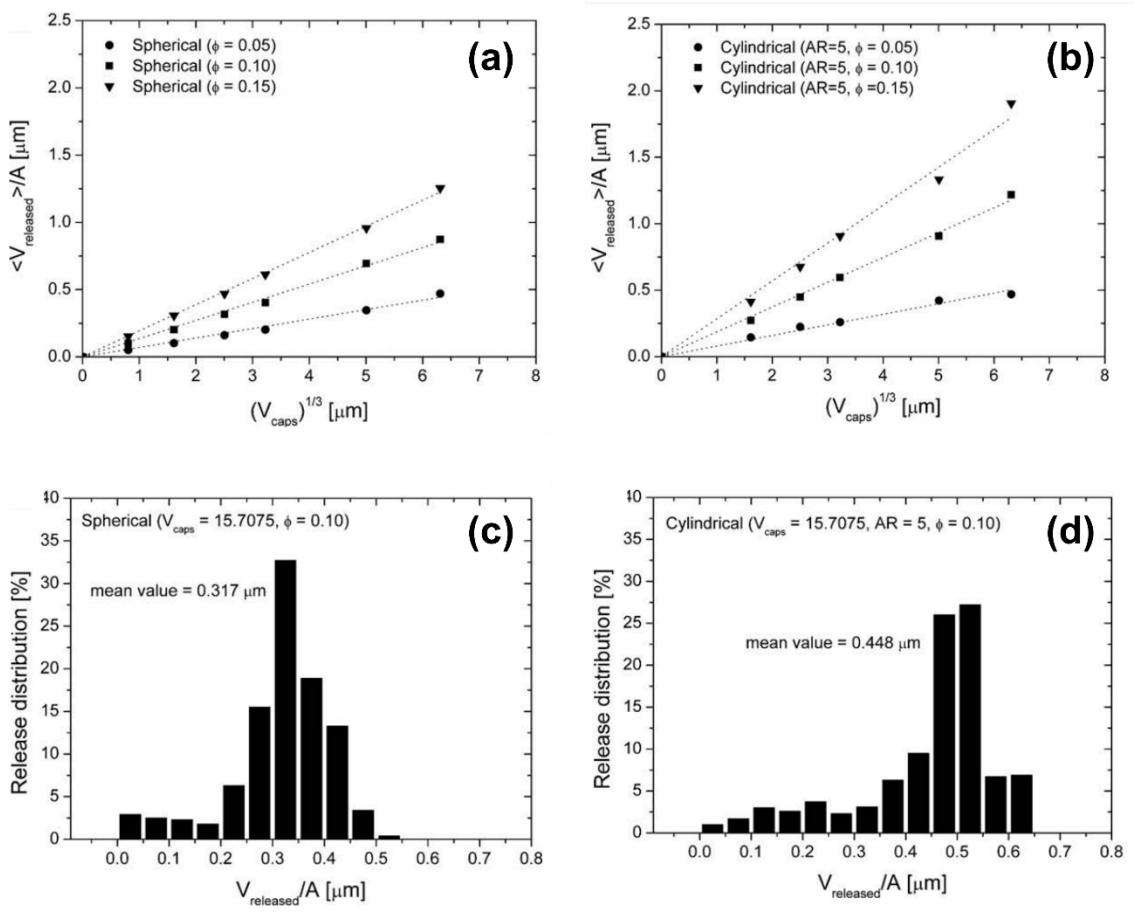

Figure 3.9: The effect of shape of capsules on volume of encapsulated healing agent released ($V_{RELEASED}$) per crack area (A) for different capsule concentrations of (a) spherical capsules and (b) cylindrical capsules where the greater distribution of the volume of healing agent released was observed for the cylindrical capsules in (d) as opposed to the spherical capsules in (c) for 1000 simulations [309]

3.8.7 Crack width

To ensure the durability and serviceability of the constituents of structural concrete, it is necessary to control the emergence of cracks as they permit water and other contaminating factors such as chloride or sulphate particles to enter into the concrete matric, thus initiating the early corruption of the network. It is vital to minimise cracks in concrete to increase its longevity and reduce maintenance requirements. Various researchers have investigated this aspect, with a primary focus on the effects of the self-healing of cracks [196, 282, 311].

The primary purpose of utilising microbial formulations is to induce the precipitation of $CaCO_3$ in order to facilitate the closure of small cracks via the direct addition of bacterial cells or spores into the cracks or embedding bacterial spores within the concrete, which have the potential to achieve growth when oxygen, water or moisture are present, along with nutrients and a precursor for the production of calcite that can promote the healing and sealing of cracks. Thus, it has been demonstrated that bacterial healing is beneficial for the recovery of the low permeability of concrete when applied to cracks that are micro-sized (or smaller). Past findings have indicated that it is possible to heal cracks up to 1mm in size in periods ranging between 3 and 14 weeks based on different factors such as the kind of bacteria, the volume and kind of biochemical agent, the biochemical processes and the width of the crack [102, 103].

Nuguroho et al. [312] demonstrated the sealing of cracks within cement mortar where bacteria was used as the self-healing agent, and the findings indicated that the bacterial self-healing agent was capable of efficiently sealing the cracks and preventing the flow of water up to 0.25 mm. Qian et al. [313] examined whether bacillus mucilaginous L3 was capable of healing samples with dimensions of 40 mm x 40 mm x 160 mm with w/c 0.4 cracks. The experimental findings showed that this method facilitated the complete healing of 50-100 µm cracks. Basically, via the inclusion of preserved bacterial spores and additional nutrients within the samples of mortar, it was possible to fully seal cracks with a width of up to 460 µm within 100 days [95]. Furthermore, the microbial precipitation of calcite via the ureolysis pathway allowed cracks with widths up to 970 µm to be mostly sealed after being immersed in water for 56 days [103]. According to the findings of Erşan et al. [177], the largest cracks they healed using bacteria in 28 days and 56 days had widths of 370 ± 20 µm and 480 ± 16 µm, respectively. Up to 85% of water tightness was recovered at the culmination of the 56-day period for a crack with a width of 465 ± 21 µm.

Conversely, a novel approach was developed for controlling the width of cracks by researchers from Cardiff University, which involves the generation of internal pre-stressing to either extant cracks to be either closed or narrowed, thus allowing them to be healed using a bacteria-based self-healing microcapsules system [314].

It was reported from previous studies that microorganisms can heal crack widths ranging from 50 µm to 970 µm. However, most of the crack widths that can be healed autogenously are limited to less than 100 µm and preferably less than 50 µm [315, 316].

3.8.8 The effect of incubation condition

The microbial precipitation of calcium carbonate has been observed in environments where concrete structures can be incubated, such as seawater [317], soils [318], and saline lakes [319].

After generating cracks, concrete specimens are exposed to certain incubation conditions, which represent the surrounding environment of application or are compatible with healing compositions. The incubation conditions for concrete specimens are a significant factor in the mechanism of bio-self-healing. In the majority of previous studies, successfully healed specimens have been either fully submerged in water for the entire incubation period or subjected to wet-dry cycles. For instance, Wang et al. [35] tested self-healing efficiency by subjecting the cracked samples in wet-dry cycles for four weeks. The specimens were immersed in tap water for 1 hour and then exposed to air with 60% RH for 11 hours at a temperature of 20°C. Although the contact time between the specimens and water was reduced to 2 hours per day, self-healing efficiency was achieved. Luo et al. [109] investigated three different incubation conditions: (1) immersion in water; (2) 90% RH; and (3) wet-dry cycles. The temperature for all three incubation conditions was 25℃. During incubation the specimens were immersed in water for 12 hours and exposed to air for 12 hours. The results revealed that healed cracks were observed for specimens incubated in water and dry-wet cycles. By contrast, no healed cracks were observed for specimens incubated in dry conditions. This is because carbonation needs a suitable medium to give the carbon dioxide a chance to dissolve, and therefore the concrete will maintain the pH at a higher level. As a result of the lack of water in certain practical situations, the use of a hydrogel as a carrier (protection) for the bacterial spores in the mixing and hydration process to serve as a water vessel was suggested. Samples containing hydrogel and bacteria exhibited a significantly enhanced ability to heal cracks. Complete healing of cracks less than 0.3 mm wide was achieved. For cracks with widths between 0.3 and 0.4 mm, the proportion

of healing ranged between 40 and 90%. The largest crack healed had a width of 0.5 mm [103].

In general, either distilled water or tap water is utilised, but it may additionally contain aggressive materials like dilute chloride solution [22, 320, 321] and de-icing salts [322]. For example, the crack healing capacity of bacteria-based techniques was investigated in a low-temperature marine environment by Palin et al. [99]. The samples were submerged in artificial sea water at a temperature of 8°C for 56 days. The results showed that the permeability of 0.4 and 0.6mm wide cracks decreased by 95% and 93% respectively. As well as aggressive materials, water can also potentially contain a favourable agent, such as a nutrient source that can trigger bacterial activity. Xu and Yao [112] investigated the efficiency of self-healing for specimens submerged in a medium containing bacterial spores, yeast extract, and calcium source. The results showed that crack widths ranging from 0.1 to 0.4 mm were completely sealed by calcium carbonate. Table 3.2 summarising the different healing incubation conditions and the healing efficiency for different studies.

Table 3.2: Overview of crack healing in concrete in different incubation

Type of bacteria	Incubation condition	Incubation period (weeks)	Crack width healing (mm)	References
Bacillus phaericus	Immersed in water with wet-dry cycles	4	Up to 0.5	[35]
Bacillus mucilaginous	Immerged in tap water and exposed to the atmosphere with adequate supply of CO2	-	0.4	[111]
Bacillus sphaericus	submerged in water with wet-dry cycle	8	Up to 0.97	[103]
Bacillus sphaericus	Closed jar with R.H more than 90%	-	Not Applicable	[102]
Bacillus cohnii	Immersed in tap water	4	Up to 0.79	[68]
Sporosarcina pasteurii	wet-dry cycles	4	Up to 0.417	[263]
Bacillus sphaericus	submerged in urea and demineralised water	4	0.45	[264]
Not Applicable	Immersed in tap water at room temperature	2	0.15	[6]
Not Applicable	Immersed in medium containing bacterial spores, calcium source and yeast extract	-	0.1 - 0.4	[112]

As shown in Table 3.2, the bacterial based self-healing technique for concrete has been tested in different incubation conditions. However, Luo et al. [109] found that the best results were achieved in water incubation. Several factors may have contributed to this, including the presence of moisture, dissolved oxygen (because it is important for bacteria to preserve high metabolic activity) [323], and partial pressure of carbon dioxide. Additionally, in some cases the presence of beneficial agents such as a carbon source can promote bacterial activity as the autotrophic pathways of precipitation

include oxygenic and anoxygenic photosynthesis and non-methylotrophic methanogenesis [283].

Luo et al. [109] also claimed that a self-healing agent could migrate to the crack surface for specimens incubated in water due to the difference in concentration between specimen compositions and the crack surface.

3.8.9 Duration of healing

In the studies reviewed, a broad range of different healing times can be observed, which has considerable dependence on the type of healing technique adopted. Capsules containing cyanoacrylate are capable of healing a crack in under one minute [20], whereas autogenous healing can persist for up to two years [134, 226] even though, as observed by In et al. [320] for samples immersed in a solution of artificial sea water and affirmed by Maes et al. [78], a vast proportion of the autogenous healing is achieved within 35 to 50 days. On the other hand, the activation of bacterial spores only occurs several days after water has entered as germination does not occur immediately. Wiktor and Jonkers [95] observed that bacterial crack healing was initiated 20 days after samples had been immersed in water and this persisted until the 100^{th} day of immersion. The technique used for delivering bacterial spores also plays a significant role. The direct addition of spores can accelerate the healing process as the spores are in direct contact with moisture when they ingress through cracks. By contrast, a certain amount of time is needed for encapsulated spores to be released from their carer, especially if the capsules are coated by protective materials.

3.9 Field application of self-healing concrete

Minimal research has focused on determining the degree of self-healing in practical applications. While self-healing could seem to have potential according to laboratory findings, such results are relatively meaningless without the application of self-healing methods presented in the literature to actual structures.

The first person who scaled self-healing concrete technologies to the field was Dry (1999) [324]. She cast four reinforced concrete bridge decks (approximately 1.2m x 6.1m x 76mm, w/c = 0.38), as well as one control deck and three with various glass fibres

comprising adhesives and sealant (Figure 3.10a). The transverse shrinkage cracking that was encountered by the bridge decks caused the embedded fibres to break. The fibres embedded in the concrete broke after one month; however, those exposed on the top surface did not, consequently causing a transverse line of repaired microcracks which generated a controlled expansive joint (Figure 3.10b). Furthermore, most capsules that embedded partially on the surface broke after two months. Subsequently, a pneumatic jack at mid-span was used at mid-span to create load-induced cracks after several months [121]. Repair adhesive flowed onto the surface when bridge decks were loaded to yielding. The bridge decks were reloaded after a longer period of time in order to test the effectiveness of the adhesives and sealant in repairing the load-induced cracks; also, the decks were loaded for the third time after another three weeks. In comparison with the control deck, all bridge decks that contained repair adhesives gained more strength. The two bridge decks that exhibited optimal performance had indications of newly opened cracks during reloading prior to the reopening of the initial cracks. Repair adhesives were re-released during the second and third loadings for all of the decks that contained such adhesives.

Content removed due to copyright reasons

Figure 3.10: (a) Casting reinforced concrete bridge decks with dimensions of 1.2m x 6.1m x 76mm, (b) release of repair sealant at the designed ‘expansive joint’ [325]

Via a collaboration with the Dutch firm Verdygo, a wastewater treatment tank was built in Limburg, the Netherlands utilising self-healing concrete. The materials used in the

construction of the tank were steel reinforcements along with prefabricated elements and its dimensions are 23 ft. X 5 ft. X 1 ft., (Figure 3.11) [326].

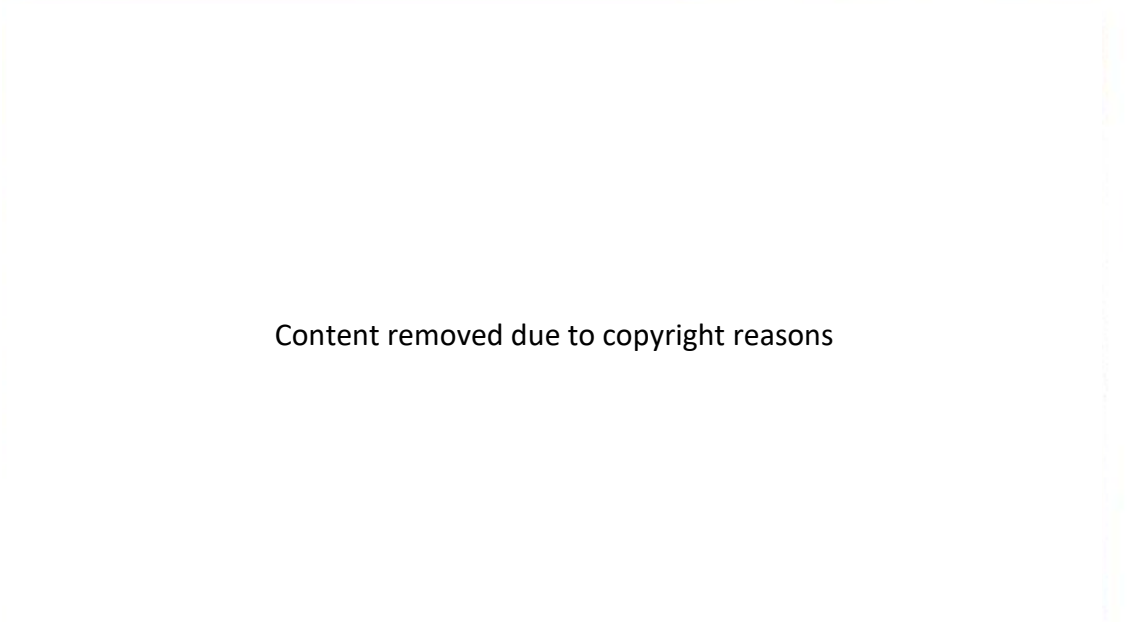

Figure 3.11: Concrete wastewater treatment tank in Limburg was casted using self-healing concrete [326]

Researchers from Delft University of Technology (TU Delft) are working on the development of self-healing concrete based on bacteria [114]. In this process, bacteria are included in the concrete mix, which metabolises the added calcium lactate to generate calcium carbonate. Several large-scale field experiments have been conducted by the research group, the first of which consisted of the implementation of 3m-long concrete linings in an irrigation channel in Ecuador (Figure 3.12), which contained lightweight aggregates with alkaliphilic spore-generating bacteria embedded. The cast concrete exhibited no indications of cracks or degradation after five months, meaning that it was not possible to assess its healing effectiveness.

Content removed due to copyright reasons

Figure 3.12: Using lightweight aggregates impregnated with alkaliphilic spore-forming bacteria in irrigation canal [327]

The first implementation of self-healing concrete in a structure was performed by the TU Delft group (Figure 3.13). This involved the construction of a lifeguard station using bacteria-based concrete. Nevertheless, it was not possible to find any results in the literature in terms of its current performance.

Content removed due to copyright reasons

Figure 3.13: A lifeguard station constructed with bacterial-based concrete [328]

As a result of the accomplishments of a limited study conducted on a garage in Vlissingen, the Netherlands, a similar self-healing liquid repair system was implemented in two stages in the construction of an intermediate floor in the Parking Garage Apeldoorn [329]. The objective of this study was to stop the intermediate floor leaking and ensure that vehicles and the reinforcement were not damaged. The project involved the use of a bacterial liquid repair system covering an overall area of 12,000 m^2. The initial stage was implemented in October 2014, followed by the second stage in March 2015. Each of the floor areas had an identical surface area of 50,165 m^2 [330]. The selection of the liquid repair system was made as it allowed external application at low pressure compared to standard injections that have the potential to harm the extant polymer topcoat [329]. A different application was used in each stage, where scrubbing machines were used to apply the liquid solution to the first area (Figure 3.14a), and high-pressure spraying equipment was utilised to distribute the solution over the second (Figure 3.14b). enabled the liquid to facilitate the required calcium carbonate production. Hence, it was necessary to apply several layers to the topcoat to ensure that the bacterial liquid applied was not unevenly distributed.

Content removed due to copyright reasons

Figure 3.14: (a) Application of bacterial liquid with scrubbing machines, (b) Application of bacterial liquid with hand-carried spraying device [329]

Basilisk Concrete presented findings showing clear results after six weeks, as limestone had formed within drilled cores, where a vast proportion of the limestone was found at greater depths in the cracks. Additional research showed that water penetration was

reduced. Up to 6 months later, no wet spots were detected on the surfaces, even after periods of rain.

Throughout the period of implementation, various tests were conducted to assess the performance of the bacterial liquid. Testing of the repair system was conducted periodically to analyse the extent to which water had penetrated at the location of the crack. This process involved the placement of wooden frameworks at particular sites on the floor. A total of 8.8 L of water was used to fill these frames and testing of the water penetration rate was performed in line with a protocol whereby the amount of continuous drops each minute was recorded. Before applying treatment to the tracks, a measurement of 45 drops per minute per crack (200µm to 300µm wide) was registered. However, four months after the treatment had been applied, this measurement was lowered to only one drop per minute [329].

3.10 Concluding Remarks

This review reported recent research on the autonomic self-healing mechanism of cementitious materials. It focused on factors that affect the performance of self-healing, the main findings of which were as follows:

- In contrast to chemical agents, bacterial agents have the ability to reduce steel corrosion by consuming oxygen, which increases the chance of corrosion.
- In previous studies, pH was mostly investigated in terms of its effect on the growth of bacteria. However, there is not enough information on the effect of the pH of the surrounding incubation conditions on healing performance.
- In previous studies, bacterial based self-healing was primarily explored under submerged conditions, including immersion in tap water, marine environment, urea and demineralised water, and dry and wet cycles. However, to the best of the author's knowledge, no previous research has investigated the healing behaviour of self-healing concrete in ground conditions.
- The research conducted in this thesis will investigate the effect of the different incubation of ground conditions on healing ability.

Chapter Four

Experimental Programme: Materials and Methods

4.1. Overview

This chapter is divided into two sections. The first section describes the materials and methods used to prepare the cement mortar specimens and the bacterial healing agent. The second section covers the testing methods and procedures carried out to assess the efficiency of self-healing. These included the tests used to assess the self-healing performance quantitatively (i.e., compressive strength tests, water permeability tests, water absorption tests, and light microscope to monitor crack closure process) and also the methods used to assess the self-healing performance qualitatively such as Scanning Electron Microscope (SEM) and Energy Dispersive X-ray diffraction (EDX). The flowchart illustrated in Figure 4.1, shows the outline of the experimental program adopted for this research.

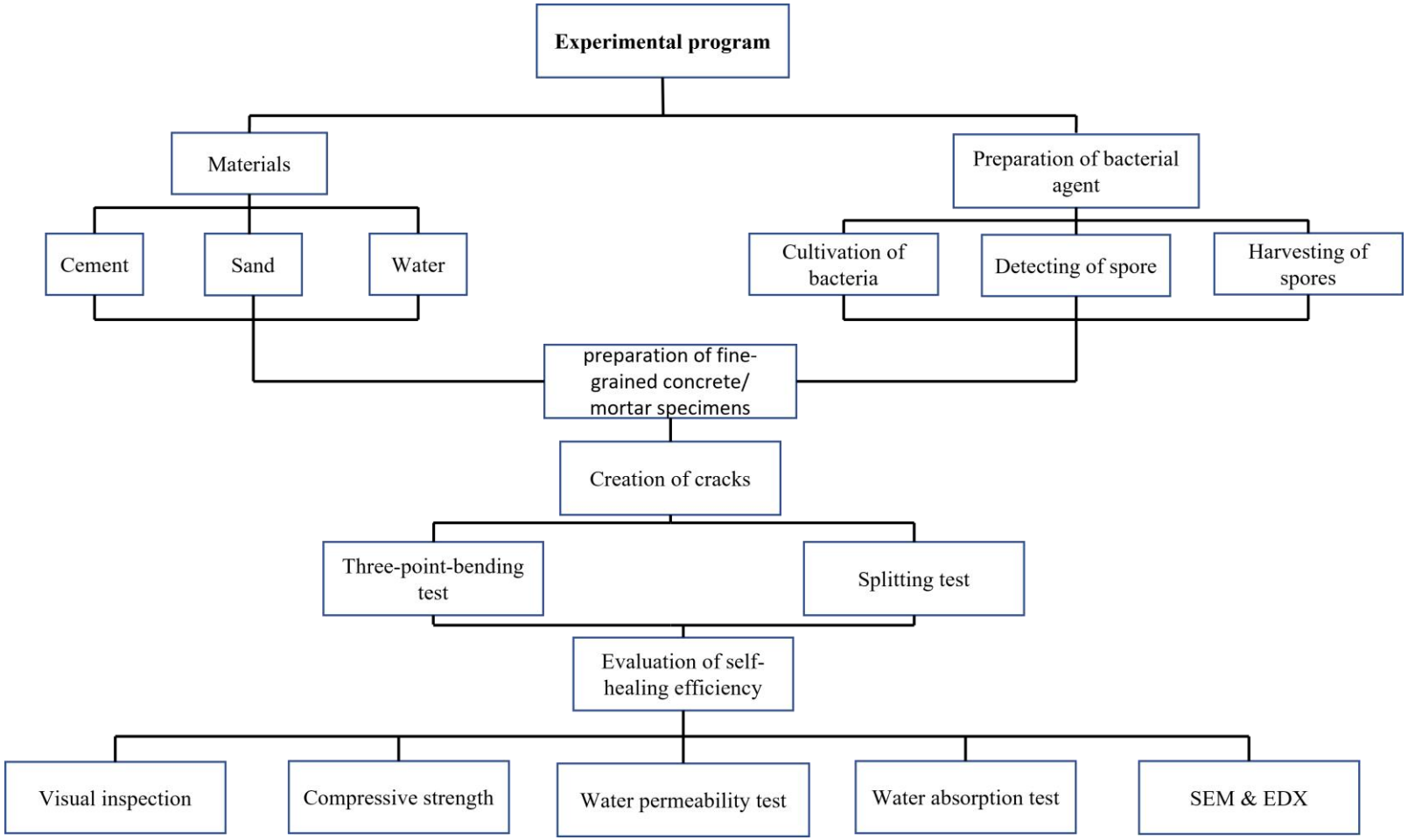

Figure 4.1: Flowchart shows the outline of the experimental program

4.2 Materials and preparation of cement mortar specimens

4.2.1 Cement

The Blue Circle Cement was used for the preliminary phase of this research. It is Ordinary Portland cement (Type I Portland cement, commercially available in the UK) and a quality-assured requirement of EN 197-1:2000 (BS EN197-1:2000 CEM II/A-LL 32,5R). The cement is used for making conventional concrete, and suitable for general purposes i.e., for use in concrete, mortars, renders, screeds, and grouts.

For the main phase of testing, where specimens are incubated into the soil with expected sulphate attack, the Hanson Sulphate Resisting Cement (CEM III/A +SR supplied from the UK) was used to limit the ettringite form of sulphate attack. The cement's quality meets the requirements of BS 8500 Part 2 Concrete – Complementary British Standard to BS EN 206-1 Part 2: Specification for constituent materials. Sulphates (which may present in groundwater and soil) react with the tri-calcium aluminate (C_3A) existing in most Portland types of cement resulting in deterioration of the concrete. In order to minimise the risk of this reaction, Hanson Sulphate-Resisting Cement is manufactured with low ratios of tri-calcium aluminate.

4.2.2 Fine Aggregate (Sand)

The fine aggregate (used for producing cement mortar) is comprised of sand with a maximum particle size of 2 mm and Specific Gravity of 2.63. The sand is commercially available, and it was sourced from Travis Perkins in the UK. In cementitious composites, sand can enhance the compaction, maximises the bond strength, and provides a good casting finish.

The particle size distribution of this sand was examined using a standard sieve test (BS EN 933). The sieve test (Figure 4.2) indicated that the sand has a uniform distribution, with 90 to 95% of the material between 150 µm to 2.36 mm and only around 5 % smaller than 63µm.

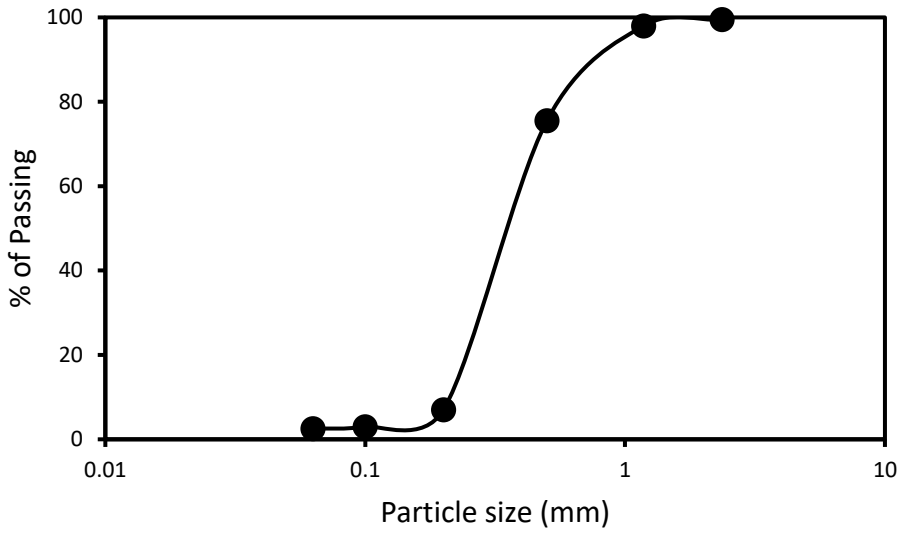

Figure 4.2: Particle size distribution of the fine aggregate

4.2.3 Physical properties of light weight aggregates

In this research, lightweight aggregate (Perlite) has been added to the cement mortar as a carer to protect the bacterial agents. As with any other additive materials, perlite may influence the mechanical properties of soft and hardener concrete. Therefore, some of the properties of the perlite (that influence the concrete/mortar characteristics) were investigated as follow:

- Sieve analysis according to BS EN 933-1:2012 [331]: In this test, the grain size distribution of aggregate particles is typically found by illustrating the relationship between the percentage of passing and sieve opening size in semi-log scale.

- Unit weight of aggregate: which can be defined as the weight of the aggregate required to fill a container of a specified unit volume. This test is usually carried out according to BS EN 1097-3:1998 [332].

- Apparent density: This can be defined as the ratio between the apparent volume and dry specimen mass of a perlite sample.

- Absorption and surface moisture according to BS EN 1097-6:2013 [333]. In this method, a pyknometer is used to find out the particle densities and water

absorption of lightweight aggregates, using a soaking time of 24 h. The absorption rate can be defined as the difference between the weight of oven-dry aggregate and the weight of fully saturated and dry surface aggregate conditions.

4.2.4 Water

The water used in this study was tap water. Neville [65] stated that "there is no clear standard for the quality of mixing water. However, it should be clean water and does not include significant organic or inorganic substances".

The pH test of the tap water was inspected using a handheld device, and the measurement confirmed that the pH value is approximately 7.

4.3 Preparation of bacterial agent and growth medium

4.3.1 Cultivation of bacteria

It is important that, in the bio self-healing mechanism, the bacterial agent ought to be able to transform organic nutrients into insoluble inorganic calcite crystals, thereby blocking the cracks. Any used nutrients and bacteria for effective crack healing ought not to disturb the integrity of the concrete matrix, neither should they have an adverse impact on other hardened and fresh attributes of concrete.

Many types of bacteria have been employed in self-healing concrete studies by different researchers such as *Bacillus alkalinitrilicus* [95], *Bacillus cohnii* [68, 106], *Sporosarcina pasteurii* [263], *Bacillus subtilis* [108, 334], *B. pseudofirmus* [106] etc. In this study, *Bacillus subtilis* H50620/9 (supplied by Philip Harris, UK) was utilised. It was selected based on prior literature [108, 334] using similar strains and that this is primarily driven by the ability of this genus to form long-lived resistant spores and also this type of bacteria has the ability to produce calcium carbonate. The Bacterial strains were cultivated in three different liquid media. The ingredients of the selected three growth media (GM1, GM2 and GM3) were used in proportions similar to those reported in the literature by other researches [96, 108, 335], respectively.

The ingredients of the growth media were summarized in Table 4.1. After adding the stated amounts of the compositions to a clean glass bottle containing one litre of

distilled water, the liquid medium was sterilized by autoclaving it at 120 °C for 20 min. The medium was left until its temperature matched the room temperature and later was filled in 100 ml labelled flasks covered with silver foil. The culture was incubated in a shaker at (36 °C, 120 rpm) for 72 hours until spores were formed as shown in Figure 4.3.

Table 4.1: The amount of the compositions of growth mediums

Components (g/l)	G.M1	G.M2	G.M3
peptone	-	-	5
meat extract	-	-	3
Calcium acetate	5	-	-
Manganese sulfate	0	-	0.01
Yeast extract	1	-	-
nutrient broth (Difco)	-	8	-
KCl	-	1	-
Magnesium sulfate	-	0.25	-
Buffering components			
$Ca(No_3)_2$	-	10^{-3} M	-
$MnCl_2$	-	10^{-4} M	-
$FeSo_4$	-	10^{-6} M	-
100 mM $Na_3C_6H_5O_7$	5.2	-	-
50 mM $NaHCO_3$	4.2	-	-

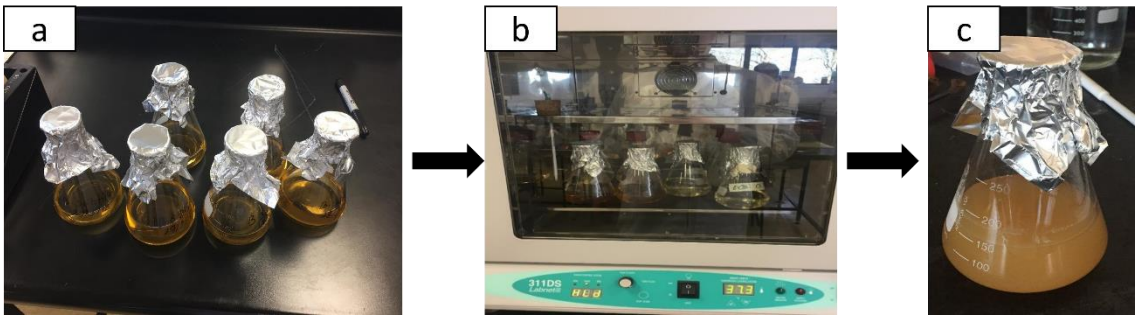

Figure 4.3: (a) Cultivation of *B. subtilis* in jars containing 100 ml of growth medium, (b) Incubation of the medium in a shaker at (36 °C, 120 rpm), (c) Formation of bacterial spores after 72 hours of incubation.

4.3.2 Detecting the spore formation by using Spore Stain Method (SSM)

In this research, the Spore Stain Method (SSM) was used to assess sporulation before using the bacterial culture as described by James and Natalie [336]. The use of microscopy to visualize spore formation is considered the most significant technique to evaluate sporulation. The used materials and test procedures are explained as follow:

4.3.2.1 Materials and tools

These tools include Malachite green, aqueous Eosin, glass slides, burner, torch, streaking loop, culture media, and microscope (LABOPHOT-2, Nikon).

4.3.2.2 Procedures

- Sterilize the table surface by using ethanol and clean tissues.
- Sterilize the streaking loop by passing it over a burner until the loop gets red.
- Place a drop of bacterial culture over apportion of the glass slide and smear the drop by using the streaking loop.
- Fix the smear by passing the glass plate over the burner 3 to 5 times.
- Place the glass slide on a staining rack and flood the fixed smear with 5% aqueous malachite green solution.

- Apply heat to the underside of the slide by using the torch until the stain starts to steam. Once the stain begins steaming, keep applying the heat under the slide for 5 minutes and make sure not to boil the stain.
- Cool the slide at room temperature and wash it gently with tap water.
- Flood the slide with 5% of aqueous Eosin and leave it for 2 minutes.
- Rinse the slide with tap water and blot it dry.
- Examine the slide under the microscope (LABOPHOT-2, Nikon) with an oil immersion lens. The spores strain appears in green whereas the vegetative cells strain appears in pink as shown in Figure 4.4.

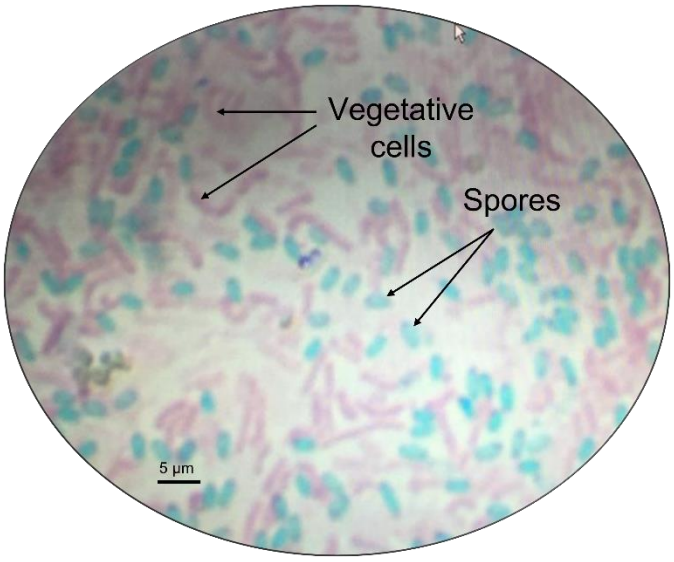

Figure 4.4: Identification of spore formation under the microscope

4.3.3 Harvesting and washing of spores

To minimize the presence of vegetative cells, spores were harvested with the use of a centrifuge machine, where the culture was filled in 50 ml falcon tubes and then spun at very high speed (3390 RCF) for 10 min and then washed twice using distilled water. The centrifugal force causes heavier particles to move away from the axis of rotation, resulting in the deposition of spores at the bottom of the test tube forming what is

known by a pellet., and the remaining solution was taken out of the tube. The spores were washed by adding distilled water twice to the spores (See Figure 4.5).

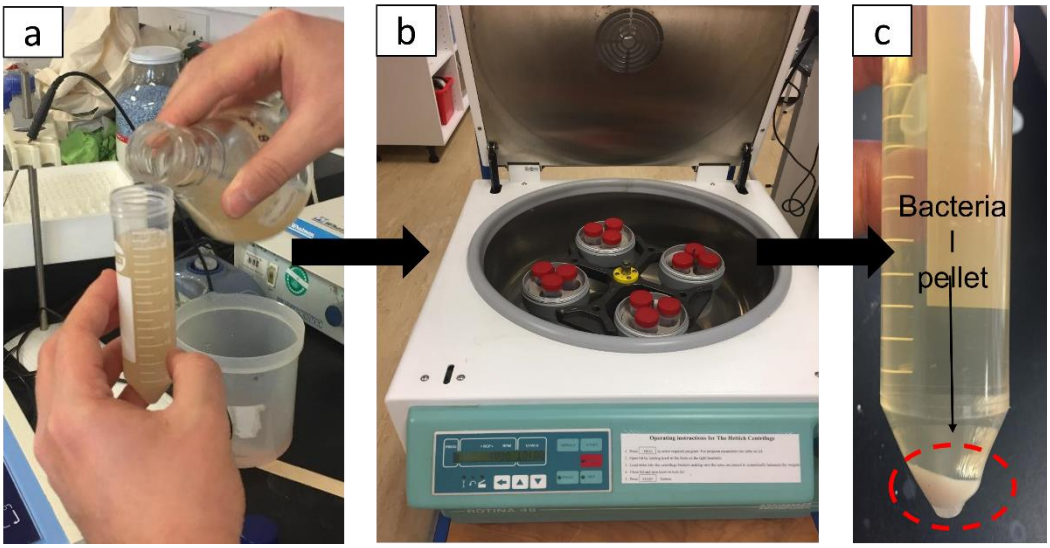

Figure 4.5: The process of spores harvesting using a centrifuge machine. (a) Filling falcon tubes by bacterial culture, (b) Harvesting the spores using a centrifuge machine, (c) Deposition of spores at the bottom of the tube after the centrifuging process

4.3.4 Colony Forming Unit (CFU)

Colony Forming Unit (CFU) is a microbiology term used to measure the viability of bacterial spores either if they are in suspension or encapsulated. In the direct microscopic counts' method, all cells including dead, and living are counted, whilst CFU measures only viable cells using the serial dilutions method. In this research, the number of bacterial colonies was estimated using serial dilutions according to James and Natalie [336].

4.3.4.1 Materials and tools

A nutrient gar plates, burner, culture media, pipet, and glass spreader rod.

4.3.4.2 Procedures

- Serial dilution was prepared by using Phosphate Buffered Saline (PBS) bottles (10:1).
- The bacterial suspension was diluted into a series with a 10-fold dilution by adding 1 ml of bacterial suspension to 9 ml of PBS to produce the first dilution 1/10.
- The second dilution was made by adding 1 ml from the first dilution to 9 ml of PBS to produce the second dilution 1/100, as shown in Figure 4.6.
- The last step was repeated until the dilution of $1/10^9$.
- 100 µml of each dilution were plated in two agar plates and then incubated at 36 ℃ for 24 hours.
- The CFU is calculating by using this formula:

$$CFU/ml = N_p \times D_f \times P_{0.1} \quad (4.1)$$

Where:

N_p = the number of colonies on the plate

D_f = the dilution factor

$P_{0.1}$ = the plated dilution out of 0.1 ml

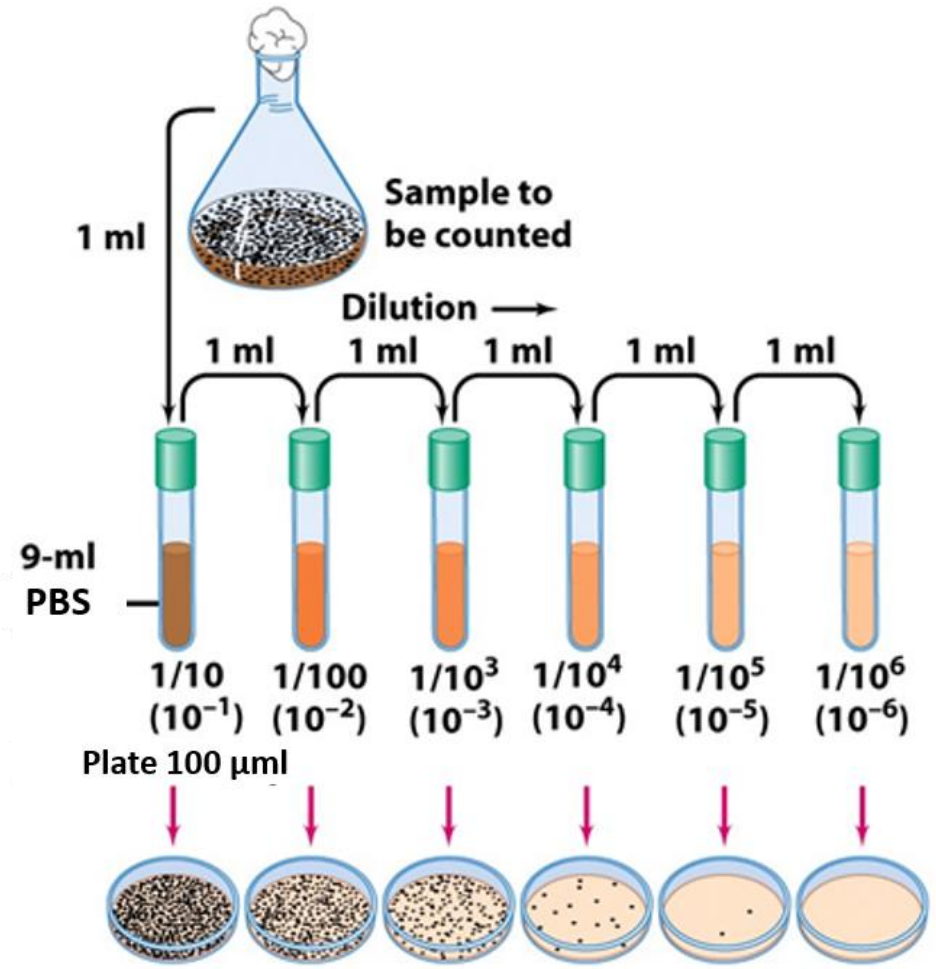

Figure 4.6: Preparation process of serial dilution test [336]

4.4 Preparation of cement mortar specimens

4.4.1 Mixing and casting process

After weighing out all of the mixed ingredients in the correct proportions (See Table 5.4) by using a digital scale, the mixing procedure was carried out according to BS EN 196-1 [337]. The cement mortar specimens were prepared by mixing the cement with water in a digital mortar mixer (Controls Testing Equipment Ltd, Figure 4.7) for about 30 seconds at a low speed (140 ± 5 r/m). Then, the sand was added gradually to the cement paste, and the mixing continued for 30 seconds with high speed (285 ± 10) - according to Table 2 BS EN 196-1 [337]. The mixer was stopped for one minute to scrape the adhering paste from the mixer's walls, and then it was operated again at high speed for two minutes.

Figure 4.7: Mixer used to prepare the cement mortar specimens

After the mixing, the mortar was cast in three different moulds' geometries: prisms (40mm x 40mm x 160mm), cylinders (Ø100mm x 40mm), and cubes (40mm x 40mm x 40mm). These geometries accommodate the three different testing adopted in the experimental programme. Figure 4.8 shows the three moulds and specimens.

The prisms specimens were reinforced by placing a fibre mesh at the mid of the specimen to avoid any failing during the propagation of cracks. During the casting, the specimens were gently compacted by using a special rod and vibration table to remove any trapped air in the cement mortar and then followed by levelling the top surface of the specimens to smooth it up by using a spatula. The moulds (with the specimens) were covered with wet cloths and left for 24h in a curing room, where the air temperature and humidity were about 23℃ and 50-55%, respectively.

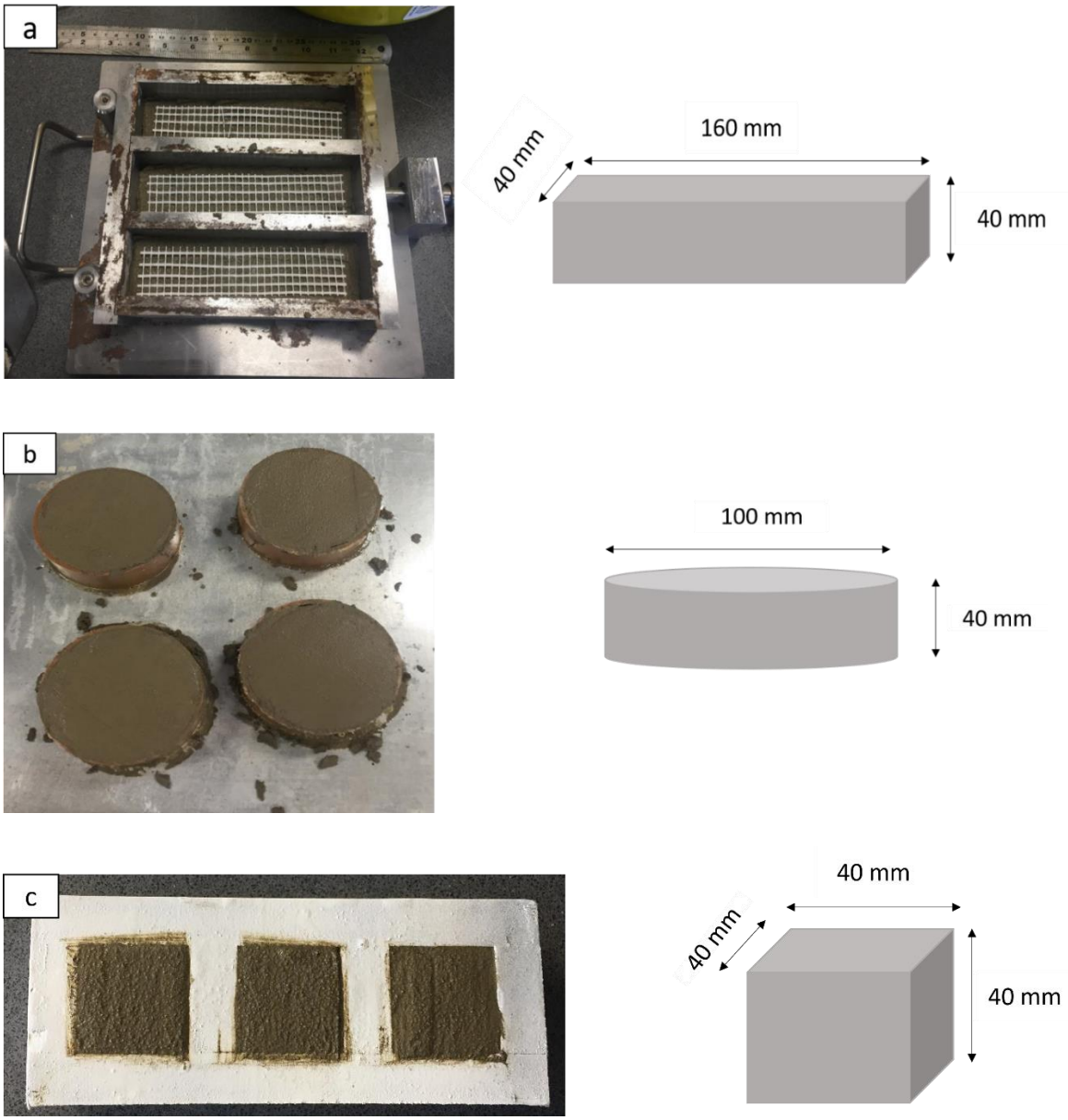

Figure 4.8: Casting and levelling of mortar specimens (a) Prisms, (b) Cylinders specimens, (c) Cubes

4.4.2 Demoulding and curing of specimens

Curing is one of the most significant steps performed after casting specimens. The specimens must be carefully cured to achieve their maximum potential strength. Inevitable collapse during the process of crack creation under stresses is possible, if the specimens could not achieve appropriate strength.

In this study, the 24h old specimens were removed from their moulds using a hand drill to remove the screws. After the demoulding, the specimens were labelled and then immersed in water at 20°C for 28 days. The water of the tank (in which the specimens were cured) are regularly renewed every seven days.

Figure 4.9: Cement mortar specimens after demoulding

4.5 Creation of cracks

The mortar specimens were cracked using two different methods that suit their dimensions and shapes. These methods are explained as follow.

4.5.1 Three-point-bending test

After 28 days of curing, the prismatic specimens were wiped out of the water, dried at room temperature, and then subjected to mechanical testing using a three-point-bending test to generate cracks. The prism was installed at two parallel beams at the bottom of the sample (specimen), with the distance between these beams measuring approximately two-thirds of the sample's total length. The top surface of the sample was compressed by one central beam, as shown in Figure 4.10. The induced cracks were controlled via Linear Variable Differential Transducers (LVDT) attached to the bottom of the specimens. The load was applied gradually with a velocity of 0.001 mm s^{-1} until a crack was formed. The velocity was then decreased to allow the crack to be formed

around the specimen without failing it, and then the specimen was unloaded, giving cause to a decrease in crack width.

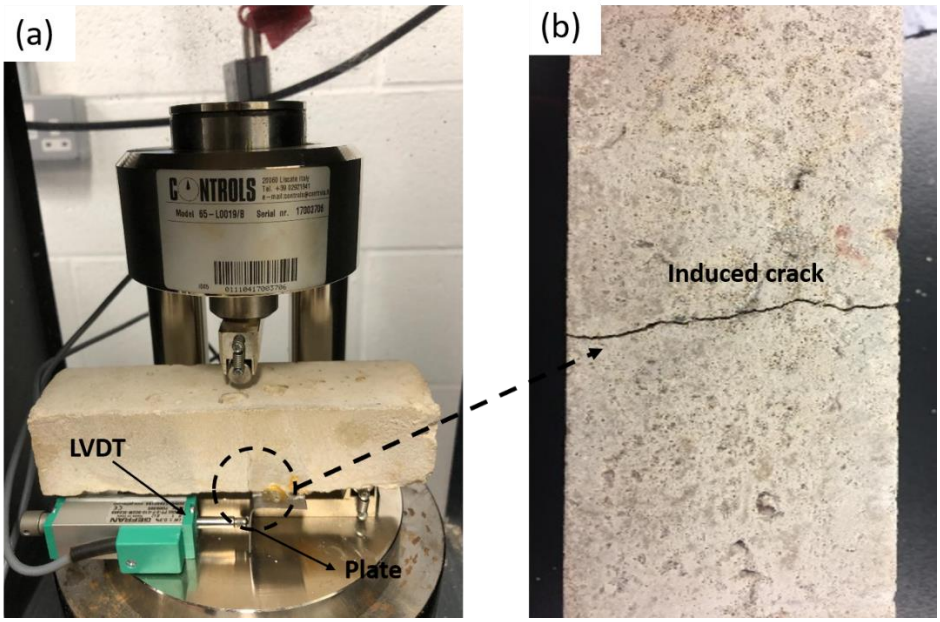

Figure 4.10: Automatic compression machine used for the three-point load bending test to generate initial cracks (a) Installing a prismatic specimen between the parallel beams (b) The specimen after crack creation

4.5.2 Splitting test

After 28 days of curing, the cylindrical specimens were wiped out of the water and then dried at room temperature before cracking them using the splitting test. In preparation for this test, the cylindrical specimens (of 100 mm in diameter and 40 mm in thickness) were wrapped with carbon fibre adhesive tape to prevent collapse during the process of crack creation under indirect tensile stresses. After placing the specimen horizontally between the upper and bottom plates in the uniaxial compressive strength test machine, the machine was turned on and operated with a low speed of 0.001 mm s^{-1} until a crack was formed on both sides of the cylinder as shown in Figure 4.11. At this point, the loading was stopped immediately.

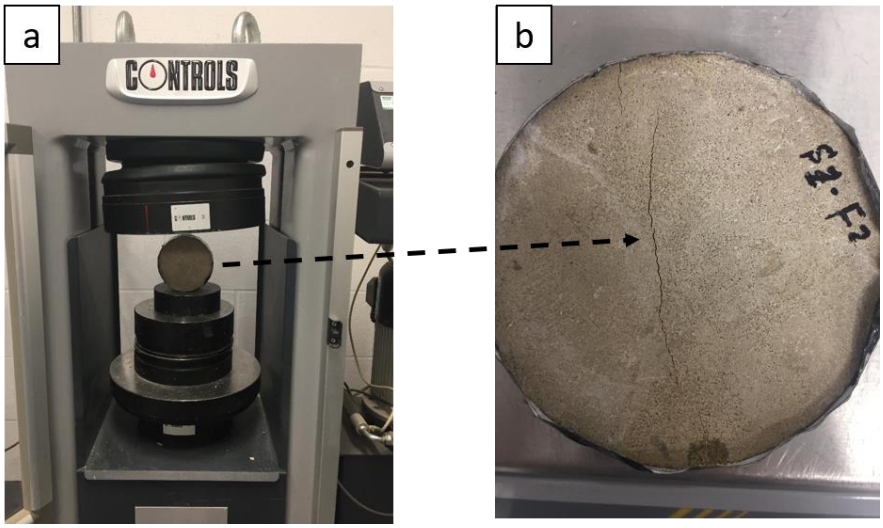

Figure 4.11: Automatic compression machine used for the splitting test (indirect tensile test) to generate initial cracks: (a) Installing a cylindrical specimen between the upper and bottom plates (b) The cracked specimen

4.6 Evaluation of self-healing efficiency

According to recent studies, several techniques have been used to evaluate the crack closure, i.e., assess quantitatively and qualitatively the efficiency of self- healing. For quantitative assessment, different experiments have been adopted, such as concrete compressive strength, water permeability, ultrasonic measurements, chloride ion permeability, uniaxial tensile test. The qualitative assessment of the efficiency of self-healing concrete has been conducted visually by taking imaging using electronic microscopes or by more advanced techniques such as Scanning Electron Microscope (SEM) and Energy Dispersive X-ray (EDX) technologies. In this study, the following methods/experiments were adopted as follows:

4.6.1. Visual inspection

The visual inspection of crack closures was conducted under a light microscope (Nikon, Japan). Immediately after the cracks were created, each crack was marked up at 3 to 4 positions, distributed homogeneously along the crack length. Before the incubation process commenced, initial images were taken. Additionally, final photos were taken

after specific lengths of incubation. In each image, crack width at each position nearby the marker were measured using Shuttlepix Editor software (Figure 4.12).

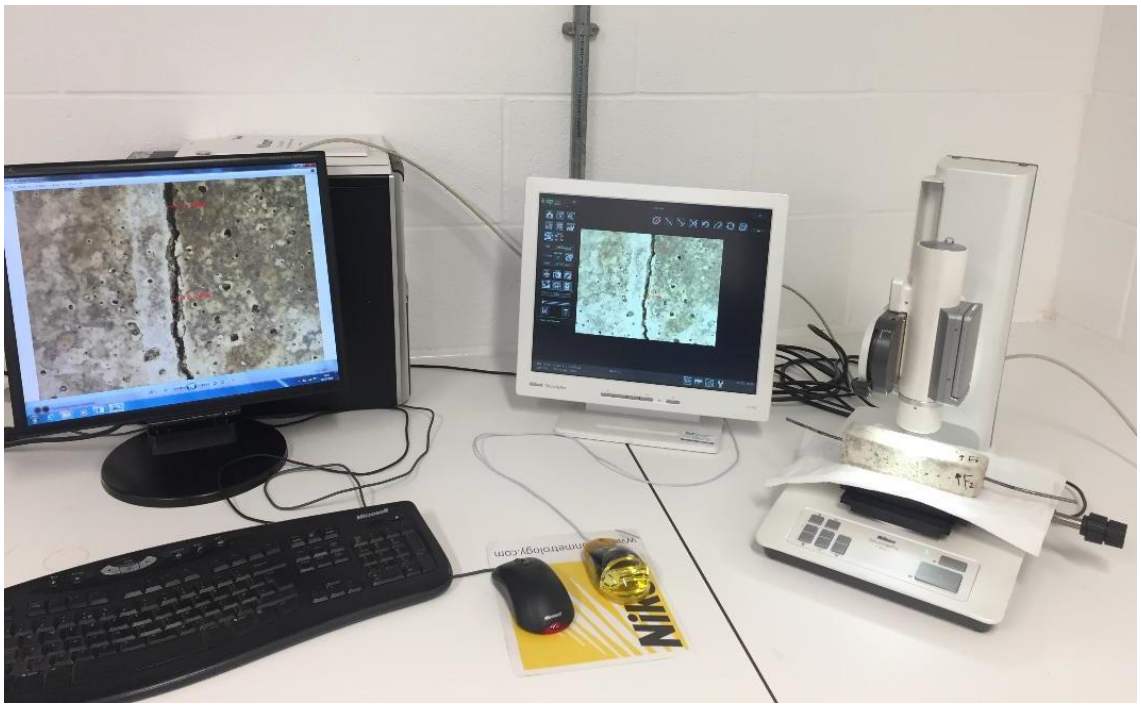

Figure 4.12: Visual inspection of a cracked specimen under the microscope (Nikon)

The assessment of the healing performance has to start from quantification of the crack closure, comparing the area of cracks before and after the incubation [322]. Therefore, in this research, the crack healing ratio was evaluated using an image processing programme called “image j”. Image j is a general image processing program that enables the users to measure distances, angles, creates density histograms and analyse images.

The healing percentage was taken as the decrease in area fraction corresponding to the cracks present in a microscopic image after incubation. The healing percentage was calculated using equation 4.1. As shown in Figure 4.13, cracks are identified by the black pixels of the images and at 400 magnifications, each pixel is equivalent to approximately 200µm.

Figure 4.14 shows an example of a comparison between area of cracks before and after the healing period.

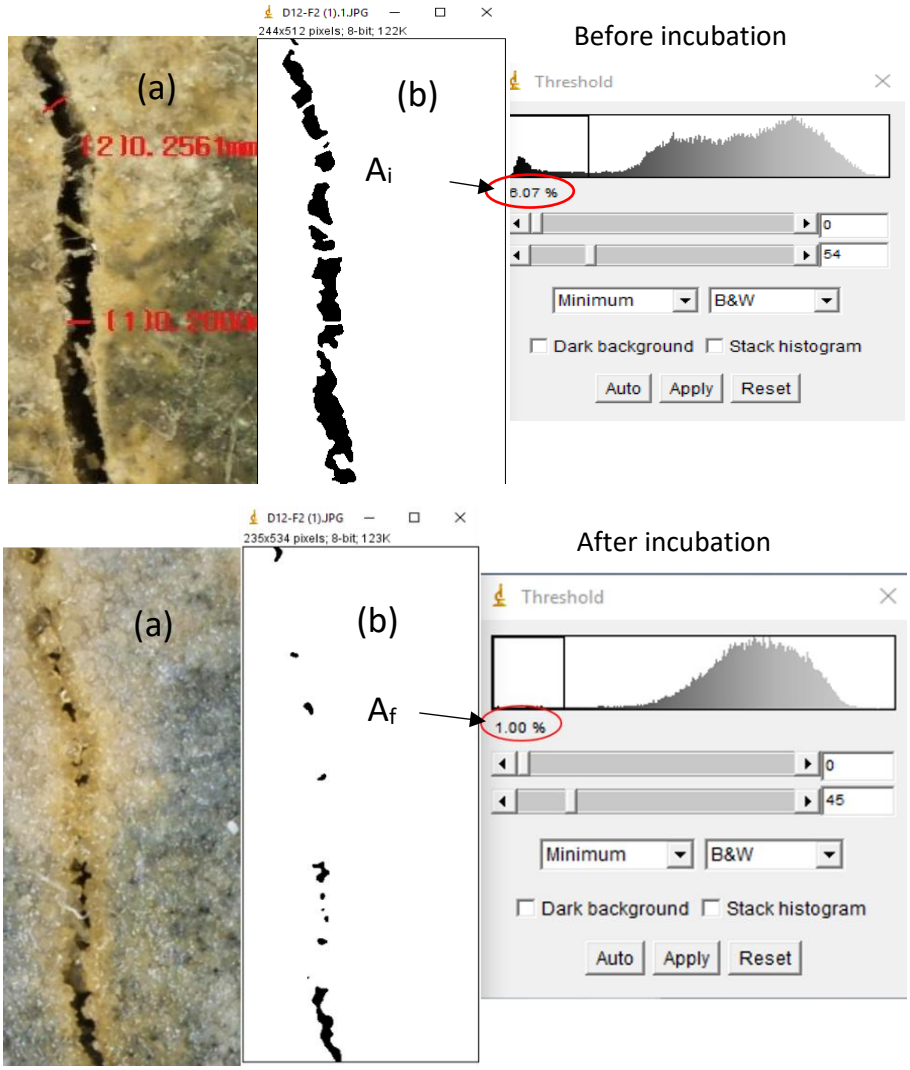

Figure 4.13: Analysis of crack images before and after incubation using image j programme. (a) Cracks under the microscope, (b) Binary images of crack

$$Healing\ ratio\ \% = \frac{Ai - Af}{Ai}\ x\ 100 \qquad (4.2)$$

Where:

Ai = the initial area of crack

Af = the final area of crack

(a)

Summary

File Edit Font

Slice	Count	Total Area	Average Size	%Area	Mean
D4-F1 (1).JPG	38	11095	291.974	6.063	69.483
D4-F1 (2).JPG	20	10220	511.000	2.329	89.300
D4-F1 (3).JPG	21	10944	521.143	3.951	49.474
D4-F1 (4).JPG	27	6441	238.556	2.870	49.073
D4-F1 (5).JPG	22	7005	318.409	3.056	67.316
D4-F2 (1).JPG	28	26129	933.179	10.997	40.481
D4-F2 (2).JPG	27	32704	1211.259	16.951	50.876
D4-F2 (3).JPG	13	27840	2141.538	6.434	47.753
D5-F1 (1).JPG	35	10770	307.714	4.803	69.529
D5-F1 (2).JPG	23	11295	491.087	5.038	49.272
D5-F1 (3).JPG	13	15906	1223.538	7.094	80.246
D5-F1 (4).JPG	20	18403	920.150	8.208	80.427
D5-F1 (6).JPG	65	14469	222.600	4.621	48.107
D5-F2 (1).JPG	26	984	37.846	0.313	8.916
D5-F2 (2).JPG	31	6958	224.452	3.103	41.447
D5-F2 (3).JPG	24	8482	353.417	3.783	44.909
D6-F1 (1).JPG	46	4498	97.783	1.995	70.119
D6-F1 (2).JPG	13	10039	772.231	4.474	65.327
D6-F1 (3).JPG	23	15997	695.522	7.097	58.171
D6-F1 (4).JPG	9	17155	1906.111	7.738	34.283
D6-F2 (1).JPG	26	27116	1042.923	10.769	62.909
D6-F2 (2).JPG	22	28482	1294.636	9.981	51.582
D6-F2 (3).JPG	16	22691	1418.188	10.226	42.903
D6-F2 (4).JPG	20	22518	1125.900	8.039	51.825

(b)

Summary

File Edit Font

Slice	Count	Total Area	Average Size	%Area	Mean
D4-F1 (1).JPG	26	1117	42.962	0.798	25.448
D4-F1 (2).JPG	28	2081	74.321	0.929	24.589
D4-F1 (3).JPG	27	3670	135.926	1.637	24.966
D4-F1 (4).JPG	35	3836	109.600	1.711	33.759
D4-F1 (5).JPG	37	3091	83.541	1.405	39.118
D4-F2 (1).JPG	74	12001	162.176	4.292	50.480
D4-F2 (2).JPG	20	7038	351.900	3.136	33.503
D4-F2 (3).JPG	49	8672	176.980	2.237	30.968
D5-F1 (1).JPG	34	2828	83.176	1.067	17.203
D5-F1 (2).JPG	56	7652	136.643	3.473	48.375
D5-F1 (3).JPG	60	6088	101.467	2.715	40.539
D5-F1 (4).JPG	61	7596	124.525	3.472	50.548
D5-F1 (5).JPG	46	4732	102.870	0.980	17.450
D5-F1 (6).JPG	16	824	51.500	0.240	5.657
D5-F2 (1).JPG	16	382	23.875	0.170	6.237
D5-F2 (2).JPG	29	2041	70.379	0.933	27.723
D5-F2 (3).JPG	33	2683	81.303	1.228	30.783
D6-F1 (1).JPG	1	2	2.000	7.213E-4	255.000
D6-F1 (2).JPG	4	378	94.500	0.168	232.738
D6-F1 (3).JPG	30	5143	171.433	2.351	35.440
D6-F1 (4).JPG	29	6272	216.276	2.797	42.792
D6-F2 (1).JPG	46	14303	310.935	3.967	50.103
D6-F2 (2).JPG	23	13904	604.522	5.857	24.843
D6-F2 (3).JPG	23	6381	277.435	2.727	34.613
D6-F2 (4).JPG	29	11640	401.379	4.510	36.390

Figure 4.14: A comparison between the area of cracks. (a) Area of cracks before the healing, (b) Area of cracks after the healing period

4.6.2 Compressive strength test

Compressive strength can be defined as the efficiency of a material or structure to resist compressive loads. The compressive strength is the most significant character for concrete, subsequently investigating the effect of adding a bacterial agent or capsules to the concrete mix should be focused on.

In this research, different encapsulation techniques of bacteria were first used to investigate the effect of these techniques on healing performance. Perlite and calcium alginate beads were used as encapsulation materials. These materials have their own physical properties which differ from the main ingredient of cement mortar (cement and sand), therefore affecting the compressive strength of the mortar.

The prepared cubes of fresh mortar were tested for compressive strength, according to BS 1881-116:1983 [338], by an automatic compression machine (Controls-PILOT). The

cubes were placed between the two parallel discs, as shown in Figure 4.15. The reference rate of the load was accelerated by 0.30±0.05 N/(mm^2.s) until the concrete cubes failed.

Figure 4.15: Automatic compression machine used for the compressive strength test

4.6.3 Water permeability test

A number of techniques have been used to assess the performance or to quantify the quality of bacterial self-healing in cementitious materials. The water permeability test is considered a non-destructive and reliable test that can be conducted in the laboratory to assess the water tightness of cement mortar at different stages during the healing process. In general, the relationship between cracks in concrete and water permeability is direct proportion, where water permeability increases with the increase of crack size. Within the literature [201, 339], falling or constant head water permeability tests have been extensively used to evaluate the permeability of cracked and healed concrete specimens by observing the flow rate, or by quantifying the water passing through the cracked samples. In this study, the cylindrical specimens were subjected to a falling head permeability test both before and after healing. The test was adapted from Van Tittelboom et al. [26] to estimate the efficiency of the self-healing process (i.e. crack closure).

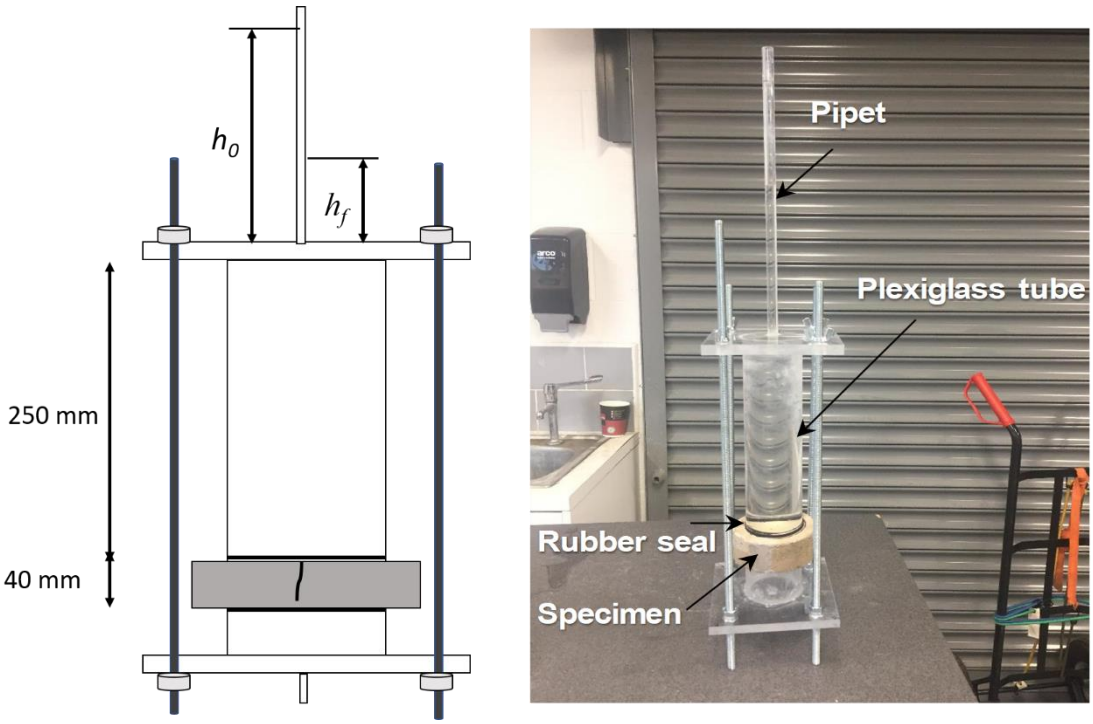

Figure 4.16: Schematic view of water permeability test.

4.6.3.1 Test procedures

- **Apparatus set-up**

The apparatus of the falling head permeability test was assembled in the lab. Two rings of Plexiglas, with 70 mm outer diameter, 62 mm inner diameter, and 250 mm high, (supplied by Simply plastics, UK) were glued with two square plates of Plexiglas, with dimensions of (150 x 150 x 12mm). One Plexiglas plate with a pipette was glued on the top Plexiglas, and the second plate, with a drain tube, was glued on the bottom ring as shown in Figure 4.16. The assembled parts were supported by for threaded bars, one at each corner.

- **Preparation of specimens.**

Before and after healing, the cylindrical specimens were first placed in container filled with tap water for at least 24 hours in order to remove any trapped air inside the specimens. After removal from the container, two discs of rubber washer seal, 71 mm outer diameter and 56 mm inner diameter were mounted at both top and bottom sides

of the specimen to avoid any loss of water between the specimen and Plexiglas ring. The rest of the specimen was dried with a paper towel and coated with fast-hardener epoxy to prevent any leakage through the extended cracks while testing the specimen as shown in Figure 4.17.

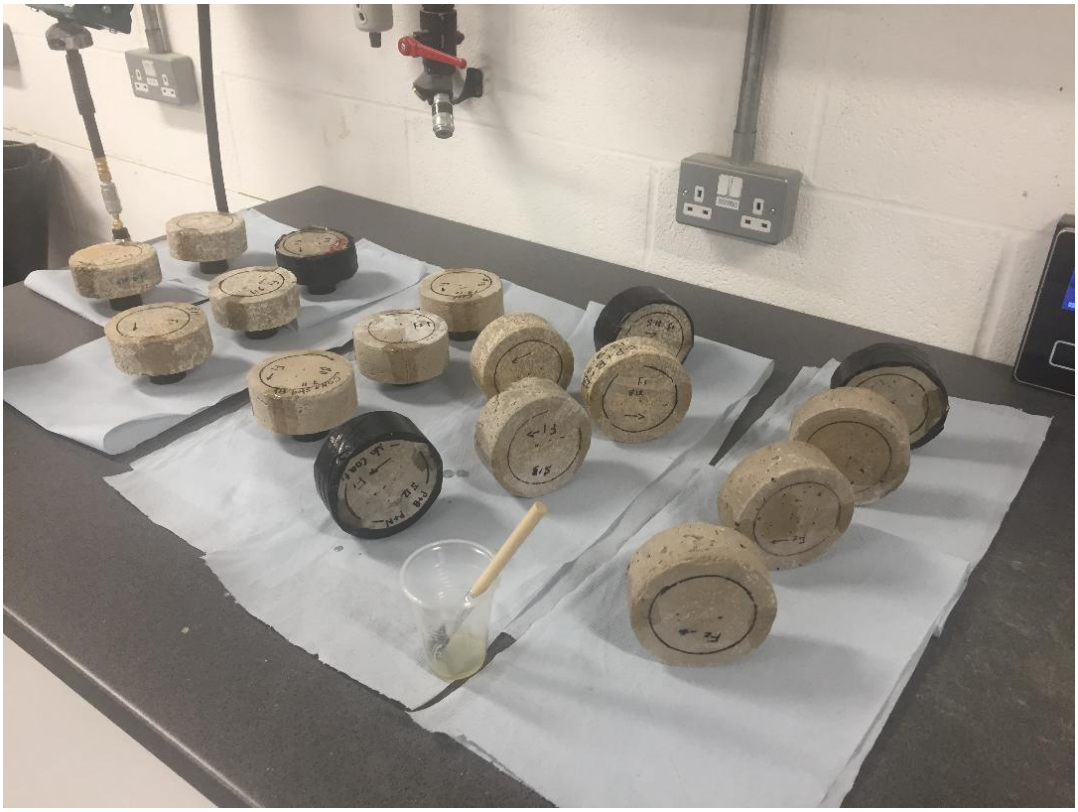

Figure 4.17: Coating the extended cracks by fast-hardener epoxy

- **Permeability measurement.**

After finishing the preparation step, the specimen was placed between the Plexiglas rings, and then the threaded bars' nuts were screwed to fix the specimen. The test was started by filling the pipette with water until h_0 level. The water dropped from top to bottom as a result of the pressure head, which was around 300 mm of water. The time was recorded when the test started, and the water drop was measured at regular time intervals, depending on the flow rate of water through the specimen. The permeability coefficient (k) was calculated according to the following equations based on Darcy's law for a falling water head.

$$\frac{dQ}{dt} = -\frac{a\,dh}{dt} = k\,\frac{h}{T}\,A \tag{4.3}$$

$$= -\frac{dh}{h} = k\,\frac{h\,A}{a\,T}\,dt \tag{4.4}$$

By integrating from h_0 to h_f:

$$k = \frac{a\,T}{A\,t}\,ln\,\frac{h0}{hf} \tag{4.5}$$

Where:

k = water permeability coefficient (m s^{-1})

a = cross-sectional area of pipette (m^2)

A = cross-sectional area of specimen (m^2)

T = specimen thickness (m)

t = time (s)

h_0 and h_f = initial and final water heads (cm), respectively.

In order to evaluate the mechanism of self-healing using the permeability tests, Roig-Flores et al. [143] proposed to use formulas similar to the one used for crack closure, where the data from unhealed specimens used as a reference to be compared with healed specimens by using the following equation.

$$Healing\ ratio\ \% = \frac{Ki - Kf}{Ki}\ x\ 100 \tag{4.6}$$

Where:

K_i = initial water permeability coefficient (m s^{-1})

K_f = final water permeability coefficient (m s^{-1})

4.6.4 Capillary water absorption test

The concrete healing efficiency can be evaluated by a number of properties such as water absorption and chloride diffusion. Each of these properties can be measured using standardized methods. Capillary water absorption is a non-destructive test linked to crack tightness and therefore can be used to quantify the water tightness of the specimens before and after cracking.

According to Martys and Ferraris [340], the capillary suction can be interpreted as a result of unequal surface tension forces between the fluid-fluid and fluid-solid interfaces. In this test, the water absorption rate by capillary suction of oven-dried mortar specimens is measured to calculate the sorption coefficient of specimens before and after the healing process.

In this research, mortar prisms of 40 x 40 x 160 mm were oven-dried at temperature of 40 ℃ for a minimum period of one week, until the mass change in 2 hours was less than 0.2%. Before starting the capillarity test, the prisms were left at room temperature overnight.

4.6.4.1 Test procedures

- Before starting the test procedures, all mortar prisms sides were coated with epoxy resin as a waterproof material. The bottom surface was also coated with epoxy except for a small area of 20 mm x 40 mm around the crack as shown in Figure 4.18.

- The initial weight of all specimens was recorded and then the test face of each specimen was placed on two plastic strips in a tray fitted with a loose lid to prevent air movement around the specimens during the test. The try was filled with distilled water to a depth of about (2 ± 1) mm over the level of the plastic strips as shown in Figure. 4.19.

- The water absorption rate was measured using an electronic balance with an accuracy of 0.01 g. To remove surface water, the specimens were wiped using dampened cloth before each weighting. The water uptake was measured for 6

hours frequently (after 12 minutes, 30 minutes, 1 hour, 2 hours, 3 hours, 4 hours, and 6 hours),

The absorption and the sorptivity coefficient (S) were calculated according to BS EN 13057:2002 [341] using the following equations.

$$I = \frac{mt}{a\ x\ d} \tag{4.7}$$

$$S = \frac{I}{\sqrt{t}} \tag{4.8}$$

Where:

m_t = change in specimen mass in grams at the time t

a = exposed area of the specimen in mm^2

d = density of the water in g. mm^3

The healing percentage was calculated according to the following equation.

$$\text{Healing ratio} = \frac{(Si - Sf)}{Si}\ x\ 100 \tag{4.9}$$

Where:

S_i = coefficient of Sorption before incubation

S_f = coefficient of Sorption after incubation

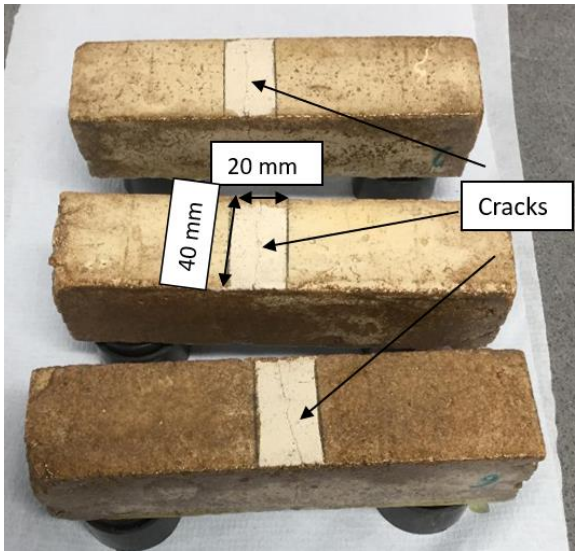

Figure 4.18: Isolation of mortar prisms using epoxy resin

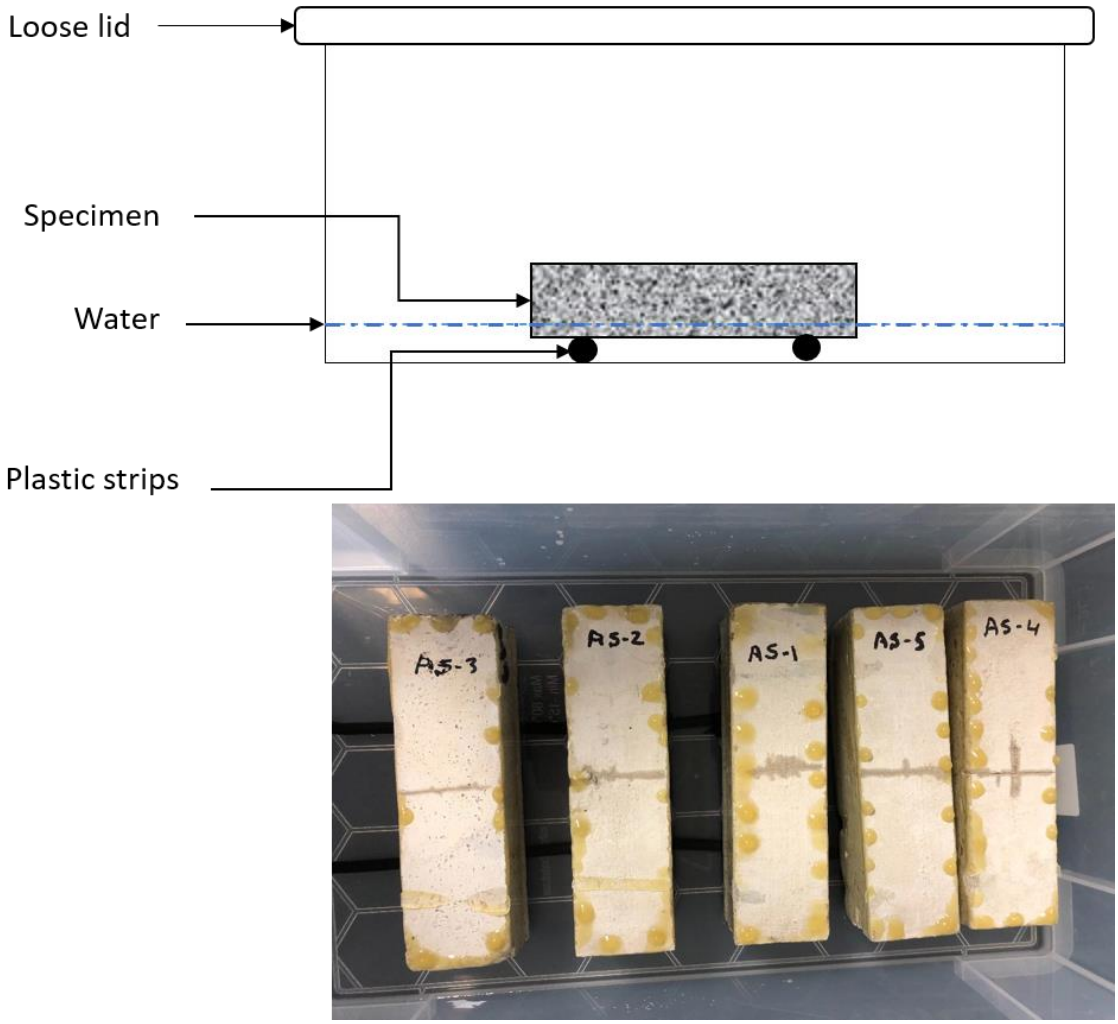

Figure 4.19: Schematic illustration of the capillary water absorption test set-up

4.6.5 Scanning Electron Microscope (SEM)

Healing quality is potentially affected by the type of self-healing compound/product, sealing the cracks. In this research, the precipitated material (healing product) was inspected using Scanning Electron Microscope (SEM) and Energy Dispersive X-ray (EDX) technologies. These techniques allowed the investigation of the crystalline structure and chemical compositions of self-healing products, which is a useful technique when used to verify the chemical compositions of self-healing products.

The SEM is a scientific instrument and one of the most powerful tools that have been widely used in the field of engineering to examine the structure characterization of any objective. SEM has the ability to produce images with high magnification and special resolution with minimum acceleration voltage area [342].

4.6.5.1 Procedures

In order to enable the electron beam to travel in straight lines and produce a suitable sample to be viewed in SEM, specimens were required to be processed as follows.

- **Preparation of specimens**

The specimens were left for 48 hours at room temperature until they got completely dry and then they were cut to small pieces around the healed crack where the calcium carbonate was precipitated to fit the chamber of SEM and reduce the porous.

- **Fixation**

The small piece (approximately 20 x 10 x 10 mm) of the sample was mounted on a special chamber to be ready for coating as shown in Figure 4.20.

Figure 4.20: Fixing the sample on the cylindrical disc chamber

- **Sputter Coating**

In order to enhance and improve the imaging quality of samples, the specimens were gold coated with a sputter coating Emitech K575 before using them in the field of electron microscopy. The specimens were placed in a cylindrical disc chamber provided by several holes to fix the sample in (Figure 4.21) for 10 minutes to create a conductive layer of metal on the specimen surface deposited by low vacuum coating of the sample. The coating prevents charging, and improves the signal of the secondary electron required for topographic examination in the SEM.

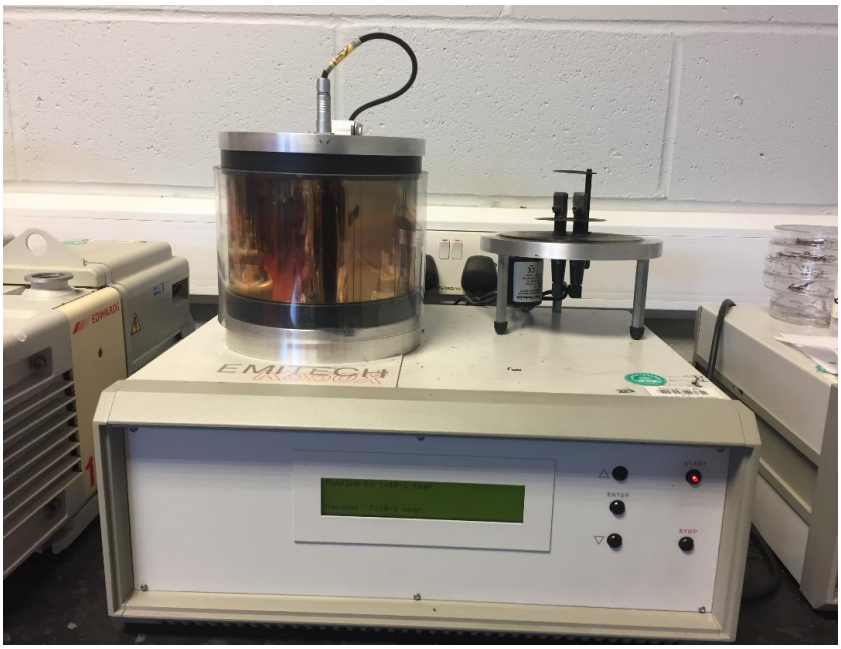

Figure 4.21: Sputter coating camber

- **SEM scanning**

After coating the specimens, they were analysed with an SEM instrument (TESCAN – VEGA 3 Dual-Beam Electron Microscope). The specimens were first placed at the SEM cylindrical disc chamber for scanning. The samples were first pumped under high vacuum conditions to remove any trapped air inside the samples and then followed by releasing an electron beam at a point on the top surface of the sample to measure the resulting electrons with a detector. An image was formed, pixel by pixel by doing this in a raster pattern across the sample's surface.

Figure 4.22: Scanning Electron Microscope (SEM)

Chapter 5

The effect of delivery techniques of bacterial agent on the efficiency of self-healing system of concrete

5.1 Introduction

Concrete durability can be restored by using a novel technique that comprises bacterial-induced precipitation of calcium carbonate. In this approach, concrete micro-cracks can be healed by precipitating calcium carbonate where bacterial activity providing heterogeneous crystal nucleation sites in super-saturated $CaCO_3$ solution. However, this technique raised several challenges for engineers to overcome especially for the survival of the bacterial agent inside the concrete matrix.

To improve the viability of bacteria and crack healing efficiency, engineers and materials scientists have attempted to investigate different techniques to deliver the healing agent including using a vascular system [106] or using capsules such as expanded clay particles [95], modified alginate hydrogel [107], hydrogel [35], and silica gel [101]. However, most of the capsules suffer from serious limitations and drawbacks, such as a change in volume due to cement hydration and being non-sensitive to cracks.

For successful implementation of bio-concrete the delivery (encapsulation) methods must be suitable for inclusion in the concrete matrix, sensitive enough to allow the release of the healing agents, stable in volume, and must not absorb water. Most importantly, the encapsulation must have minimum impact on the physical and mechanical properties of the concrete such as permeability and compressive strength [343].

This chapter investigates the effect of using polymer materials (i.e. calcium alginate) and lightweight aggregate (i.e. perlite) as protective materials on the compatibility with the cement mortar and the efficiency of self-healing. Furthermore, the viability of *Bacillus subtilis* spores within these capsules was also investigated. The aspects of the most appropriate delivery technique of bacterial agent for practical application were

discussed. For this study, *Bacillus subtilis* (H50620/9) were impregnated in calcium alginate and perlite to protect the healing agent within the mortar matrix. To provide more protection for the impregnated bacteria, coating the perlite with sodium silicate was investigated. The direct add of spores was utilised as a control technique to compare the output results after calcium alginate and perlite use. The performance of the capsules and healing efficiency was quantified by conducting compressive strength tests, falling head permeability tests, and visual inspection of crack sealing. In addition, the microstructure of precipitated materials was characterised by Scanning Electron Microscope (SEM) and Energy Dispersive X-ray (EDX). Figure 5.1 summarises the used delivery techniques of healing agents and experimental program for this chapter.

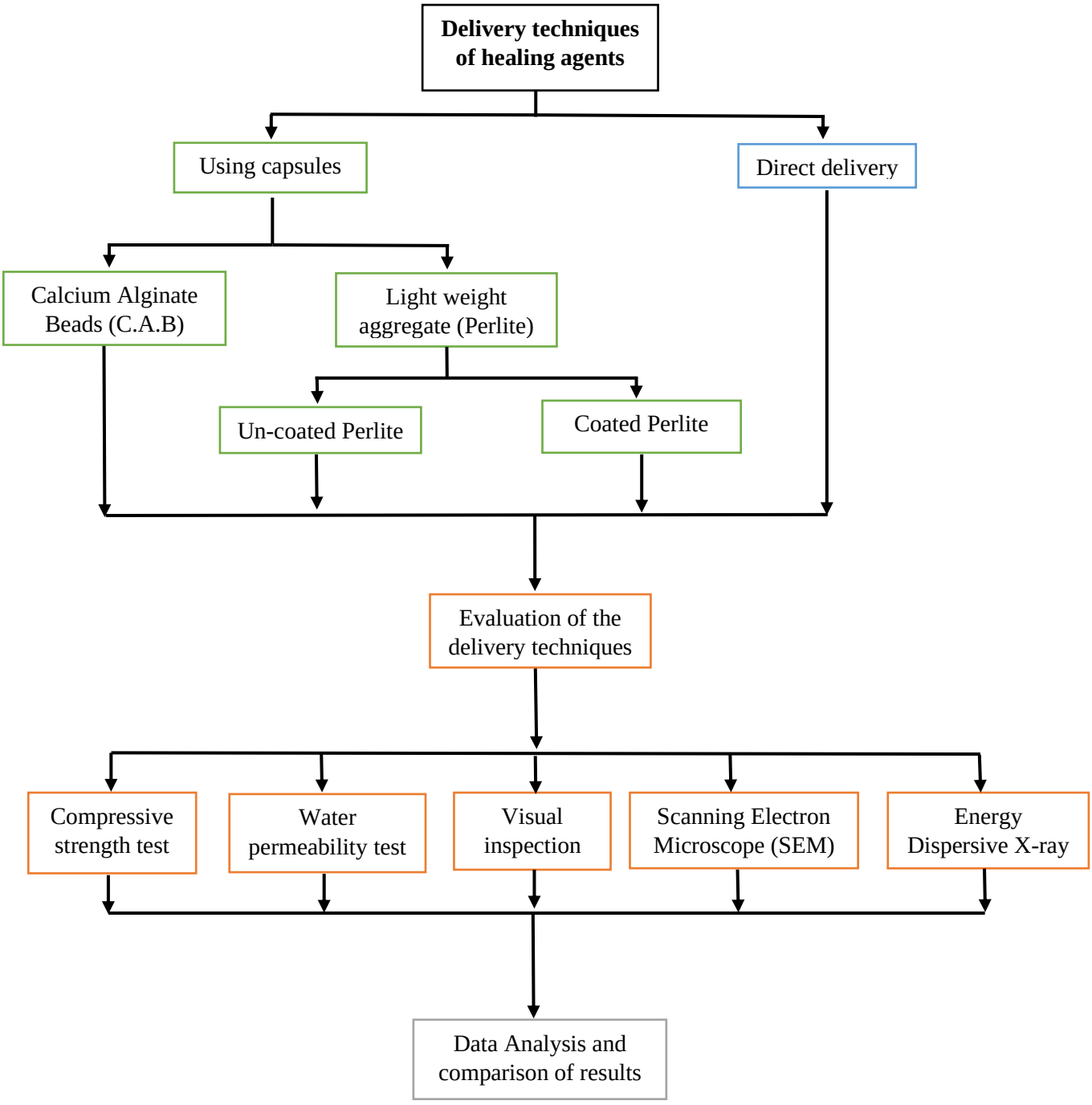

Figure 5.1: Experimental programme layout

5.2. Experimental program

5.2.1 Selection of growth media

In order to assess and find the most appropriate media for *bacillus subtilis* to grow and produce spores, three growth media were investigated in this research. The chemical compositions for the three-growth media were listed in Table 4.1.

The efficiency of the three growth media was investigated by using Spore Stain Test (SST) and Colony Forming Unit (CFU) test. The results showed that the three growth media were able to produce colonies with different concertation, whereas the spores were detected under the microscope for only G.M-2 and G.M-3. The spores stain appears in green and the vegetative cells stain appears in pink. From Figure 5.2, it can be seen that the maximum number of spores was achieved in the second growth media (G.M-2), whereas a small number of spores were noted in G.M-3. The first growth media (G.M-1) has not produced any spores. Therefore, G.M-2 has been selected to grow the *bacillus subtilis* as the highest number of spores was achieved with this media.

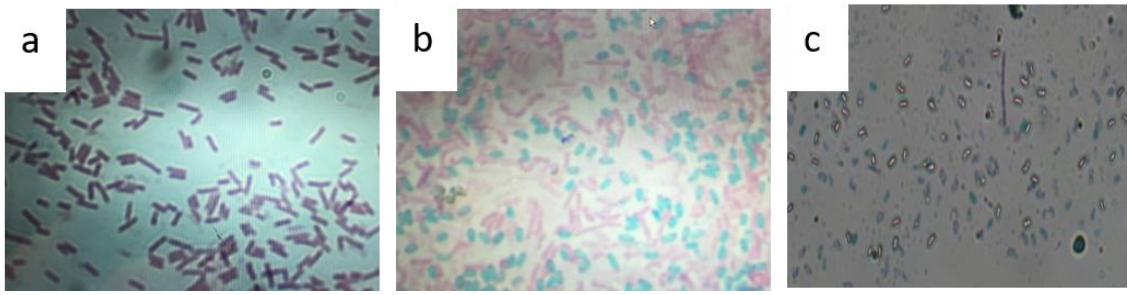

Figure 5.2: Strain of *Bacillus Subtilis* under the microscope (a) First growth media (G.M-1) (b) Second growth media (G.M-2) (c) Third growth media (G.M-3)

5.2.2 Direct adding of bacterial spores

The healing agents (bacteria and nutrients) can be incorporated directly to concrete during the mixing process. In this technique, the bacterial suspension and nutrients can be added to replace a part of mixing water to the concrete matrix. However, when bacteria are added directly into concrete, the microbial metabolic activity of bacteria is

dramatically affected due to the harsh environment such as high pH and dry condition of the concrete, which make bacteria hardily to survive [61].

In this research, the direct add of spores was used as a control technique. The bacteria were cultured in G.M-2 for 72 hours until spores were formed and then the spores were harvested and washed as explained in Chapter 4, section 4.3.3. Before starting in encapsulation process, spores were assessed and visualised under a microscope (LABOPHOT-2, Nikon) using a spore stain test, and the bacterial culture was spread in agar plates to count the Colonies Forming Units (CFU) (Figure 5.3). The centrifuged spores were re-suspended in distilled water, and the final concentration of bacteria in the suspension was 7×10^6 CFU ml^{-1}.

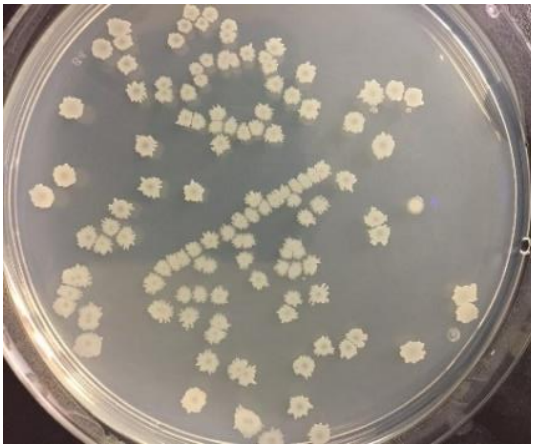

Figure 5.3: Morphology of colonies in agar plate

5.2.2.1 Proportion of cement mortar specimens

The mixing and casting process was carried out as explained in chapter 4, section 4.4.1. Three types of cement mortar specimens were prepared by mixing Portland cement type I, sand, self-healing agent and tap water. Mixture proportions are given in Table 5.1. Six cylindrical specimens with a diameter of 100 mm and 40 mm height were used for the water permeability test and three cubes of 40 x 40 x 40 mm were used for the compressive strength test. For visual inspection of crack healing efficiency, six prismatic

specimens with dimensions of 40 x 40 x160 mm were used. After 24 hours, the specimens were unmoulded and kept in water for curing until the day of the test.

Figure 5.4: Cement mortar specimens (a) Cylindrical (b) Prisms (c) Cubes

Table 5.1: Mixture proportions of cement mortar of specimens

Mixture ID.	Cement (g)	Sand (g)	Water (g)	Nutrient (g)	Bacteria liquid (mL)
M1	1200	3600	545	24	55

5.2.3 Calcium alginate beads

Alginate is considered the most vastly utilised material and widely used production technique for bioencapsulation. The alginate is originally produced from natural polysaccharide material which comes from marine plants, and its basic structural form consists of linear unbranched polymers containing d-mannuronic acid and l-guluronic acid. The thermal form of alginate is stable and biocompatible in the existence of di- or tri-cations. Furthermore, the calcium alginate beads can be easily created by extruding alginate into calcium acetate or chloride solution. The alginate capsules have been used in various implementations such as bioprocess, biomedical, pharmaceutical, food and feed [344-346]

5.2.3.1 Preparation of sodium alginate and calcium chloride solution

Sodium alginate was prepared in the Biology Laboratory at the University of Derby. 7.5 g of sodium alginate, 0.5 g of yeast extract and 7.8 g of hydrochloride as alkali buffer (0.1 mol. L^{-1}) were added and dissolved in 500 ml of distilled water. In order to make the solution more homogenous, a magnetic stirrer was used to form a 1.5 % sodium alginate solution. The solution was autoclaved for 30 minutes at a temperature of 120 ℃ and then stored overnight in a cooling fridge at 4 ℃ before using it to produce calcium alginate beads.

The calcium chloride ($CaCl_2$) solution was prepared by adding 8 g of calcium chloride and 4 g and calcium lactate as a nutrient to 400 ml of a distilled water and then mixed by using a magnetic stirrer until the liquid became homogenous to form 2% calcium chloride solution. The solution was autoclaved and stored at 4 ℃.

5.2.3.2 Encapsulation of bacterial agent into calcium alginate

Encapsulation can be defined as a process of reserving agents within a mould in particulate form to attain specific effects, such as impregnation, stabilisation or protection of healing agents.

After finishing the harvest and washing process of spores by using the centrifuge machine as explained in Chapter 4, Section 4.3.3, the spores were added to the sodium alginate solution and then mixed by using a magnetic stirrer until the solution turned homogenous. As shown in Figure 5.4, a syringe was used to produce the calcium alginate capsules. The encapsulation procedure starter by dropping sodium alginate solution at 5 cm height into the calcium chloride solution, in an autoclaved jar. A burn was used during the encapsulation process to prevent any contamination from surrounding air. The gel of calcium alginate beads was formed as a result of a chemical reaction between calcium chloride solution and sodium alginate solution. After 20 minutes, the formed beads were removed from the calcium chloride solution, washed twice using sterilised water, and dried at 37 °C for 24 h. To avoid any contamination, the dried beads were kept in a cooling fridge at 4 ℃ until the day of the mix.

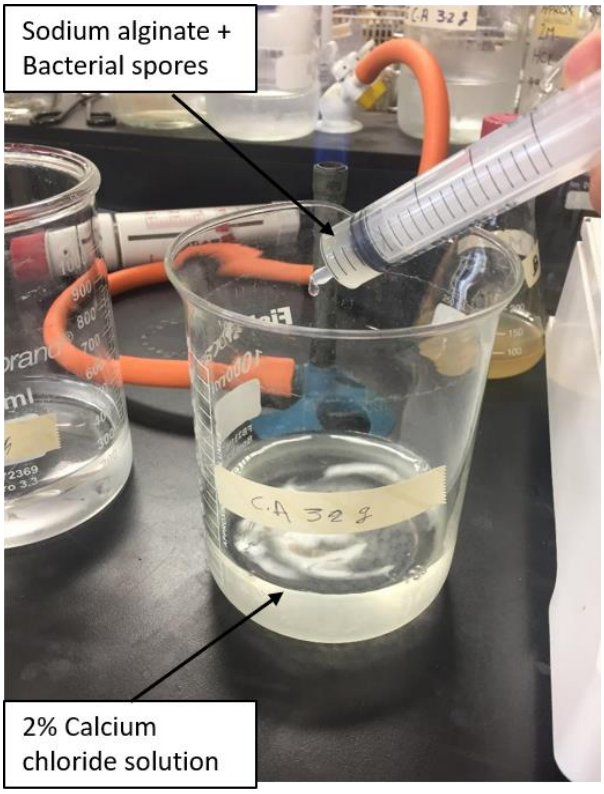

Figure 5.4: Using a syringe to produce the calcium alginate capsules

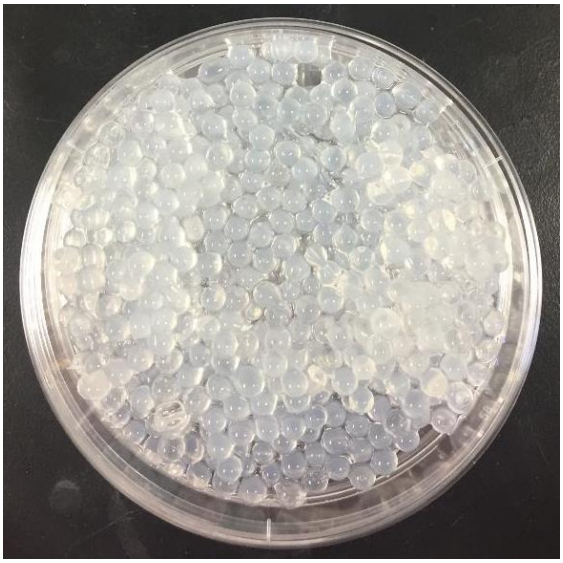

Figure 5.5: Calcium alginate capsules

5.2.3.3 Proportion of cement mortar specimens

The mixing and casting processes were carried out following BS EN 196-1 [347]. Three types of cement mortar specimens were prepared by mixing Portland cement type I, sand, and tap water. Calcium alginate beads loaded with bacterial agents and nutrients were added afterwards to the mix and mixed by using a digital mortar mixer until the mix became homogenous. Mixture proportions are given in Table 5.2.

The mortar has been cast in cylindrical specimens with a diameter of 100 mm and 40 mm height were used for water permeability test and cubes of 40 x 40 x 40 mm were used for the compressive strength test. Prismatic specimens with dimensions of 40 x 40 x160 mm were used for visual inspection of crack healing efficiency.

Table 5.2: Mixture proportions of cement mortar specimens with healing agents encapsulated within calcium alginate

Mixture ID	Cement (g)	Sand (g)	Water (g)	Calcium alginate (g)
M2	1200	3600	600	240

5.2.4 Light weight aggregate (Perlite)

Perlite is a hydrated siliceous volcanic glass (SiO_2) obtained from pumice rocks. It is typically created when the volcanic lava exposes to rapid cooling after volcanic eruption [348]. One of the main features of perlite is its ability to expand under high temperatures, where perlite volume can increase up to 20 times its original volume [349]. As a result of this physical transformation, the porous structure and water absorption of the expanded perlite is considerably increased to create a suitable hosting environment for the healing agent. Figure 5.6 shows the porous structure of perlite under SEM. Moreover, the cost of expanded perlite is very low compared to other materials such as expanded clay, exfoliated vermiculite, mineral wool or shale. This, had made perlite ideal to be used as light weight aggregate in several applications such as construction materials including concrete, agriculture, medical and chemical industry [350]. In addition, expanded perlite has been utilised to form some constructional

elements such as pipe, brick, plaster, wall and floor block or to increases the insulation quality of concrete and fire resistance [348].

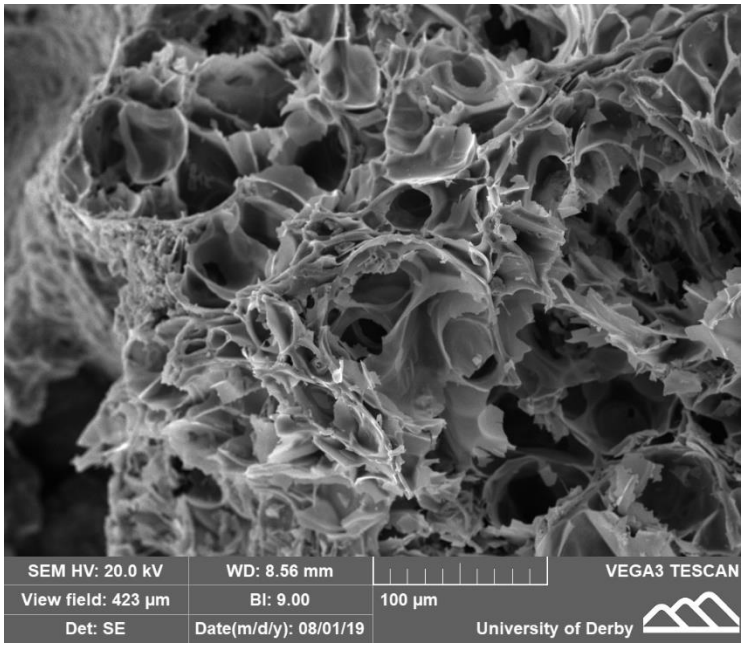

Figure 5.6: Porous structure of Perlite under SEM

5.2.4.1 Physical properties of perlite

The physical properties of used perlite were investigated according to British Standers. Table 5.3 summarising the physical properties of perlite and relative specification. The particle size distribution for coated and un-coated perlite was tested using a sieve analysis test. Before starting the test, the sieves were stacked up with the smallest one at the bottom and the large sieve at the top and a pan was placed under the sieves to collect the past particles as shown in Figure 5.7. To perform the test, 100 g of perlite was placed on the top sieve, covered, and then shaken for 10 min. After finishing the shaking, the percentage of passing was calculated, and then the relationship between the particle size and percentage of passing was illustrated on a semi-log scale as shown in Figure 5.8.

Table 5.3: Physical properties of Perlite

Property	Value	Specification
Unit weight	128 Kg/m^3	BS EN 1097-3:1998
Absorption rate	277 %	BS EN 1097-6:2013
Moisture content	22 %	BS EN 1097-6:2013

Figure 5.7: Preparation of sieves for particle size distribution test

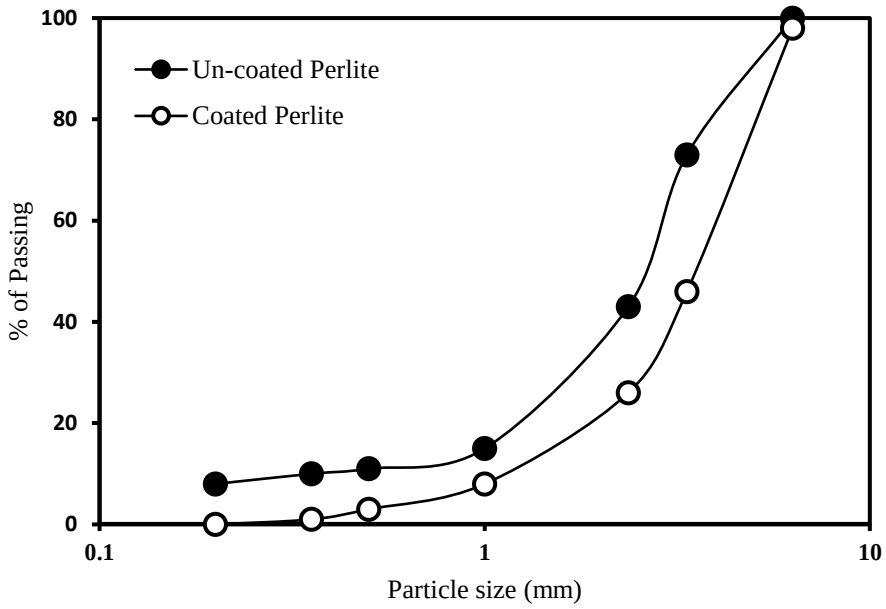

Figure 5.8: Particle size distribution of coated and un-coated perlite

5.2.4.2 Encapsulation of spores into the perlite

Uncoated perlite (UCP)

The perlite was first sterilised in the oven at a temperature of 160 °C for two days to destroy any microbes or bacteria present and remove any moisture. To impregnate the perlite with bacterial spores, it was then soaked in the bacterial suspension until the suspension was absorbed. The surface of the perlite was then sprayed with a nutrient solution containing calcium acetate (60 g l^{-1}) and yeast extract (6 g l^{-1}). For further investigation, the nutrients were impregnated in separate capsules by using the same procedures to avoid the germination of bacterial spores with nutrient before introducing cracks in the mortar specimens.

After each treatment, the perlite was dried in the oven at 40°C for two days. These produced capsules containing approximately 0.3% of nutrients by perlite weight with a spore concentration of approximately 1.6 x 10^7 CFU $gram^{-1}$.

Coating the perlite (CP)

The perlite coating technique involved the separate encapsulation of the bacteria and nutrients into perlite using the same procedures detailed in section 5.2.4.2. To protect

the healing agent inside the carrier, the perlite was coated by two layers of sodium silicate. Firstly, the impregnated perlite was immersed in sodium silicate supplied from Sigma-Aldrich, UK, until the surface of the perlite was fully covered and then was dried at 25 °C for 48 hours (Figure 5.9). The second layer of sodium silicate was applied, followed by curing the wet perlite in dry cement. The coated perlite was then cured in water for 24 hours. The mass of CP was approximately 10 times the mass of UCP.

Figure 5.9: Drying the perlite after applying the first layer of sodium silicate

5.2.4.3 Proportion of cement mortar specimens

The mix proportions and cement mortar specimens were prepared and designed as stated in Chapter 4, section 4.4.1. To cast a proper and consistent mixture that combined with the encapsulated healing agents, the coated and uncoated perlite were added to the mix to replace around 20% of the volume of the standard sand. Mixture proportions are given in Table 5.4.

Table 5.4: Mixture proportions of cement mortar specimens with healing agents encapsulated within perlite

Mixture ID	Quantities (g)								
	Cement	Sand	Water	Perlite +Bacteria +Nutrient	Perlite +Bacteria	Perlite +Nutrient	Coated perlite +Bacteria +Nutrient	Coated perlite +Bacteria	Coated perlite +Nutrient
M3	1200	2030	600	60	-	-	-	-	-
M4	1200	2880	600	-	-	-	960	-	-
M5	1200	2030	600	-	25	35	-	-	-
M6	1200	2880	600	-	-	-	-	400	560

After 28 days of curing, the prismatic specimens were cracked at the centre by using three-point test and splitting tensile test for cylindrical specimens as explained in Chapter 4, sections (4.5.1, and 4.5.2 respectively)

5.3 Results and discussion

5.3.1 Viability of the encapsulated spores

The viability rate of impregnated spores in perlite, calcium alginate and direct add was investigated at different ages (0, 10, 30 and 150 days). In this test, the serial dilution technique has been used to calculate the number of viable bacterial spores as CFU $gram^{-1}$. At different periods, one gram of spores' carers was crushed to powder in a hand-held pestle and then mixed by using a vortex mixer until the suspension became homogenous and then followed by suspension in PBS medium under sterile conditions (Figure 5.10). Subsequently serially diluted and plated on agar plates and then immediately incubated at 37 °C for 24 hours.

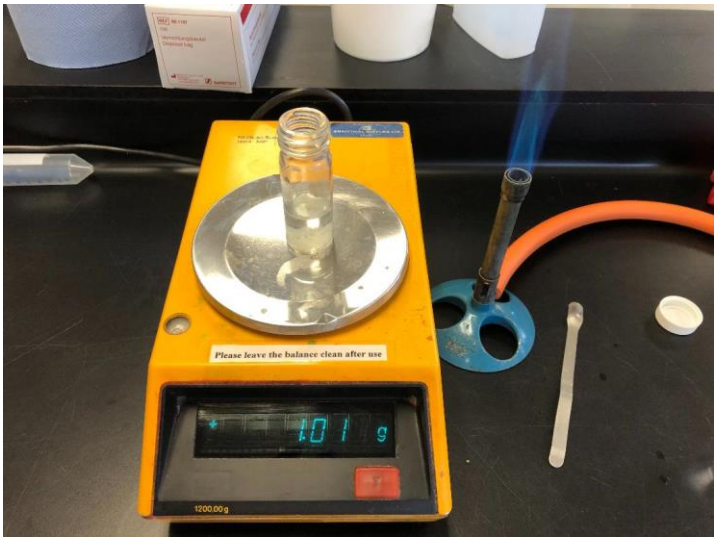

Figure 5.10: Crushed and suspended one gram of calcium alginate in PBS medium

The number of colonies was counted (Figure 5.11), and the CFU was calculated as explained in Chapter 4, equation 4.1.

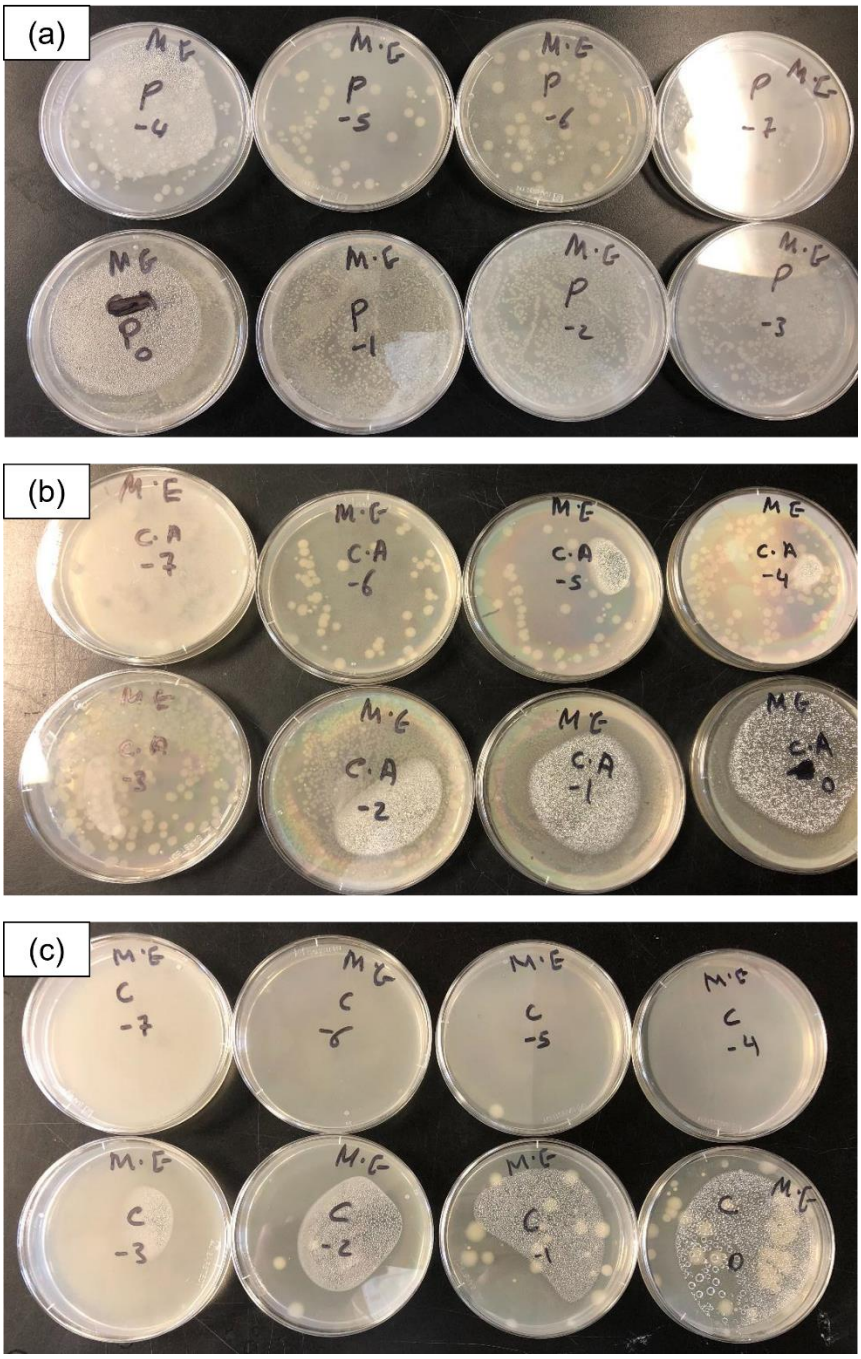

Figure 5.11: Number of colonies forming unit after 150 days: (a) Perlite, (b) Calcium alginate, (c) Cement mortar

The relationship between the log of CFU and time in days is illustrated in Figure 5.12, From the Figure, it can be clearly seen that the number of viable bacterial spores was decreased over the time. The numbers of viable spores in perlite, calcium alginate and cement mortar were recorded as 5×10^7, 4.5×10^7, and 4.3×10^7 CFU gram^{-1}, respectively,

at the age of 0 days. However, after 150 days, this number was steadily decreased for spores impregnated in perlite and calcium alginate and the number of viable spores was maximum in perlite 1.5 x 10^7 CFU $gram^{-1}$ followed by calcium alginate 2.8 x 10^6 CFU $gram^{-1}$. In contrast, the viability of spores, which were directly added to the cement mortar, was sharply decreased by around 70%.

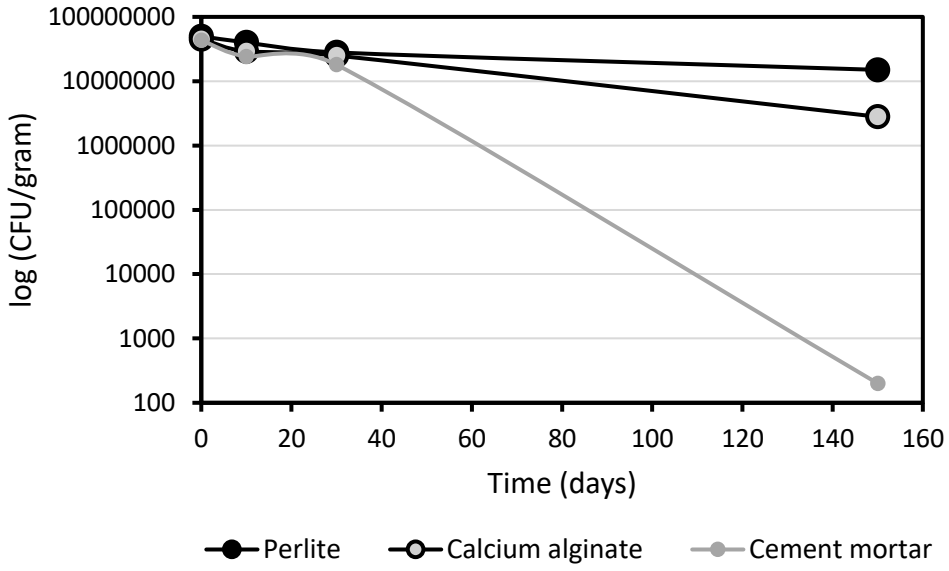

Figure 5.12: The effect of the delivery technique of spores on their viability

5.3.2 Compressive strength

Impregnation of the bacterial agent into capsules is a prerequisite of self-healing to protect the bacteria from the harsh environment within the concrete matrix. However, different studies reported that using capsules may result in an undesirable loss in compressive strength [6, 103]. Therefore, the generally unpredictable effect of capsule addition on hardened cementitious material properties means that it is necessary to investigate the influence of adding these capsules on the cementitious matrix.

After curing, all mortar specimens were subjected to compressive strength testing on days 7 and 28 post mortar mixing. Figure 5.13 illustrates the strength values of compressive strength for cement mortar specimens incorporated with different encapsulated materials. On observation, it is clear to see that the cement mortar cubes

(M1) incorporated with direct add of bacterial spores showed a significant increase in compressive strength compared to those prepared with calcium alginate (M2) (8.46 MPa), perlite (M3) (9.13 MPa) and coated perlite (M4) (7.1 MPa). The highest strength value of M1 was observed after 28 days of curing (11.43 MPa). The improvement in the compressive strength of M1 can be interpreted as the result of calcium carbonate deposition on the microorganism cell surfaces and within the pores of cement mortar, causing filling of the voids inside the mortar to occur [304]. Bacterial spores were activated immediately due to the direct delivery method [351]. The precipitation of $CaCO_3$ can increase concrete compressive strength by improving the hydrolysation of cement at faster rates [352]. Furthermore, the spores were added as a part of the mixing water and therefore would not have occupied any voids within the mortar.

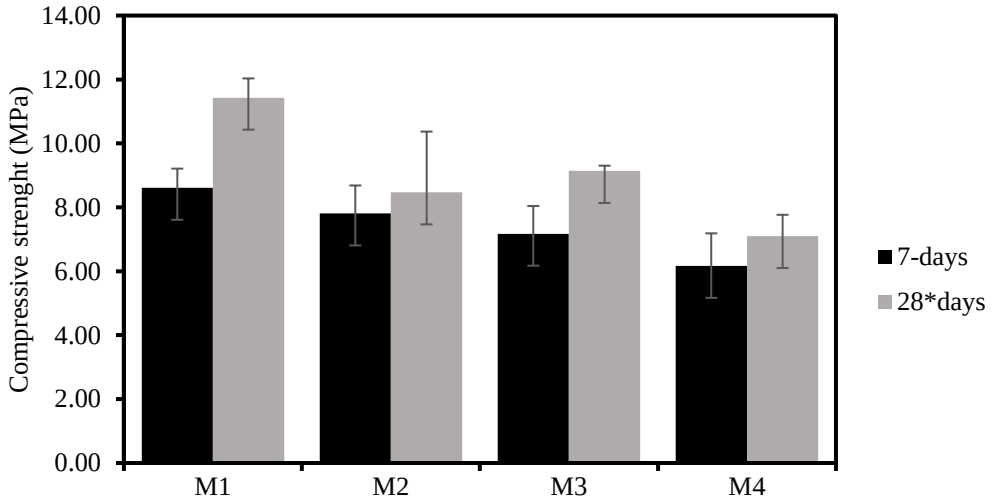

Figure 5.13: Effect of the delivery technique of bacterial agents on the Compressive Strength of Cement Mortar Cubes at 7 and 28 days.

A higher increasing rate of compressive strength after 28 days of curing was observed for all specimens and this increase accounts for the hydration of dehydrated cement particles to form calcium silicate hydrate (C-S-H) [97, 242].

The use of calcium alginate cubes (M2) led to an improvement of 9 % in compressive strength (7.81 MPa) in comparison with the uncoated perlite (M3) mortar at age 7 days (7.17 MPa), which can be attributed to an increase in the number of pores as shown in Figure 5.14. In contrast, the compressive strength (9.14 MPa) of uncoated perlite cubes (M3) at the age of 28 days was improved with respect to the compressive strength (8.47 MPa) of specimens incorporated with calcium alginate (M2). This increase in compressive strength is mainly due to the stability in the size of perlite capsules over time in comparison with calcium alginate capsules, which shrank as a result of cement hydration and left spherical void surrounding the capsules. There is also the possibility that the porous and rough texture of uncoated perlite may increase the coherence with sand-cement mortar and therefore improve the compressive strength. Specimens with coated perlite (M4) showed a decrease in strength of approximately 16% at age 7 days compared to specimens containing uncoated perlite (M3). This decrease might have been produced by the negative impact of weak layers of sodium silicate and cement powder surrounding the perlite.

Broken capsules have been frequently observed in all cementitious matrices; therefore, their compatibility with the cementitious matrix will determine if this weakens strength development or if the cement hydration procedure has an effect on it. If capsules have no notable impact on the microstructure and their detrimental effect on material properties is negligible, they are considered to be ‘compatible’. It is also essential that they are well-embedded in the adjacent matrix. Figure 5.14 shows the embedded capsules within the cementitious matrix, from the Figure, it can be clearly seen that the most compatible capsule is the perlite, which was homogeneously distributed within the specimens (M3, M4). In contrast, the alginate capsules (M2) were floated as a result of their light smooth spherical shape and therefore they were concentrated at the top of the specimens. In addition to that, the spherical void surrounding the capsules had created a weak point. In most cases cracks were crossing these voids without breaking the capsules.

In general, compatibility is commanded by the ability of capsules to keep the healing agents, stability of their size, and adhesion between the capsule's material and cementitious matrix.

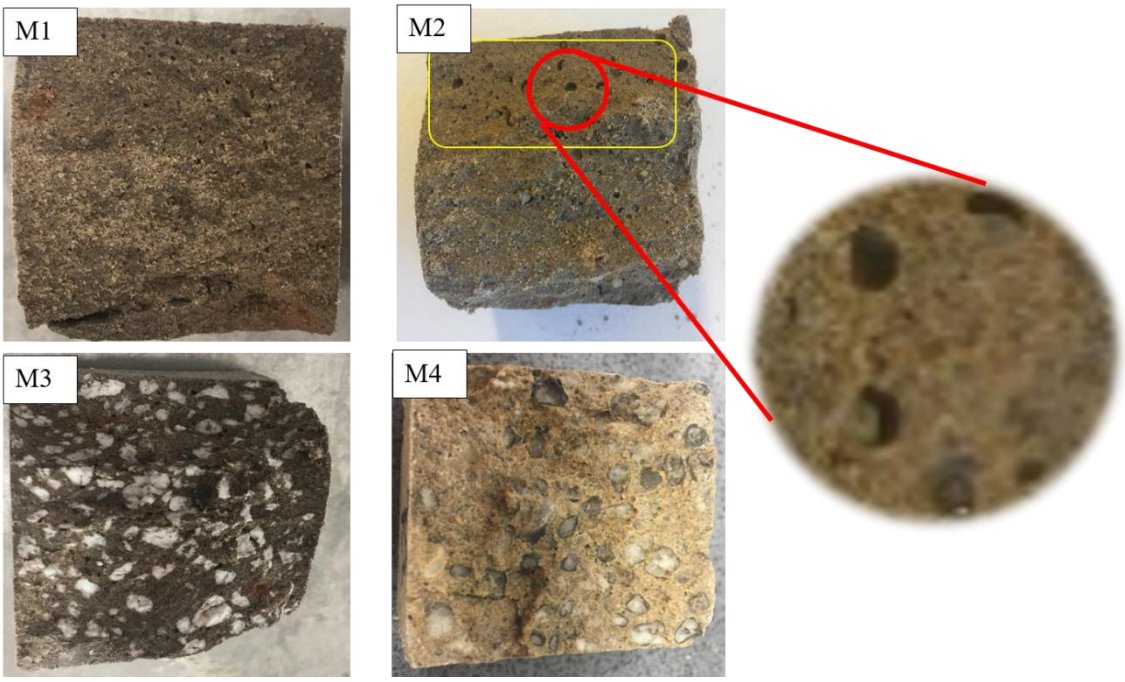

Figure 5.14: Cross-sections of cement mortar specimens show the distribution of carer materials for mixtures M1, M2, M3 and M4.

5.3.3 Visualization and determination of the crack-healing ratio

To assess and quantify the healing performance of cracks for each mix, specimens from different healing periods were inspected under a light microscope, as shown in Figure 5.15. The Figure indicates that crack-healing performance was observed before and after the healing period for most of the specimens, where white mineral precipitations of calcium carbonate filled the cracks due to bacterial activity. At the earlier stage of incubation, the specimens which were incorporated with direct add (M1) exhibited a considerable healing performance, with no further efficient healing observed over time. The early efficient performance can perhaps be interpreted as direct activation and calcium carbonate precipitation of free spores caused by the ingress of water through cracks. However, the high activity of the free spores inside the cement mortar is limited

due to the harsh alkaline environment and the lack of protection. As bacterial spores were added directly to the mix and not protected against the high pH, therefore the activity of spores decreased swiftly because spores were unable to thrive in such conditions [101]. Additionally, over time the bacteria cells are affected by a decrease in the flow rate of Oxygen and nutrients, where the faster rate of calcium carbonate deposition blocks the pores in the concrete [352].

It can be observed that the healing percentages of cracks increased with extended incubation periods, especially for specimens containing encapsulated healing agents. It can also be seen that the maximum healed crack width was approximately 570 μm after 60 days of incubation for specimens incorporated with set M3.

The change in the crack widths for all specimens before and after incubation was measured and compared to evaluate the efficiency of healing performance. Figure 5.16 shows the healing ratio of initial crack width after 28 and 65 days of healing. It is clear to see that specimens incorporated with coated perlite (M4, M6) had limited healing ratios, possibly caused by the coating materials preventing the release of the healing agents. In contrast, specimens incorporated with bacterial agents (M1, M2, M3, M5), especially the agents that were loaded into uncoated perlite (M3, M5), presented a prominent progression in crack healing ratio. The highest healing ratio was observed in small crack widths ranging from 100 μm to 300 μm in the majority of specimens, whilst only a few large cracks were completely healed.

Initially, the calcium carbonate precipitations appear in the position of bacteria at first, and subsequently slowly increase and final heal the crack in the cement mortar specimen completely. This is based on the microbial mineralisation that is utilised for self-healing concrete. In order to fill larger cracks completely, it is necessary to use more mineral precipitations, as the repair of wider cracks under continuous repair agent amounts is more difficult to repair. Contrastingly, in the case of a wide crack, the repair agent forms mineral precipitation which spread easily beyond the water environment, thereby, resulting in a partial and bad repairing effect and wasting of the healing agent [109].

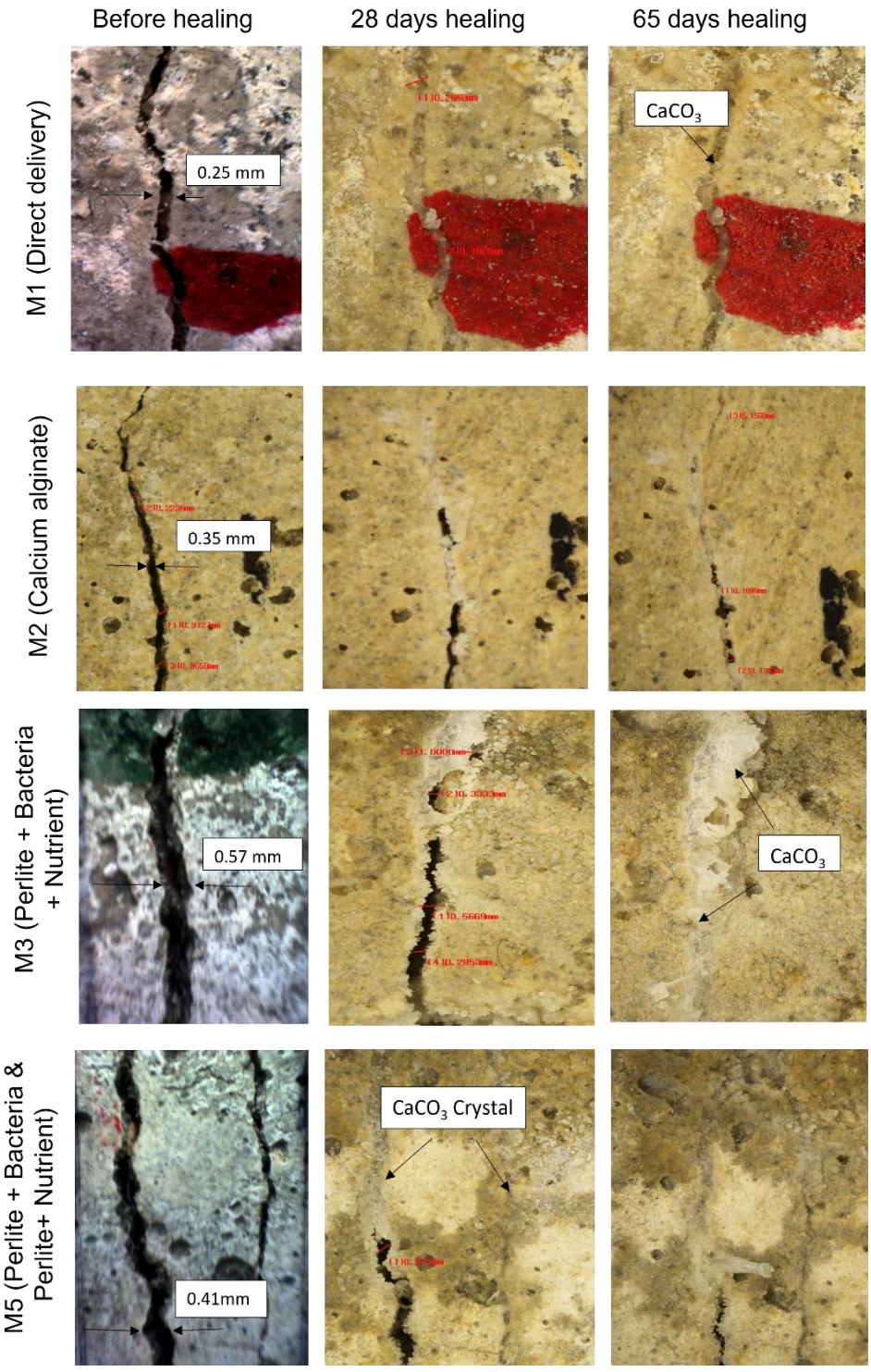
Before healing
28 days healing
65 days healing
M1 (Direct delivery)
0.25 mm
CaCO3
M2 (Calcium alginate)
0.35 mm
M3 (Perlite + Bacteria + Nutrient)
0.57 mm
CaCO3
M5 (Perlite + Bacteria & Perlite+ Nutrient)
0.41mm
CaCO3 Crystal

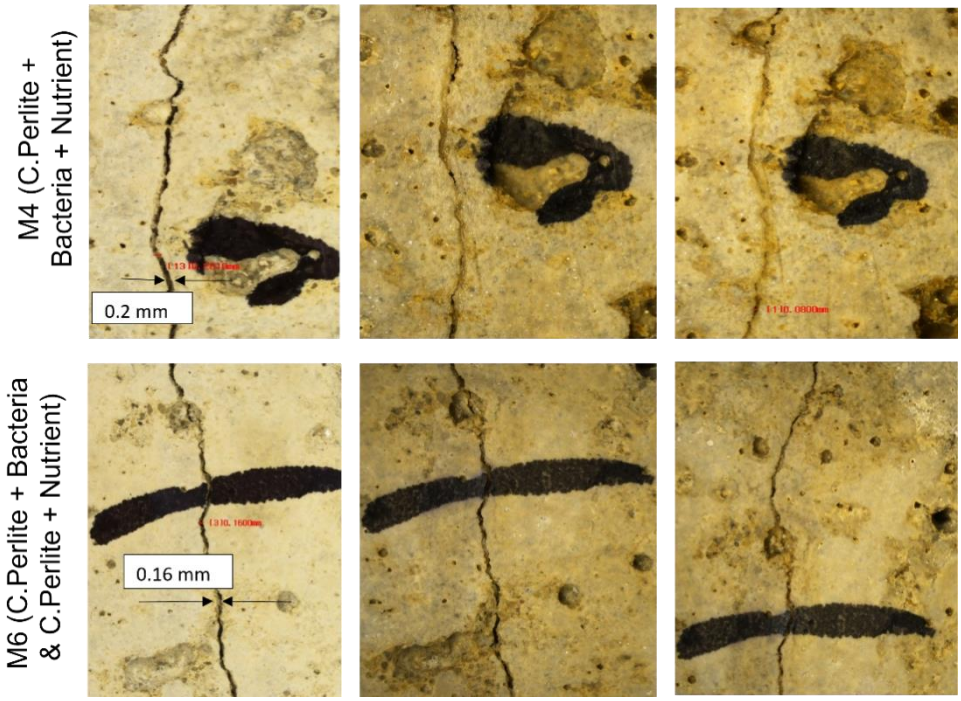

Figure 5.15: Microscopic observation of crack-healing before and after 28 and 65 days for mixtures M1 to M6

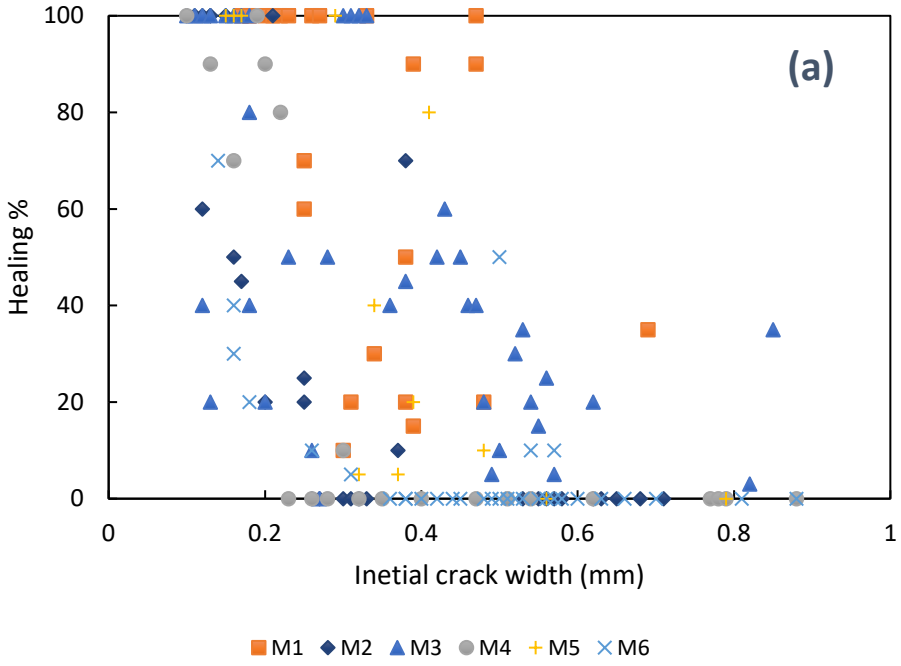

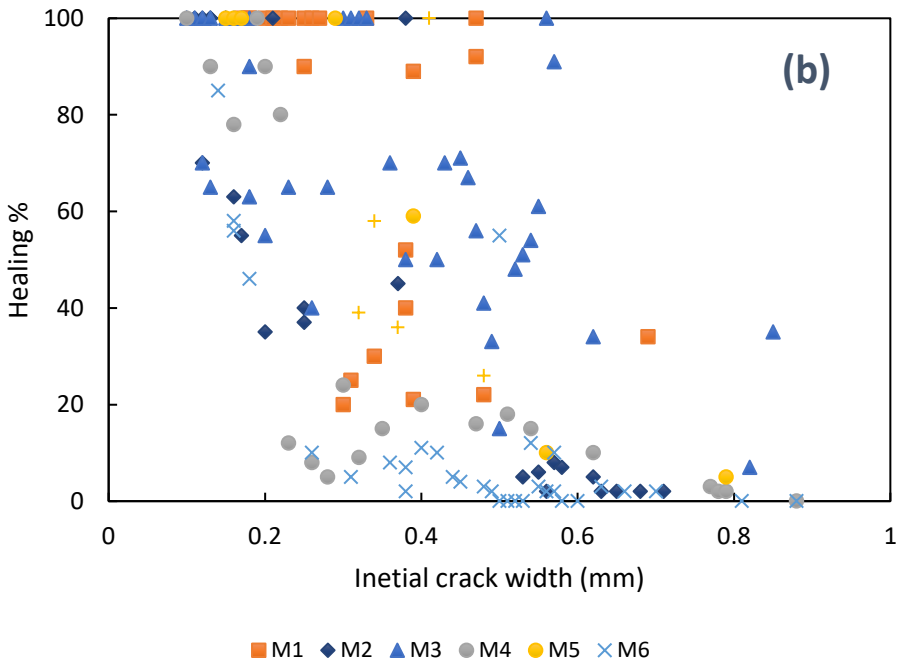

Figure 5.16: Crack healing ratio as a function of the initial crack width for mixtures M1 to M6: (a) after 28 days of incubation; (b) after 65 days of incubation

5.3.4 Water permeability test

Following the microscopic inspection of cracks, healing efficiency was investigated using a falling-head water permeability test to link the functional property (crack permeability) to the visual inspection of cracks. For this research, six cylindrical cracked specimens were tested before and after 4 weeks of healing treatment for each mixture. Permeability test results for all mixtures are presented in Figure 5.17. The Figure indicates that the initial coefficients of water permeability for all mixtures were within the range of 10^{-5} m.s^{-1} to 10^{-6} m.s^{-1} as all cracks ranged between 100 µm to 450 µm. Moreover, after 28 days of treatment, the water permeability of all mixtures was decreased.

A promising reduction of 28%, 26% and 21% were identified in mixtures M1, M3, and M5 respectively as a result of precipitation of the healing products in the crack surfaces as evident in the SEM results of the healed cracks (Figure 5.18). The deposition of calcium carbonate fills pores and continuous channels that passing the water, and therefore, limiting the seeping of aggressive materials such as sulphates and chlorides which can lead to excessive corrosion of reinforced steel bars and thus deteriorating of the whole structure. Comparison between direct add and other specimens revealed a relative reduction in permeability, and this could be explicated by the homogenous distribution and faster activation of spores in the direct add. In addition, it was noticed that a thin layer of calcium carbonate crystals was formed at the uncracked surface due to the bacterial activity at the top surface where spores can be found. This thin layer has blocked the porous and internal channels and therefore reduced the water permeability coefficient. On the other hand, lower percentages of permeability reduction were attained for the same healing period for mixtures M4 and M6, and this could be probably attributed to incomplete healing processes due to the delay in releasing the healing agents. The water permeability results were consistent with the visual inspections and indicated that the permeability behaviour was related to the crack width closure, and therefore, it can be concluded that $CaCO_3$ precipitation had a feasible impact on reducing water permeability. This impact depended on the crack width, and amount of $CaCO_3$ precipitation.

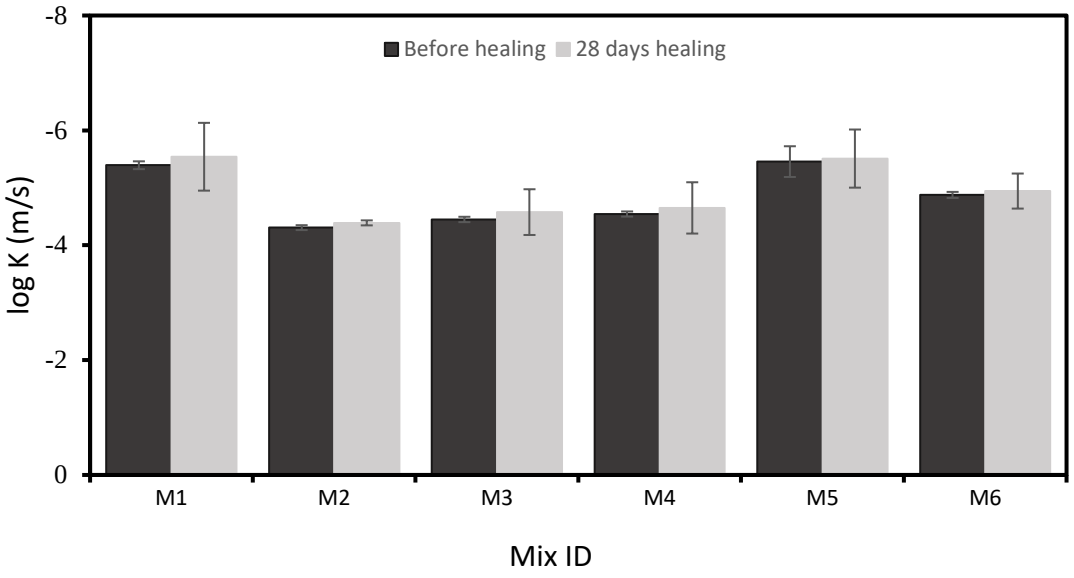

Figure 5.17: Coefficient of permeability (K) results for mixtures M1 to M6 before and after 28 days healing

5.3.5 Microstructural observation and analysis of the healing production

To characterise the microstructure and compositions of self-healing, Scanning Electron Microscope (SEM) and Energy Dispersive X-ray diffraction (EDX) were utilised. Small fractures of each mix were cut around the sealed cracks. Prior to the scanning, the small fractures were then sputter-coated with a thin layer of gold in a vacuum for 10 min to make them electrically conductive. As observed under the SEM (see Figure 5.18), a full growth of crystals with distinct sizes and shapes of hexagonal structure of calcium carbonate crystals for M1, M2, and M5 mixes, and other phases with spherical shapes of calcium carbonate crystals for M3, M4, and M6 mixes. These crystals were confirmed to be similar to the crystals which were reported in Wiktor and Jonkers' study [95]. The observed mineral precipitations of $CaCO_3$ on crack surfaces were formed due to the metabolic conversion of nutrients during the respiration of bacteria with the presence of Oxygen. However, according to Cacchio et al. [290] the formation of various morphologies of calcium carbonate crystals are still not clearly understood and could be affected by different factors such as the chemical characteristics of the cell wall of the bacteria.

Results of EDX analysis of the depicted crystals shown in Figure 5.19, demonstrated that the major elements of the white coloured precipitate are calcium (Ca), carbon (C), and Oxygen (O). It can, therefore, be interpreted those cracks were sealed by precipitated calcium carbonate ($CaCO_3$) product due to the presence of an active bacterial agent.

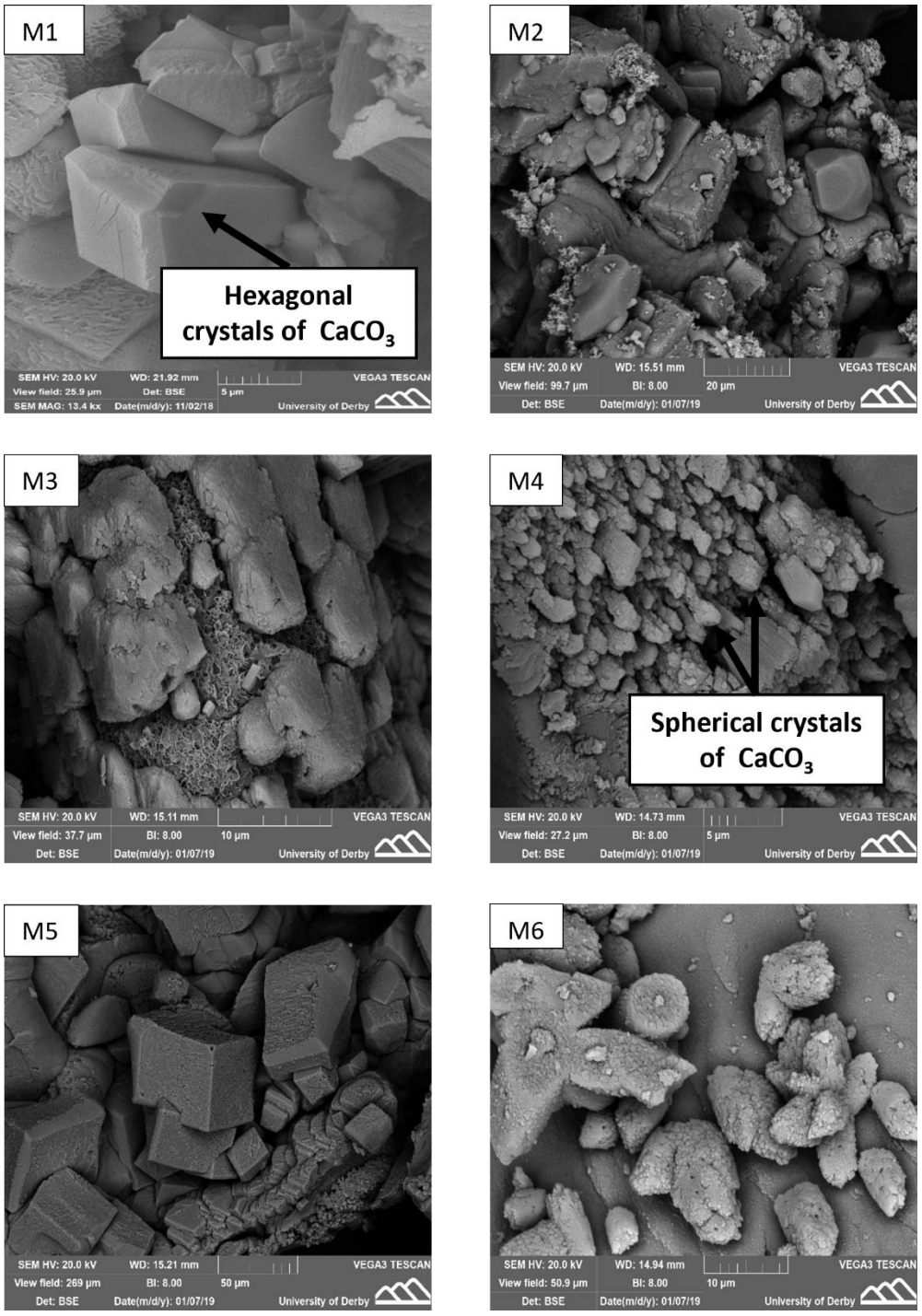

Figure 5.18: Result of SEM of white precipitated product in healing fracture for mixtures (M1 to M6)

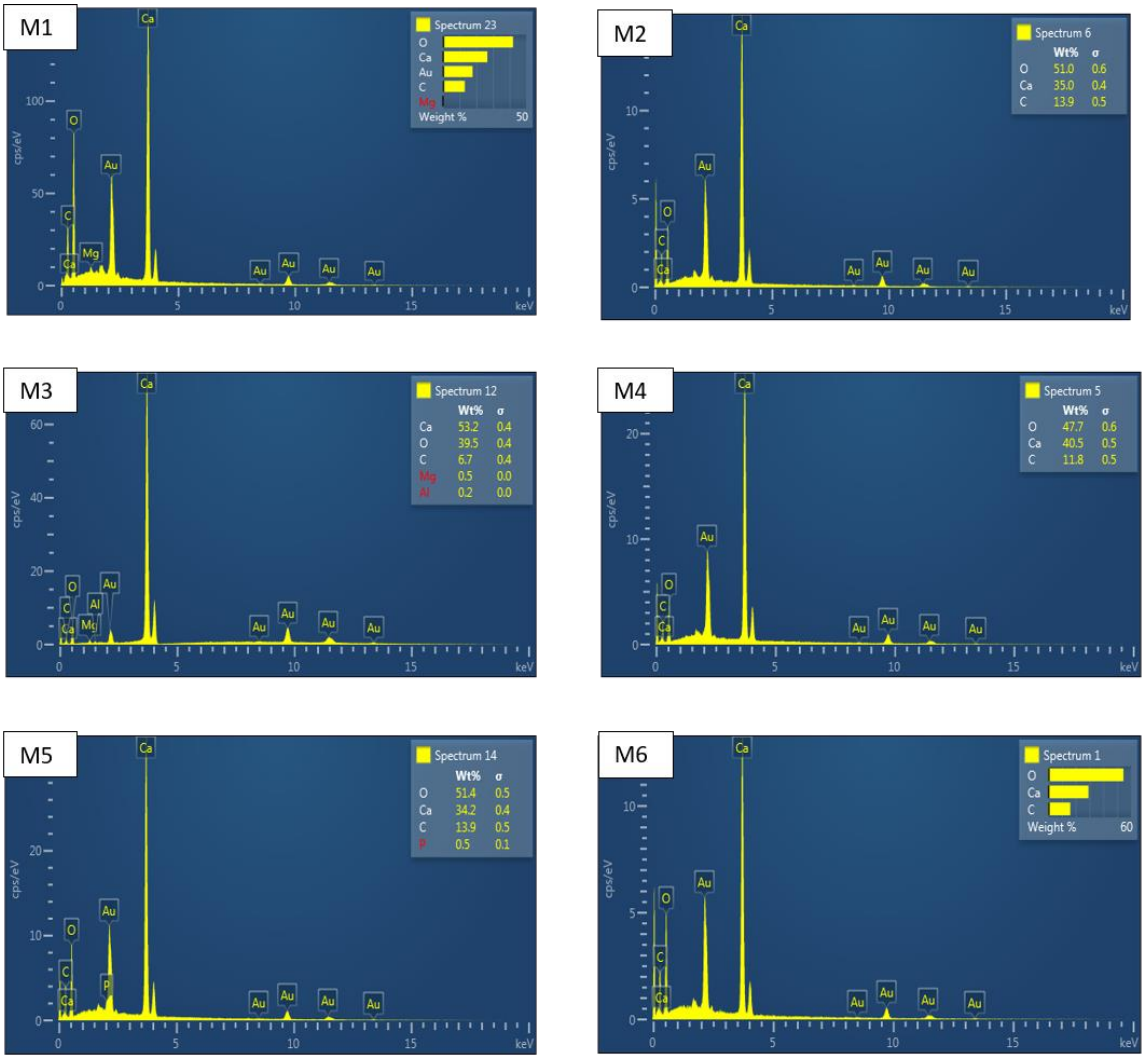

Figure 5.19: Result of EDX analysis of white precipitated product in healing fracture for mixtures (M1 to M6)

5.4 Concluding remarks

In the preliminary phase of the research work, different delivery techniques of bacterial agents were investigated to assess the effect of these techniques on self-healing efficiency and compatibility with the cement mortar matrix.

Based on the results of the viability of spores, compressive strength, visual inspection, water permeability and SEM and EDX tests, the following conclusions can be drawn:

- The viability of spores over the time has been affected by the type of capsules. After 150 days, the maximum number of viable spores was in perlite capsules. In contrast, direct add of spores resulted in loosing around 70% of their colonies.
- The volume stability of the perlite capsules has made them more compatible with the cement mortar matrix in comparison with calcium alginate capsules. However, in general, incorporation of the healing agents within capsules had a negative impact on strength behaviour.
- Voids were formed around the calcium alginate beads due to cement hydration. In most cases, cracks were crossing these voids without breaking the capsules, whereas perlite capsules were not affected by cement dehydration.
- The direct delivery of bacteria provides homogenous distribution of the bacterial agent in concrete specimens, and the healing performance was more efficient at the early stages of incubation and was less efficient after long-term incubation. It could be interpreted that the viability of spores was reduced as a result of the high alkaline environment within the cement matrix.
- The visual evaluation showed that, the maximum crack-healing capacity was achieved for specimens incorporated with uncoated perlite.
- Self-healing was achieved in both cases either by impregnating nutrients with spores or in separate capsules. This means that the activated spores feed on nutrients released from their capsules and carried to the crack surface during the incubation period.
- Coating the perlite using sodium silicate to protect the impregnated bacteria may have a negative impact on healing performance, where the coating layer delays the release of the bacterial agents, therefore impeding the crack healing process.
- The SEM and EDX results presented that the mineral precipitations on crack surfaces are calcium carbonate.

Chapter 6

The effect of soil incubation conditions on the efficiency of self-healing concrete

6.1 Overview

This chapter aims to understand the effect of different ground conditions on the efficiency of bio self-healing in cementitious materials. The chapter presents three experimental stages based on the types of soils and their conditions where the bio self-healing of cement mortar specimens was examined as explained below. The full experimental program presented in this chapter is shown in Figure 6.1.

The first stage investigates the effect of the presence of microbial and organic materials within the soil on the performance of self-healing by incubating mortar specimens into sterilized and non-sterilized soil. This stage aims to investigate if the existing bacteria in the soil can produce any self-healing.

In the second stage, the investigation focused on the bio self-healing in specimens incubated in coarse-grained soil (sand). The soil was subjected to fully and partially saturated cycles and conditioned with different pH and sulphate levels representing industrially recognised classes of exposure (namely, X0, XA1, and XA3). These classes were selected according to BS EN 206:2013+A1:2016 - based on the risk of corrosion and chemical attack from an aggressive ground environment, where X0 represents no risk and XA3 a very high risk.

Finally, in the third stage, cement mortar specimens were incubated into fully and partially saturated fine-grained soil (clay) with similar aggressive environments as in stage 2.

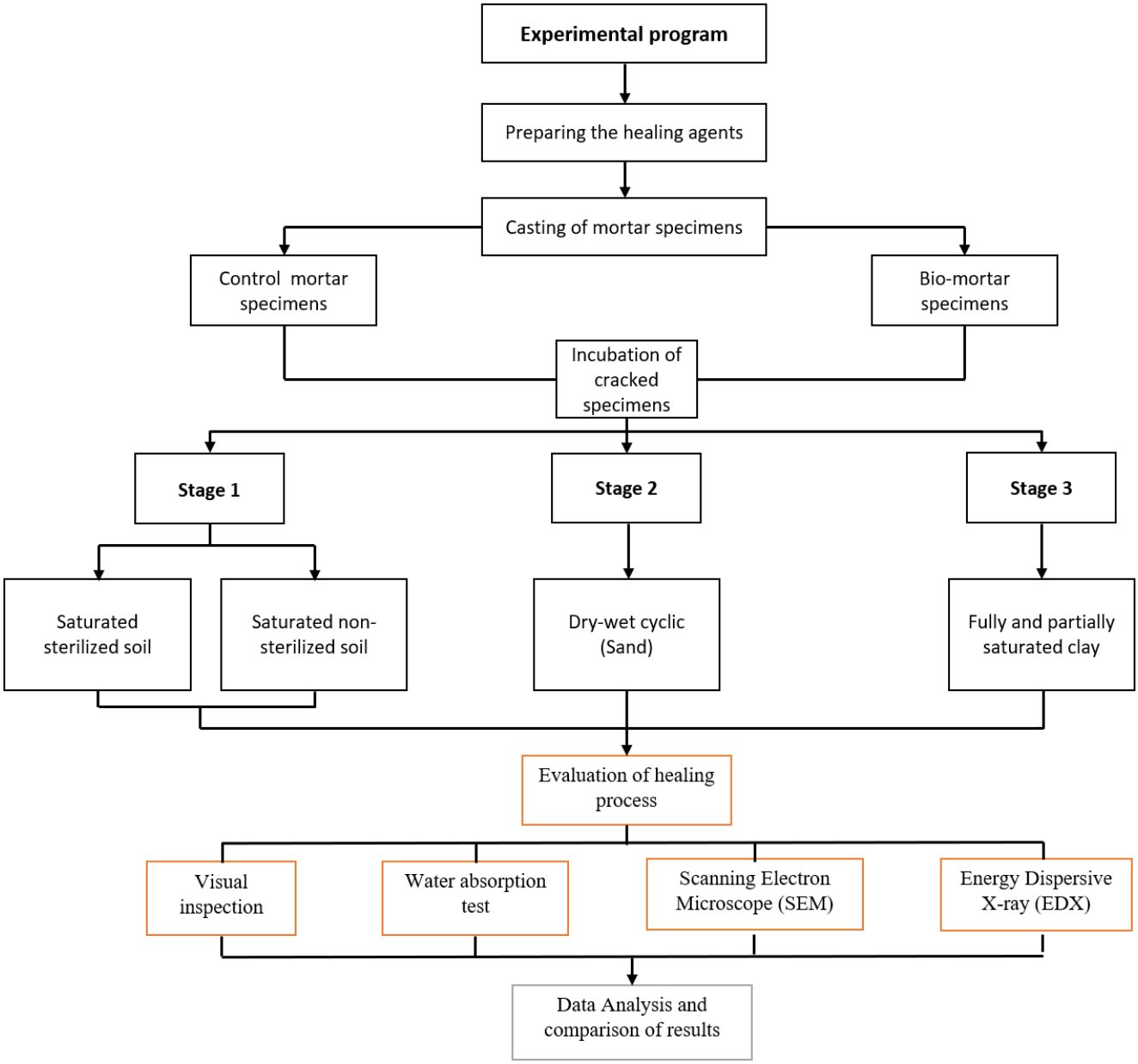

Figure 6.1: Experimental programme layout

6.2 Experimental program

6.2.1 The effect of growth media's pH on the growth of bacteria (Preliminary testing)

One of the primary factors that can have an impact on bacterial growth within the growth media is the pH level [296]. Therefore, in order to investigate the effect of pH value on the growth of *bacillus subtilis* bacteria and on the amount of precipitated calcium carbonate, first, the bacterial spores were cultivated in three medias with

different pH values. 900 ml of growth media were prepared by adding 7.2 g of nutrient broth (Difco), 0.225 g of magnesium sulphate, and 0.9 g of potassium chloride. The solution was divided into three bottles and every bottle contains 300 ml of growth media. The first bottle was considered as a control and the pH value was around 7. The pH value for the second and third bottles was adjusted by adding hydrochloric acid (Hcl) with a concentration of 1M to the solution with different concentrations and then followed by mixing the solution using a magnetic stirrer to make the solution more homogenous resulted in a solution with pH values of 6 and 4 for the second and third bottles respectively as shown in Figure 6.2. The solution was autoclaved for 20 minutes at a temperature of 120 ℃, and then it was left until its temperature matched the room temperature and later buffers of Ca $(NO_3)_2$, $MnCl_2$, and $FeSo_4$ were added with percentages as explained in Chapter 4.

Three cultures of *bacillus subtilis* were cultivated for each pH value by adding 100 ml of growth media to clean autoclaved flask and then they were incubated in a shaker at (36 °C, 125 rpm) for 72 hours. After the incubation, the spores were tested under the microscope using Spore Stain Test (SST) and then were spread over agar plates to quantify the colonies using CFU test for every culture.

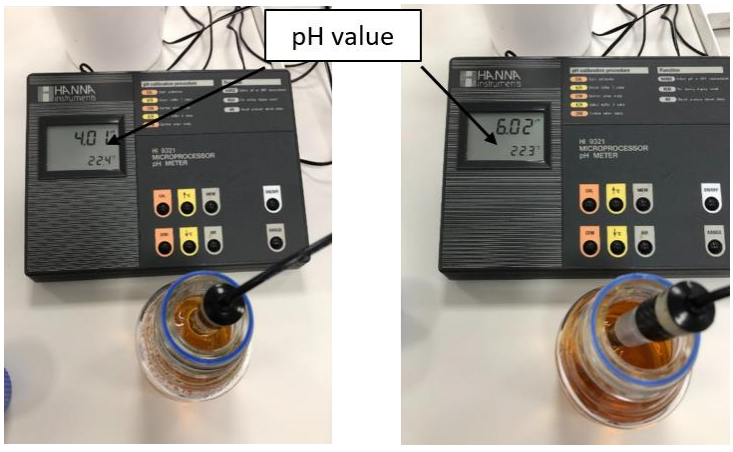

Figure 6.2: Preparation and measuring the pH values of growth media

In this test, the effect of pH value on the amount of precipitated calcium carbonate was also investigated by growing bacterial spores in 9 flasks with different pH values (7,6, and 4). Each one of the 3 flasks has the same pH and every flask was filled with 100 ml of sterilized water with a different pH value (adjusted as explained in the first stage) and 5 g of calcium lactate and 0.5 g of yeast extract as nutrients. 1 ml of *bacillus subtills* spores was added to every flask and then the cultures were incubated in a shaker at (36 °C, 125 rpm) for different periods of 3, 6 and 10 days. After each period, the solutions were centrifuged in 15 ml falcon tubes at high-speed (4000 RPM) for 10 min to separate the precipitated materials of calcium carbonate, and organic materials from the culture solution as shown in Figure 6.3. The precipitated materials at the bottom of the falcon tubes were mixed with 1ml of sterilized water and vortexed for 1 min. The homogenous suspension was filtrated using ultra-fine filter paper with retention down to 0.7 µm in liquids and the retained materials were left in the oven at 36℃ until they get dry. After drying, the precipitated were collected and weighted using a digital scale with an accuracy of 0.1 mg. The weight of precipitated calcium carbonate was calculated by taking the average weight for each pH. The precipitated materials were also scanned under the SEM to verify the formation of crystal morphology and chemical compositions.

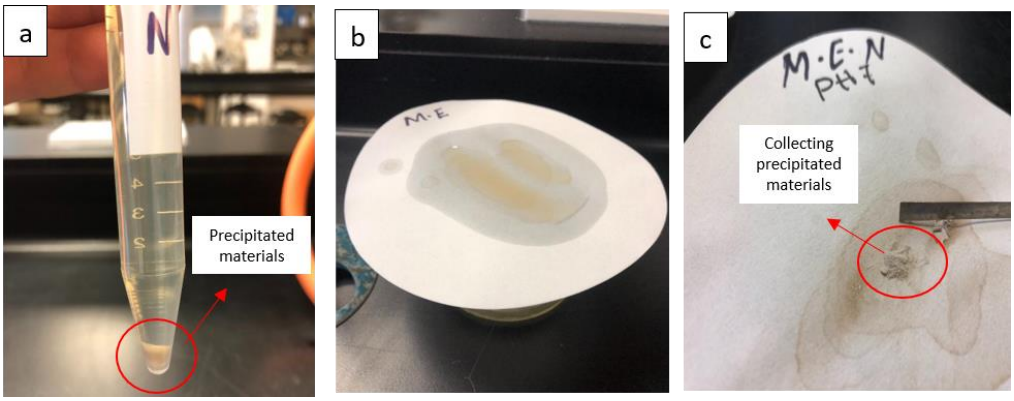

Figure 6.3: Process of collecting precipitated materials of calcium carbonate and organic materials. (a) A pellet of deposition of precipitated materials at the bottom of the test tube after centrifuge, (b) Using ultra-fine filter paper to filter the suspension, (c) Scratching and collecting the precipitated materials after drying.

6.2.2 Preparation of cement mortar specimens and crack creation

Four different types of mixes were prepared according to BS EN 196-1 [337] as presented in Table 6.1. The bacterial spores were encapsulated with nutrients into perlite as explained in Chapter 5, section 5.2.4.2. The produced capsules containing approximately 0.3% of nutrients by perlite weight with a spore concentration of approximately 6.4 x 10^7 CFU $gram^{-1}$.

The sand was first mixed with Hanson Sulphate Resisting Cement (CEM III/A +SR supplied from the UK) and tap water. Subsequently, perlite loaded with bacterial spores and nutrients were added afterwards to the mix and mixed by using a digital mortar mixer until the mix became homogenous. For the first stage experimental program, the healing agents (bacterial spores and nutrients) were added directly to the cementitious matrix during the mixing process.

Table 6.1: Mixing proportion of the cement mortar specimens

Mixture ID.	Cement (Kg/m^3)	Sand (Kg/m^3)	Water (Kg/m^3)	Perlite + Bacteria + Nutrients (Kg/m^3)	Perlite (Kg/m^3)	Bacterial spores (Kg/m^3)	Nutrient (Kg/m^3)
M 6.1	450	1350	200	-	-	25	9
M 6.2	450	1350	225	-	-	-	9
M 6.3	450	761	225	22.5		-	-
M 6.4	450	761	225	-	22.5	-	-

Two specimen geometries were prepared: (i) cylindrical specimens (with a diameter of 100 mm and a height of 40 mm) were used for the visual inspection of crack sealing, and (ii) prismatic specimens (40 x 40 x 160 mm) were used for water absorption testing. To avoid complete failure during crack propagation, the prisms specimens were reinforced by a fibre mesh placed at the centre of the specimens during casting. After 24 h, the mortar specimens were removed from their moulds and cured for 28 days until they were tested. After curing, the specimens were cracked using standard mechanical testing. A three-point-bending test was used for the prisms and a splitting test for the cylinders as explained in Chapter 4 (Sections 4.5.1, and 4.5.2 respectively).

Subsequently, the specimens were visually inspected under a light microscope (Nikon) where the widths of cracks were measured at regular intervals using Shuttlepix Editor software.

The inspection indicated that various cracks were generated with widths ranging between 60 µm to 350 µm as a result of the mechanical loading. Measuring and classifying these cracks were necessary to ensure each incubation environment would equally have all ranges of crack widths.

6.2.3 Characterisation of soil and incubation process

6.2.3.1 The effect of the presence of microbial and organic materials within soil on the efficiency of self-healing (stage one)

The natural soil consists of five major ingredients, which contain minerals, organics, air, water and living microorganisms. The soil environment can be defined as the outer loose district of the earth's surface that supports the life of plants and other organisms. From the engineering viewpoint, the soil is the hosting environment that supports the substructure of any construction such as foundations, bridge bears and retaining walls through active and passive pressure. Microbiologically, the soil is considered one of the most active regions of microbiological interactions in nature. It is the site where most of the physical, biological and biochemical reactions related to decay of organic materials, impairment, and mineral transformation exist and cycling of nutrients [353]. These transformations may have a significant impact on the performance of bacterial based self-healing concrete.

In this stage, incubating control specimens M6.2 (with nutrient only), bio-mortar specimens (with bacterial spores + nutrient) in sterilized and non-sterilized soil were conducted to investigate the effect of microbial and organic materials within soil on the efficiency of self-healing concrete.

The soil was locally resourced from a natural field within the University of Derby. The soil was first examined visually to determine its class. It was classified as natural alluvial soft to firm dark brown silty slightly sandy clay. This alluvial clay would contain a wide range of bacteria that naturally existed within the ground. The soil had neutral pH values

of 6.5 to 7.6, measured by a hand-held soil pH tester. Further analysis of the soil using Particle Size Distribution (PSD) testing indicated a very high content of fine-grained material (more than 35% of clay) and less than 7.4% sand and gravel. As the fine-grained material is highly impermeable, an additional amount (about 15%) of medium-grained sand was added to the soil to slightly improve its permeability. The soil was sterilized using the oven at a temperature of 120℃ for three days (Figure 6.4) to destroy the microbes and organic materials within soil.

Figure 6.4: Sterilizing the soil using the oven at a temperature of 120℃

The soil incubation process was conducted within plastic containers with dimensions of (600 x 350 x 400 mm) as shown in Figure 6.5. The cracked specimens were incubated into the soil at depth of 100 mm from the bottom side and 150 mm above the top surface. Each container hosted six specimens of the same type, and the initial condition of the soil was made fully saturated where negative pore water pressure (suction) should be almost zero.

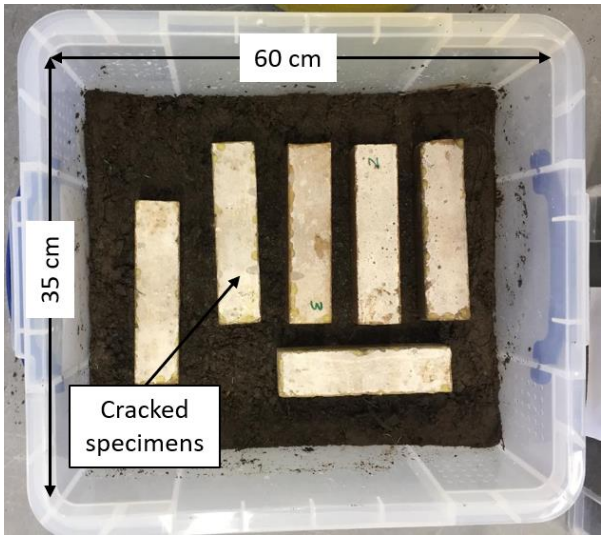

Figure 6.5: Incubation of cracked specimens within sterilized and non-sterilized natural soil

6.2.3.2 The effect of aggressive environment of exposure on the efficiency of self-healing

World widely concrete is considered as one of the most popular materials selected in the underground structures exposed to aggressive environmental conditions such as foundations, tunnels and water tanks buried in the earth due to its high performance and durability [354]. However, the presence of sulphates in soils, groundwater, or industrial effluent surrounding a concrete structure may cause a serious problem to the long-term durability, especially for the underground concrete structures. The sulphate attack of concrete could lead to major threads such as cracks, an increase in permeability, and loss of strength. Therefore, in order to ensure durable concrete with high performance for structures in direct contact with soil containing sulphates, bacterial based self-healing concrete could be utilized to seal concrete micro-cracks caused by sulphate attack or any other reason which can cause cracks to concrete. This is especially important because in some cases it is impossible to repair the micro-cracks of underground structures and the durability of concrete structures is becoming an increasingly serious economic and ecological issue.

However, the different concentrations of sulphates, pH, soil permeability, and the lack of oxygen within soils play significant roles in the activity of bacterial agents and therefore, in the efficiency of self-healing concrete.

This stage aims to investigate the effect of these parameters on the healing performance by incubating cracked cement mortar specimens in clay and sandy soil with different concentrations of sulphates exposed to different ground regime including, fully and partially saturation, and dry-wet cycles. The non-cohesive soil (sand) and cohesive soil (clay) used for the incubation of cracked specimens were prepared as follows.

Non-cohesive soil (sand – stage two)

Non-cohesive soil can be defined as any free-running type of soil and the particles lie side by side without bonding, such as gravel or sand. In this study, a high-quality premium and free chemical with sub rounded grain shape sandy soil was used for the incubation of bio and control mortar specimens.

To characterise the soil, Particle Size Distribution (PSD) analysis (Figure 6.6) was conducted using a sieve test in accordance with BS EN 933. The stack of sieves was shaken using a designated shaker for about 10 min and then retained soil on each sieve was weighed. The test confirmed that the soil was medium to fine sand (BS 5930:1981), with 95-97% of the material between 100 and 700µm and only around 3-5% smaller than 63µm. This sand is considered a permeable material with quick water drainage. Therefore, any induced change in water content or saturation degree (e.g. fully and partially saturated cycles required during the test) is expected to take effect quickly. In contrast to clay soils, such a change in water content could take an inordinately long time due to poor permeability [355].

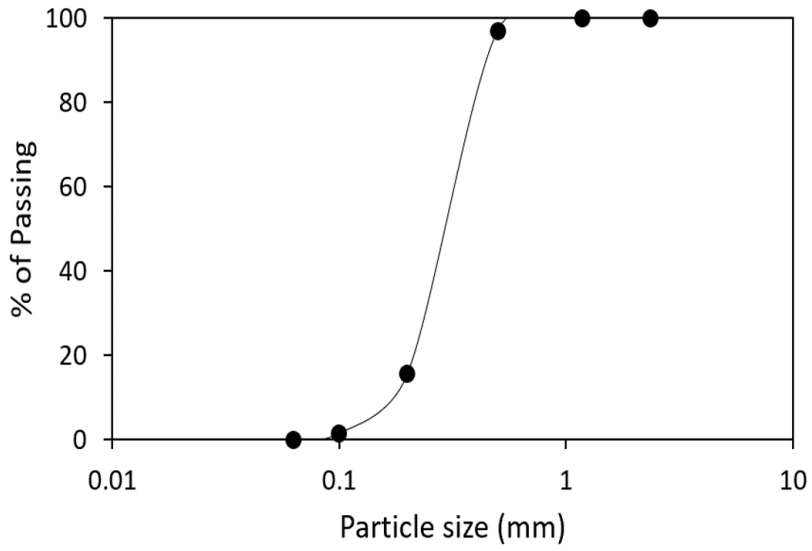

Figure 6.6: Particle Size Distribution of the soil (sand) used for incubation.

The chemical composition of the sand was also investigated under SEM and EDX, as shown in Figure 6.7. The results indicated that the sand was mainly composed of (SiO_2) Silicon dioxide, (K_2O) potassium oxide, (Al_2O_3) aluminium oxide, (Fe_2O_3) iron oxide, and (MgO) Magnesium oxide. This was similar to the SEM and EDX results conducted on the sand used for preparing the mortar mixture.

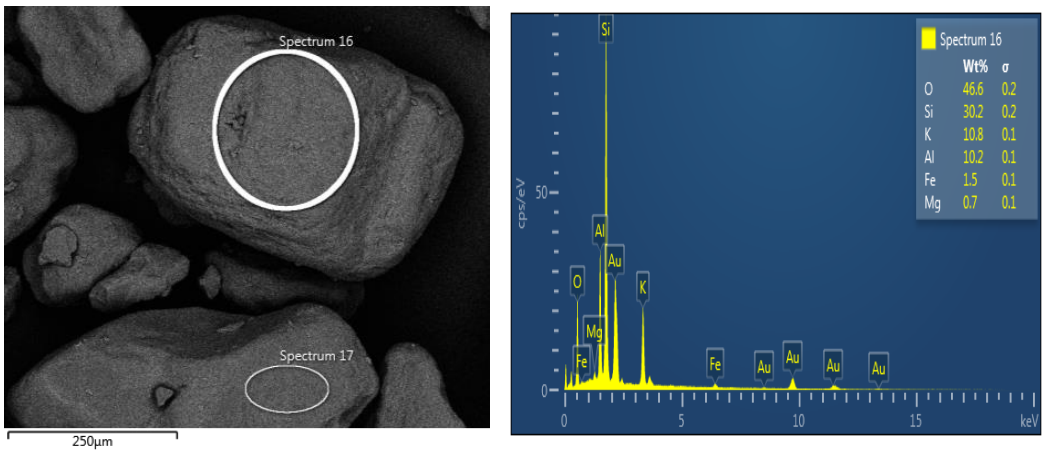

Figure 6.7: Result of SEM and EDX analysis of the sand used for incubation

The sand density (of 20.4 ± 0.5 kN/m3) was controlled by maintaining a constant drop height and flow rate. The sand was placed in plastic boxes (with dimensions of 600 x 350

x 400 mm), and up to six specimens were placed within each plastic box, which was outfitted with a filtration system. A porous sheet, thin gravel layer, and outlet at the base of these boxes were added for controlled drainage. This setup (see Figure 6.8) facilitated the creation of fully and partially saturated cycles during incubation time and crack healing.

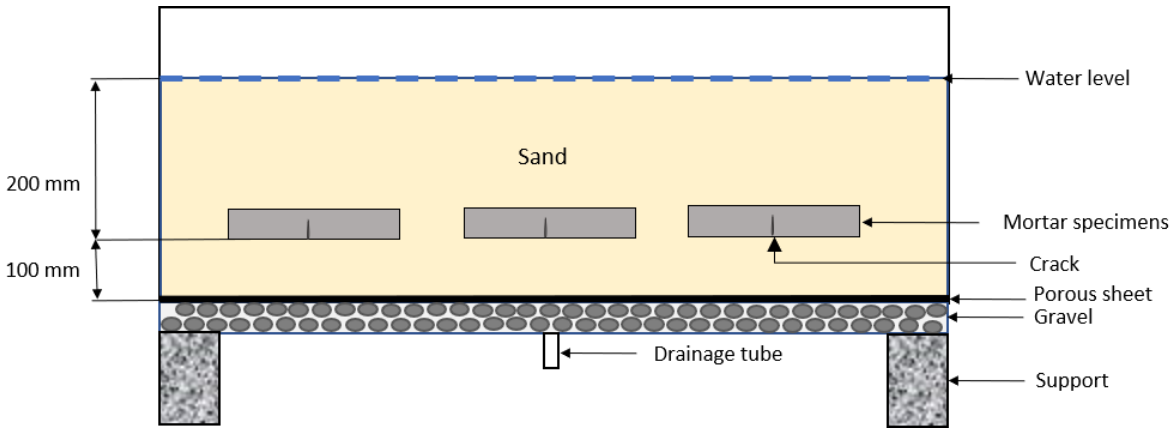

Figure 6.8: Schematic illustration of an incubation box containing cracked specimens within non-cohesive soil (Sand)

The pH value of the soil was adjusted to match the aggressive chemical environments with three categories X0, XA1, and XA3 classified in accordance with Table 2, BS EN 206:2013+A1:2016.

X0 was the control class with a neutral pH value of around 7; whereas the pH values for classes XA1 and XA3 were adjusted to be approximately 6 (moderately acidic environment) and 4.5 (extremely acidic), respectively. As stated in BS 1377-3:1990, calcium sulphate is considered the sulphate salt that is most commonly found in soil. Therefore, the soil pH was reduced to the required level by mixing the soil with calcium sulphate (supplied by Sigma-Aldrich Ltd, UK) in the percentages shown in Table 6.2. For confirmation, the soil pH was measured using a portable pH meter, as shown in Figure 6.9.

Table 6.2: Limiting values of calcium sulphate to achieve the desired exposure classes

Exposure class	X0	XA1	XA3
Calcium sulphate (mg/Kg)	0	≥ 2000 and ≤ 3000	>12000 and ≤ 24000
pH range	< 7.4 and ≥ 7	≤ 6.5 and ≥ 5.5	≤ 4.5 and ≥ 4
Achieved pH	7± 0.2	5.9± 0.2	4.5± 0.2

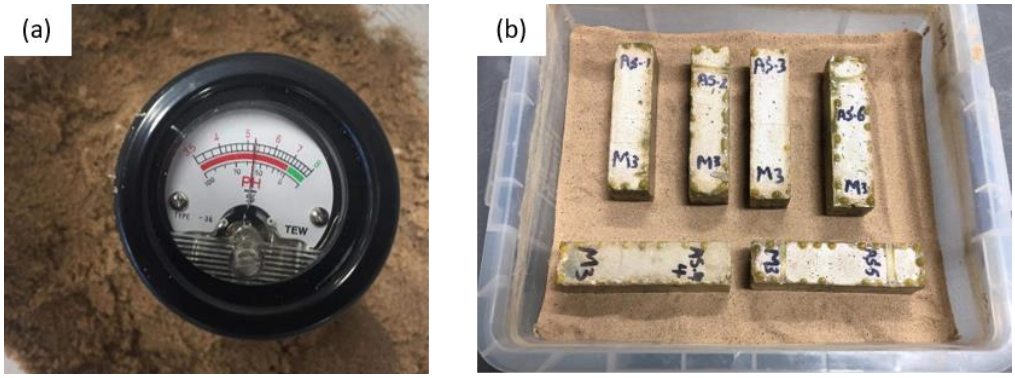

Figure 6.9: (a) Using portable pH meter to measure soil pH, (b) incubating the cracked specimens into the sand

The cracked specimens were first visually inspected and tested for water absorption and then incubated at a depth of 200 mm from the bottom surface. The bio (BMS) and control mortar specimens (CMS) were incubated in separate boxes to avoid cross-contamination i.e. immigrating the spores and nutrients from the crack zone of BMS specimens to CMS through water seepage within the soil.

The soil (with the cracked specimens) was then subjected to fully and partially saturated cycles for 120 days. For each cycle, the soil was fully saturated for 20 days by adding water from the soil surface, then partially saturated for 10 days by allowing water to drain away from the system at the bottom of the incubation box (Figure 6.10). Control and bio-mortar specimens were incubated in water in order to be used as a control exposure class. All incubations were conducted at a room temperature of approximately 23°C.

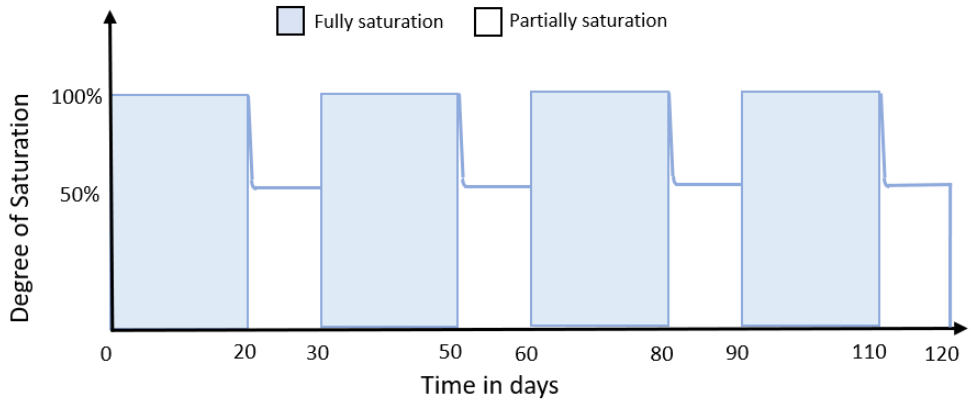

Figure 6.10: Schematic illustration for fully and partially saturated cycles of incubation

Cohesive soil (clay - stage three)

The cohesive soil is characterized as sticky soil, and can be designated as loam, clay or silty clay. The clay used in this work is commercially available and it was supplied from Pot-clays in the UK - mainly containing clay with some silt to be used for incubating the cement-mortar specimens. This type of soil was considered for the experiment because it is widely encountered in construction sites, not only in the UK [31] but also in many other regions worldwide. The clay content is comprised of kaolinite which has been widely used in fundamental studies in geotechnical engineering [32]. The soil was tested to characterise its physical properties, including plasticity and grading, according to British Standers [33]. The particle size distribution (PSD) of the soil mixture was 100% smaller than 63µm, including 68% pure clay (i.e. < 2µm). Table 6.3 summarises the physical properties of the clay, indicating it is silty clay with intermediate plasticity.

Table 6.3: Physical properties of the soil (classification)

Basic Property	Average Value
Liquid limit	45%
Plastic limit	24%
Plastic Index	21
Clay content	68%
Silt content	32%
Specific Gravity	2.8

Clay soils are generally water-sensitive where pore-water pressure (u) significantly depends on the variation of moisture content and degree of saturation. For an instant, when the clay is fully saturated, u value is positive but can become negative (suction) in a partially saturated condition. For the majority of the tests, the soil was planned to be in fully-saturated condition (FSC); therefore it was important to find out the minimum moisture content at which the pore-water pressure would be positive or approximately within the normal, 'equilibrium', values (u = 0). This was determined by examining the soil suction at different moisture contents. The soil suction was measured using a Miniature-Tensiometer (UMS T5 by Labcell LTD) connected to a compatible data logger. The laboratory measurements of the suction and moisture content were plotted in Figure 6.11, which can be reasonably considered as an overall approximation of the soil-water characteristics curve [356].

As shown in Figure 6.11, the suction depends primarily on the moisture content and increased with soil dehydration. Accordingly, the following moisture contents 47% and 25% were considered for the fully and partially saturated conditions, respectively. For both conditions, we had also to control the densities as this influence the saturation. Table 6.4 summarises the soil parameters considered in both conditions (FSC and PSC).

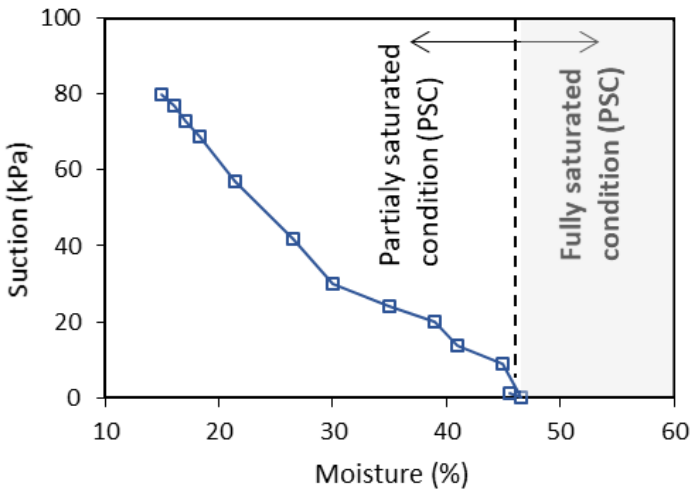

Figure 6.11: The relationship between the measured suction and average moisture content of the soil. The moisture contents of 47% and 25% were considered for the fully and partially saturated conditions, respectively

Table 6.4: Soil parameters under the two water regimes/ conditions

Property	Fully saturation condition (FSC)	Partially saturation condition (PSC)
Density (Mg/m^3)	1.78 ± 0.1	1.58 ± 0.1
Moisture content (%)	47 ± 2	25 ± 2
Suction (kPa)	0 ± 1	49 ± 1

The soil was conditioned to represent two hydrological regimes, including partially and fully saturated conditions (PSC and FSC, respectively). For FSC, three different aggressive environments were prepared by adding calcium sulphate to soil (see Table 6.5) to represent three exposures classes according to BS EN 206:2013+A1:2016, namely X0, XA1 and XA3 as stated in stage two. For the PSC, only class X0 was considered.

Table 6.5: Limiting values of calcium sulphate used to achieve the desired exposure classes

Exposure class	X0	XA1	XA3
Calcium sulphate (mg/Kg)	0	≥ 2000 and ≤ 3000	>12000 and ≤ 24000
pH range	< 7.4 and 7 ≥	≤ 6.5 and 5.5 ≥	≤ 4.5 and 4 ≥
Achieved pH	7.2 ± 0.2	5.9 ± 0.2	4.3 ± 0.2

Immediately after the inspection of the cracks, six mortar specimens were incubated for each exposure class for 120 days within the clay, which was pre-prepared according to properties specified in Tables 6.3 and 6.4. Plastic boxes - with dimensions of (600 x 350 x 400 mm), were used for the incubation, as shown in Figure 6.12. The soil was prepared in workable slurry (slump) with the required moisture content and lightly compacted in layers where the first layer reached 100 mm from the bottom before placing the mortar specimens. Then, the second layer was placed around the specimens creating a thickness of 200mm.

In order to avoid cross-contamination, the bio-mortar specimens (BMS) and the control mortar specimens (CMS) were incubated in separate soil boxes.

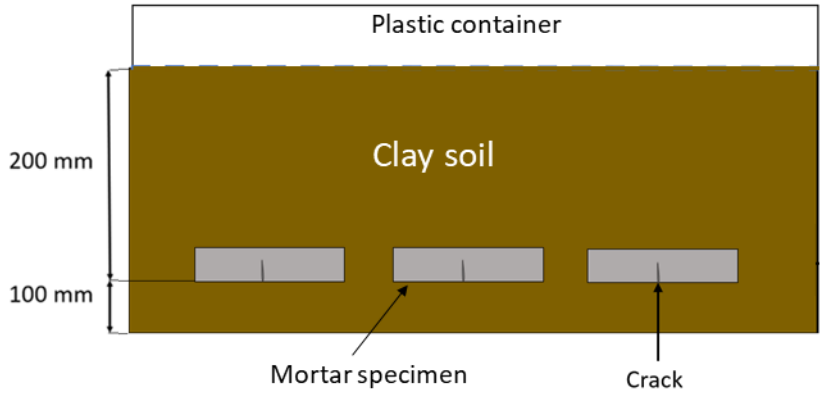

Figure 6.12: Schematic illustration of pre-cracked specimens incubated within the clay soil

6.3 Results and discussion

6.3.1 The effect of pH value on the growth of bacteria and the amount of precipitated calcium carbonate

After 72 hours of incubation, the three growth media with different pH values were taken out of the shaker to investigate the growth of the bacteria. It was observed that the flasks that containing growth media with pH of 6 and 7 were turned cloudy evident of the presence of spores, whereas flasks that contain growth media with pH 4 had the same colour of media (see Figure 6.13).

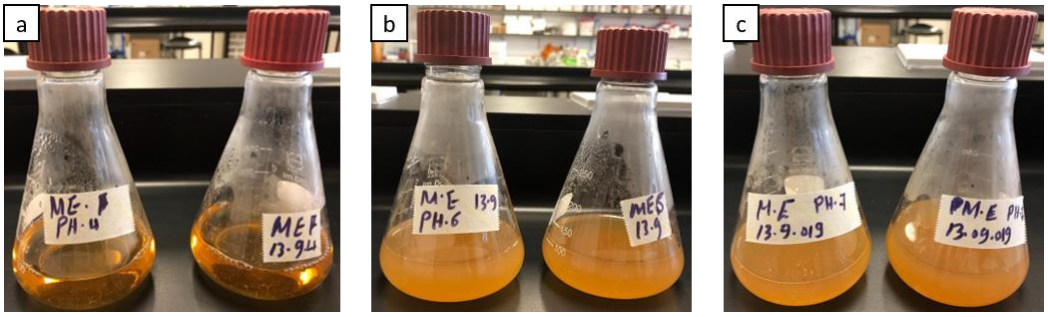

Figure 6.13: Growth medias with different pH values after incubation, (a) pH 4, (b) pH 6, (c) pH 7.

The centrifuged spores were investigated under the microscope using the spore stain test as shown in Figure 6.14. From the Figure, it can be clearly seen that the number of

spores in the growth media with pH 7 was much higher than in the growth media with pH 6 and the spores were barely seen in the growth media with pH 4 which means that the pH value has a major effect on the growth of spores. These results were also confirmed through the CFU test by using serial dilution and agar plates as shown in Figure 6.15. As shown in the Figure, the number of colonies for the growth media with pH 7 was almost twice the number of colonies of the growth media with pH 6 for the same plate with a dilution of (-4). Few colonies were observed from the growth media with pH 4.

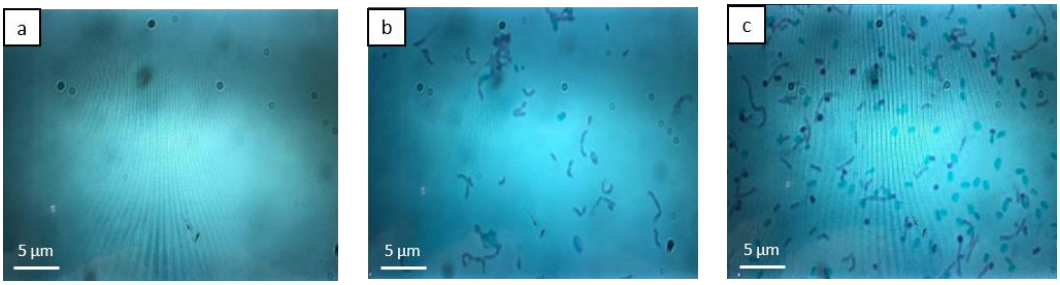

Figure 6.14: Spores of *bacillus subtills* under the microscope. (a) Growth media with pH4. (b) Growth media with pH6 (c) Growth media with pH7

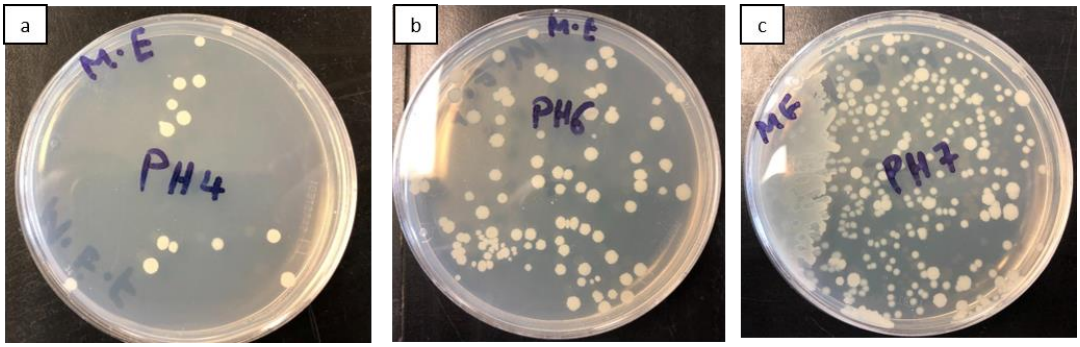

Figure 6.15: Morphology of colony-forming unit in agar plate with a dilution of -4, (a) Growth media with pH 4. (b) Growth media with pH 6 (c) Growth media with pH 7.

The effect of pH on the amount of produced calcium carbonate was also investigated for periods of 3, 6, and 10 days and the results were illustrated in Figure 6.16. From the Figure, it can be clearly seen that the amount of precipitation was significantly affected

by the pH value. It was observed that at each period of incubation the amount of calcium carbonate produced by the suspension with pH 7 was the highest compared to the amount produced by suspensions with pH 6 and 4. On observation, the highest amounts were recorded at age of 10 days of incubation (109, 100, 67 mg) for suspensions with pH 7, 6, and 4 respectively. These results were also evident in Figure 6.17, where the highest amount of precipitation was identified for tube (c).

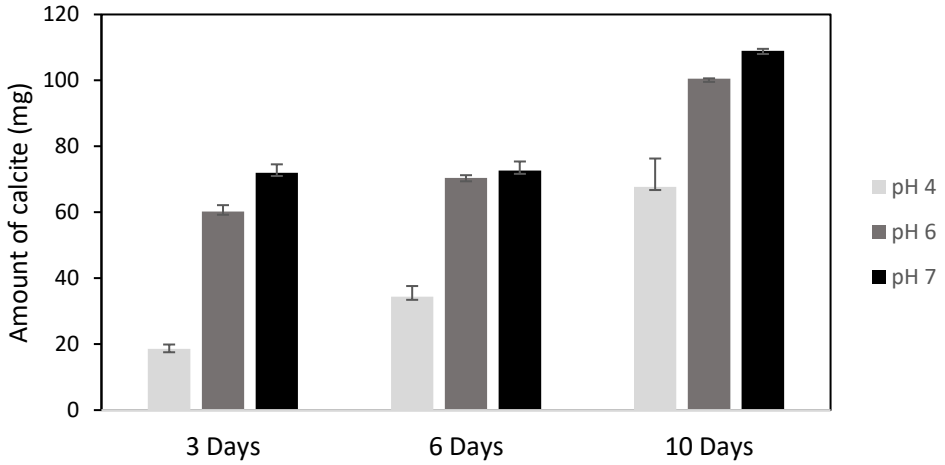

Figure 6.16: The effect of pH value on the amount of calcium carbonate produced

The produced calcium carbonate was also confirmed using SEM and EDX analysis. As shown in Figure 6.18 the crystals of calcium carbonate were detected using SEM and the chemical compositions of these crystals were ensured as calcium (Ca), carbon (C), and Oxygen (O). It can, therefore, be interpreted that the produced calcium carbonate ($CaCO_3$) was due to the activity of bacteria during incubation.

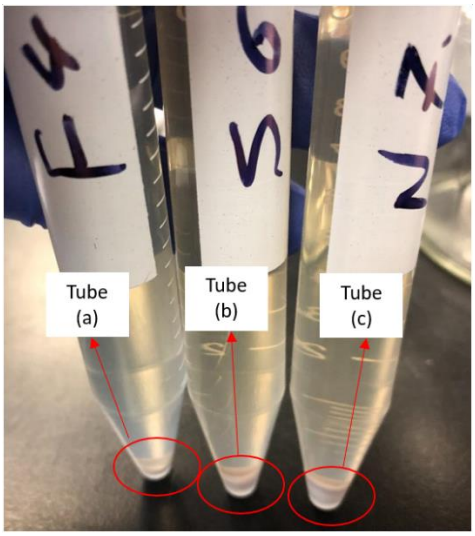

Figure 6.17: The amount of precipitated materials in falcon tubes after centrifuging. (a) pH 4 (b) pH 6 (c) pH 7

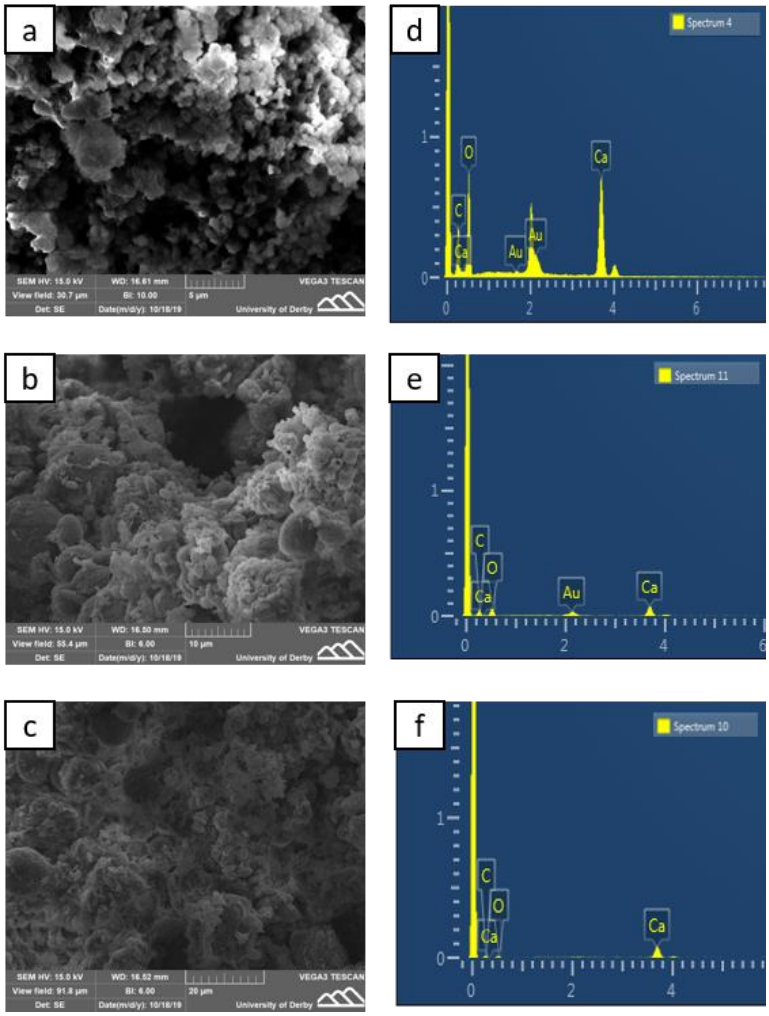

Figure 6.18: Results of SEM (a) pH4, (b) pH 6, (c) pH 7, and EDX analysis (d) pH4, (e) pH 6, (f) pH 7

6.3.2 The effect of the presence of microbial and organic materials within soil on the efficiency of self-healing (stage one)

6.3.2.1 Visual evaluation of crack and healing quantification

After incubation, the specimens were taken out from their incubation environments and then immersed in water for ultrasound cleaning before being visually inspected under the microscope to evaluate the crack closure and quantify the self-healing efficiency. Figure 6.19 shows images of CM (M6.2) and BM (M6.1) specimens incubated in different environmental conditions. It can be clearly seen that BM specimens were sealed by white precipitation. Specimens incorporated with only nutrient (CM) incubated in non-sterilized soil (NSS) were partially healed by white precipitated material. In contrast, no healing was observed for CM specimens incubated in sterilized soil (SS).

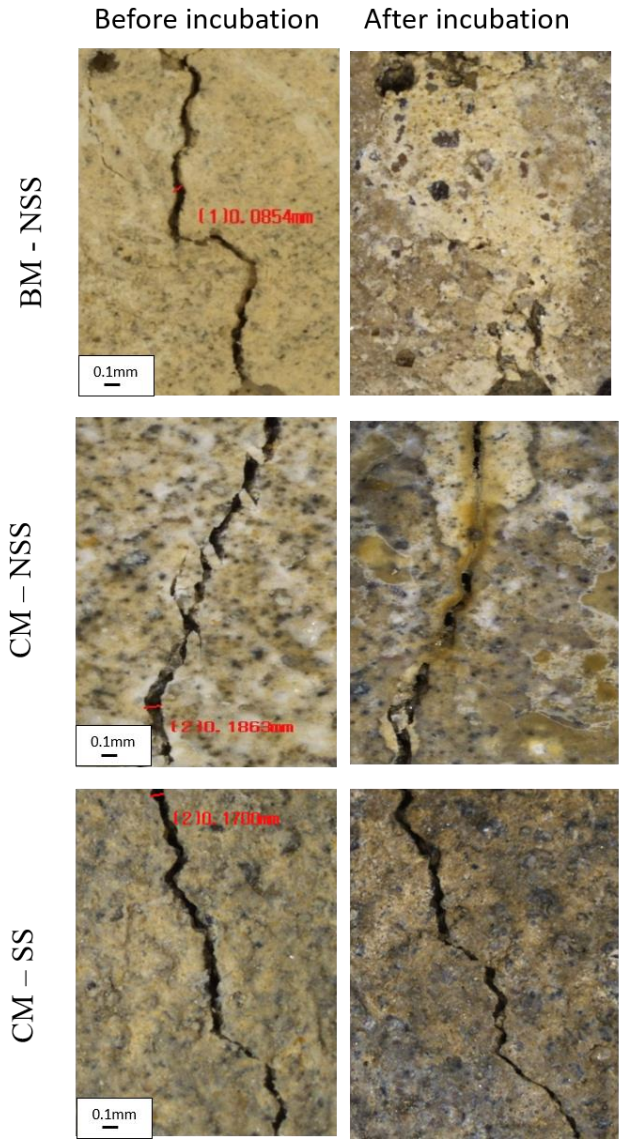

Figure 6.19: Microscopic images of cracks before and after incubation for mixtures BM and CM

To quantify the healing ratio, images of cracks before and after incubation were analysed using “image J” software. The healing ratio for all mixes and incubation conditions are presented in Table 6.6, where specimens containing bacterial agent (BM) exhibit a greater healing ratio (about 76%) compared to the other specimens not containing bacterial agent (CM) (around 46% in NSS and 29% in SS). In comparison with CM specimens incubated in SS, CM incubated in NSS showed a relative increase in healing ratio and this could be explicated by the metabolic conversion of nutrients by bacteria.

Table 6.6: Statistical results of the crack healing ratio of CM and BM specimens incubated under different exposure classes (SS and NSS)

Healing ratio (%)	Exposure classes		
	CM		BM
	NSS	SS	NSS
Min	9.15	1.03	5.25
Max	76.73	61.58	88.15
Average	46.12	29.40	75.98
St. Deviation	27.19	23.84	31.51

6.3.2.2 Capillary water absorption test results

The relationship between the mass of absorbed water per unit inflow area and the square root of time was plotted in Figure 6.20. As illustrated in the Figure, the change in a sorptivity index value of the CM specimens incubated in NSS (1.170×10^{-4} mm/√sec) is overall higher than those of the CM specimens incubated in SS (8.308×10^{-5} mm/√sec). This implies that the presence of bacteria within soil led to around 34% reduction in the sorptivity index values in comparison with the values observed in the CM incubated in SS. The lowest post-incubation absorption rate was attained for specimens incorporated with a bacterial agent (BM) incubated in NSS, as a result of the deposition of healing products which fills pores and continuous channels that passing the water and therefore reduce the amount of water taken up in the crack by capillary suction. Where the sorptivity index value was 2.412×10^{-5} mm/√sec. The absorption results were consistent with the visual inspection and indicated that the absorption behaviour was related to the crack healing ratio.

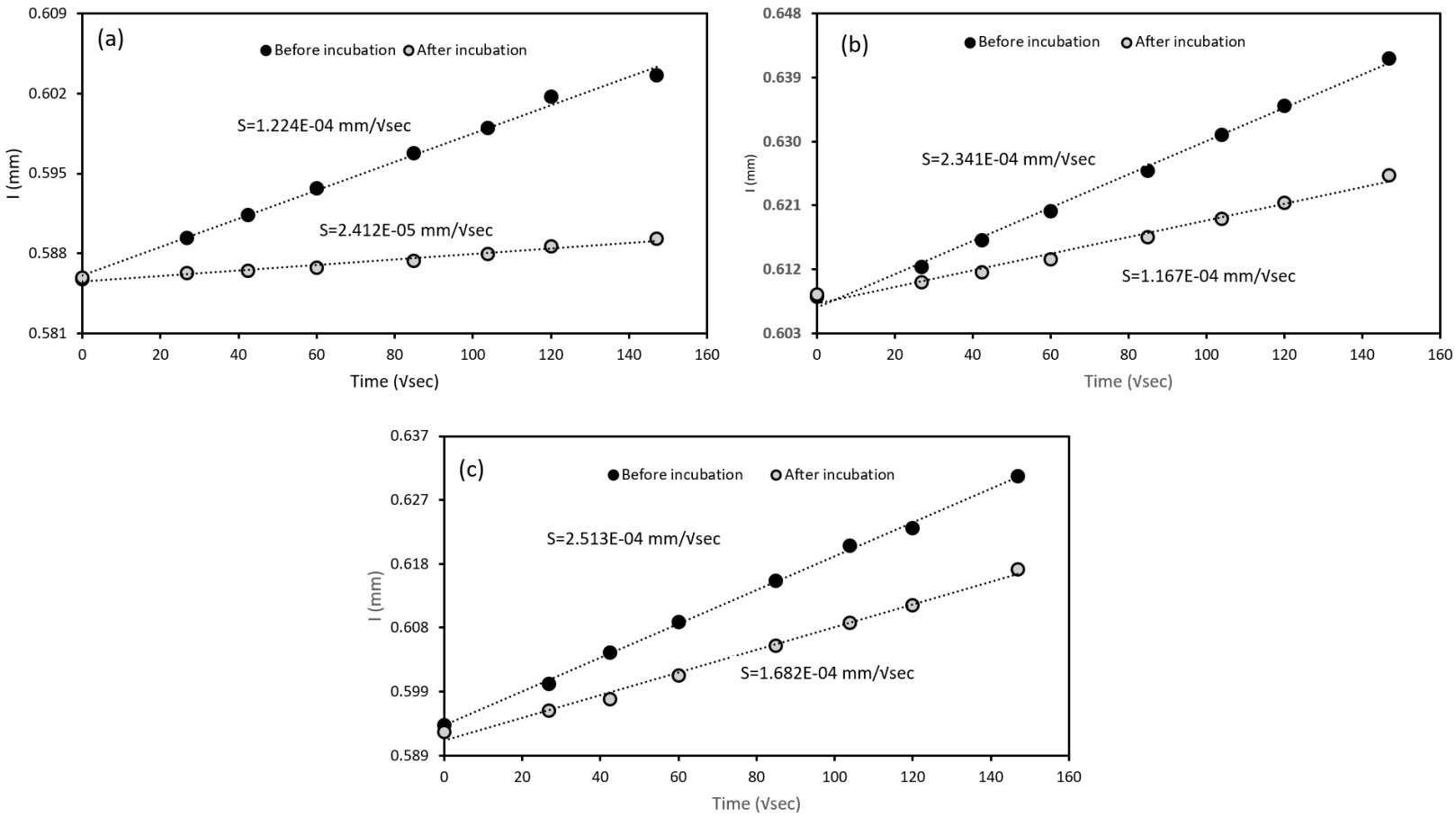

Figure 6.20: Change in water absorption of the cracked specimens before and after incubation. (a) BM specimens incubated in NSS, (b) CM incubated in NSS, (c) CM incubated in SS

The healing percentages of BM and CM based on the change in water absorption rate before and after incubation is presented in Figure 6.21. These results indicate that healing ratio of BM incubated in NSS was almost double at those of CM incubated in the same identical exposure conditions. The lowest healing ration (33%) was recorded for CM incubated in SS.

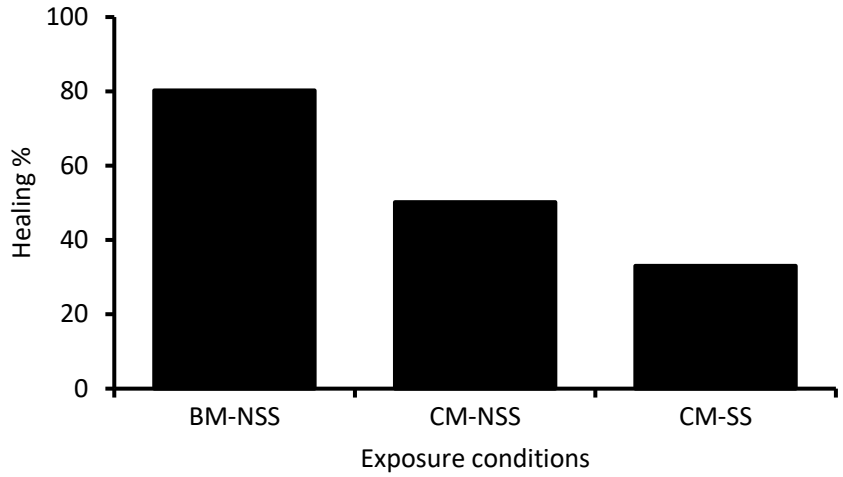

Figure 6.21: The healing percentages of BM and CM based on the change in water absorption rate before and after incubation under different exposure conditions

6.3.2.3 Microstructure analysis of healing products

The SEM and EDX analysis indicated that the microstructure of precipitated material at crack surfaces of BM and CM specimens incubated in NSS were crystals of calcium carbonate and the major elements of the mineral precipitate were calcium, carbon, and oxygen. Therefore, it can be concluded that cracks were sealed by precipitated calcium carbonate crystals. The microstructure analysis of CM specimens incubated in SS showed that the main structure was formed by crystals of calcium hydroxide and ettringite, which was formed as a result of the reaction of sulphate compounds with calcium aluminate in the cement. Calcium carbonate crystals were also observed and the probable reason for that is due to the reaction of carbon dioxide present in water

with the calcium hydroxide produced by hydration of calcium oxide [357]. The major elements were characterized by EDX were silicate and oxygen which can be attributed to forming calcium silicate hydrate (C-S-H) due to the ongoing hydration of cement particles. Therefore, we conclude that cracks were sealed by precipitated calcium carbonate crystals, and that the process was enhanced in the presence of naturally occurring soil bacteria.

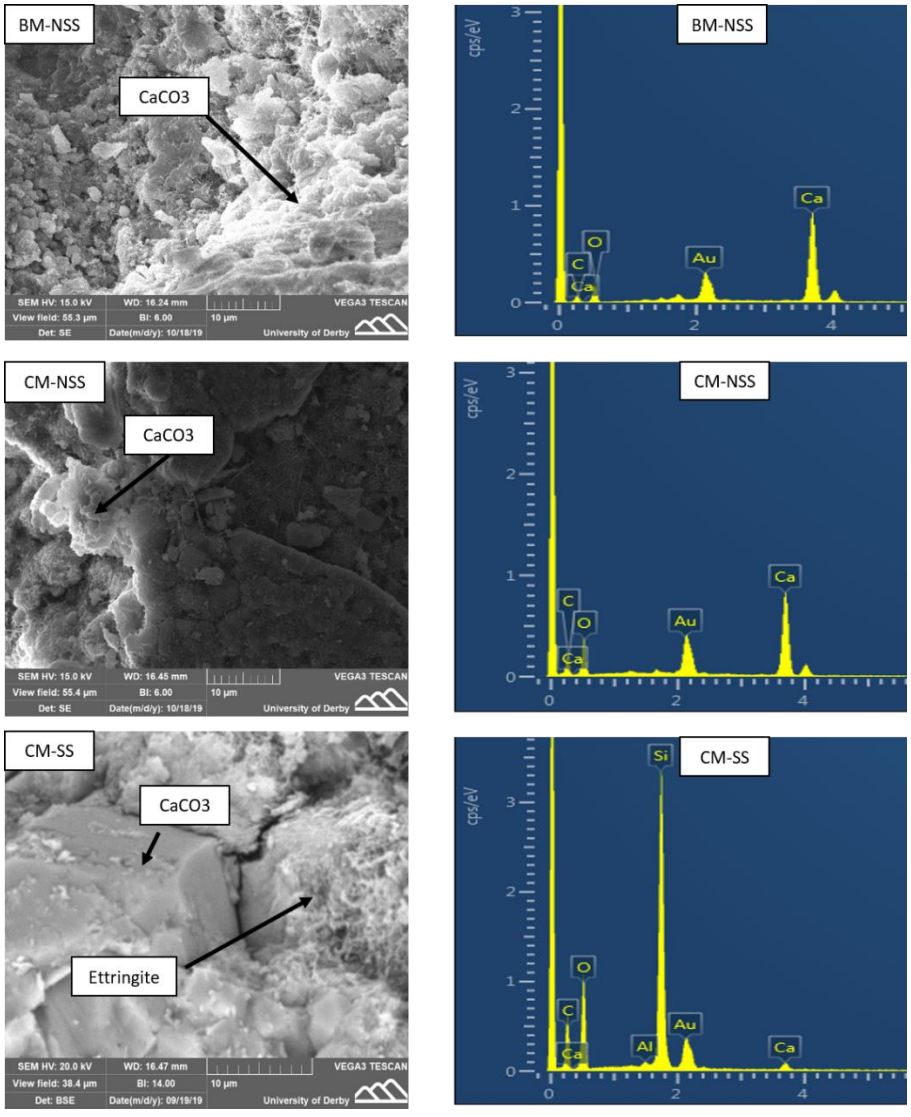

Figure 6.22: SEM images and EDX analysis of precipitations at cracks surface

6.3.3 The effect of exposure conditions on the efficiency of self-healing cement mortar specimens incubated into non-cohesive soil (sand) exposed to dry and wet cycles (stage two)

6.3.3.1 Visual evaluation of crack and healing quantification

After 120 days of incubation, the control (CMS M6.4) and bio-mortar specimens (BMS M6.3) were removed from their incubation environments and visually inspected under the microscope to evaluate the crack closure. Figure 6.23 depicts several top views of the crack surface of BMS before and after the healing process in four different exposure conditions. As shown, the widths of completely healed cracks were significantly larger in specimens incubated in water and pH neutral soil (X0) (280 and 260µm, respectively) than specimens incubated in XA1 and XA3 (180 and 110 µm, respectively). In addition, only a few locations were completely healed for specimens incubated in XA3, which can be attributed to the effects of a high concentration of calcium sulphate and low soil pH.

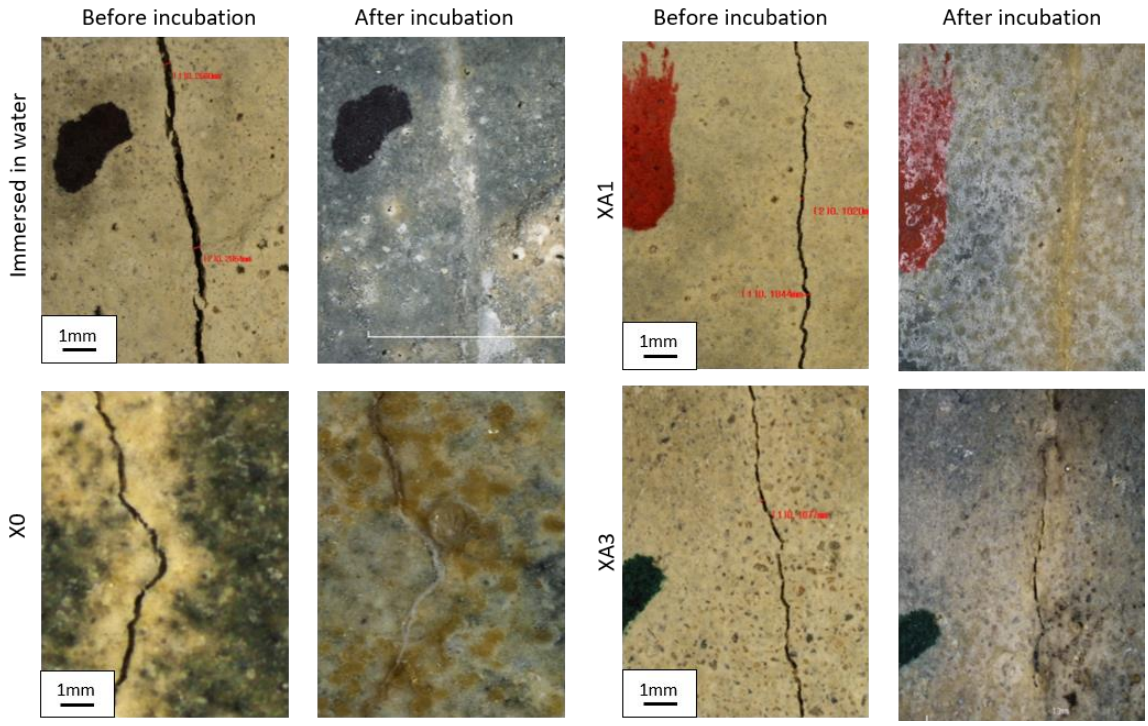

Figure 6.23**:** Microscopic observation of crack healing of (BMS) before and after incubation

The results of the microscopic inspection of CMS are presented in Figure 6.24. This shows that most of the small cracks (< 100 µm) incubated under different conditions were autogenously healed (as a result of exposing the un-hydrated cement particles within the crack area to secondary hydration) and the maximum healed crack width was approximately 120 µm.

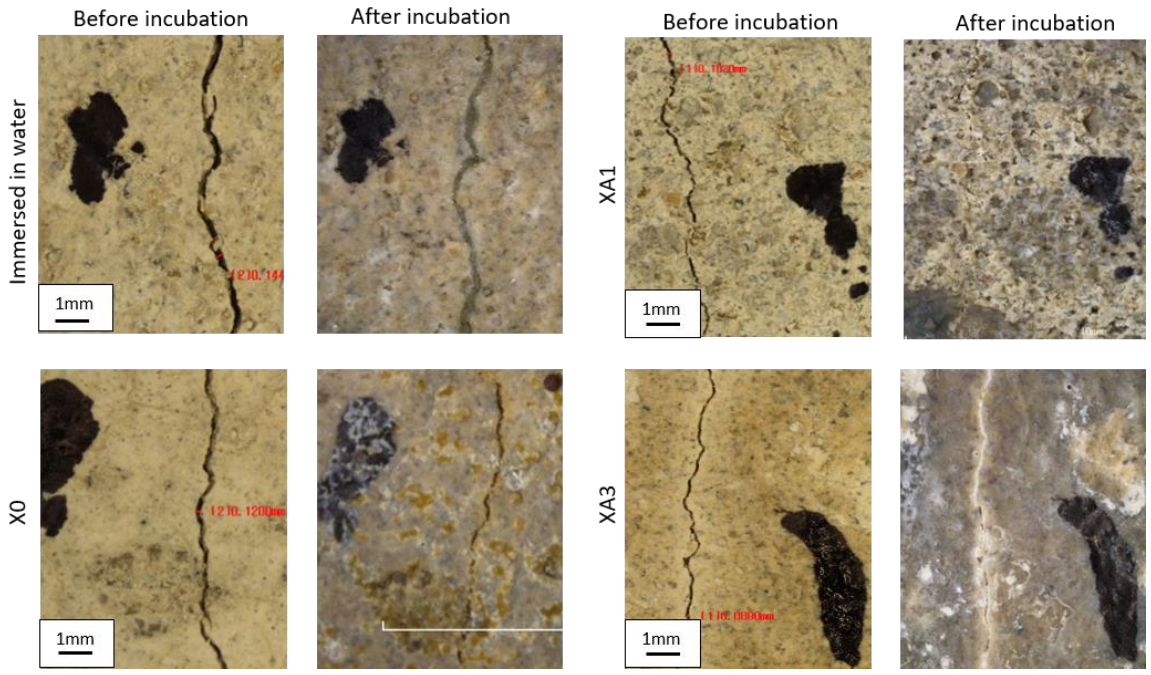

Figure 6.24: Microscopic observation of crack healing of (CMS) before and after incubation

Table 6.7 presents the statistical results using “image J” software for the crack healing ratio of CMS and BMS specimens incubated in different exposure classes. The results of the image analysis were consistent with the microscopic observation. Furthermore, the relationship between the crack width and healing ratio for CMS and BMS was inverse in that the smaller the crack width, the higher the healing percentage.

Table 6.7: Statistical results of the crack healing ratio of CMS and BMS incubated under different exposure classes

Healing ratio (%)	Exposure classes							
	Water immersed		X0		XA1		XA3	
	CMS	BMS	CMS	BMS	CMS	BMS	CMS	BMS
Min	1.075	17.96	0.249	17.08	6.85	19.80	0.66	3.38
Max	99.062	99.74	84.71	100	94.15	99.96	90.27	99.05
Average	42.63	90.15	38.11	82.65	37.66	64.78	33.4	47.2
St. Deviation	29.10	19.01	29.08	22.46	26.39	19.10	26.66	22.67

As Table 6.7 shows, the healing percentage of CMS immersed in water was relatively high (42%) compared to the healing percentage of CMS in the soil of the exposure classes (38%, 37%, and 33%for X0, XA1, and XA3 respectively). This can be attributed to the reaction of carbon dioxide present in water with the calcium hydroxide produced by the hydration of calcium oxide [6, 86, 103].

The healing efficiency of specimens incubated in XA3 is also slightly lower than for X0, which might explain the effect of the soil pH, as this was lower in the XA3-soil (pH = 4.5) than in the X0-soil (pH = 7). This result is in agreement with previous studies [254, 298, 358] which found that a higher pH can provide a suitable environment for carbon dioxide to dissolve and react with calcium hydroxide.

Larger healing ratios were observed for all BMS compared to CMS; this accounts for the white mineral precipitation of calcium carbonate caused by the metabolic conversion of nutrients by bacteria [292], as evidenced by the EDX analysis. As indicated in Table 6.7, the soil pH influences the performance of bio self-healing as the healing percentage of BMS incubated in XA3 is significantly lower (47%) than in the specimens incubated in X0 (82%). The highest healing percentage was approximately 90% for specimens immersed in water. This can be attributed to the high concentration of oxygen dissolved in water and light exposure, which stimulates the photosynthesis pathway of calcium carbonate precipitation [86].

These results indicate that using bacteria with cement-mortar could effectively improve the healing performance of cracks incubated within the ground. Moreover, a more efficient healing capacity was exhibited with specimens incubated in water and X0 than with those incubated in XA1 and XA3. The reduction in healing performance of BMS incubated in XA1 and XA3 can be attributed to the lower pH value in the surrounding environment.

6.3.3.2 Capillary water absorption test results

The effect of each environmental exposure condition on the water absorption rate for CMS and BMS was examined before and after incubation (Figure 6.25). The rate of water absorption through cracks due to capillarity water suction before and after incubation was compared to determine the direct relation between crack closure and absorption rate. The relationship between the mass of absorbed water per unit inflow area and the square root of time is illustrated in the plots depicted in Figures 6.26 and 6.27. The results show that after incubation, the sorptivity value for both types of specimens (CMS and BMS) decreased as a result of crack healing. However, this reduction was more evident in BMS i.e. specimens impregnated with the bacterial agent.

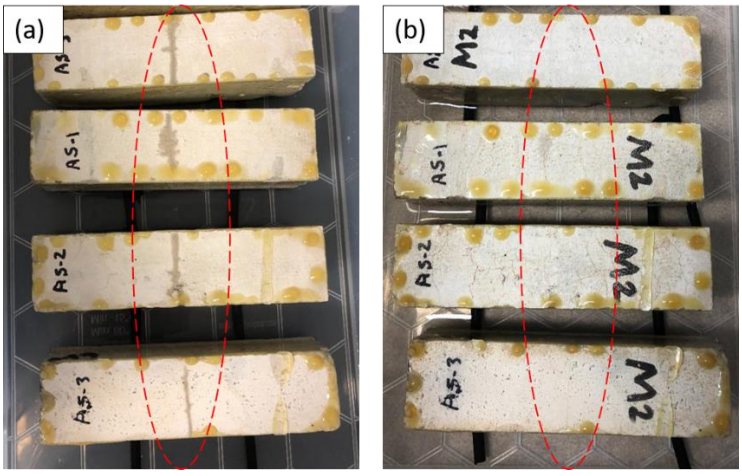

Figure 6.25: Comparison of water absorbed by BMS after two hours of absorption (a) Specimens before incubation, (b) The same specimens after incubation

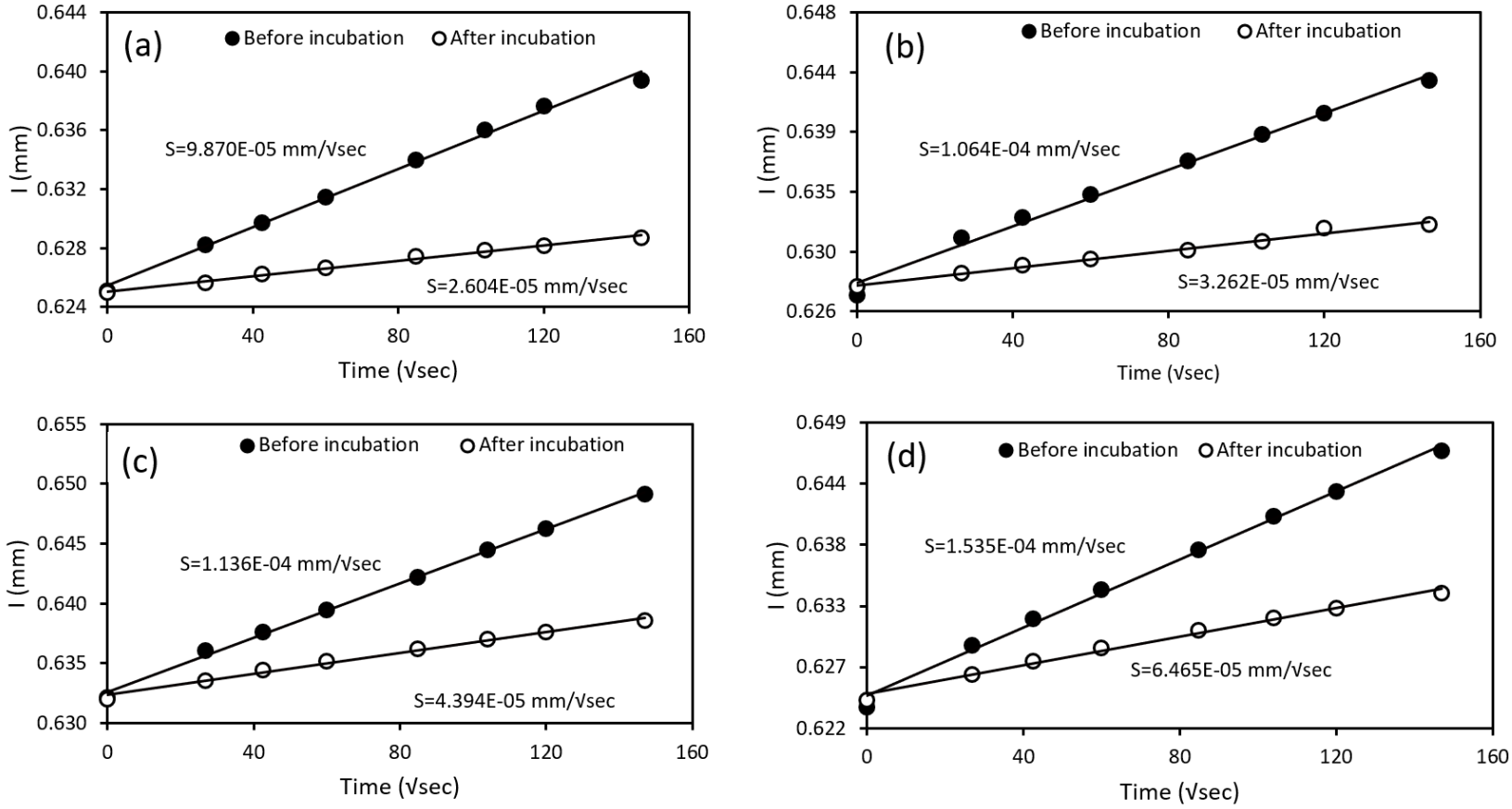

Figure 6.26: Change in capillary water absorption of the BMS before and after 120 days of incubation in different environmental exposure conditions: (a) immersed in water, (b) X0-soil, (c) XA1-soil, and (d) XA3-soil

The results also indicated that BMS incubated in exposure class X0 exhibited a higher reduction in absorption rate than specimens incubated in XA1 and XA3. For instance, the sorptivity indexes of the specimens incubated in X0, XA1, and XA3 were 3.262 x 10^{-5}, 4.394 x 10^{-5} and 6.465 x 10^{-5} mm/√sec, respectively. As evident in the microscopic images and SEM results (presented in sections 6.3.3.1 and 6.3.3.3, respectively), the high deposition of calcium carbonate filled the cracks, pores, and continuous channels that passed through the water and therefore reduced the absorption rate.

The absorption rate was higher and generally similar for CMS in all the exposure classes (X0, XA1 and XA3). However, a slight increase in absorption rate was observed for all specimens incubated in XA3.

It is evident that the sorptivity index values of the BMS were lower than those of the CMS in all environmental exposure conditions. For instance, the change in sorptivity index values for the BMS and CMS after incubation in X0 was 7.378 x 10^{-5} mm/ √sec and 4.379 x 10^{-5} mm/√sec, respectively. This implies that using bacteria with the cement mortar led to a 41% reduction in the sorptivity index values.

A relatively high reduction change in the sorptivity index of 8.914 x 10^{-6} and 7.242 x 10^{-5} mm/√sec was indicated for CMS and BMS immersed in water, respectively. This reduction was also observed in image analysis. Hence, as the crack closure (healing percentage) increases, the sorptivity index decreases because this alters the transport of moisture into the cracks of the tested specimens.

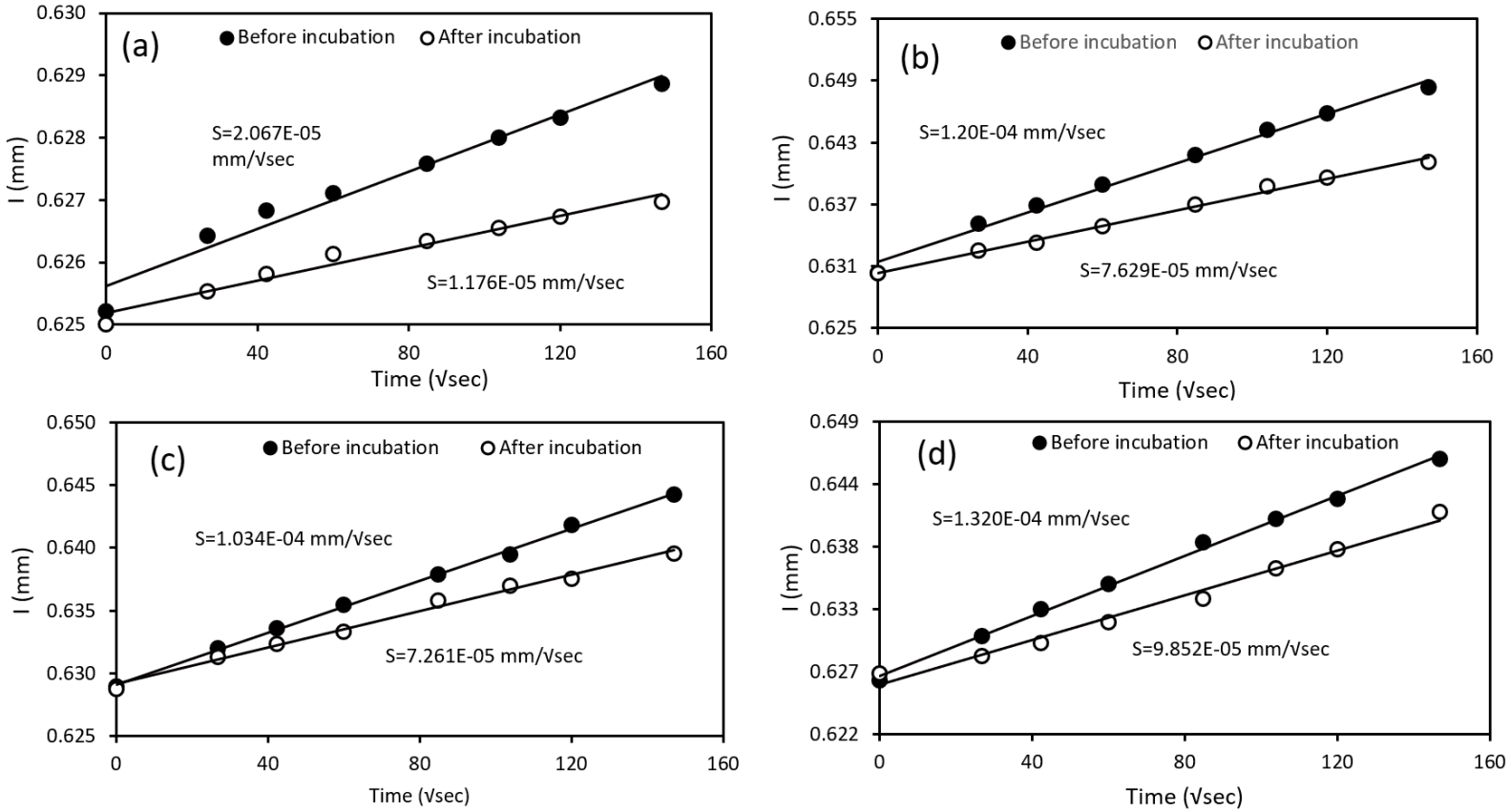

Figure 6.27: Change in capillary water absorption of the CMS before and after 120 days of incubation (in different exposure conditions) (a) immersed in water, (b) X0-soil, (c) XA1-soil, and (d) XA3-soil.

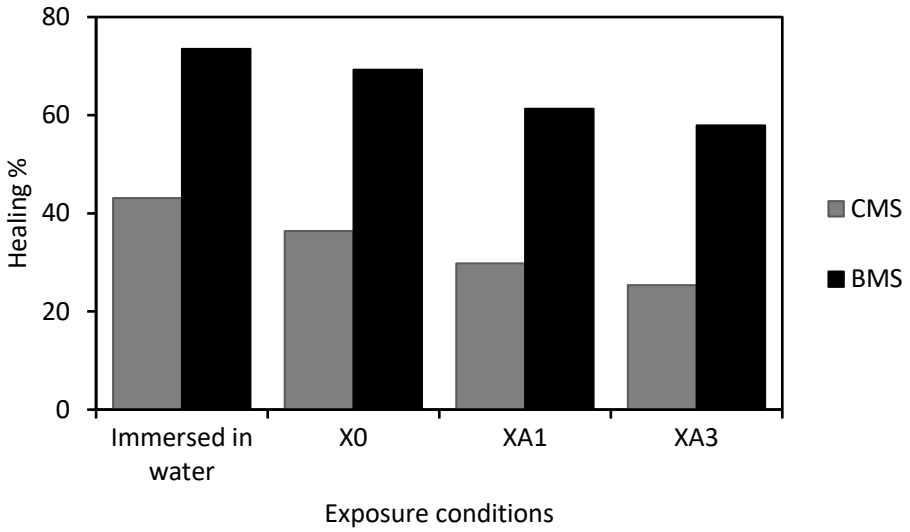

Figure 6.28: The healing percentages of BMS and CMS based on the change in water absorption rate before and after incubation under different conditions

6.3.3.3 Microstructure analysis of healing products

Figures 6.29 and 6.30 present the SEM and EDX analysis of CMS and BMS, respectively. The SEM analysis revealed that all specimens (BMS) incorporated with the bacterial agent contained regular and dense structure crystals of calcium carbonate. However, the density of the calcium carbonate crystals of the specimens incubated in XA3 was less than that of specimens incubated in X0 and XA1 (Figure 6.30). This could be a result of the severe exposure condition and low pH (i.e. acidic environment).

The results of the EDX analysis of the healing products of BMS confirmed that the white precipitated materials on the crack surfaces were calcium carbonate, which is in line with the results obtained by other researchers [359, 360]. Therefore, it can be concluded that cracks were filled with calcium carbonate as a result of microbiologically induced calcite precipitation. By contrast, the microstructure analysis of CMS revealed that the main structure was formed by crystals of calcium hydroxide and ettringite (calcium sulphoaluminate) (Figure 6.29). These were created as a result of the reaction of sulphate compounds with calcium aluminate in the cement and were similar to the crystals reported in a study conducted by Alghamri et al. [97]. The creation of ettringite

crystals lowers the amount of CH and C_3A in the cement-based matrix and the pressure of salt crystallisation inside the pores of the cement mortar [280, 361]. For all CMS, the EDX analysis of healing products in the cracks indicated the presence of Si and O. This can be attributed to the formation of calcium silicate hydrate (C-S-H) caused by the ongoing hydration of cement particles.

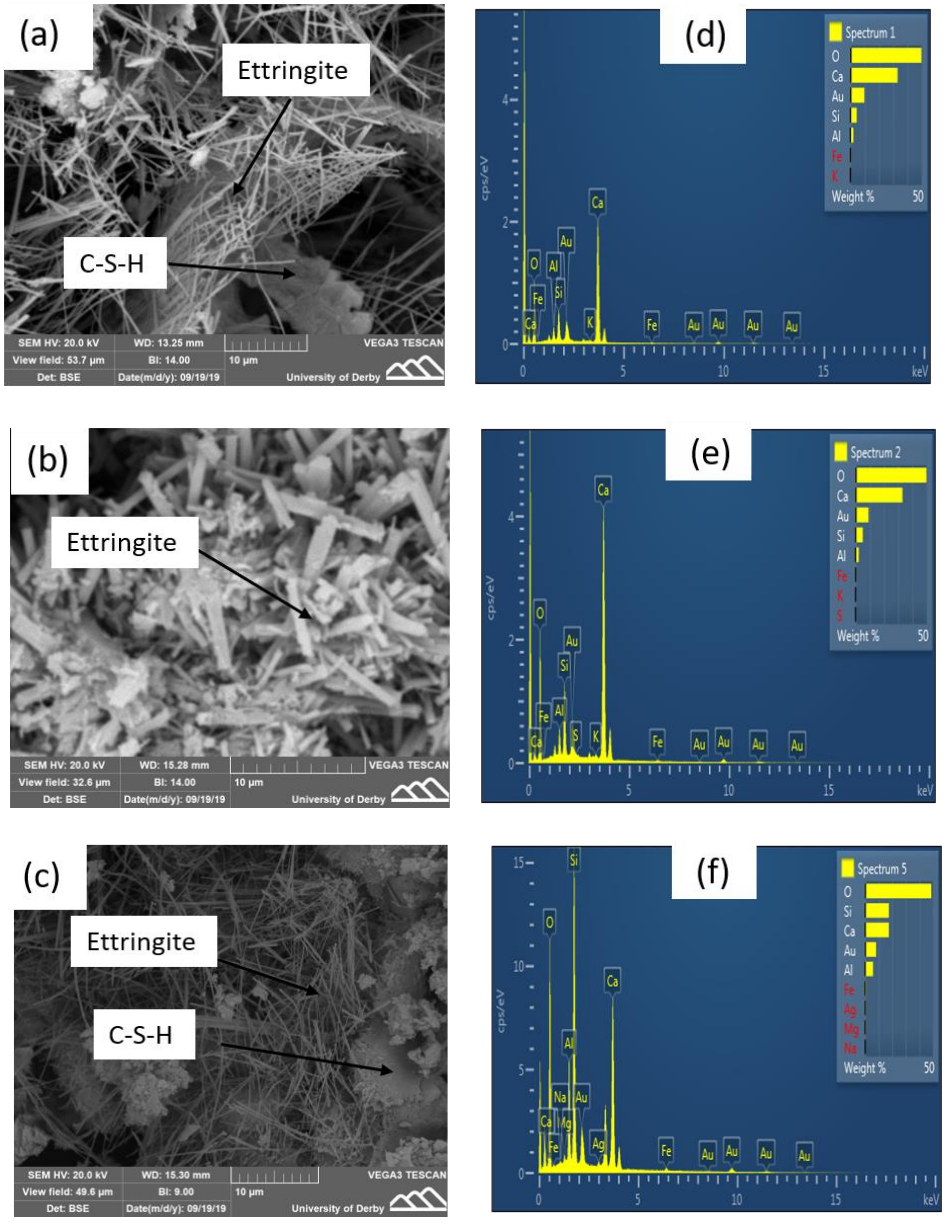

Figure 6.29: SEM and EDX results for healing products of CMS. (a, b, and c) SEM images of healing products of CMS incubated in X0, XA1, and XA3 respectively. (d, e, and f) EDX analysis of healing products of CMS incubated in X0, XA1, and XA3 respectively

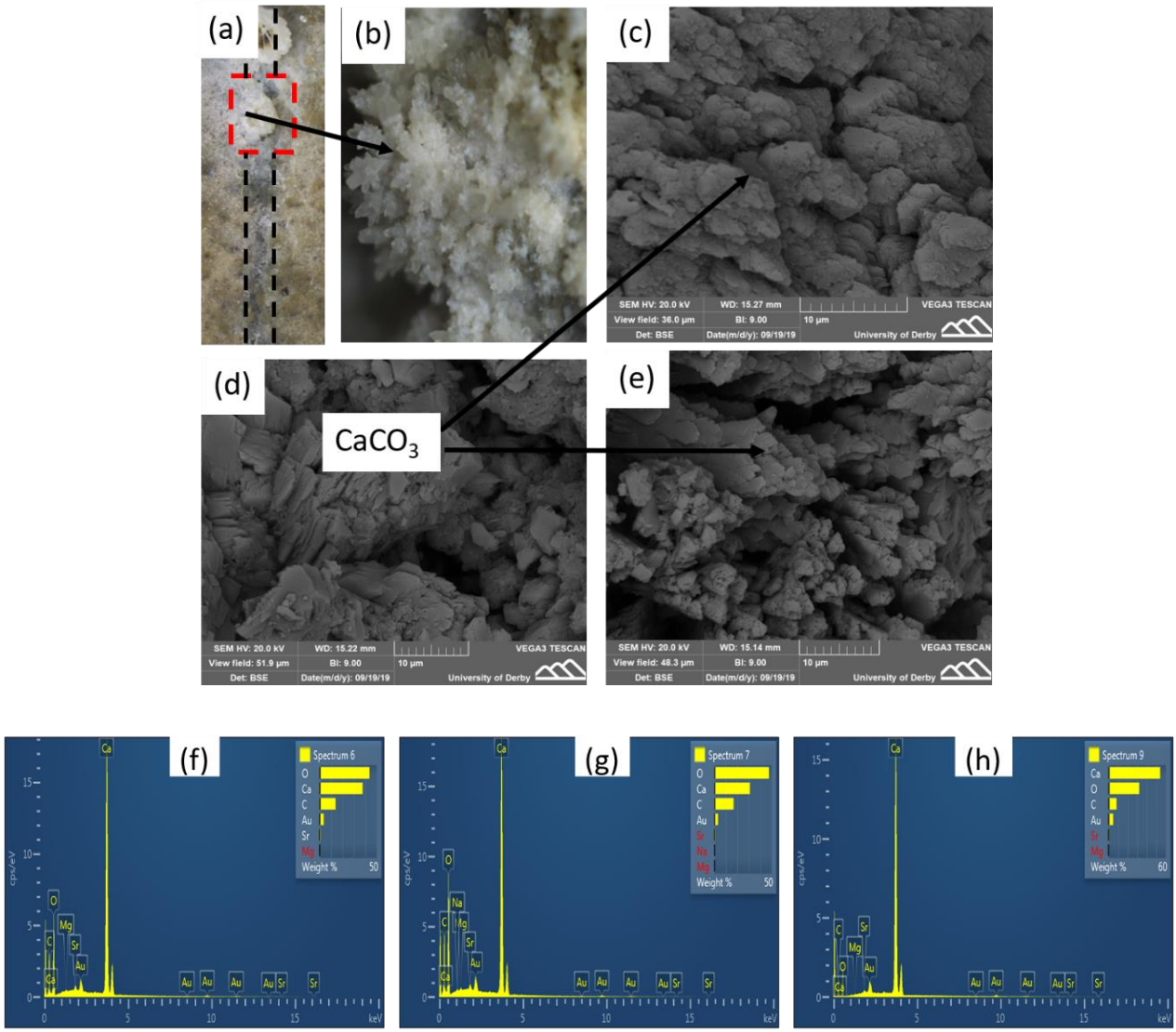

Figure 6.30: SEM and EDX results for healing products of BMS. (a) Microscopic image of crack-filled with white precipitation of calcium carbonate. (b) Stereomicroscopic close-up image (indicated by dotted square in image (a)) of calcium carbonate crystals. (c, d, and e) SEM images of healing products of BMS incubated in X0, XA1, and XA3 respectively. (f, g, and h) EDX analysis of healing products of BMS incubated in X0, XA1, and XA3 respectively

6.3.4 The effect of exposure conditions on the efficiency of self-healing cement mortar specimens incubated into cohesive soil (clay) exposed to fully and partially saturation regime (stage three)

6.3.4.1 Visual evaluation of crack and healing quantification

After incubation in the fully (FSC) and partially saturated clay (PSC), the control (CMS) and bio-mortar specimens (BMS) were first removed from soil (their incubation environments) and then immersed in water for ultrasound cleaning before being visually inspected under the microscope to evaluate the crack closure. Figure 6.31 shows typical top views of the crack surface of the maximum healed crack widths of bio-mortar specimens (BMS) before and after the incubation in four different exposure conditions (FSC-X0, FSC-XA1, FSC-XA3, and PSC-X0). As shown, the widths of completely healed cracks were relatively larger in specimens incubated in fully saturated, pH neutral soil (FSC-X0) (250µm) than the specimens incubated in FSC-XA1 and FSC-XA3 (220 and 189 µm, respectively). For bio-mortar specimens (BMS) incubated in partially saturated pH neutral soil (PSC-X0), only a few locations were completely healed, and the maximum healed crack width was around 170 µm. It was also noted that a thin and discontinued layer of calcium carbonate crystals were formed at the top of the cracks (Figure 6.32).

The microscopic inspection of the control mortar specimens (CMS) showed that the crack was more difficult to repair autogenously with the increase of average crack width. Based on the microscopic inspection (Figure 6.33), the autogenous healing as a result of the late hydration of un-hydrated cement particles was effective for average crack width of 60–120 µm where most of the cracks within this range were healed.

To quantify the healing ratio, images of cracks before and after incubation were processed to obtain the crack binarisation images using “image J” software. Table 6.8 presents the statistical results for the crack healing ratio of the control and bio-mortar specimens incubated in different exposure classes.

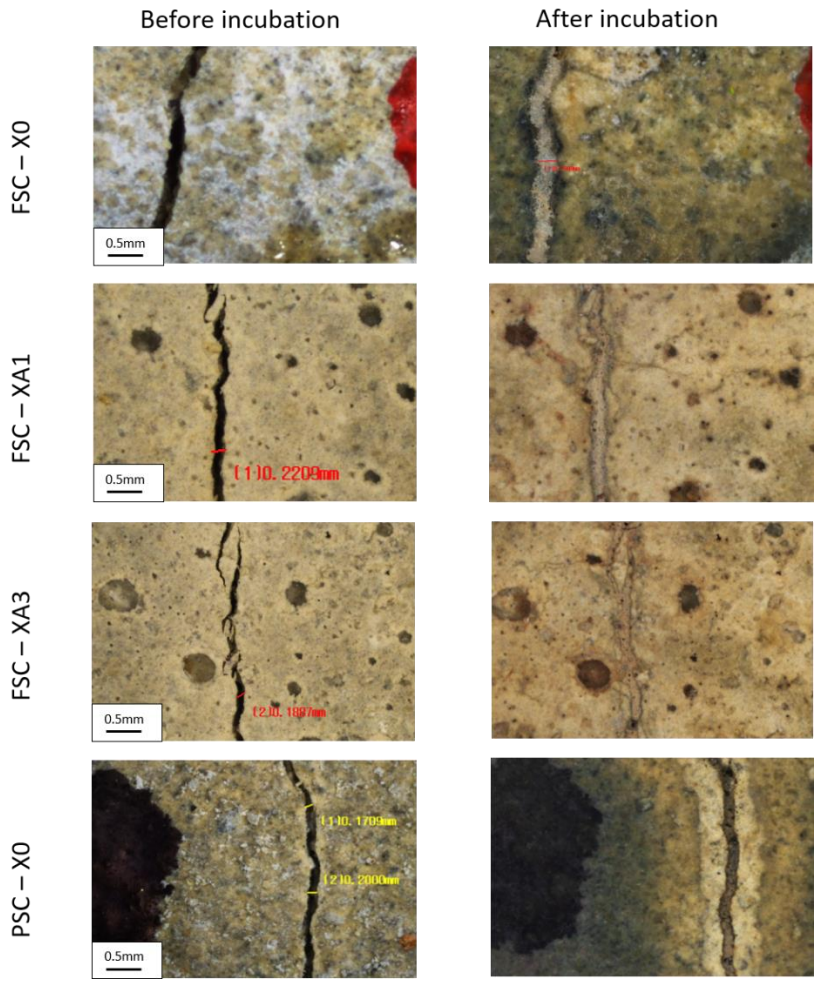

Figure 6.31: Microscopic observation of crack healing of bio-mortar specimens (BMS) before and after incubation in fully and partially saturated clay (FSC and PSC, respectively)

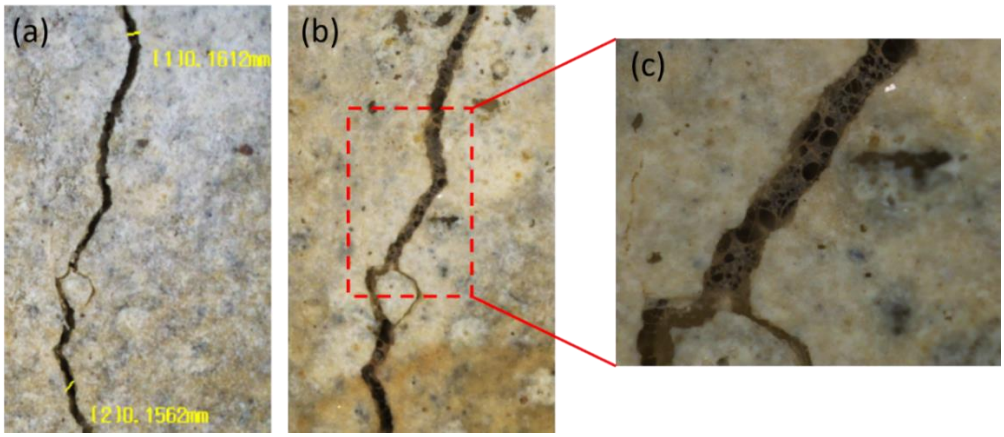

Figure 6.32: Microscopic observation of crack healing of bio-mortar specimens (BMS) incubated in partially saturated condition (PSC), (a) Before incubation, (b) After incubation, (c) Stereomicroscopic close-up image

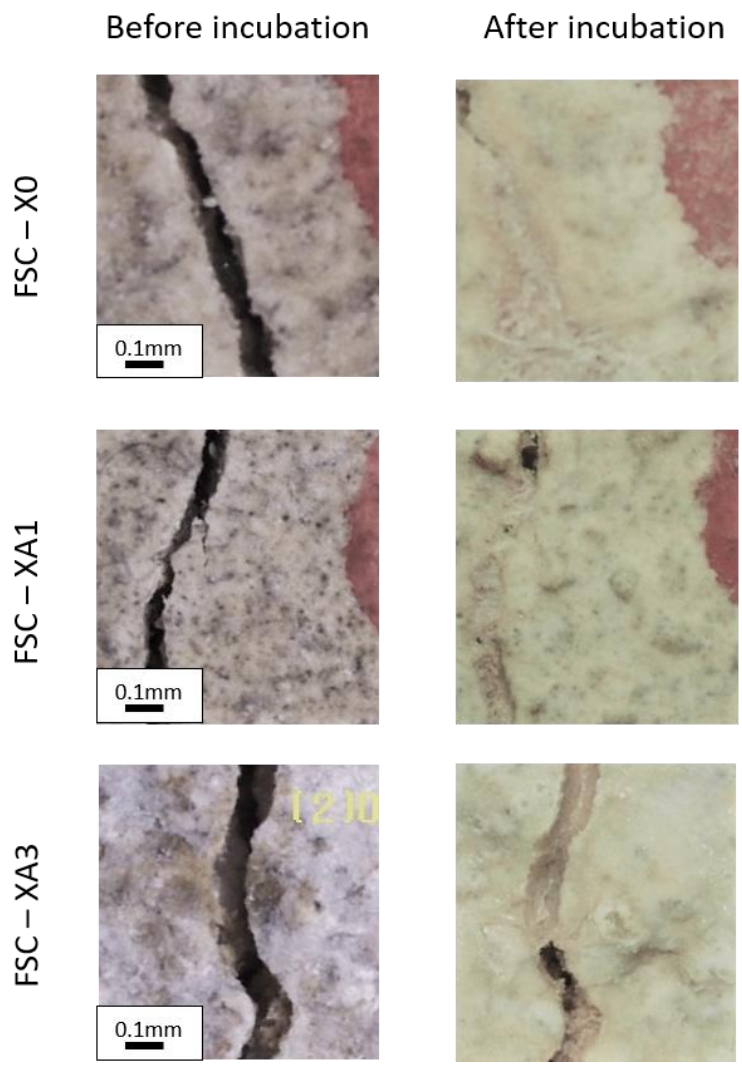

Figure 6.33: Microscopic observation of crack healing of control mortar specimens (CMS) before and after incubation in fully saturated clay (FSC)

Table 6.8: Statistical results of the crack healing ratio of the control and bio-mortar incubated under different exposure classes

Healing ratio (%)	Exposure classes							
	FSC-X0		FSC-XA1		FSC-XA3		PSC-X0	
	CMS	BMS	CMS	BMS	CMS	BMS	CMS	BMS
Min	2..80	11.39	1.49	16.52	3.04	10.19	2.804	2.35
Max	97.18	98.62	90.51	99.24	95.16	96.29	87.182	92.10
Average	31.29	63.73	29.14	62.89	33.86	59.07	15.34	38.02
St. Deviation	21.14	20.23	27.06	24.83	25.20	18.63	31.47	24.71

As Table 6.8 shows, the healing ratios for all bio-mortar specimens (BMS) are almost two-folds of healing ratios of control mortar specimens (CMS) for all exposure classes. This accounts for the white mineral precipitation of calcium carbonate caused by the metabolic conversion of nutrients by bacteria [38], as evidenced by the EDX analysis. It was also indicated that the soil pH has a slight influence on the healing performance of bio mortar specimens. For instance, the healing percentage of bio-mortar specimens incubated in FSC-XA3 was around 7% lower than in the specimens incubated in FSC-X0. The reduction in healing performance of BMS incubated in XA1 and XA3 can be attributed to the lower pH value in the surrounding environment. This is supported by a previous study by Knoll [39], which found that a high pH favours the formation of carbonates from bicarbonates. However, the repairability of the microbial agent was more noticeably limited in the specimens incubated within the partially saturated condition (PSC-X0), where the corresponding healing ratio was approximately 38%.

Looking at the healing percentage of the control mortar specimens (which did not have any bio healing agent), it is evident that the healing ratio was low and relatively similar in the three different exposure classes (31%, 29%, and 33% for FSC-X0, FSC-XA1, and FSC-XA3 respectively) – despite these were all incubated in fully saturated condition FSC. However, the healing percentage of the control mortar specimens incubated in PSC-X0 was significantly lower (15%) than in specimens incubated in FSC. The autogenous healing of cementitious materials has a certain capacity, and this capacity is mainly affected by the composition of the matrix and the environmental exposure conditions. In FSC exposure class, the hydration of the un-hydrated cement particles and swelling of the hydration products were more effective than in PSC, due to the presence of water.

6.3.4.2 Capillary water absorption test results

Figures 6.34 and 6.35 show the change in capillary water absorption of the cracks before and after the soil incubation. The results showed that after incubation, the sorptivity coefficient for all specimens (CMS and BMS) decreased due to crack healing. Based on the change in the sorptivity coefficient (S), the healing ratio was calculated and plotted in Figure 6.36. For the BMS incubated in fully saturated clay (FSC), a relatively lower

water absorption rate was obtained for all exposure classes in comparison with the BMS incubated in PSC. For instance, the change in sorptivity indexes of the BMS specimens incubated in X0-FSC, XA1-FSC, and XA3-FSC were 4.051 x 10^{-5}, 4.322 x 10^{-5} and 2.774 x 10^{-5} mm/√sec, respectively, whereas the change in sorptivity indexes of the BMS incubated in X0-PSC was 2.051 x 10^{-5} mm/√sec. According to the concept of bio self-healing concrete [40], one of the main factors is that enough self-healing agents should be transported to the crack surface and activated by water contact. For the fully saturated condition (where moisture content = 47%), all of the pore space is filled with liquid and no matric suction in the soil (i.e. according to the Tensiometer measurement, Figure 6.11). Therefore, the bacteria would be exposed at the crack surfaces and activated as soon as they became in contact with water ingress from the surrounding fully saturated soil. Then, the precipitations of calcium carbonate form due to the metabolic conversion of nutrients under the respiration of bacteria.

In contrast, for the partially saturated condition (PSC), a layer of moisture covering the soil particles and a menisci shape layer at the contact points with the cracked specimens were formed as a result of the capillary and adsorptive forces (suction), whereas the rest of the pore space was occupied by air. In such conditions, the soil attracts water molecules that become less available in the cracks leading to the lack of necessary conditions for the self-healing process. This implies that self-healing performance is significantly affected by the moisture content of the soil.

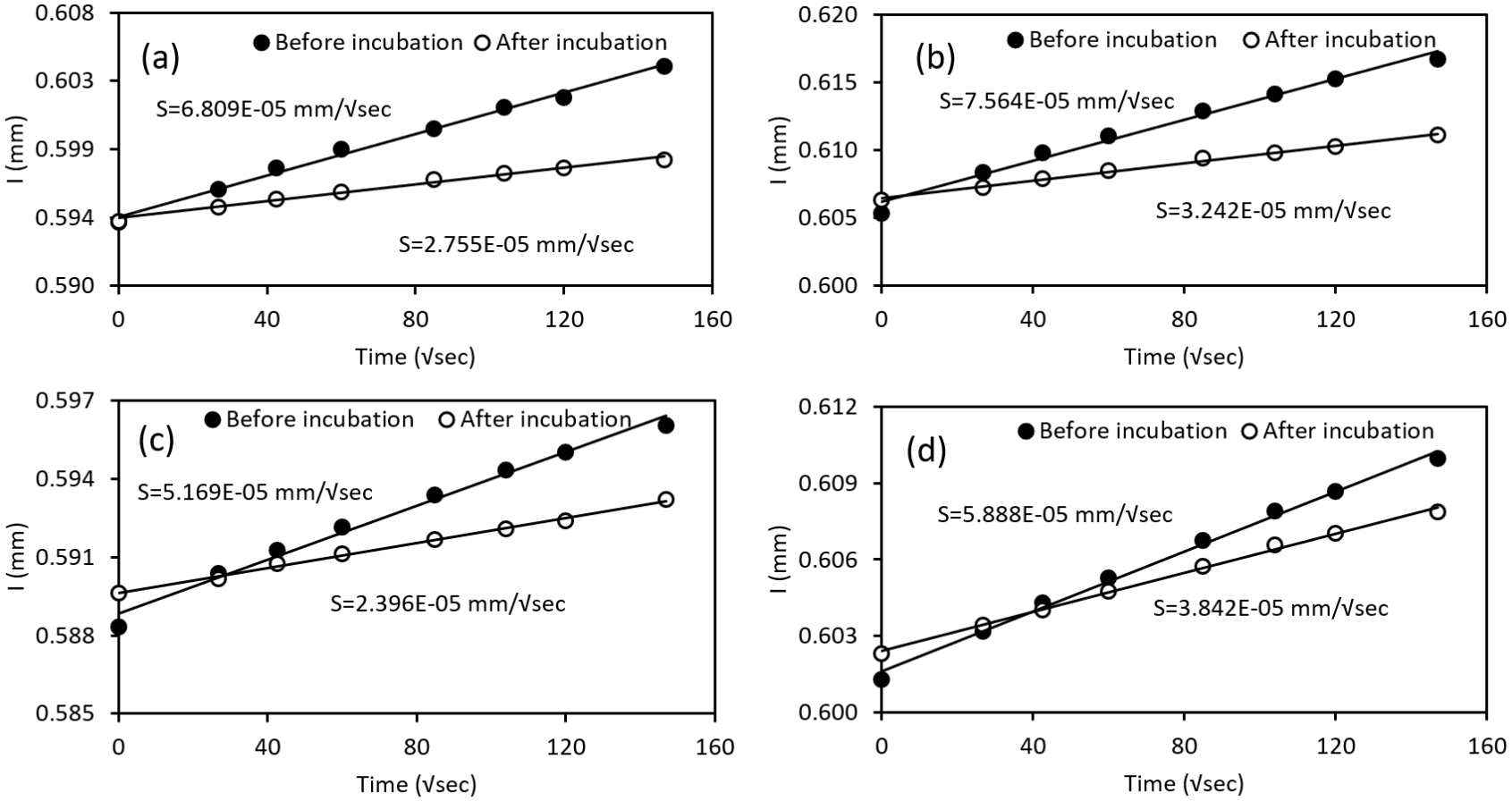

Figure 6.34**:** Change in capillary water absorption of the bio-mortar specimens (BMS) before and after incubation in different environmental exposure conditions: (a) X0-FSC, (b) XA1-FSC, (c) XA3-FSC, and (d) X0-PSC.

On the other hand, the pre-cracked CMS were autogenously healed and exhibited lower healing ratios in comparison with BMS, and the change in sorptivity indexes of the CMS incubated in X0-FSC, XA1-FSC and XA3-FSC were 1.967 x 10^{-5}, 2.069 x 10^{-5} and 1.677 x 10^{-5} mm/√sec, respectively. However, in all relevant reaction processes for autogenous healing, like secondary hydration of un-hydrated cement particles, and swelling of hydration products, water is the key element to proceed with such reactions. Therefore, all these reactions would be significantly influenced or not happen without the presence of water. Therefore, the healing percentage of the CMS incubated in partially saturated condition (X0-PSC) was relatively lower (11.7%) in comparison with the healing percentage of specimens incubated in X0-FSC and identical exposure class (27.1%).

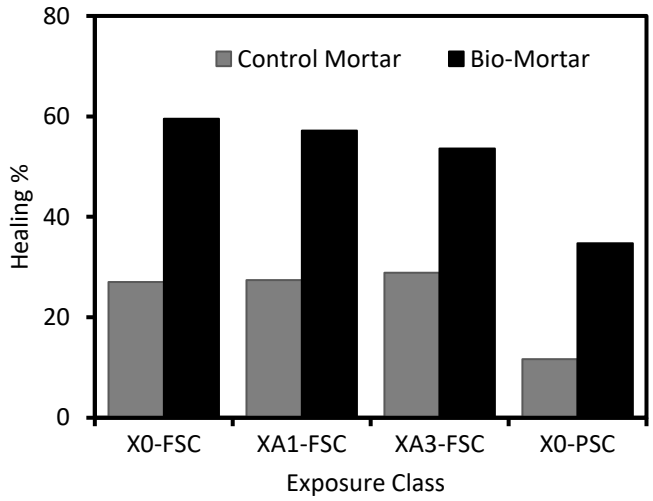

Figure 6.36**:** The healing percentages of the bio and control mortar specimens based on the change in water absorption rate before and after soil incubation under different exposure conditions

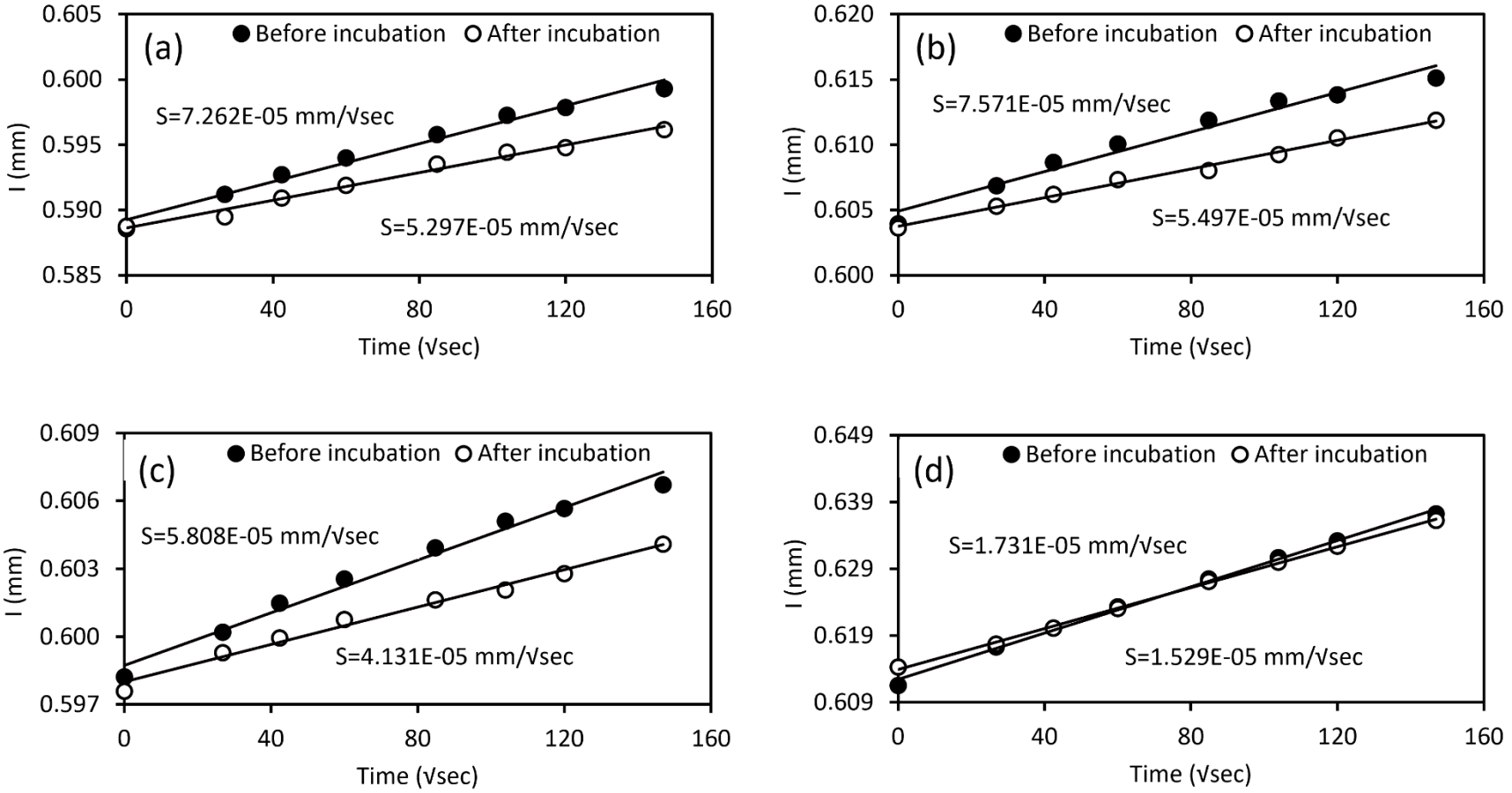

Figure 6.35**:** Change in capillary water absorption of the control mortar specimens (CMS) before and after incubation (in different exposure conditions) (a) X0-FSC, (b) XA1-FSC, (c) XA3-FSC, and (d) X0-PSC.

In summary, it was clearly noticed that a significant decrease in the absorption rate of bio-mortar specimens in comparison with the control specimens in all environmental exposure classes (e.g. Figure 6.36). As evident from the SEM images (see next section), the deposition of crystals of calcium carbonate on the crack surface resulted in a decrease in the permeation properties.

6.3.4.3 Microstructure analysis of healing products

The SEM images of the precipitations at the cracks surface for the bio and control mortar specimens are shown in Figures 6.37, and 6.38, respectively. From Figure 6.37 (a, b, and c), it can be found that the structure of the calcium carbonate crystals appears granular blocky and laminar close packing morphology. These structures were attached to the crack wall. The result of the element composition analysis using EDX revealed that the precipitation at cracks surface was essentially an association of oxygen, carbon, and calcium atoms (Figure 6.37 d, e, and f). Therefore, it can be concluded that cracks were blocked with calcium carbonate crystals as a result of microbiologically induced calcite precipitation.

SEM images for the healing products of the control specimens for the three different exposure classes were taken at the crack areas, as shown in Figure 6.38 (a, b, and c). It can be seen that after incubation, the developed healing product was mainly discrete crystals of ettringite and calcium silicate hydrate.

The EDX analysis of the healing product (i.e. of the control specimens' cracks) indicated the presence of Ca, Si, and O. This can be attributed to the formation of calcium silicate hydrate (C-S-H) caused by the ongoing hydration of unhydrated cement particles.

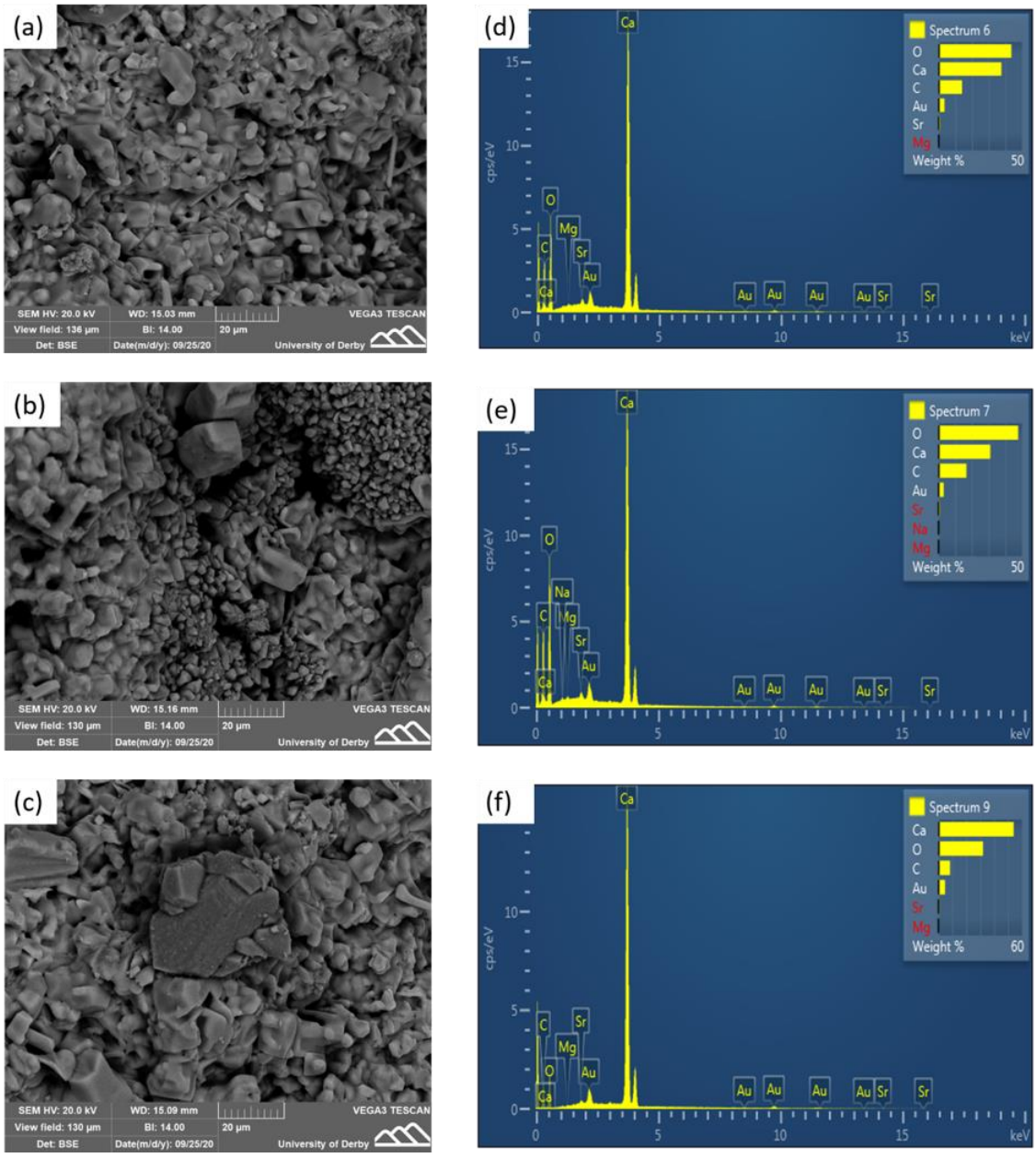

Figure 6.37: (a, b, and c) SEM images of the healing products of the bio-mortar specimens incubated in X0, XA1, and XA3 respectively. (d, e, and f) EDX analysis of the healing products of the bio mortar specimens incubated in X0, XA1, and XA3 respectively

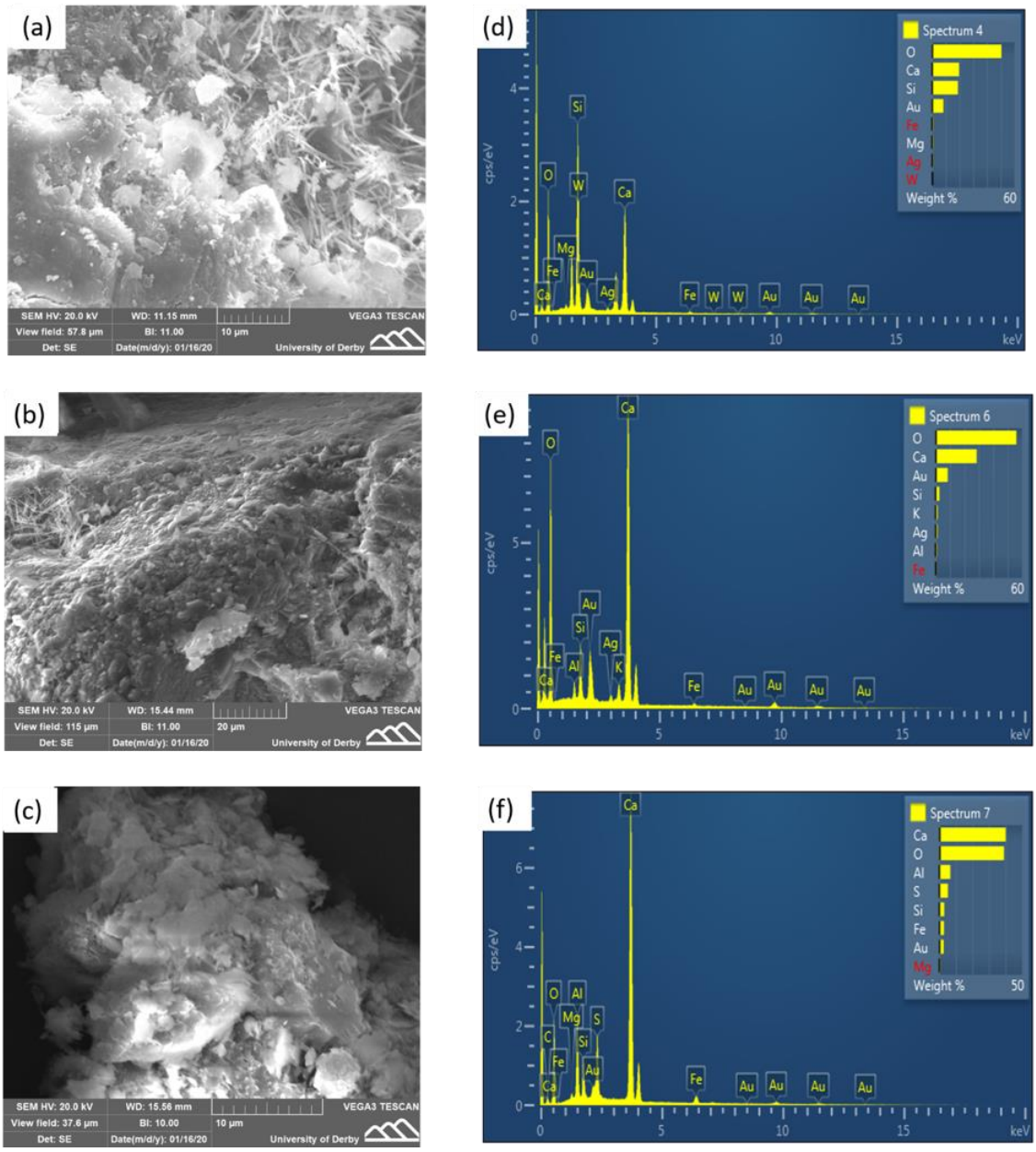

Figure 6.38: (a, b, and c) SEM images of the healing products of the bio mortar specimens incubated in X0, XA1, and XA3, respectively. (d, e, and f) EDX analysis of the healing products of the control mortar specimens incubated in X0, XA1, and XA3 respectively

6.4 Conclusion

This chapter investigated the effect of different ground exposure conditions included the influence of naturally occurring microbes presented within soil, type of soil, pH value, and different ground regime included partially fully saturated and dry-wet cycles

on the efficiency of bio self-healing concrete. The feasibility and efficiency of self-healing were evaluated with reference to crack healing ratio and water tightness while the microstructure of the healing products was analysed and verified using SEM and EDX. From the results, the main conclusions can be drawn as follow:

- The healing percentage of BMS incubated in NSS is significantly higher (37%) compared to CMS incubated in the same identical condition.
- Indigenous bacteria naturally present within soil can enhance the mortar self-healing process.
- Using bacteria with cement mortar improved the crack healing ratio by more than 50% and reduced water absorption by more than 45% for specimens incubated in sand with exposure class X0 (pH = 7).
- Water incubation was found to be the most favourable environment for self-healing as maximum healing ratios were observed for both types of specimens.
- For non-cohesive soil (sand), the reduction in pH of the incubation environment affected bio self-healing performance. For instance, the healing percentage in the crack closure of specimens incubated in XA3 (pH = 4.5) was 43% lower than in specimens incubated in X0 (pH = 7). However, for cohesive soil (clay) the healing ratios of bio self-healing of specimens incubated in the same identical exposure conditions were almost similar, with better results observed in the pH neutral condition.
- The healing efficiency of CMS and BMS incubated in sand was remarkably higher than those incubated in clay with the same identical exposure conditions. This could be attributed to the increase in dissolved carbon dioxide and oxygen concentrations, where during the wet cycles, CO_2 dissolve when fresh water is added and during the dry cycles, oxygen can easily move to the embedded specimens through pores of soil.
- The efficiencies of control and bio-mortar specimens were significantly affected by the soil's moisture content, where the healing performance of bio-mortar specimens incubated in fully saturated condition was around 40% higher than partially saturated condition. This indicates that the mineral precipitation of

calcium carbonate caused by the metabolic conversion of nutrients by bacteria is heavily reliant on the moisture content of soil. The hydration of un-hydrated cement particles representing the primary source of autogenous healing is also influenced by soil moisture content.

- The SEM and EDX results indicated that the mineral precipitations on the crack surfaces of the bio-mortar specimens were calcium carbonate and that the healing products of control specimens were ettringite and C-S-H.
- In general, it can be inferred that the bio self-healing was more efficient for all exposure classes in comparison with autogenous healing experienced by the control specimens.

Chapter 7

Monitoring the self-healing performance of concrete [embedded within the soil] using electrical resistivity technique

7.1 introduction

Non-destructive techniques can be used to provide information on the healing process of concrete cracks. These techniques have been indirectly used in different studies to investigate the performance of self-healing of cracks, such as thermogravimetric analysis [101], rapid chloride permeability [43, 362], steel corrosion [363] ultrasonic pulse velocity method [364] and x-ray scan [40]. For instance, Alghamri et al. [97] assessed the self-healing efficiency of concrete mixed with light weight aggregate using the ultrasonic pulse velocity technique. Their results indicated that the time of the ultrasonic waves reduced, as the crack sealed with the depositions and fillings. Xu et al. [363] investigated the inhibition of steel corrosion using ureolysis-based microbial calcium carbonate precipitation. In their study, they found that the steel corrosion was successfully inhibited by the crack closure from precipitation of calcium carbonate. In another study, eight Acoustic Emission (AE) sensors were attached to the concrete surface in order to evaluate crack healing. The results revealed that, the accuracy of transmitter localization was lost in the presence of 0.3 mm wide crack and improved as the crack was healed [365]. Even though these techniques supply valuable information related to the self-healing process, but they do not give an accurate indication about the change in the crack width measurement.

The transport attributes of concrete can be changed when cracks are present in the microstructure. Cracks change the electrical properties of concrete because they change the connectivity of pore structures. Identification and monitoring of the initiation and propagation of cracks in concrete can be achieved by using the electrical resistivity method. However, Ranade et al. [366] determined, with greater accuracy, the development of microcracks in cementitious composite materials using electrical

resistivity under tensile strength. Some performance characteristics of concrete correlate electrical resistivity well; such properties include water absorption, chloride diffusion coefficient and the corrosion rate of steel reinforcement [367]. The electrical resistivity of concrete was defined by Sengul [368] as 'the resistance of concrete against the flow of an electric current through the concrete'. Moreover, non–destructive testing (NDT) may be defined as concrete's ability to resist the exchange of particles that are subject to an electrical field. Concrete resistance to chloride penetration can be assessed by using concrete resistivity, similarly to the rapid chloride penetration (RCP) test [367]. Resistivity measurement can, in this environment, be used to assess the level of the interconnectivity of pores. The electrical resistivity of concrete, which is independent of the geometry of the sample, is an intrinsic attribute of a material.

In this research, the specimens were incubated within soil environment. Therefore, observing the healing process during the incubation period was complicated. Therefore, and in order not to disturb the specimens during the healing process, electrical resistivity testing was used for this purpose to monitor the crack healing performance.

7.2 Experimental program

7.2.1 Preparation of specimens

7.2.1.1 Specimens for electrical resistivity measurements

The control and bio cement mortar mixes were prepared according to BS EN 196-1 [337] as detailed in Table 7.1. The bacterial spores were encapsulated with nutrients into perlite as explained in Chapter 5, Section (5.2.4.2). The produced capsules containing approximately 0.3% of nutrients by perlite weight with a spore concentration of approximately 5.2 x 10^6 CFU $gram^{-1}$. The mix process was conducted as explained in Chapter 6, Section (6.2.2).

Table 7.1: Mixing proportion of the cement mortar specimens

Mixture ID.	Cement (Kg/m^3)	Sand (Kg/m^3)	Water (Kg/m^3)	Perlite + Bacteria + Nutrients (Kg/m^3)	Perlite (Kg/m^3)
Control	450	761	225	-	22.5
Bio	450	761	225	22.5	-

Plain waved carbon fibre (CF) fabric sheet of 375 g/m^2, supplied by East Coast Fiberglass Supplies, UK, was used in each specimen as electrodes as shown in Figure 7.1 (a). The carbon fibre electrodes were prepared by cutting the carbon fibre sheet into parcels of 100 x 35 mm. Perforated plastic meshes were glued to the carbon fibre electrodes to keep the electrodes straight (Figure 7.1 b).

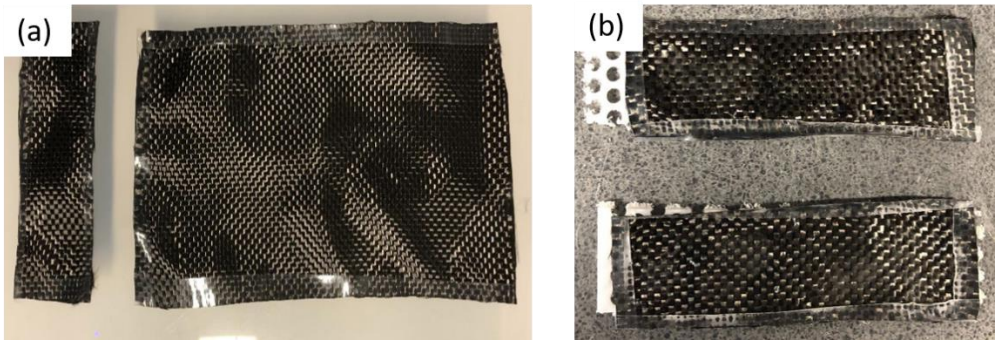

Figure 7.1: (a) Carbon fibre sheet, (b) Perforated plastic meshes glued to the carbon fibre sheet

The prepared paste was cast into prismatic moulds (40 x 40 x 160 mm). The total number of specimens for each mix group was 12 prisms. Nine cubes with dimensions of 50 x 50 x 50 mm for each mix were also cast for porosity calculations.

In order to make the carbon electrodes straight during the casting, small wooden pieces were used as shown in Figure 7.2. The wooden pieces were removed 15 minutes later after finishing the casting.

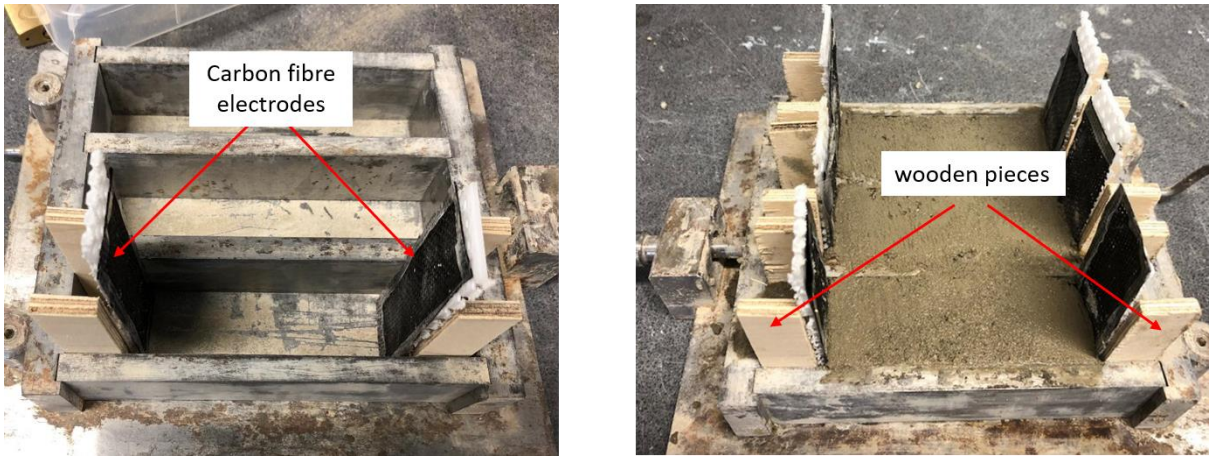

Figure 7.2: Fixing the carbon fibre electrodes during the casting

After 24 h, the mortar specimens were gently removed from their moulds and cured for 28 days until they were tested.

7.2.1.2 Specimens for steel corrosion measurements

The corrosion approach of reinforcement steel bars is partially governed by the transport of ions through the microstructure of the cementitious matrix. When ions charges, the ability of a material to resist the transfer of charge is dependent upon the electrical resistivity. Therefore, a connection could be expected between the steel corrosion and the electrical resistivity. In this test, the same mix design, control and bio-mortar were prepared for steel corrosion measurements. For this work, the 10 mm steel bars were cut into 12 segments (6 segments for each mix) with a length of 220 mm and then immediately cleaned using a wire wheel cup brush as shown in Figure 7.3. Both ends of steel bars, exposed to the environment, were coated with epoxy resin to avoid corrosion except a small part at the top of the bar to be connected to a voltmeter. The epoxy was sprinkled uniformly using a brush over the required area. This step was conducted twice to ensure that the whole area was covered.

Figure 7.3: Cleaning the steel bars

Before casting the mortar, the steel bars were fixed in the mid of the prisms as shown in Figure 7.4. After two days, the mortar specimens were gently removed from the moulds and cured for 28 days until they were tested.

Figure 7.4: Casting of prisms mortar specimens with steel bars

7.2.2 Crack creation and incubation process

After curing, all specimens were cracked using a three-point-bending test as explained in Chapter 4 (Sections 4.5.1). During the cracking process, the carbon fibre sheets used to prepare specimens for electrical resistivity were separated from the cementitious matrix due to the low cohesive contact between carbon sheets and cementitious matrix (Figure 7.5). Therefore, copper wire mesh electrodes were used to replace the carbon fibre sheets. A pure copper wire mesh with 0.6 mm of wire diameter and a square mesh

of 1.5 mm was used as an electrode as shown in Figure 7.6. The copper mesh electrodes were embedded within the cementitious matrix parallel with a distance of 120 mm between the two electrodes using the same process used in casting carbon electrodes.

Figure 7.5: Separation of carbon fibre sheets during crack creation process

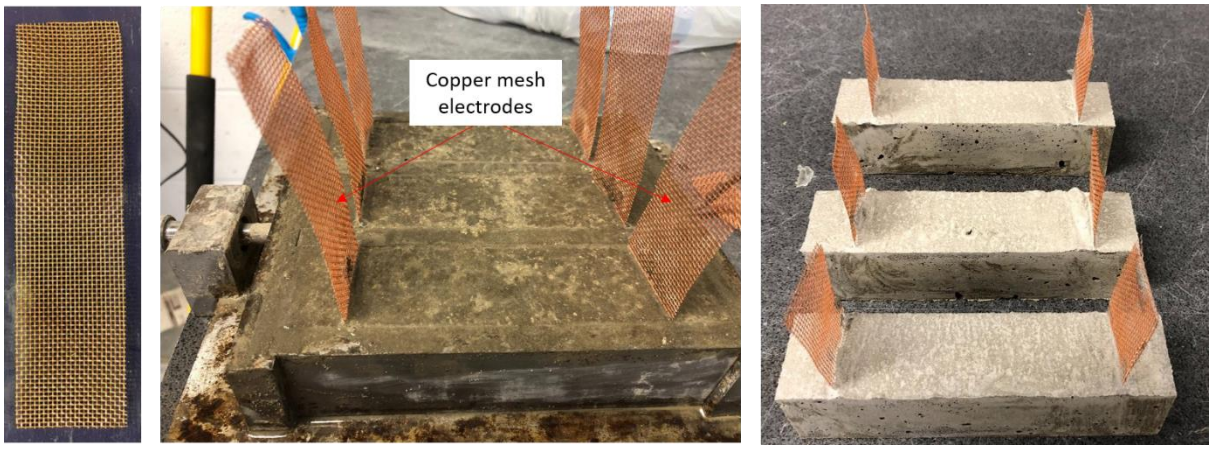

Figure 7.6: Using copper mesh electrodes with cementitious matrix

Immediately, after the creation of the cracks, their widths were measured at regular intervals using Shuttlepix Editor software. Various cracks were generated in the control and bio-mortar specimens with widths ranging between 100µm to 280µm. The cracked specimens (control and bio-mortar) prepared for the electrical resistivity tests were incubated in separate plastic boxes containing water and fully saturated soil.

Sandy soil widely exists in civil engineering projects. Therefore, the soil used in this investigation was a sub-rounded grain shape sand with free chemicals. The mechanical and chemical characteristics of this non-cohesive soil are presented in Chapter 6, Section 6.2.3.2.

The cracked specimens (control and bio-mortar) prepared for steel corrosion measurements were only incubated in water only.

Figure 7.7: Incubation of cracked specimens within the soil

7.2.3 Absolute Porosity measurement

Concrete resistivity is significantly affected by absolute porosity, where resistivity decreases as the absolute porosity increases. In this study, the absolute porosity of control and bio-mortar specimens were measured for three different periods (7, 28, and 90 days) to investigate the effect of bio healing agent on the porosity of the cementitious matrix.

The prepared cube specimens were immersed in water and then, they were oven-dried at 100±5°C until getting constant weight to determine the oven-dry mass. The saturated surface-dry mass was determined using an electronic scale (Figure 7.8) with 0.01g

accuracy. The absolute porosity of concrete was calculated according to Bioubakhsh [369] as follows:

$$A_P\ \% = \left(\frac{Ws - Wd}{V}\right) / \rho \times 100 \qquad (7.1)$$

Where:

A_P = the absolute porosity

ρ = the density of water

W_s = the saturated surface-dry mass of the specimen

W_d = the oven-dry mass of the specimen

V = the volume of sample

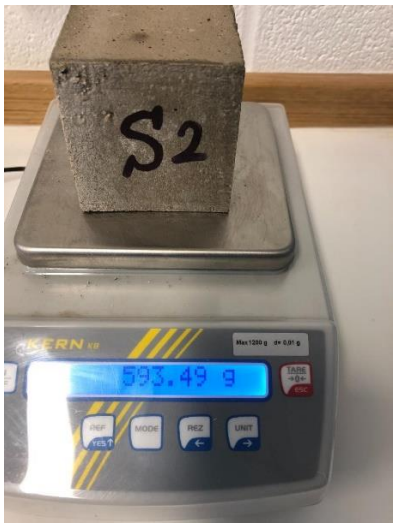

Figure 7.8: Weighing of specimens using high precision electronic scale

Therefore, the absolute porosity of concrete representing the proportion of the volume of pore space to the volume of the specimen and its' value usually expressed as a percentage of the specimen volume.

7.2.4 Electrical resistivity measurement

A two-probe or four-probe strategy can be used to measure the electrical resistivity of concrete. Previously, this involved the use of four electrical contacts, the inner two being for voltage estimation and the outer two for passing current, resulting in the contact resistance not being included in the measured resistance. The two-probe strategy involves the utilisation of two electrical contacts, each of which is for both voltage and current.

In this research, the two-electrode technique was adapted to measure the concrete resistivity. An A.C Voltage of 3V was applied across the two electrodes from a function generator, the power supplied at a frequency of 60 Hz to eliminate the influences of Polarization [370].

Numerous studies conducted previously [371-373] indicate that, over time, direct current (DC) increases resistance because of the polarization effect. This can be clarified by stating that the electric current passing through the cementitious matrix produces liberated oxygen and hydrogen, resulting in there being a thin film between the cementitious matrix and the electrodes [374]. Consequently, this film reduces the electric current at a given applied voltage. Therefore, alternating current (AC) at a 60 Hz frequency was utilised to resolve the polarisation problems partially, as also shown in Chen's study [375].

In order to calculate the concrete resistivity, two readings were obtained from the measured current (I) and voltage (V). The electrical resistivity of the concrete is then calculated as follows [376]:

$$\rho = \mathrm{R}\,\frac{\mathrm{A}}{\mathrm{L}} \tag{7.2}$$

$$\mathrm{R} = \frac{\mathrm{V}}{\mathrm{I}} \tag{7.3}$$

Where:

ρ = electrical resistivity of concrete

R = electrical resistance

A = cross-sectional area of the electrode perpendicular to the current flow (35 x 40 mm^2)

L = distance between two electrodes (120 mm)

V = applied voltage

I = measured current

The two electrodes were embedded into concrete and have free sides to be used as electrodes as shown in Figure 7.9.

The readings of concrete resistivity were measured every seven days for all samples (with and without the bacterial agent) incubated within soil and water to observe the resistivity differences which reflect the healing performance of cracks.

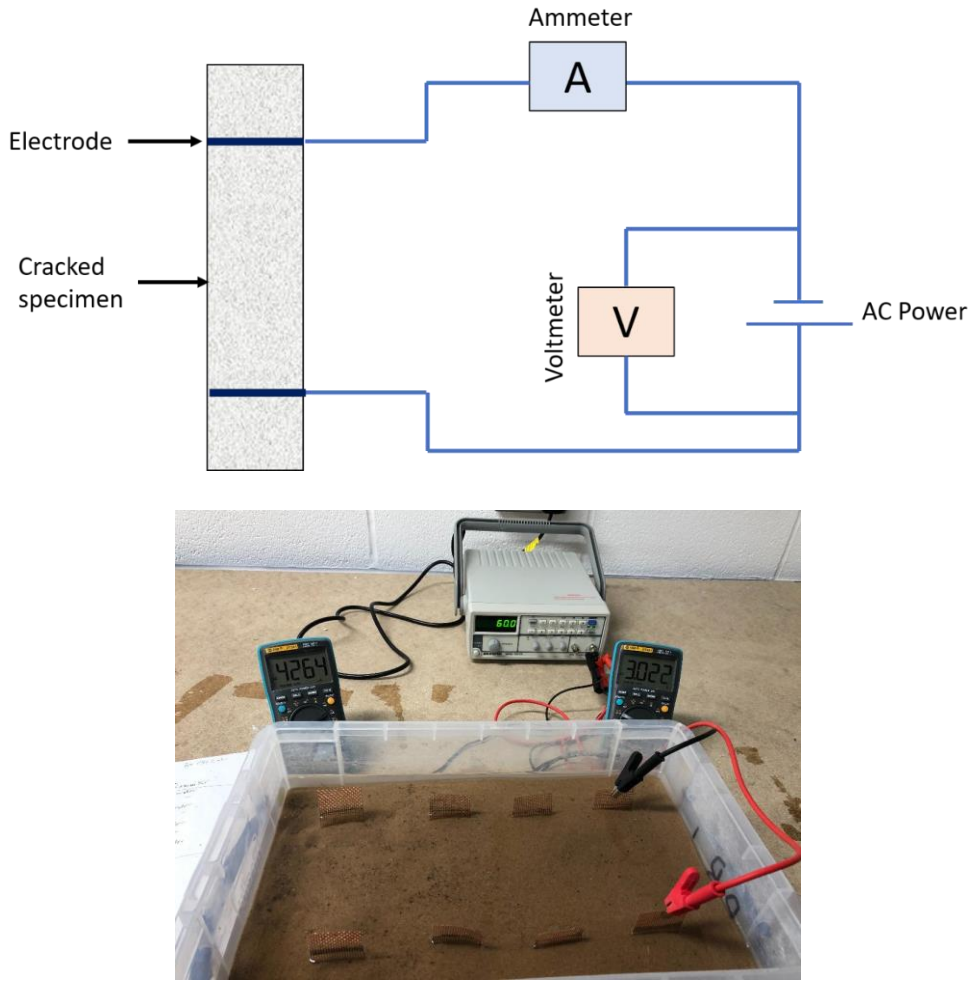

Figure 7.9: Simplified test arrangement for concrete resistivity measurements

The literature indicated that temperature has an impact on ionic mobility and that the electric current flow in concrete is caused by ionic movement within the pores. Consequently, in the course of the experimental measurements of this work, consideration was also given to the impact of temperature on electrical resistivity. Ionic mobility generally increases with temperature, which resultantly reduces electrical resistivity. Since it is evident that a 1.8°F (1°C) change can cause a 3 per cent change in the electrical resistivity of concrete [367], it is essential that, when concrete samples for electrical resistivity are tested, temperature changes are monitored.

7.2.5 Reinforcement corrosion measurement

It has been argued that bacterially induced carbonate precipitation could be a new and ecologically friendly strategy to prevent reinforcement corrosion in cement-based materials [363]. In order to study the effect of crack closure on the development of corrosion of steel bars while still embedded in concrete, half-cell potential measurements were adapted for this investigation.

Half-cell potential measurements are considered the most commonly used method of observing steel corrosion in concrete structures. In the 1970s, Richard F. Stratfull has introduced the method in North America and then it was approved by ASTM as standard in 1980 [377]. The Half-cell potential method is especially suitable because it can be used to assess the anticipation of steel corrosion before damage appearing at the surface of a structure. The steel corrosion activity can be classified by using the Half-cell potential measurements and also it can indicate the locations where the steel is probably corroded; nevertheless, the rate of corrosion of steel or concrete condition can be evaluated by potentials [378]. The Half-cell potential technique can be used for ordinary structures or stainless-steel reinforcement, and it can be also applied to evaluate the corrosion of prestressing steel in concrete in the same manner, but it cannot be performed on prestressing steel in the ducts of posttensioned cables.

The test set-up of half-cell potential measurement contains a voltmeter with two leads. The first lead is linked to a reference electrode, made of copper sulphate, laid on the concrete face. The second lead is linked to the steel bars through a voltmeter, while the

reference electrode passes a current to the surface of the concrete by using a sponge soaked with an electrolytic solution (Figure 7.10). The main purpose of this apparatus is to measure the voltage or the variation in potential between the reference electrode and the steel bars. As copper is higher than steel in galvanic series, therefore the reference electrode in the half-cell potential behaves as the cathode.

The half-cell measurements were taken at three different positions for each specimen as shown in Figure 7.10, and the mean was used to evaluate the average of the half-cell potential values for the total measurement period, which could be calculated as follows:

$$P_{ave} = \frac{\sum_{i=1}^{n} Pi}{n} \quad (7.4)$$

Where:

P_{ave} = the average of the half-cell potential values for the total measurement period

n= the total number of half-cell potential measurements

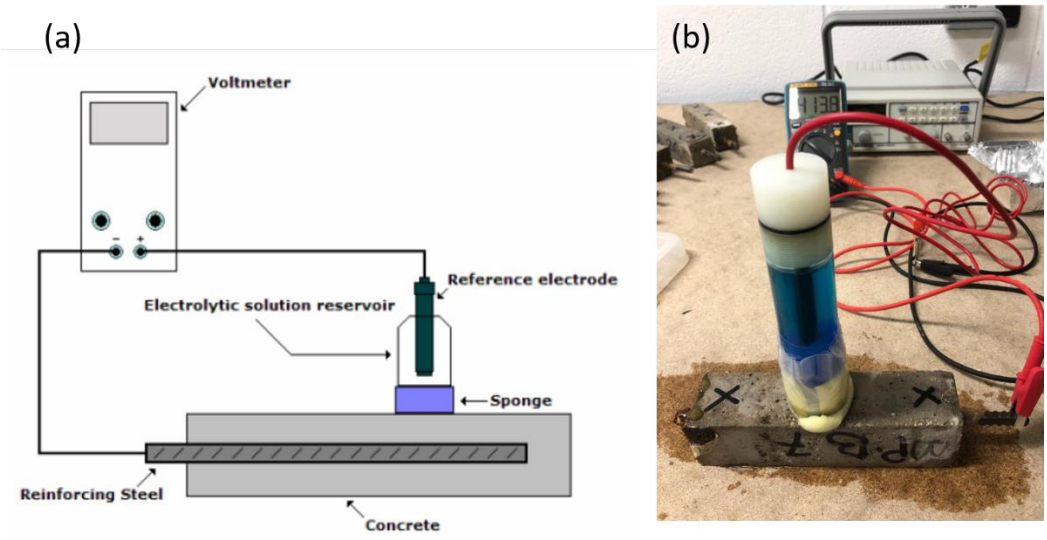

Figure 7.10: (a) Simplified test arrangement of half-cell (adopted in this study after Guthrie et al. [378]). (b) Half-cell potential device used in the lab.

7.3 Results and discussion

7.3.1 Absolute Porosity

The absolute porosity of the control and bio-mortar specimens was calculated (as discussed above), and the average values were presented graphically. Figure 7.11 illustrates the results of the absolute porosity as a percentage. As can be seen from the Figure, the differences in the absolute porosity values between the control and bio-mortar specimens at the first 7 days were very small (2.01 %). Therefore, the influence of the porosity change on electrical resistivity measurements can be neglected at this stage.

It can also be clearly seen that the absolute porosity for bio-mortar specimens was decreased with time, and this could be attributed to the growth of calcium carbonate crystals near the external surface of the specimens and therefore decreasing the porosity of bio-mortar specimens. On another hand, the porosity of bio-mortar specimens after 90 days was 22.5 % less than those of control specimens indicating the effect of bacteria on the impregnated mortar.

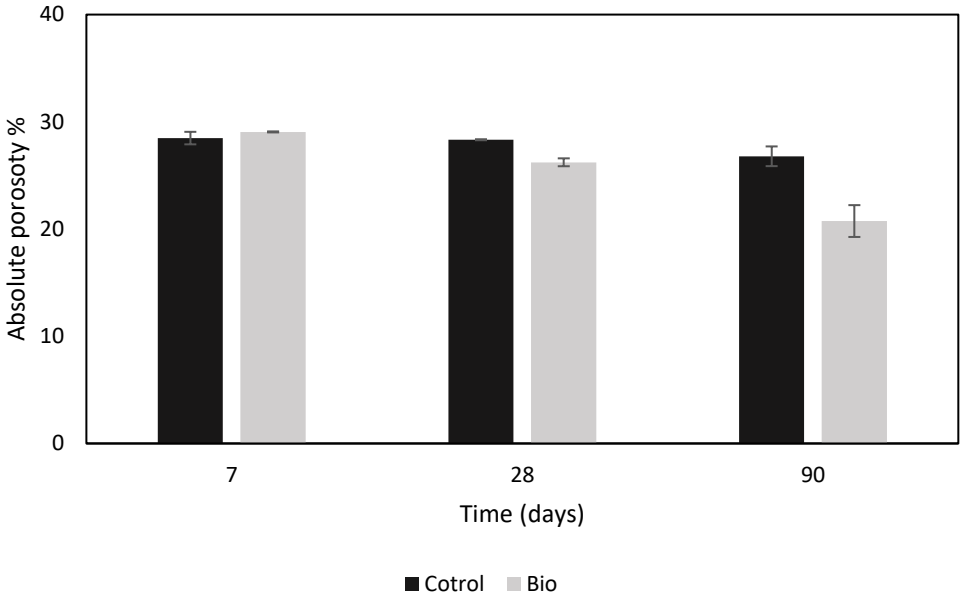

Figure 7.11: The absolute porosity values for the control and bio-mortar specimens at different periods

7.3.2 Electrical resistivity

The electrical resistivity for both types of cracked specimens (control and bio-mortar) was measured during the healing process. The relationship between the electrical resistivity and time of incubation for these specimens in water and soil is presented in Figures 7.12 and 7.13, respectively. From the Figures, it can be observed that the electrical resistivity for all specimens was increased over time. For specimens incubated in water, the increase in resistivity in the first four weeks of incubation was almost similar for both types of specimens. However, after 28 days the increase in resistivity of bio-mortar specimens was higher than the control specimens. After around 70 days of incubation, the final increase for bio and control specimens observed was around 106%, and 63% respectively. The remarkable improvement in electrical resistivity of the bio-mortar specimens can be interpreted as a result of calcium carbonate deposition within the cracks as shown in Figure 7.14.

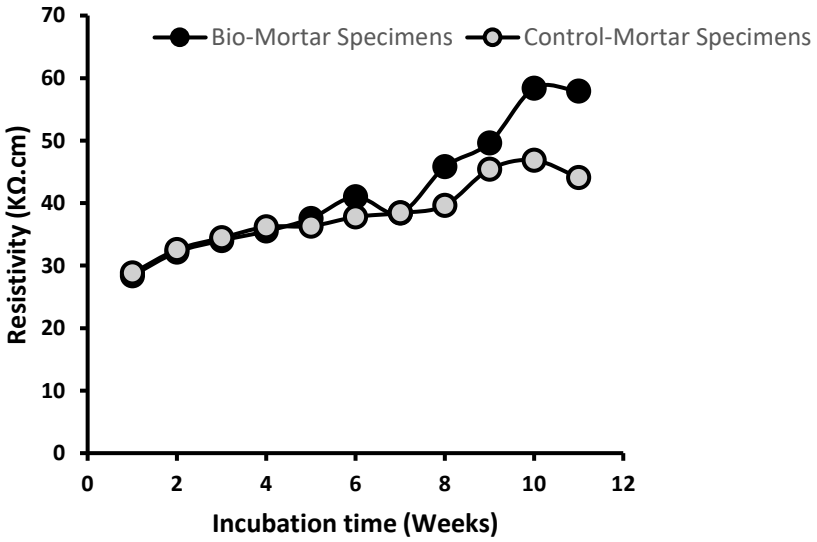

Figure 7.12: The relationship between the electrical resistivity and time of incubation of bio and control specimens incubated in water

For soil incubated specimens, the electrical resistivity for both types of specimens (bio and control) increased over time with some fluctuations, however, after 70 days of

incubation, the final increase of resistivity for bio-mortar specimens was around 64%, whereas the final increase of resistivity for control specimens was around 37%.

In general, the increase in the electrical resistivity of both types of specimens incubated in water was higher than at those incubated in soil, and this attributed to the increase in healing performance in water in comparison with soil incubation. The presence of soil matrix might have influenced the transportation of oxygen and other resources to the microbes, which could limit their capacity for the production of CO_2 and Calcium Carbonate sealing the cracks.

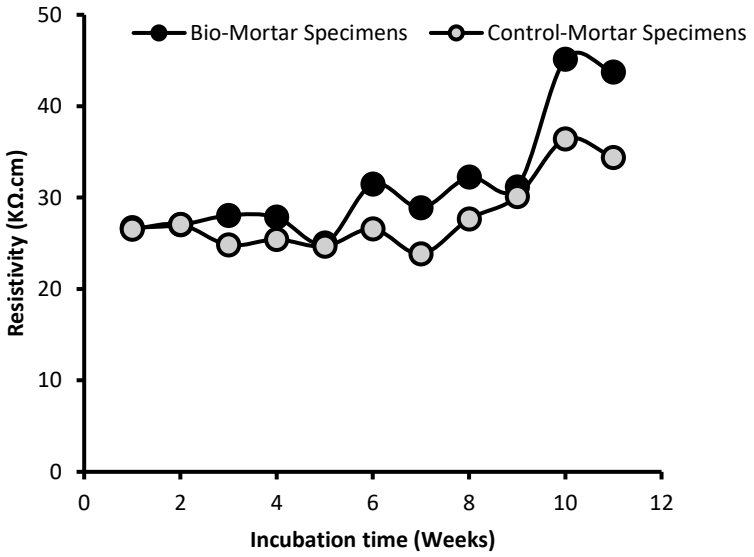

Figure 7.13: The relationship between the electrical resistivity and time of incubation of bio and control specimens incubated in soil

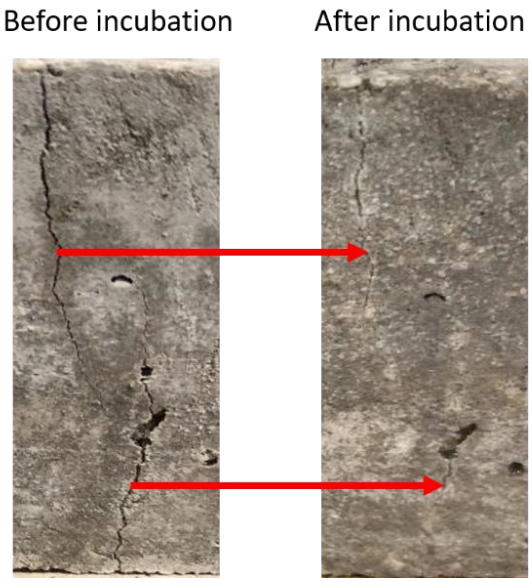

Figure 7.14: Observation of crack healing before and after incubation for bio-mortar specimens

7.3.3 Steel corrosion

The relationship between the corrosion potential and time of incubation for the control and bio-mortar specimens is illustrated in Figure 7.15. It can be seen that the corrosion potential just before incubation in water was low and similar for both types of specimens and this implies that there was no rust, and the overall surface of the rebar is smooth.

The corrosion rate for all specimens was approximately -300 mV in the first 14 days of incubation, then shifted to more negative potential after 3 weeks (Figure 7.15). This indicates that the corrosion tendency increased with time. The control specimens showed a higher corrosion tendency (-694.3 mV) than the bio-mortar specimens (-464 mV) at the end of the incubation period.

Before cracking, the electrical potential of both types of specimens was around -100 mV, which indicates the passivity of reinforcements when the concrete cover was intact. Normally, the reinforcement will not corrode as a result of the formation of a passive film layer on the steel surface. After cracking, the electrical potential values increased gradually during the incubation period for both types of specimens except for the bio-mortar specimens whose corrosion current did not highly increase from 21 days to the end of the incubation period.

After cracking, corrosive species, mainly moisture, carbon dioxide CO_2, and chloride ions Cl^-, will penetrate the concrete and result in damage to the passive film. In this study, deterioration of reinforcement was initiated by the carbonation-induced corrosion since no chloride ions were included. Therefore, the reinforcement corrosion can be effectively prevented by restraining the ingress of moisture and CO_2 as a result of the healing process of the cracks. For the bio-mortar specimens, the developed bio-mineral was able to block pores and seal cracks, thereby leading to a delay of water-born ions within specimens by which steel reinforcement's passivity towards corrosion is protected by a diffusion barrier of oxygen.

These results are consistent with the results obtained from electrical resistivity, implying that the electrochemical properties of concrete and reinforcement corrosion are consistent.

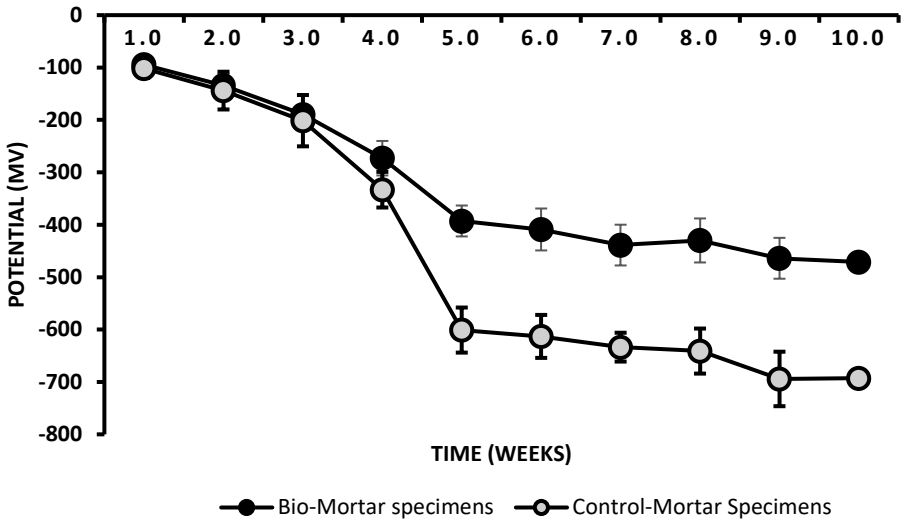

Figure 7.15: Electrical potential of control and bio-mortar specimens

7.4 Conclusion

This chapter presented an investigation of the feasibility of using concrete electrical resistivity technique to evaluate the healing performance of bio-self healing of cracks.

The results showed that the improvement in electrical resistivity of bio-mortar specimens was remarkably higher in comparison with control specimens, particularly, for water incubation where bio healing agents can work more effectively. This improvement can be referred to the healing performance of bio-mortar specimens in comparison with autogenous healing in control specimens.

In the absence of chlorides, reinforcement corrosion can be inhibited by the microbial induced calcium precipitation process due to its effective crack closure capability. Moreover, oxygen consumption by bacteria and the formation of calcium carbonate to avoid the ingress of moisture and CO_2 into concrete has reduced the propagation of corrosion of reinforcement bars. However, the bio-healing agent has provided crack healing but could not completely avoid corrosion initiation.

Chapter 8

Conclusions and Further Work

8.1 Introduction

This thesis has investigated the efficiency of bio self-healing concrete incubated within soil. To better understand the bio self-healing mechanism and the effect of incubation environment on healing performance, several factors were investigated in this research work such as the effect of the delivery technique of healing agents, type of soil, exposure conditions, and ground regime (partially, and fully saturated as well as different cycles), and finally, a new method of assessing the efficiency of the self-healing system of specimens embedded within soil using concrete electrical resistivity was also investigated in this research.

This chapter brings together the conclusions drawn from the research work reported in this thesis and recommends appropriate future work for continued investigations on bio self-healing concrete incubated within soil. For more specific conclusions the reader is referred to the individual conclusions of each part at the end of each chapter.

8.2 Conclusions

A list of specific research objectives was described in Chapter 1. The research presented in this thesis, and summarised below, has been undertaken to satisfying these objectives and has led to the following conclusions:

8.2.1 Phase One (The effect of delivery technique of bacterial agent on the efficiency of self-healing system of concrete):

The first phase of this study was conducted to evaluate the effect of using polymer materials (i.e. calcium alginate), and lightweight aggregate (i.e. perlite) as carer materials on the compatibility with the cementitious mortar and the efficiency of self-healing. To provide more protection for the impregnated bacteria, coating the perlite with sodium silicate was investigated. The direct add of spores was used as a control

technique to compare the findings after calcium alginate and perlite use. Moreover, the viability of spores within these capsules was also investigated. Based on this investigation, the following conclusion can be drawn.

- The calcium alginate beads were shrunk due to cement hydration; therefore, voids were formed around the capsules. In most cases, cracks were crossing these voids without breaking the beads. In contrast, the volume of perlite capsules was stable.
- In the direct delivery of the healing agent, the viability of spores was reduced as a result of the high alkaline environment within the cement matrix. However, the direct delivery provided a homogenous distribution of healing agent, and the healing performance was more efficient at the early stages of incubation and was less efficient after long-term incubation.
- The uncoated perlite has offered a quick release of healing agents, and therefore, better healing efficiency was exhibited during incubation.
- Using sodium silicate as a coating layer to provide more protection to the impregnated bacteria had negatively affected the healing performance, where the coating layer delays the release of the bacterial agents, therefore impeding the crack healing process.
- The volume stability of the perlite capsules has made them more compatible with the cement mortar matrix in comparison with calcium alginate capsules.
- Self-healing was achieved in both cases either by impregnating nutrients with spores or in separate capsules. This means that the activated spores feed on nutrients released from their capsules and carried to the crack surface during the incubation period.

8.2.2 Phase Two (The effect of type of soil, exposure conditions, and ground regime on the healing efficiency of self-healing concrete):

The second phase of this research was performed to evaluate the effect of different ground conditions on self-healing efficiency. In particular, the influence of the aggressive

environment of exposure classified with according to BS EN 206-1 2000 namely X0, XA1 and XA3 on the healing performance of cement mortar specimens incubated into non-cohesive soil (sand) exposed to dry and wet cycles, and cement mortar specimens incubated into fully and partially saturated cohesive soil (clay). Based on these investigations, the conclusions are presented as follow:

- The microbially induced calcium carbonate on the crack surface has the potential to improve the durability of cementitious materials and therefore increasing the service life of concrete structures. Based on the results reported in Chapter 6, the results showed efficient and notable self-healing for bio-mortar specimens in comparison with control specimens in all exposure conditions.
- For non-cohesive soil (sand), the reduction in pH of the incubation environment affected bio self-healing performance. For example, the healing percentage in the crack closure of specimens incubated in XA3 (pH = 4.5) was 43% lower than in specimens incubated in X0 (pH = 7). However, for cohesive soil (clay) the healing ratios of bio self-healing of specimens incubated in the identical exposure conditions were almost similar, with better results observed in the pH neutral condition.
- The efficiencies of control and bio-mortar specimens were significantly affected by the soil's moisture content, where the healing performance of bio-mortar specimens incubated in fully saturated conditions was around 40% higher than partially saturated condition. This indicates that the mineral precipitation of calcium carbonate caused by the metabolic conversion of nutrients by bacteria is heavily reliant on the moisture content of the soil. The hydration of un-hydrated cement particles representing the primary source of autogenous healing is also influenced by soil moisture content.

In summary, this work has shown that bio self-healing solutions would be applicable to concrete structures incubated into soils such as foundations, bridge piers, and tunnels in a range of standard exposure conditions, and that this is facilitated by the commonly applied bacterial agent *Bacillus subtilis*.

8.2.3 Phase Three (Monitoring the self-healing performance of concrete embedded within the soil using electrical resistivity technique):

In this phase, the electrical resistivity technique was used to assess the healing performance of cracked specimens incubated within the soil. The main conclusion obtained from this investigation is presented as follows:

- The results revealed a remarkable improvement in electrical resistivity of bio-mortar specimens in comparison with control specimens, particularly, for water incubation where bio healing agent can work more effectively. This improvement can be referred to the healing performance of bio-mortar specimens in comparison with autogenous healing in control specimens.

8.3 Recommendations for future work

This research has provided new information on the efficiency of bio self-healing of concrete incubated within soils. The study was motivated by problems encountered with the durability of underground concrete structures (as explained in Chapter 1). The findings from this research showed that the exposure conditions affected the healing efficiency, therefore future work should consider how formulations, application methods, and ground preparation can be optimised to achieve the best possible protection for underground concrete structures. Therefore, it is recommended that more extensive studies should be undertaken in this evolving field of advanced solutions to durability problems before using this system in the construction industry. The following future work is recommended:

- Using capsules as a protective carer has a negative impact on concrete properties such as compressive strength. In this research, all used capsules had negatively affected concrete strength; however, intensive research is needed to find a suitable capsule that does not affect concrete properties.
- In this research, it was evidenced that indigenous bacteria naturally present within the soil can enhance the mortar self-healing process. However, further

investigation is needed to find the effect of type and amount of bacteria present within the soil on the healing performance.

- Carbon dioxide dissolves in water and reacts with the hydroxide to form calcium carbonate autogenously. However, in the case of under-ground structures water not always comes from the top surface of soil such as rain. However, water can come from the increase in the water table, therefore, the effect of CO_2 dissolved in water on autogenous healing can be investigated by designing an experiment to investigate the effect of dry and wet cycles by simulating the increase of water table level instead of adding water through the top surface.
- It is necessary to optimize the pH range for microbially induced calcium carbonate for any specific bacterial strain that will be used. For instance, previous research [325] showed that at a higher pH level, the enzymatic activity of bacteria decreases and at lower pH levels carbonate tends to dissolve, and therefore decreases precipitation. Therefore, for future work, it is significant to select a suitable strain of bacteria that have the ability to precipitate calcite in the targeted environment.
- The effect of soil properties such as porosity, permeability and depth of incubation where temperature increase with depth can affect the bio healing performance. For instance, the presence of soil matrix impedes the transportation of oxygen and other resources to the bacteria, which could limit their capacity for CO_2, and these impediments depend on soil properties. Therefore, further work is required to investigate the influence of soil properties and depth of incubation on healing performance.
- Using electrical resistivity to assess the healing performance was successfully used in this research. However, further research is needed to correlate the relationship between evolved resistivity and crack closure.

References

1. Lala, R., A. Hussain, and S. Akhtar, *Self Healing Concrete.*
2. Broomfield, J.P., *Corrosion of steel in concrete: understanding, investigation and repair*. 2006: CRC Press.
3. Bamforth, P.B., *Early-age thermal crack control in concrete*. Vol. 660. 2007: Ciria.
4. Mihashi, H. and T. Nishiwaki, *Development of engineered self-healing and self-repairing concrete-state-of-the-art report.* Journal of Advanced Concrete Technology, 2012. **10**(5): p. 170-184.
5. Basheer, P.A.M., S.E. Chidiact, and A.E. Long, *Predictive models for deterioration of concrete structures.* Construction and Building Materials, 1996. **10**(1): p. 27-37.
6. Jonkers, H.M., *Bacteria-based self-healing concrete.* Heron, 56 (1/2), 2011.
7. Liu, Y., *Modeling the time-to corrosion cracking of the cover concrete in chloride contaminated reinforced concrete structures.* 1996.
8. Koch, G.H., et al., *Corrosion cost and preventive strategies in the United States*. 2002.
9. Sangadji, S., *Can self-healing mechanism helps concrete structures sustainable?* Procedia engineering, 2017. **171**: p. 238-249.
10. Cailleux, E. and V. Pollet. *Investigations on the development of self-healing properties in protective coatings for concrete and repair mortars*.
11. Treasury, H.M. and I. Uk, *Infrastructure cost review: technical report.* HM Treasure and Infrastructure UK, London, UK, 2010.
12. Solomon, I., M.F. Bird, and B. Phang, *An economic solution for the cathodic protection of concrete columns using a conductive tape system.* Corrosion science, 1993. **35**(5-8): p. 1649-1660.
13. Ahn, T.-H. and T. Kishi, *Crack self-healing behavior of cementitious composites incorporating various mineral admixtures.* Journal of Advanced Concrete Technology, 2010. **8**(2): p. 171-186.
14. Broek, A.V., *Self-healing concrete*. 2009, FORBES INC 60 FIFTH AVE, NEW YORK, NY 10011 USA.
15. Yunovich, M. and N.G. Thompson, *Corrosion of highway bridges: Economic impact and control methodologies.* Concrete International, 2003. **25**(1): p. 52-57.
16. Van Breugel, K. *Is there a market for self-healing cement-based materials*.
17. Schlangen, E. and S. Sangadji, *Addressing infrastructure durability and sustainability by self healing mechanisms-recent advances in self healing concrete and asphalt.* Procedia Engineering, 2013. **54**: p. 39-57.
18. van der Zwaag, S., *An introduction to material design principles: Damage prevention versus damage management*, in *Self healing materials*. 2007, Springer. p. 1-18.
19. Dry, C., *Matrix cracking repair and filling using active and passive modes for smart timed release of chemicals from fibers into cement matrices.* Smart Materials and Structures, 1994. **3**(2): p. 118.
20. Van Tittelboom, K. and N. De Belie, *Self-healing in cementitious materials—A review.* Materials, 2013. **6**(6): p. 2182-2217.
21. Souradeep, G. and H.W. Kua, *Encapsulation technology and techniques in self-healing concrete.* Journal of Materials in Civil Engineering, 2016. **28**(12): p. 04016165.
22. Li, M. and V.C. Li, *Cracking and Healing of Engineered Cementitious Composites under Chloride Environment.* ACI Materials Journal, 2011. **108**(3).
23. Ter Heide, N., *Crack healing in hydrating concrete.* Delft University of Technology, 2005.
24. ter Heide, N. and E. Schlangen. *Self-healing of early age cracks in concrete*.

25. Van Tittelboom, K. and N. De Belie, *Self-healing concrete: suitability of different healing agents.* International Journal of 3R's, 2010. **1**(1): p. 12-21.
26. Van Tittelboom, K., et al., *Self-healing efficiency of cementitious materials containing tubular capsules filled with healing agent.* Cement and Concrete Composites, 2011. **33**(4): p. 497-505.
27. Brown, E.N., S.R. White, and N.R. Sottos, *Retardation and repair of fatigue cracks in a microcapsule toughened epoxy composite—Part II: In situ self-healing.* Composites Science and Technology, 2005. **65**(15-16): p. 2474-2480.
28. Blaiszik, B.J., et al., *Microcapsules filled with reactive solutions for self-healing materials.* Polymer, 2009. **50**(4): p. 990-997.
29. Kessler, M.R., N.R. Sottos, and S.R. White, *Self-healing structural composite materials.* Composites Part A: applied science and manufacturing, 2003. **34**(8): p. 743-753.
30. Vekariya, M.S. and J. Pitroda, *Bacterial concrete: new era for construction industry.* International journal of engineering trends and technology, 2013. **4**(9): p. 4128-4137.
31. Pacheco-Torgal, F. and J.A. Labrincha, *Biotech cementitious materials: some aspects of an innovative approach for concrete with enhanced durability.* Construction and Building Materials, 2013. **40**: p. 1136-1141.
32. Tziviloglou, E., et al., *Bio-based self-healing mortar: An experimental and numerical study.* Journal of Advanced Concrete Technology, 2017. **15**(9): p. 536-543.
33. Gupta, S., S. Dai Pang, and H.W. Kua, *Autonomous healing in concrete by bio-based healing agents–A review.* Construction and Building Materials, 2017. **146**: p. 419-428.
34. Hamza, O., et al., *The effect of soil incubation on bio self-healing of cementitious mortar.* Materials Today Communications, 2020. **24**: p. 100988.
35. Wang, J.Y., et al., *Application of hydrogel encapsulated carbonate precipitating bacteria for approaching a realistic self-healing in concrete.* Construction and building materials, 2014. **68**: p. 110-119.
36. Poursaee, A., *Corrosion of steel in concrete structures*. 2016: Woodhead Publishing.
37. Horrigmoe, G., *Future needs in concrete repair technology.* Proceedings, Concrete Technology for a Sustainable Development in the 21st Century, ed. by OE Gjørv and K. Sakai (E & FN Spon London and New York, 2000), 2000: p. 332-340.
38. Talaiekhozan, A., et al., *A review of self-healing concrete research development.* Journal of Environmental Treatment Techniques, 2014. **2**(1): p. 1-11.
39. Abd_Elmoaty, A.E.M., *Self-healing of polymer modified concrete.* Alexandria Engineering Journal, 2011. **50**(2): p. 171-178.
40. Sangadji, S., et al. *Injecting a liquid bacteria-based repair system to make porous network conrete healed*. Magnel Laboratory for Concrete Research.
41. Khushefati, W.H.A., *Healing of cracks in concrete.* 2004.
42. Song, H.-W., et al., *Predicting carbonation in early-aged cracked concrete.* Cement and Concrete Research, 2006. **36**(5): p. 979-989.
43. Achal, V., A. Mukerjee, and M.S. Reddy, *Biogenic treatment improves the durability and remediates the cracks of concrete structures.* Construction and Building Materials, 2013. **48**: p. 1-5.
44. Grieve, T.K.e.a., *Non-structural cracks in concrete*, ed. TR22. 2010.
45. Graves, H., et al., *Expanded material degradation assessment (EMDA), Volume 4: Aging of concrete.* Technical Rep. NUREG/CR-7153, ORNL/TM-2011/545, United State Nuclear Regulatory Commission, Rockville, MD, 2014.
46. Shaikh, F.U.A., *Effect of cracking on corrosion of steel in concrete.* International Journal of Concrete Structures and Materials, 2018. **12**(1): p. 1-12.

47. Otieno, M.B., M.G. Alexander, and H.D. Beushausen, *Corrosion in cracked and uncracked concrete–influence of crack width, concrete quality and crack reopening.* Magazine of Concrete Research, 2010. **62**(6): p. 393-404.
48. Scott, A. and M.G. Alexander, *The influence of binder type, cracking and cover on corrosion rates of steel in chloride-contaminated concrete.* Magazine of Concrete Research, 2007. **59**(7): p. 495-505.
49. Pettersson, K., O. Jorgenson, and P. FidjestolI, *The effect of cracks on reinforcement corrosion in high-performance concrete in a marine environment.* Special Publication, 1996. **163**: p. 185-200.
50. Arya, C. and F.K. Ofori-Darko, *Influence of crack frequency on reinforcement corrosion in concrete.* Cement and Concrete Research, 1996. **26**(3): p. 345-353.
51. Arya, C. and L.A. Wood, *The relevance of cracking in concrete to corrosion of reinforcement*. 1995: Concrete Society.
52. Beeby, A.W., *Cracking, cover, and corrostion of reinforcement.* Concrete international, 1983. **5**(2): p. 35-40.
53. Micallef, M., *Crack control in base-restrained reinforced concrete walls.* 2015.
54. Kattilakoski, J., *Crack control of concrete structures in special cases.* 2013.
55. Shahinpoor, M. *Intelligent civil engineering materials, structures and systems revisited*. ASCE.
56. Pang, J.W.C. and I.P. Bond, *A hollow fibre reinforced polymer composite encompassing self-healing and enhanced damage visibility.* Composites Science and Technology, 2005. **65**(11-12): p. 1791-1799.
57. Huang, H., G. Ye, and D. Damidot, *Effect of blast furnace slag on self-healing of microcracks in cementitious materials.* Cement and concrete research, 2014. **60**: p. 68-82.
58. Al-Ansari, M., et al., *Performance of modified self-healing concrete with calcium nitrate microencapsulation.* Construction and Building Materials, 2017. **149**: p. 525-534.
59. Kanellopoulos, A., P. Giannaros, and A. Al-Tabbaa, *The effect of varying volume fraction of microcapsules on fresh, mechanical and self-healing properties of mortars.* Construction and Building Materials, 2016. **122**: p. 577-593.
60. Tziviloglou, E., et al., *Bacteria-based self-healing concrete to increase liquid tightness of cracks.* Construction and Building Materials, 2016. **122**: p. 118-125.
61. Jonkers, H.M., et al., *Application of bacteria as self-healing agent for the development of sustainable concrete.* Ecological engineering, 2010. **36**(2): p. 230-235.
62. Edvardsen, C., *Water permeability and autogenous healing of cracks in concrete.* Materials Journal, 1999. **96**(4): p. 448-454.
63. Ghosh, S.K., *Self-healing materials: fundamentals, design strategies, and applications*. 2009: John Wiley & Sons.
64. Davies, R. and A. Jefferson, *Micromechanical modelling of self-healing cementitious materials.* International Journal of Solids and Structures, 2017. **113**: p. 180-191.
65. De Rooij, M., et al., *Self-healing phenomena in cement-Based materials: state-of-the-art report of RILEM technical committee 221-SHC: self-Healing phenomena in cement-Based materials*. Vol. 11. 2013: Springer.
66. Hassanein, N.M., *The application of neural networks to service life prediction of concrete structures.* 1996.
67. Hearn, N., *Self-sealing, autogenous healing and continued hydration: what is the difference?* Materials and structures, 1998. **31**(8): p. 563.
68. Zhang, J., et al., *Immobilizing bacteria in expanded perlite for the crack self-healing in concrete.* Construction and Building Materials, 2017. **148**: p. 610-617.

69. Vijay, K., M. Murmu, and S.V. Deo, *Bacteria based self healing concrete–A review.* Construction and building materials, 2017. **152**: p. 1008-1014.
70. Li, V.C., et al., *Recovery against Mechanical Actions*, in *Self-Healing Phenomena in Cement-Based Materials*. 2013, Springer. p. 119-215.
71. Yang, Y., et al., *Autogenous healing of engineered cementitious composites under wet–dry cycles.* Cement and Concrete Research, 2009. **39**(5): p. 382-390.
72. Schlangen, E., N. Ter Heide, and K. Van Breugel, *Crack healing of early age cracks in concrete*, in *Measuring, Monitoring and Modeling Concrete Properties*. 2006, Springer. p. 273-284.
73. Reinhardt, H.-W. and M. Jooss, *Permeability and self-healing of cracked concrete as a function of temperature and crack width.* Cement and concrete research, 2003. **33**(7): p. 981-985.
74. Hosoda, A. *Self healing of crack and water permeability of expansive concrete*.
75. Yamada, K. *Crack self healing properties of expansive concretes with various cements and admixtures*.
76. Sisomphon, K., O. Copuroglu, and E.A.B. Koenders, *Self-healing of surface cracks in mortars with expansive additive and crystalline additive.* Cement and Concrete Composites, 2012. **34**(4): p. 566-574.
77. Yu, J.H. and E.H. Yang, *RETRACTED: Microstructure of self-healed PVA engineered cementitious composites under wet-dry cycles.* Advances in Applied Ceramics, 2010. **109**(7): p. 399-404.
78. Maes, M., D. Snoeck, and N. De Belie, *Chloride penetration in cracked mortar and the influence of autogenous crack healing.* Construction and building materials, 2016. **115**: p. 114-124.
79. Yang, Y., E.-H. Yang, and V.C. Li, *Autogenous healing of engineered cementitious composites at early age.* Cement and concrete research, 2011. **41**(2): p. 176-183.
80. Zwaag, S., *Self healing materials: an alternative approach to 20 centuries of materials science*. Vol. 30. 2008: Springer Science+ Business Media BV Dordrecht, The Netherlands.
81. Cappellesso, V.G., et al., *Self-healing phenomenon evaluation in cementitious matrix with different water/cement ratios and crack opening age.* Int. J. Civ. Environ. Eng, 2019. **13**: p. 144-151.
82. Lepech, M. and V.C. Li, *Water permeability of cracked cementitious composites.* 2005.
83. Suleiman, A.R. and M.L. Nehdi, *Effect of environmental exposure on autogenous self-healing of cracked cement-based materials.* Cement and Concrete Research, 2018.
84. Hearn, N. and C.T. Morley, *Self-sealing property of concrete—Experimental evidence.* Materials and structures, 1997. **30**(7): p. 404-411.
85. Hager, M.D., et al., *Self-healing materials.* Advanced Materials, 2010. **22**(47): p. 5424-5430.
86. Seifan, M., A.K. Samani, and A. Berenjian, *Bioconcrete: next generation of self-healing concrete.* Applied microbiology and biotechnology, 2016. **100**(6): p. 2591-2602.
87. Li, V.C., Y.M. Lim, and Y.-W. Chan, *Feasibility study of a passive smart self-healing cementitious composite.* Composites Part B: Engineering, 1998. **29**(6): p. 819-827.
88. Lee, H.X.D., H.S. Wong, and N.R. Buenfeld, *Potential of superabsorbent polymer for self-sealing cracks in concrete.* Advances in Applied Ceramics, 2010. **109**(5): p. 296-302.
89. Qian, S.Z., J. Zhou, and E. Schlangen, *Influence of curing condition and precracking time on the self-healing behavior of engineered cementitious composites.* Cement and concrete composites, 2010. **32**(9): p. 686-693.
90. Janssen, D., *Water encapsulation to initiate self-healing in cementitious materials.* Master's Thesis, Delft University, Delft, 2011.

91. Sisomphon, K. and O. Copuroglu. *Self healing mortars by using different cementitious materials*.
92. White, S.R., et al., *Autonomic healing of polymer composites.* Nature, 2001. **409**(6822): p. 794.
93. Joseph, C., *Experimental and numerical study of the fracture and self-healing of cementitious materials*. 2008: Cardiff University.
94. Wu, M., B. Johannesson, and M. Geiker, *A review: Self-healing in cementitious materials and engineered cementitious composite as a self-healing material.* Construction and Building Materials, 2012. **28**(1): p. 571-583.
95. Wiktor, V. and H.M. Jonkers, *Quantification of crack-healing in novel bacteria-based self-healing concrete.* Cement and Concrete Composites, 2011. **33**(7): p. 763-770.
96. Alazhari, M., et al., *Application of expanded perlite encapsulated bacteria and growth media for self-healing concrete.* Construction and Building Materials, 2018. **160**: p. 610-619.
97. Alghamri, R., A. Kanellopoulos, and A. Al-Tabbaa, *Impregnation and encapsulation of lightweight aggregates for self-healing concrete.* Construction and Building Materials, 2016. **124**: p. 910-921.
98. Liu, X.Y., et al., *Experimental study on self-healing performance of concrete.* J. Build. Mater, 2005. **2**: p. 184-188.
99. Palin, D., V. Wiktor, and H.M. Jonkers, *A bacteria-based self-healing cementitious composite for application in low-temperature marine environments.* Biomimetics, 2017. **2**(3): p. 13.
100. Wang, J.Y., N. De Belie, and W. Verstraete, *Diatomaceous earth as a protective vehicle for bacteria applied for self-healing concrete.* Journal of industrial microbiology & biotechnology, 2012. **39**(4): p. 567-577.
101. Van Tittelboom, K., et al., *Use of bacteria to repair cracks in concrete.* Cement and Concrete Research, 2010. **40**(1): p. 157-166.
102. Wang, J., et al., *Use of silica gel or polyurethane immobilized bacteria for self-healing concrete.* Construction and building materials, 2012. **26**(1): p. 532-540.
103. Wang, J.Y., et al., *Self-healing concrete by use of microencapsulated bacterial spores.* Cement and Concrete Research, 2014. **56**: p. 139-152.
104. Mostavi, E., et al., *Evaluation of self-healing mechanisms in concrete with double-walled sodium silicate microcapsules.* Journal of materials in civil engineering, 2015. **27**(12): p. 04015035.
105. Dong, B., et al., *Smart releasing behavior of a chemical self-healing microcapsule in the stimulated concrete pore solution.* Cement and Concrete Composites, 2015. **56**: p. 46-50.
106. Alazhari, M., *The effect of microbiological agents on the efficiency of bio-based repair systems for concrete.* 2017.
107. Wang, J., et al., *Application of modified-alginate encapsulated carbonate producing bacteria in concrete: a promising strategy for crack self-healing.* Frontiers in microbiology, 2015. **6**: p. 1088.
108. Kalhori, H. and R. Bagherpour, *Application of carbonate precipitating bacteria for improving properties and repairing cracks of shotcrete.* Construction and Building Materials, 2017. **148**: p. 249-260.
109. Luo, M., C.-x. Qian, and R.-y. Li, *Factors affecting crack repairing capacity of bacteria-based self-healing concrete.* Construction and building materials, 2015. **87**: p. 1-7.
110. Jonkers, H.M. and E. Schlangen. *Development of a bacteria-based self healing concrete*. Citeseer.

111. Qian, C., et al., *Self-healing of early age cracks in cement-based materials by mineralization of carbonic anhydrase microorganism.* Frontiers in microbiology, 2015. **6**: p. 1225.
112. Xu, J. and W. Yao, *Multiscale mechanical quantification of self-healing concrete incorporating non-ureolytic bacteria-based healing agent.* Cement and concrete research, 2014. **64**: p. 1-10.
113. Achal, V., X. Pan, and N. Özyurt, *Improved strength and durability of fly ash-amended concrete by microbial calcite precipitation.* Ecological Engineering, 2011. **37**(4): p. 554-559.
114. Jonkers, H.M. and E. Schlangen, *Self-healing of cracked concrete: a bacterial approach.* Proceedings of FRACOS6: fracture mechanics of concrete and concrete structures. Catania, Italy, 2007: p. 1821-1826.
115. Chahal, N., R. Siddique, and A. Rajor, *Influence of bacteria on the compressive strength, water absorption and rapid chloride permeability of concrete incorporating silica fume.* Construction and Building Materials, 2012. **37**: p. 645-651.
116. Ramakrishnan, V., et al. *Improvement of concrete durability by bacterial mineral precipitation*.
117. Ghosh, P., et al., *Use of microorganism to improve the strength of cement mortar.* Cement and Concrete Research, 2005. **35**(10): p. 1980-1983.
118. Ghosh, S., et al., *Microbial activity on the microstructure of bacteria modified mortar.* Cement and Concrete Composites, 2009. **31**(2): p. 93-98.
119. Mihashi, H., et al., *Fundamental study on development of intelligent concrete characterized by self-healing capability for strength.* Transactions of the Japan Concrete Institute, 2000. **22**: p. 441-450.
120. Joseph, C., et al., *Experimental investigation of adhesive-based self-healing of cementitious materials.* Magazine of Concrete Research, 2010. **62**(11): p. 831-843.
121. Dry, C.M., *Three designs for the internal release of sealants, adhesives, and waterproofing chemicals into concrete to reduce permeability.* Cement and Concrete Research, 2000. **30**(12): p. 1969-1977.
122. Trask, R.S. and I.P. Bond, *Biomimetic self-healing of advanced composite structures using hollow glass fibres.* Smart Materials and Structures, 2006. **15**(3): p. 704.
123. Toohey, K.S., et al., *Self-healing materials with microvascular networks.* Nature materials, 2007. **6**(8): p. 581.
124. Huang, H., G. Ye, and Z. Shui, *Feasibility of self-healing in cementitious materials–By using capsules or a vascular system?* Construction and Building materials, 2014. **63**: p. 108-118.
125. Sangadji, S. and E. Schlangen. *Porous network concrete: A new approach to make concrete structures self-healing using prefabricated porous layer*. Citeseer.
126. Giannaros, P., *Laboratory and field investigation of the performance of novel microcapsule-based self-healing concrete.* 2017.
127. Sangadji, S. and E. Schlangen, *Self Healing of Concrete Structures-Novel approach using porous network concrete.* Journal of Advanced Concrete Technology, 2012. **10**(5): p. 185-194.
128. Li, Y. *A Review: Novel Routes towards the Realization of Self-Healing Function in Cementitious Materials*. IOP Publishing.
129. Lv, Z. and D. Chen, *Overview of recent work on self-healing in cementitious materials.* Materiales de Construcción, 2014. **64**(316): p. 034.
130. Tang, W., O. Kardani, and H. Cui, *Robust evaluation of self-healing efficiency in cementitious materials–a review.* Construction and Building Materials, 2015. **81**: p. 233-247.

131. Ferrara, L., et al., *Experimental characterization of the self-healing capacity of cement based materials and its effects on the material performance: A state of the art report by COST Action SARCOS WG2.* Construction and Building Materials, 2018. **167**: p. 115-142.
132. Jaroenratanapirom, D. and R. Sahamitmongkol, *Self-crack closing ability of mortar with different additives.* Journal of Metals, Materials and Minerals, 2011. **21**(1).
133. Snoeck, D. and N. De Belie, *Mechanical and self-healing properties of cementitious composites reinforced with flax and cottonised flax, and compared with polyvinyl alcohol fibres.* Biosystems Engineering, 2012. **111**(4): p. 325-335.
134. Ferrara, L., V. Krelani, and F. Moretti, *Autogenous healing on the recovery of mechanical performance of High Performance Fibre Reinforced Cementitious Composites (HPFRCCs): Part 2–Correlation between healing of mechanical performance and crack sealing.* Cement and Concrete Composites, 2016. **73**: p. 299-315.
135. Karaiskos, G., et al., *Performance monitoring of large-scale autonomously healed concrete beams under four-point bending through multiple non-destructive testing methods.* Smart Materials and Structures, 2016. **25**(5): p. 055003.
136. Pease, B.J., et al. *Photogrammetric assessment of flexure induced cracking of reinforced concrete beams under service loads*.
137. Homma, D., H. Mihashi, and T. Nishiwaki, *Self-healing capability of fibre reinforced cementitious composites.* Journal of Advanced Concrete Technology, 2009. **7**(2): p. 217-228.
138. Jaroenratanapirom, D. and R. Sahamitmongkol, *Self-crack closing ability of mortar with different additives.* Journal of Metals, Materials and Minerals, 2011. **21**(1): p. 9-17.
139. Qian, S., et al., *Self-healing behavior of strain hardening cementitious composites incorporating local waste materials.* Cement and Concrete Composites, 2009. **31**(9): p. 613-621.
140. Snoeck, D., et al., *Visualization of water penetration in cementitious materials with superabsorbent polymers by means of neutron radiography.* Cement and Concrete Research, 2012. **42**(8): p. 1113-1121.
141. Van Tittelboom, K., et al., *Acoustic emission analysis for the quantification of autonomous crack healing in concrete.* Construction and Building Materials, 2012. **28**(1): p. 333-341.
142. Giannaros, P., A. Kanellopoulos, and A. Al-Tabbaa, *Sealing of cracks in cement using microencapsulated sodium silicate.* Smart Materials and Structures, 2016. **25**(8): p. 084005.
143. Roig-Flores, M., et al., *Self-healing capability of concrete with crystalline admixtures in different environments.* Construction and Building Materials, 2015. **86**: p. 1-11.
144. Mechtcherine, V. and M. Lieboldt, *Permeation of water and gases through cracked textile reinforced concrete.* Cement and Concrete Composites, 2011. **33**(7): p. 725-734.
145. Jacobsen, S., J. Marchand, and H. Hornain, *SEM observations of the microstructure of frost deteriorated and self-healed concretes.* Cement and Concrete Research, 1995. **25**(8): p. 1781-1790.
146. Huang, H., et al. *Application of sodium silicate solution as self-healing agent in cementitious materials*. RILEM Publications SARL: Hong Kong, China.
147. Ferrara, L., V. Krelani, and M. Carsana, *A "fracture testing" based approach to assess crack healing of concrete with and without crystalline admixtures.* Construction and Building Materials, 2014. **68**: p. 535-551.
148. Van Belleghem, B., et al. *Analysis and visualization of water uptake in cracked and healed mortar by water absorption tests and X-ray radiography*.

149. Van Tittelboom, K., et al., *Use of neutron radiography and tomography to visualize the autonomous crack sealing efficiency in cementitious materials.* Materials and structures, 2013. **46**(1-2): p. 105-121.
150. Van den Heede, P., et al., *Neutron radiography based visualization and profiling of water uptake in (un) cracked and autonomously healed cementitious materials.* Materials, 2016. **9**(5): p. 311.
151. Thomas John Van, D., *Guidelines for early-opening-to-traffic portland cement concrete for pavement rehabilitation*. 2005: Transportation Research Board.
152. Van Tittelboom, K., et al., *Comparison of different approaches for self-healing concrete in a large-scale lab test.* Construction and building materials, 2016. **107**: p. 125-137.
153. Snoeck, D. and N. De Belie, *Repeated autogenous healing in strain-hardening cementitious composites by using superabsorbent polymers.* Journal of Materials in Civil Engineering, 2015. **28**(1): p. 04015086.
154. Snoeck, D., et al., *X-ray computed microtomography to study autogenous healing of cementitious materials promoted by superabsorbent polymers.* Cement and Concrete Composites, 2016. **65**: p. 83-93.
155. Wang, J., et al., *X-ray computed tomography proof of bacterial-based self-healing in concrete.* Cement and Concrete Composites, 2014. **53**: p. 289-304.
156. Mihashi, H., et al. *Advanced monitoring sensor and self-repairing system for cracks in concrete structures*. RILEM Publications SARL.
157. Wan, K.T. and C.K.Y. Leung, *Applications of a distributed fiber optic crack sensor for concrete structures.* Sensors and Actuators A: Physical, 2007. **135**(2): p. 458-464.
158. Rodríguez, G., J.R. Casas, and S. Villaba, *Cracking assessment in concrete structures by distributed optical fiber.* Smart Materials and Structures, 2015. **24**(3): p. 035005.
159. Wen, S. and D.D.L. Chung, *Electrical-resistance-based damage self-sensing in carbon fiber reinforced cement.* Carbon, 2007. **45**(4): p. 710-716.
160. McCarter, W.J., et al., *Activation energy and conduction in carbon fibre reinforced cement matrices.* Journal of materials science, 2007. **42**(6): p. 2200-2203.
161. Ding, Y., et al., *Nano-carbon black and carbon fiber as conductive materials for the diagnosing of the damage of concrete beam.* Construction and Building Materials, 2013. **43**: p. 233-241.
162. Teomete, E., *Measurement of crack length sensitivity and strain gage factor of carbon fiber reinforced cement matrix composites.* Measurement, 2015. **74**: p. 21-30.
163. Peled, A., et al., *Electrical impedance spectra to monitor damage during tensile loading of cement composites.* ACI Materials Journal, 2001. **98**(4): p. 313-322.
164. Torrents, J.M., et al., *Analysis of the impedance spectra of short conductive fiber-reinforced composites.* Journal of Materials Science, 2001. **36**(16): p. 4003-4012.
165. Wen, S. and D.D.L. Chung, *Piezoresistivity in continuous carbon fiber cement-matrix composite.* Cement and Concrete Research, 1999. **29**(3): p. 445-449.
166. Wang, S. and D.D.L. Chung, *Piezoresistivity in continuous carbon fiber polymer-matrix composite.* Polymer Composites, 2000. **21**(1): p. 13-19.
167. Goldfeld, Y., et al. *Integrated monitoring of TRC using carbon fibers*.
168. Goldfeld, Y., et al., *Integrated self-monitoring of carbon based textile reinforced concrete beams under repeated loading in the un-cracked region.* Carbon, 2016. **98**: p. 238-249.
169. Goldfeld, Y., et al., *Sensory carbon fiber based textile-reinforced concrete for smart structures.* Journal of Intelligent Material Systems and Structures, 2016. **27**(4): p. 469-489.

170. Yildirim, G., et al., *Estimating the self-healing capability of cementitious composites through non-destructive electrical-based monitoring.* Ndt & E International, 2015. **76**: p. 26-37.
171. Nijland, T.G., et al. *Self healing phenomena in concretes and masonry mortars: a microscopic study*.
172. Çopuroğlu, O., et al., *Experimental techniques used to verify healing*, in *Self-Healing Phenomena in Cement-Based Materials*. 2013, Springer. p. 19-63.
173. Sisomphon, K., O. Copuroglu, and A. Fraaij, *Application of encapsulated lightweight aggregate impregnated with sodium monofluorophosphate as a self-healing agent in blast furnace slag mortar.* Heron, 56 (1/2), 2011.
174. Bundur, Z.B., et al., *Impact of air entraining admixtures on biogenic calcium carbonate precipitation and bacterial viability.* Cement and Concrete Research, 2017. **98**: p. 44-49.
175. Chen, H., C. Qian, and H. Huang, *Self-healing cementitious materials based on bacteria and nutrients immobilized respectively.* Construction and Building Materials, 2016. **126**: p. 297-303.
176. Erşan, Y.Ç., et al., *Self-protected nitrate reducing culture for intrinsic repair of concrete cracks.* Frontiers in microbiology, 2015. **6**: p. 1228.
177. Erşan, Y.Ç., et al., *Enhanced crack closure performance of microbial mortar through nitrate reduction.* Cement and Concrete Composites, 2016. **70**: p. 159-170.
178. Fan, S. and M. Li, *X-ray computed microtomography of three-dimensional microcracks and self-healing in engineered cementitious composites.* Smart materials and structures, 2014. **24**(1): p. 015021.
179. Ferrara, L., V. Krelani, and F. Moretti, *On the use of crystalline admixtures in cement based construction materials: from porosity reducers to promoters of self healing.* Smart Materials and Structures, 2016. **25**(8): p. 084002.
180. Jiang, Z., et al., *Self-healing of cracks in concrete with various crystalline mineral additives in underground environment.* Journal of Wuhan University of Technology-Mater. Sci. Ed., 2014. **29**(5): p. 938-944.
181. Ma, H., S. Qian, and Z. Zhang, *Effect of self-healing on water permeability and mechanical property of medium-early-strength engineered cementitious composites.* Construction and Building Materials, 2014. **68**: p. 92-101.
182. Sangadji, S., et al., *The Use of Alkaliphilic Bacteria-based Repair Solution for Porous Network Concrete Healing Mechanism.* Procedia engineering, 2017. **171**: p. 606-613.
183. Xu, J., W. Yao, and Z. Jiang, *Non-ureolytic bacterial carbonate precipitation as a surface treatment strategy on cementitious materials.* Journal of Materials in Civil Engineering, 2013. **26**(5): p. 983-991.
184. Ramachandran, V.S. and J.J. Beaudoin, *Handbook of analytical techniques in concrete science and technology: principles, techniques and applications*. 2000: Elsevier.
185. Yuan, X.Z., W. Sun, and X.B. Zuo. *Study of feasibility of heat melt adhesive being used in crack self-healing of cement-based materials*. Trans Tech Publ.
186. Song, Y.-K., et al., *Sunlight-induced self-healing of a microcapsule-type protective coating.* ACS applied materials & interfaces, 2013. **5**(4): p. 1378-1384.
187. Jonkers, H.M. and A. Thijssen. *Bacteria mediated remediation of concrete structures*.
188. Sabir, B.B., S. Wild, and M. O'Farrell, *A water sorptivity test for martar and concrete.* Materials and Structures, 1998. **31**(8): p. 568.
189. Snoeck, D., et al., *Self-healing cementitious materials by the combination of microfibres and superabsorbent polymers.* Journal of Intelligent Material Systems and Structures, 2014. **25**(1): p. 13-24.

190. Şahmaran, M., et al., *Self-healing of mechanically-loaded self consolidating concretes with high volumes of fly ash.* Cement and Concrete Composites, 2008. **30**(10): p. 872-879.
191. Feiteira, J., E. Gruyaert, and N. De Belie, *Self-healing of moving cracks in concrete by means of encapsulated polymer precursors.* Construction and Building Materials, 2016. **102**: p. 671-678.
192. Araujo, M., et al., *Cross-linkable polyethers as healing/sealing agents for self-healing of cementitious materials.* Materials & Design, 2016. **98**: p. 215-222.
193. Van Belleghem, B., et al., *Capillary water absorption in cracked and uncracked mortar–A comparison between experimental study and finite element analysis.* Construction and Building Materials, 2016. **110**: p. 154-162.
194. Zaccardi, Y.A.V., N.M. Alderete, and N. De Belie, *Improved model for capillary absorption in cementitious materials: Progress over the fourth root of time.* Cement and Concrete Research, 2017. **100**: p. 153-165.
195. Rimmelé, G., et al., *Heterogeneous porosity distribution in Portland cement exposed to CO2-rich fluids.* Cement and Concrete Research, 2008. **38**(8-9): p. 1038-1048.
196. Aldea, C.-M., et al., *Extent of healing of cracked normal strength concrete.* Journal of materials in civil engineering, 2000. **12**(1): p. 92-96.
197. Ahn, T.H., M. Morita, and T. Kishi. *Innovative repair methods for civil infrastructures based on crack self-healing technologies using cementitious materials*.
198. Nishiwaki, T., et al., *Development of self-healing system for concrete with selective heating around crack.* Journal of Advanced Concrete Technology, 2006. **4**(2): p. 267-275.
199. Brandt, A.M., *Cement-based composites: materials, mechanical properties and performance*. 2005: CRC Press.
200. Aldea, C.M., S.P. Shah, and A. Karr, *Permeability of cracked concrete.* Materials and structures, 1999. **32**(5): p. 370-376.
201. Wang, K., et al., *Permeability study of cracked concrete.* Cement and concrete research, 1997. **27**(3): p. 381-393.
202. Van Tittelboom, K., et al., *Methyl methacrylate as a healing agent for self-healing cementitious materials.* Smart Materials and structures, 2011. **20**(12): p. 125016.
203. Roig-Flores, M., et al., *Effect of crystalline admixtures on the self-healing capability of early-age concrete studied by means of permeability and crack closing tests.* Construction and Building Materials, 2016. **114**: p. 447-457.
204. Formia, A., et al., *Experimental analysis of self-healing cement-based materials incorporating extruded cementitious hollow tubes.* Journal of Intelligent Material Systems and Structures, 2016. **27**(19): p. 2633-2652.
205. Gruyaert, E., et al. *Non-destructive testing techniques to evaluate the healing efficiency of self-healing concrete at lab-scale*. CRC Press.
206. Gruyaert, E., et al., *Self-healing mortar with pH-sensitive superabsorbent polymers: testing of the sealing efficiency by water flow tests.* Smart Materials and Structures, 2016. **25**(8): p. 084007.
207. Tziviloglou, E., et al. *Evaluation of experimental methodology to assess the sealing efficiency of bacteria-based self-healing mortar: round robin test*. RILEM.
208. Yang, Z., et al., *A self-healing cementitious composite using oil core/silica gel shell microcapsules.* Cement and Concrete Composites, 2011. **33**(4): p. 506-512.
209. Yildirim, G., et al., *Influence of cracking and healing on the gas permeability of cementitious composites.* Construction and Building Materials, 2015. **85**: p. 217-226.
210. Akhavan, A. and F. Rajabipour, *Evaluating ion diffusivity of cracked cement paste using electrical impedance spectroscopy.* Materials and structures, 2013. **46**(5): p. 697-708.

211. Win, P.P., M. Watanabe, and A. Machida, *Penetration profile of chloride ion in cracked reinforced concrete.* Cement and concrete research, 2004. **34**(7): p. 1073-1079.
212. Astm, C., *597, Standard test method for pulse velocity through concrete.* ASTM International, West Conshohocken, PA, 2009.
213. Aïtcin, P.-C., *Binders for durable and sustainable concrete*. 2014: CRC Press.
214. Wang, X., et al., *Experimental study on cementitious composites embedded with organic microcapsules.* Materials, 2013. **6**(9): p. 4064-4081.
215. Darquennes, A., et al., *Self-healing at early-age, a way to improve the chloride resistance of blast-furnace slag cementitious materials.* Construction and Building Materials, 2016. **113**: p. 1017-1028.
216. Sahmaran, M., G. Yildirim, and T.K. Erdem, *Self-healing capability of cementitious composites incorporating different supplementary cementitious materials.* Cement and Concrete Composites, 2013. **35**(1): p. 89-101.
217. Ismail, M., et al., *Effect of crack opening on the local diffusion of chloride in cracked mortar samples.* Cement and concrete research, 2008. **38**(8-9): p. 1106-1111.
218. Sahmaran, M., M. Li, and V.C. Li, *Transport properties of engineered cementitious composites under chloride exposure.* ACI Materials Journal, 2007. **104**(6): p. 604.
219. Klieger, P., *Significance of tests and properties of concrete and concrete-making materials*. Vol. 169. 1994: ASTM International.
220. Lee, H.X.D., H.S. Wong, and N. Buenfeld. *Self-sealing cement-based materials using superabsorbent polymers*.
221. Song, M., S. Jeon, and Y. Song. *The change of osmosis pressure by crack self-healing of cementitious materials*.
222. Carlos Jr, C., *Microscopic observations of internal frost damage and salt scaling*. 2008: University of California, Berkeley.
223. Nishiwaki, T., et al., *Experimental study on self-healing capability of FRCC using different types of synthetic fibers.* Journal of Advanced Concrete Technology, 2012. **10**(6): p. 195-206.
224. Nishiwaki, T., et al., *Self-healing capability of fiber-reinforced cementitious composites for recovery of watertightness and mechanical properties.* Materials, 2014. **7**(3): p. 2141-2154.
225. Ferrara, L., et al., *Natural Fibres As Promoters Of Autogeneous Healing In HPFRCCS: Results From On-Going Brazil-Italy Cooperation.* Special Publication, 2015. **305**: p. 11-1.
226. Ferrara, L., et al., *Effects of autogenous healing on the recovery of mechanical performance of High Performance Fibre Reinforced Cementitious Composites (HPFRCCs): part 1.* Cement and Concrete Composites, 2017. **83**: p. 76-100.
227. De Nardi, C., et al., *Effect of age and level of damage on the autogenous healing of lime mortars.* Composites Part B: Engineering, 2017. **124**: p. 144-157.
228. De Nardi, C., et al., *Effectiveness of crystalline admixtures and lime/cement coated granules in engineered self-healing capacity of lime mortars.* Materials and Structures, 2017. **50**(4): p. 191.
229. Granger, S., et al., *Experimental characterization of the self-healing of cracks in an ultra high performance cementitious material: Mechanical tests and acoustic emission analysis.* Cement and Concrete Research, 2007. **37**(4): p. 519-527.
230. Kuang, Y.-c. and J.-p. Ou, *Passive smart self-repairing concrete beams by using shape memory alloy wires and fibers containing adhesives.* Journal of Central South University of Technology, 2008. **15**(3): p. 411-417.
231. Joseph, C., et al., *Experimental investigation of adhesive-based self-healing of cementitious materials.* Magazine of Concrete Research, 2010. **62**(11): p. 831-843.

232. Thao, T.D.P., et al., *Implementation of self-healing in concrete–Proof of concept.* The IES Journal Part A: Civil & Structural Engineering, 2009. **2**(2): p. 116-125.
233. Pelletier, M.M., et al., *Self-healing concrete with a microencapsulated healing agent.* Cem. Concr. Res, 2011.
234. Xing, F., et al. *Self-healing mechanism of a novel cementitious composite using microcapsules*.
235. Yang, Z., et al., *Laboratory assessment of a self-healing cementitious composite.* Transportation Research Record, 2010. **2142**(1): p. 9-17.
236. Dry, C., M. Corsaw, and E. Bayer, *A comparison of internal self-repair with resin injection in repair of concrete.* Journal of adhesion science and technology, 2003. **17**(1): p. 79-89.
237. Sun, L., W.Y. Yu, and Q. Ge. *Experimental research on the self-healing performance of micro-cracks in concrete bridge*. Trans Tech Publ.
238. Thao, T.D.P., *Quasi-Brittle Self-Healing Materials: Numerical Modelling and Applications in Civil Engineering.* 2011.
239. Kim, J.S. and E. Schlangen. *Super absorbent polymers to simulate self healing in ECC*.
240. Qian, S., et al. *Self-healing cementitious composites under bending loads*.
241. Ferrara, L., et al., *Self Healing Of Cement Based Materials Engineered Through Crystalline Admixtures: Experimental Results From A Multinational University Network.* Special Publication, 2015. **305**: p. 13-1.
242. Qureshi, T.S., A. Kanellopoulos, and A. Al-Tabbaa, *Encapsulation of expansive powder minerals within a concentric glass capsule system for self-healing concrete.* Construction and Building Materials, 2016. **121**: p. 629-643.
243. Granger, S., et al., *Monitoring of cracking and healing in an ultra high performance cementitious material using the time reversal technique.* Cement and Concrete Research, 2009. **39**(4): p. 296-302.
244. Kan, L.-L., et al., *Self-Healing Characterization of Engineered Cementitious Composite Materials.* ACI Materials Journal, 2010. **107**(6).
245. Nishiwaki, T., et al., *Experimental study on self-healing effect of FRCC with PVA fibers and additives against freeze/thaw cycles.* Proceedings, 5th ICSHM, Raileigh, USA, 2015.
246. Nanayakkara, A. *Self-healing of cracks in concrete subjected to water pressure*.
247. Jacobsen, S. and E.J. Sellevold, *Self healing of high strength concrete after deterioration by freeze/thaw.* Cement and Concrete Research, 1996. **26**(1): p. 55-62.
248. Wang, X., et al., *Self-healing concrete incorporating mineral additives and encapsulated lightweight aggregates: Preparation and application.* Construction and Building Materials, 2021. **301**: p. 124119.
249. Vermeer, C.M., et al., *From waste to self-healing concrete: A proof-of-concept of a new application for polyhydroxyalkanoate.* Resources, Conservation and Recycling, 2021. **164**: p. 105206.
250. Rajasegar, M. and C.M. Kumaar, *Hybrid effect of poly vinyl alcohol, expansive minerals, nano-silica and rice husk ash on the self-healing ability of concrete.* Materials Today: Proceedings, 2021. **45**: p. 5944-5952.
251. Qureshi, T. and A. Al-Tabbaa, *Self-Healing Concrete and Cementitious Materials*, in *Advanced Functional Materials*. 2020, IntechOpen.
252. Rai, A. and M.C. Maurya, *Eco-concrete: Opportunities and Challenges.*
253. Alazhari, M.S.A., *The effect of microbiological agents on the efficiency of bio-based repair systems for concrete.* 2017.
254. Knoll, A.H., *Biomineralization and evolutionary history.* Reviews in mineralogy and geochemistry, 2003. **54**(1): p. 329-356.

255. Jonkers, H.M., A. Thijssen, and E. Schlangen, *Ontwikkeling van zelfherstellend beton met behulp van bacteriën.* Cement, 2008. **4**: p. 78-81.
256. Achal, V., et al., *Lactose mother liquor as an alternative nutrient source for microbial concrete production by Sporosarcina pasteurii.* Journal of industrial microbiology & biotechnology, 2009. **36**(3): p. 433-438.
257. Gajjar, K.M. and M.A. Jamnu, *A Study of Performance of Bacillus Lentus on Concrete Cracks.* PARIPEX-INDIAN J. Res, 2013. **2**: p. 71-75.
258. Krishnapriya, S. and D.L.V. Babu, *Isolation and identification of bacteria to improve the strength of concrete.* Microbiological research, 2015. **174**: p. 48-55.
259. Ramachandran, S.K., V. Ramakrishnan, and S.S. Bang, *Remediation of concrete using micro-organisms.* ACI Materials Journal-American Concrete Institute, 2001. **98**(1): p. 3-9.
260. Han, N.-X. and F. Xing, *A Comprehensive Review of the Study and Development of Microcapsule Based Self-Resilience Systems for Concrete Structures at Shenzhen University.* Materials, 2016. **10**(1): p. 2.
261. Chahal, N., R. Siddique, and A. Rajor, *Influence of bacteria on the compressive strength, water absorption and rapid chloride permeability of fly ash concrete.* Construction and Building Materials, 2012. **28**(1): p. 351-356.
262. Achal, V., A. Mukherjee, and M.S. Reddy, *Microbial concrete: way to enhance the durability of building structures.* Journal of materials in civil engineering, 2010. **23**(6): p. 730-734.
263. Xu, J. and X. Wang, *Self-healing of concrete cracks by use of bacteria-containing low alkali cementitious material.* Construction and Building Materials, 2018. **167**: p. 1-14.
264. Da Silva, F.B., et al., *Production of non-axenic ureolytic spores for self-healing concrete applications.* Construction and Building Materials, 2015. **93**: p. 1034-1041.
265. Paine, K. *Bacteria-based self-healing concrete: Effects of environment, exposure and crack size*. RILEM publications SARL.
266. Soltmann, U., B. Nies, and H. Böttcher, *Cements with embedded living microorganisms–a new class of biocatalytic composite materials for application in bioremediation, biotechnology.* Advanced Engineering Materials, 2011. **13**(1-2): p. B25-B31.
267. Bundur, Z.B., M.J. Kirisits, and R.D. Ferron, *Biomineralized cement-based materials: Impact of inoculating vegetative bacterial cells on hydration and strength.* Cement and Concrete Research, 2015. **67**: p. 237-245.
268. Achal, V., A. Mukherjee, and M.S. Reddy, *Microbial concrete: way to enhance the durability of building structures.* Journal of materials in civil engineering, 2011. **23**(6): p. 730-734.
269. Andalib, R., et al., *Optimum concentration of Bacillus megaterium for strengthening structural concrete.* Construction and Building Materials, 2016. **118**: p. 180-193.
270. Ferris, F.G., et al., *Bacteriogenic mineral plugging.* Journal of Canadian Petroleum Technology, 1997. **36**(09).
271. Rivadeneyra, M.A., et al., *Biomineralization of carbonates by Halomonas eurihalina in solid and liquid media with different salinities: crystal formation sequence.* Research in Microbiology, 1998. **149**(4): p. 277-287.
272. Hammes, F., et al., *Strain-specific ureolytic microbial calcium carbonate precipitation.* Applied and environmental microbiology, 2003. **69**(8): p. 4901-4909.
273. Wang, J., et al., *Application of microorganisms in concrete: a promising sustainable strategy to improve concrete durability.* Applied microbiology and biotechnology, 2016. **100**(7): p. 2993-3007.

274. Seifan, M., A.K. Samani, and A. Berenjian, *New insights into the role of pH and aeration in the bacterial production of calcium carbonate (CaCO 3).* Applied microbiology and biotechnology, 2017. **101**(8): p. 3131-3142.
275. Silva, F.B., et al., *Industrial application of biological self-healing concrete: Challenges and economical feasibility.* Journal of Commercial Biotechnology, 2015. **21**(1).
276. Basaran, Z., *Biomineralization in cement based materials: inoculation of vegetative cells.* 2013.
277. Lee, Y.S. and W. Park, *Current challenges and future directions for bacterial self-healing concrete.* Applied microbiology and biotechnology, 2018. **102**(7): p. 3059-3070.
278. Luna-Finkler, C.L. and L. Finkler, *Bacillus sphaericus and Bacillus thuringiensis to insect control: Process development of small scale production to pilot-plant-fermenters*, in *Insecticides-Advances in Integrated Pest Management*. 2012, InTech.
279. Frankel, R.B. and D.A. Bazylinski, *Biologically induced mineralization by bacteria.* Reviews in mineralogy and geochemistry, 2003. **54**(1): p. 95-114.
280. Aye, T. and C.T. Oguchi, *Resistance of plain and blended cement mortars exposed to severe sulfate attacks.* Construction and Building Materials, 2011. **25**(6): p. 2988-2996.
281. Hammes, F. and W. Verstraete, *Key roles of pH and calcium metabolism in microbial carbonate precipitation.* Reviews in environmental science and biotechnology, 2002. **1**(1): p. 3-7.
282. De Muynck, W., N. De Belie, and W. Verstraete, *Microbial carbonate precipitation in construction materials: a review.* Ecological Engineering, 2010. **36**(2): p. 118-136.
283. Castanier, S., G. Le Métayer-Levrel, and J.-P. Perthuisot, *Ca-carbonates precipitation and limestone genesis—the microbiogeologist point of view.* Sedimentary geology, 1999. **126**(1-4): p. 9-23.
284. Castanier, S., G. Le Metayer-Levrel, and J.-P. Perthuisot, *Bacterial roles in the precipitation of carbonate minerals*, in *Microbial sediments*. 2000, Springer. p. 32-39.
285. Okafor, N., *Environmental microbiology of aquatic and waste systems*. 2011: Springer Science & Business Media.
286. Talham, D.R., *Biomineralization: Principles and Concepts in Bioinorganic Materials Chemistry Stephen Mann. Oxford University Press, New York, 2001*. 2002, ACS Publications.
287. Knorre, H.v. and W.E. Krumbein, *Bacterial calcification*, in *Microbial sediments*. 2000, Springer. p. 25-31.
288. Rusznyák, A., et al., *Calcite biomineralization by bacterial isolates from the recently discovered pristine karstic Herrenberg cave.* Applied and environmental microbiology, 2012. **78**(4): p. 1157-1167.
289. Ronholm, J., et al., *A mineralogical characterization of biogenic calcium carbonates precipitated by heterotrophic bacteria isolated from cryophilic polar regions.* Geobiology, 2014. **12**(6): p. 542-556.
290. Cacchio, P., et al., *Calcium carbonate precipitation by bacterial strains isolated from a limestone cave and from a loamy soil.* Geomicrobiology Journal, 2003. **20**(2): p. 85-98.
291. Ehrlich, H.L., *Geomicrobiology: its significance for geology.* Earth-Science Reviews, 1998. **45**(1-2): p. 45-60.
292. Perito, B. and G. Mastromei, *Molecular basis of bacterial calcium carbonate precipitation*, in *Molecular biomineralization*. 2011, Springer. p. 113-139.
293. Neville, A., *Autogenous healing—a concrete miracle?* Concrete international, 2002. **24**(11): p. 76-82.
294. Van Tittelboom, K., et al., *Influence of mix composition on the extent of autogenous crack healing by continued hydration or calcium carbonate formation.* Construction and Building Materials, 2012. **37**: p. 349-359.

295. Sahmaran, M., et al., *Repeatability and pervasiveness of self-healing in engineered cementitious composites.* ACI Materials Journal, 2015. **112**(4): p. 513-522.
296. Luhar, S. and S. Gourav, *A review paper on self healing concrete.* Journal of Civil Engineering Research, 2015. **5**(3): p. 53-58.
297. Bang, S.S., J.K. Galinat, and V. Ramakrishnan, *Calcite precipitation induced by polyurethane-immobilized Bacillus pasteurii.* Enzyme and microbial technology, 2001. **28**(4-5): p. 404-409.
298. Reddy, M.A., *Temperature Effect on Various Bacteria Used in Microbial Concrete.* International Journal of Innovative Research in Science, Engineering and Technology, 2016. **5**(4).
299. Sharma, T., et al. *The Requirements for autonomic microbiologically-induced calcite-precipitation in concrete*.
300. Schleifer, K.H., *Classification of Bacteria and Archaea: past, present and future.* Systematic and applied microbiology, 2009. **32**(8): p. 533-542.
301. Horikoshi, K., *2.5 General Physiology of Alkaliphiles.* Extremophiles handbook, 2010: p. 99.
302. Ghosh, P., et al., *Development of bioconcrete material using an enrichment culture of novel thermophilic anaerobic bacteria.* 2006.
303. Ghaz-Jahanian, M.A., et al., *Influence of small RNAs on biofilm formation process in bacteria.* Molecular biotechnology, 2013. **55**(3): p. 288-297.
304. Abdullah, M.A.H., N.A.H. Abdullah, and M.F. Tompang. *Development and Performance of Bacterial Self-healing Concrete-A Review*. IOP Publishing.
305. Ducasse-Lapeyrusse, J., et al., *Effect of calcium gluconate, calcium lactate, and urea on the kinetics of self-healing in mortars.* Construction and Building Materials, 2017. **157**: p. 489-497.
306. Rajczakowska, M., *Self-healing concrete.* 2019.
307. Zemskov, S.V., H.M. Jonkers, and F.J. Vermolen, *Two analytical models for the probability characteristics of a crack hitting encapsulated particles: Application to self-healing materials.* Computational materials science, 2011. **50**(12): p. 3323-3333.
308. Ponnusami, S.A., S. Turteltaub, and S. van der Zwaag, *Cohesive-zone modelling of crack nucleation and propagation in particulate composites.* Engineering Fracture Mechanics, 2015. **149**: p. 170-190.
309. Mookhoek, S.D., H.R. Fischer, and S. van der Zwaag, *A numerical study into the effects of elongated capsules on the healing efficiency of liquid-based systems.* Computational Materials Science, 2009. **47**(2): p. 506-511.
310. Lv, Z. and H. Chen, *Analytical models for determining the dosage of capsules embedded in self-healing materials.* Computational Materials Science, 2013. **68**: p. 81-89.
311. Edvardsen, C., *Water permeability and autogenous healing of cracks in concrete*, in *Innovation in concrete structures: Design and construction*. 1999, Thomas Telford Publishing. p. 473-487.
312. Nugroho, A. and I. Satyarno, *Bacteria as Self-Healing Agent in Mortar Cracks.* Journal of Engineering & Technological Sciences, 2015. **47**(3).
313. Qian, C., et al., *Bio-mineralization on cement-based materials consuming CO2 from atmosphere.* Construction and Building Materials, 2016. **106**: p. 126-132.
314. Pilegis, M., et al., *Delayed concrete prestressing with shape memory polymer tendons.* 2015.
315. Snoeck, D., L. Pel, and N. De Belie, *Autogenous healing in cementitious materials with superabsorbent polymers quantified by means of NMR.* Scientific reports, 2020. **10**(1): p. 1-6.

316. Dry, C. and W. McMillan, *Three-part methylmethacrylate adhesive system as an internal delivery system for smart responsive concrete.* Smart Materials and Structures, 1996. **5**(3): p. 297.
317. Morita, R.Y., *Calcite precipitation by marine bacteria.* Geomicrobiology Journal, 1980. **2**(1): p. 63-82.
318. Boquet, E., A. Boronat, and A. Ramos-Cormenzana, *Production of calcite (calcium carbonate) crystals by soil bacteria is a general phenomenon.* Nature, 1973. **246**(5434): p. 527.
319. Douglas, S. and T.J. Beveridge, *Mineral formation by bacteria in natural microbial communities.* FEMS microbiology ecology, 1998. **26**(2): p. 79-88.
320. In, C.-W., et al., *Monitoring and evaluation of self-healing in concrete using diffuse ultrasound.* NDT & E International, 2013. **57**: p. 36-44.
321. Maes, M., K. Van Tittelboom, and N. De Belie, *The efficiency of self-healing cementitious materials by means of encapsulated polyurethane in chloride containing environments.* Construction and Building Materials, 2014. **71**: p. 528-537.
322. Cuenca, E., A. Tejedor, and L. Ferrara, *A methodology to assess crack-sealing effectiveness of crystalline admixtures under repeated cracking-healing cycles.* Construction and Building Materials, 2018. **179**: p. 619-632.
323. Zhang, J.L., et al., *A binary concrete crack self-healing system containing oxygen-releasing tablet and bacteria and its Ca 2+-precipitation performance.* Applied microbiology and biotechnology, 2016. **100**(24): p. 10295-10306.
324. Dry, C.M. *Repair and prevention of damage due to transverse shrinkage cracks in bridge decks*. International Society for Optics and Photonics.
325. Dry, C.M. *Self-repair of cracks in brittle material systems*. International Society for Optics and Photonics.
326. Hernandez, M., *Using Self-Healing Concrete for Concrete Pepairs on Aging Concrete Structures.* Research and Development Office Science and Technology Program, 2016.
327. Sierra Beltran, M.G., et al. *Field application of self-healing concrete with natural fibres as linings for irrigation canals in Ecuador*.
328. Stewart, A., *The 'living concrete'that can heal itself.* CNN, updated and accessed March, 2016. **7**.
329. ., *P.g.A.* and R.S. 8. 2016.
330. Hofboer, N. *Self-Healing Concrete*. (2015, June).
331. de Normalisation, C.E., *Tests for Geometrical Properties of Aggregates.* Determination of Particle Shape. Shape Index, 1996: p. 933-4.
332. British Standards, I., *Tests for Mechanical and Physical Properties of Aggregates: Part 6 Determination of Particle Density and Water Absorption*. 2000: British Standards Institution.
333. Standard, B., *Determination of Particle Density and Water Absorption: Aggregates between 31.5 mm and 4 mm.* BS EN, 2000: p. 1097-6.
334. Pei, R., et al., *Use of bacterial cell walls to improve the mechanical performance of concrete.* Cement and Concrete Composites, 2013. **39**: p. 122-130.
335. Sonenshein, A.L., et al., *Isolation and characterization of rifampin-resistant and streptolydigin-resistant mutants of Bacillus subtilis with altered sporulation properties.* Journal of bacteriology, 1974. **120**(1): p. 253-265.
336. James, C. and S. Natalie, *Microbiology. A laboratory manual*. 2014: Pearson Education.
337. En, B.S., *196-1: 2016.* Methods of Testing Cement. Determination of Strength, 2016.
338. Standard, B., *Testing concrete-Part 116: method for determination of compressive strength of concrete cubes.* BS, 1881. **116**: p. 1983.

339. Suleiman, A.R. and M.L. Nehdi, *Effect of environmental exposure on autogenous self-healing of cracked cement-based materials.* Cement and Concrete Research, 2018. **111**: p. 197-208.
340. Martys, N.S. and C.F. Ferraris, *Capillary transport in mortars and concrete.* Cement and concrete research, 1997. **27**(5): p. 747-760.
341. En, B.S., *13057: 2002, Determination of resistance of capillary absorption.* British Standards Institution, 2002. **20**: p. 685.
342. Todokoro, H. and M. Ezumi, *Scanning electron microscope*. 1999, Google Patents.
343. Luo, M. and C. Qian, *Influences of bacteria-based self-healing agents on cementitious materials hydration kinetics and compressive strength.* Construction and Building Materials, 2016. **121**: p. 659-663.
344. Chan, E.-S., et al., *Encapsulation of herbal aqueous extract through absorption with ca-alginate hydrogel beads.* Food and Bioproducts Processing, 2010. **88**(2-3): p. 195-201.
345. Gbassi, G.K., et al., *Microencapsulation of Lactobacillus plantarum spp in an alginate matrix coated with whey proteins.* International journal of food Microbiology, 2009. **129**(1): p. 103-105.
346. Shilpa, A., S.S. Agrawal, and A.R. Ray, *Controlled delivery of drugs from alginate matrix.* Journal of Macromolecular Science, Part C: Polymer Reviews, 2003. **43**(2): p. 187-221.
347. Bsi, *BS EN 196-1: 2005: Methods of testing cement. Determination of strength*. 2005, BSI London, UK.
348. Celik, A.G., A.M. Kilic, and G.O. Cakal, *Expanded perlite aggregate characterization for use as a lightweight construction raw material.* Physicochemical Problems of Mineral Processing, 2013. **49**.
349. Sengul, O., et al., *Effect of expanded perlite on the mechanical properties and thermal conductivity of lightweight concrete.* Energy and Buildings, 2011. **43**(2-3): p. 671-676.
350. Ciullo, P.A., *Industrial minerals and their uses: a handbook and formulary*. 1996: William Andrew.
351. Siddique, R. and N.K. Chahal, *Effect of ureolytic bacteria on concrete properties.* Construction and Building Materials, 2011. **25**(10): p. 3791-3801.
352. Nain, N., et al., *Enhancement in strength parameters of concrete by application of Bacillus bacteria.* Construction and Building Materials, 2019. **202**: p. 904-908.
353. Sylvia, D.M., et al., *Principles and applications of soil microbiology*. 2005: Pearson Prentice Hall Upper Saddle River, NJ:.
354. Monteiro, P.J.M. and K.E. Kurtis, *Time to failure for concrete exposed to severe sulfate attack.* Cement and Concrete research, 2003. **33**(7): p. 987-993.
355. Hamza, O. and J. Ikin, *Electrokinetic treatment of desiccated expansive clay.* Géotechnique, 2020. **70**(5): p. 421-431.
356. Gonzalez-Ollauri, A. and S.B. Mickovski, *Plant-soil reinforcement response under different soil hydrological regimes.* Geoderma, 2017. **285**: p. 141-150.
357. Wang, J., et al., *Self-healing concrete by use of microencapsulated bacterial spores.* Cement and Concrete Research, 2014. **56**: p. 139-152.
358. Achal, V. and A. Mukherjee, *A review of microbial precipitation for sustainable construction.* Construction and Building Materials, 2015. **93**: p. 1224-1235.
359. Gupta, S., H.W. Kua, and S. Dai Pang, *Healing cement mortar by immobilization of bacteria in biochar: An integrated approach of self-healing and carbon sequestration.* Cement and Concrete Composites, 2018. **86**: p. 238-254.
360. Son, H.M., et al., *Ureolytic/Non-Ureolytic Bacteria Co-Cultured Self-Healing Agent for Cementitious Materials Crack Repair.* Materials, 2018. **11**(5): p. 782.

361. Lee, B.Y. and K.E. Kurtis, *Effect of pore structure on salt crystallization damage of cement-based materials: Consideration of w/b and nanoparticle use.* Cement and Concrete Research, 2017. **98**: p. 61-70.
362. Chahal, N. and R. Siddique, *Permeation properties of concrete made with fly ash and silica fume: Influence of ureolytic bacteria.* Construction and Building Materials, 2013. **49**: p. 161-174.
363. Xu, J., et al., *Application of ureolysis-based microbial CaCO3 precipitation in self-healing of concrete and inhibition of reinforcement corrosion.* Construction and Building Materials, 2020. **265**: p. 120364.
364. Liu, S., et al., *Evaluation of self-healing of internal cracks in biomimetic mortar using coda wave interferometry.* Cement and Concrete Research, 2016. **83**: p. 70-78.
365. Tsangouri, E., et al., *Assessment of acoustic emission localization accuracy on damaged and healed concrete.* Construction and Building Materials, 2016. **129**: p. 163-171.
366. Ranade, R., et al., *Influence of micro-cracking on the composite resistivity of engineered cementitious composites.* Cement and Concrete Research, 2014. **58**: p. 1-12.
367. Layssi, H., et al., *Electrical resistivity of concrete.* Concrete International, 2015. **37**(5): p. 41-46.
368. Sengul, O., *Factors affecting the electrical resistivity of concrete*, in *Nondestructive Testing of Materials and Structures*. 2013, Springer. p. 263-269.
369. Bioubakhsh, S., *The penetration of chloride in concrete subject to wetting and drying: measurement and modelling.* 2011.
370. Chacko, R.M., N. Banthia, and A.A. Mufti, *Carbon-fiber-reinforced cement-based sensors.* Canadian Journal of Civil Engineering, 2007. **34**(3): p. 284-290.
371. Banthia, N., S. Djeridane, and M. Pigeon, *Electrical resistivity of carbon and steel micro-fiber reinforced cements.* Cement and Concrete research, 1992. **22**(5): p. 804-814.
372. Zhang, K., B. Han, and X. Yu, *Nickel particle based electrical resistance heating cementitious composites.* Cold Regions Science and Technology, 2011. **69**(1): p. 64-69.
373. Yoo, D.-Y., I. You, and S.-J. Lee, *Electrical properties of cement-based composites with carbon nanotubes, graphene, and graphite nanofibers.* Sensors, 2017. **17**(5): p. 1064.
374. Yoo, D.-Y., I. You, and S.-J. Lee, *Electrical and piezoresistive sensing capacities of cement paste with multi-walled carbon nanotubes.* Archives of Civil and Mechanical Engineering, 2018. **18**: p. 371-384.
375. Chen, B., K. Wu, and W. Yao, *Conductivity of carbon fiber reinforced cement-based composites.* Cement and Concrete Composites, 2004. **26**(4): p. 291-297.
376. Sengul, O., *Use of electrical resistivity as an indicator for durability.* Construction and Building Materials, 2014. **73**: p. 434-441.
377. Hansson, C.M., A. Poursaee, and S.J. Jaffer, *Corrosion of reinforcing bars in concrete.* R&D Serial, 2007. **3013**.
378. Guthrie, W.S., T.M. Pinkerton, and D.L. Eggett, *Sensitivity of half-cell potential measurements to properties of concrete bridge decks*. 2008.